University of Strathclyde

Department of Pure and Applied Chemistry

Development of Biologically Relevant Assays for the Detection of Disease DNA Using SERS

By

Kirsten Gracie

A thesis presented to the Department of Pure and Applied Chemistry, University of Strathclyde, in fulfilment of the requirements for the degree of Doctor of Philosophy.

2014

This thesis is the result of the authors original research. It has been composed by the author and has not been previously submitted for examination which has led to the award of a degree.

Signed: Date:

Acknowledgements

First and foremost I would like to thank my supervisors Dr Karen Faulds and Professor Duncan Graham for the opportunity to carry out this research and for their continued support and encouragement throughout my PhD.

The majority of this research was carried out in collaborations with other academics and universities. Firstly, I would like to thank Professor Ewen Smith for his help and guidance throughout several research projects. I would like to thank Professor Roy Goodacre and Dr Elon Correa from the University of Manchester for their invaluable help with chemometric analysis, to Professor Pradeepkumar from IIT Bombay for his help with the G-quadruplex study and to Professor David Birch, Dr Jens Stutter and Philip Yip from the Physics Department at Strathclyde for allowing me to carry out the fluorescence studies in their laboratories.

I would also like to thank everyone within the Centre of Nanometrology for their help and advice throughout my PhD. In particular, I would like to thank Samantha, Rachel, Hayleigh and Sarah for being great friends and making my PhD bearable…sans oublier Alex. I would also like to thank Dr Kristy McKeating and Dr Samuel Mabbott for their help with data analysis and more importantly thesis corrections.

Finally, I would like to thank my amazing family for all their support throughout the years. To Seonaid, for understanding my mental moments and always being there to listen, to Ian and Kelly for putting up with the "leech" and the support they have given me especially in the last few months and to my nephews and niece (Cameron, Ross and Olivia) for always keeping me smiling. I would like to thank Liam for his endless support and encouragement and for not running a mile when I have been extremely stressed. Most of all, I would like to thank my mum Shona, without your love and support I would never have come this far, hopefully all the tantrums and tears have been worth it.

"Minimise the variables, maximise the constants." – I. Gracie, 2014

Abstract

DNA is the fundamental material responsible for storing the genetic coding required for the development of all living organisms. Since its discovery, there has been an intense amount of research into biorecognition events and the detection of DNA sequences coding for specific diseases. The development of the polymerase chain reaction (PCR) involved the amplification of small quantities of DNA allowing for subsequent analysis. However, fluorescence-based methods such as PCR have their limitations, for example the difficulties encountered when detecting multiple targets simultaneously. Therefore, there is a need for novel techniques that overcome these limitations associated with fluorescence-based methods. This research involves the use of SERS for the multiplex detection of target DNA, investigating the possible interactions between fluorescent dyes and DNA and SERS analysis of G-quadruplex formations.

A SERS-based detection assay was designed for the simultaneous detection of three bacterial meningitis pathogens; *Neisseria meningitidis*, *Haemophilus influenzae* and *Streptococcus pneumoniae*. By using SERS instead of fluorescence-based methods, multiplex detection was readily achieved and by using chemometric analysis it was the first report of pathogen quantification post-assay.

To gain an understanding into interactions that can occur between fluorescent dyes (FAM and TAMRA), DNA and spermine, fluorescence and SERS studies were undertaken. Fluorescent studies gave an insight into the interactions that happen off the nanoparticle surface, while the SERS studies demonstrated the competitive interactions that occur between the nanoparticle surface and the two fluorescent dyes. These studies highlighted the consideration needed when selecting fluorescent dyes and target DNA sequences when designing a multiplex SERS assay.

SERS was then applied to the detection of G-quadruplex formation. Previous reports used fluorescence-based methods, for example FID assays. Three ligands that selectively bind to and stabilise G-quadruplex DNA, previously used in fluorescence studies, were used and shown to have the ability to aggregate nanoparticles and act as Raman reporters. These ligands allowed for the design of the “on to off” SERS analysis of three G-quadruplex sequences.

Abbreviations

360A	3-amino-quinolinium pyridine
3AQN	3-amino-quinolinium naphthyridine
6AQN	6-amino-quinolinium naphthyridine
A	Adenine
A.U.	Arbitrary Units
BHQ	Black Hole Quencher
BSA	Bovine Serum Albumin
C	Cytosine
CD	Circular Dichroism
CPS	Counts per Second
CSF	Cerebral Spinal Fluid
DLS	Dynamic Light Scattering
DNA	Deoxyribonucleic Acid
dNTPs	Deoxynucleotide Triphosphates
EtBr	Ethidium Bromide
FAM	6-carboxyfluorescein
FID	Fluorescence Intercalator Displacement
FISH	Fluorescence In Situ Hybridisation
F-ITC	Fluorescein Isothiocyanate
FRET	Förster/Fluorescence Resonance Energy Transfer
FWHH	Full Width Half Height
G	Guanine
HEG	Hexaethylene glycol
HPLC	High Performance Liquid Chromatography

KCl	Potassium Chloride
LSPR	Localised Surface Plasmon Resonance
$MgSO_4$	Magnesium Sulfate
mRNA	Messenger Ribonucleic Acid
NaCl	Sodium Chloride
NMR	Nuclear Magnetic Resonance
NRMSE	Normalised Root –Mean-Square Error
OSN	Oligonucleotide Silver Nanoparticle
PBS	Phosphate Buffered Saline
PCA	Principle Component Analysis
PCR	Polymerase Chain Reaction
PLS	Partial Least Squared
PMMA	Poly (methyl methacrylate)
PNA	Peptide Nucleic Acid
QPCR	Quantitative Polymerase Chain Reaction
RNA	Ribonucleic Acid
RRS	Resonance Raman Scattering
RS	Raman Scattering
RT-PCR	Real Time – Polymerase Chain Reaction
SEF	Surface Enhanced Fluorescence
SERRS	Surface Enhanced Resonance Raman Scattering
SERS	Surface Enhanced Raman Scattering
SNA	Spherical Nucleic Acid
SPR	Surface Plasmon Resonance
T	Thymine
Taq	Thermus Aquaticus

TAMRA	Tetramethylcarboxyrhodamine
TEA	Triethylamine
TR-ITC	Tetramethylcarboxyrhodamine Isothiocyanate
tRNA	Transfer Ribonucleic Acid
UV-Vis	Ultraviolet-Visible Spectrometry

Contents

1. Introduction

In the field of molecular diagnostics, there is a growing need for sensitive and specific methods for the detection of certain diseases. The most common biomolecules of interest are DNA and proteins, and a significant amount of research has been undertaken towards developing novel methods of disease detection using these biomolecules. Since the completion of the human genome project,[1] there has been a considerable amount of interest in the detection of DNA coding for particular diseases. DNA detection of specific sequences has become increasingly important in the diagnosis and treatment of infectious diseases. Numerous diagnostic assays have been developed in recent years due to the advanced analytical techniques available and the desire for highly sensitive methods capable of detecting very low quantities of DNA. However, there is still a constant strive towards simpler and faster methods of disease diagnosis.

1.1 Deoxyribonucleic Acid (DNA)

DNA is a fundamental genetic material as it stores the genetic coding required to control the functions, behaviour, and development of all living organisms. The biological importance of DNA has resulted in an extensive amount of research in the field of molecular biology.[2] Nucleic acids are polymeric macromolecules which consists of two forms; Deoxyribonucleic acid (DNA) and Ribonucleic acid (RNA).[3, 4]

1.1.1 Primary Structure

Nucleic acids were first isolated by Friedrich Miescher in 1869[5] and following this discovery Phoebus Levene demonstrated that the larger nucleic acid structure is composed of smaller components known as nucleotides.[5, 6] Nucleotides are the repeating units that form a nucleic acid strand. Nucleotides are composed of three main components: a deoxyribose

sugar (2'-deoxyribose), a nitrogenous base and a phosphate group. The nitrogenous base is attached to the deoxyribose sugar via an *N*-glycosidic bond and the phosphate group is attached to the sugar at the 5' position (Figure 1.1).

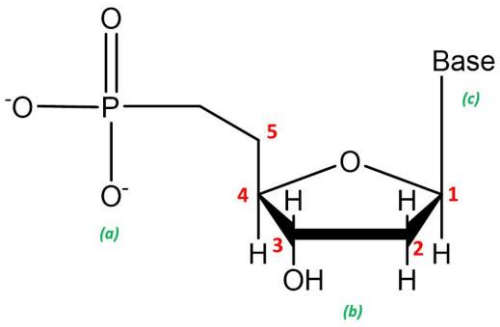

Figure 1.1 The structure of a nucleotide consisting of (a) the phosphate group, (b) the deoxyribose sugar and (c) the nitrogenous base.

There are four nitrogenous bases that can form a strand of DNA. The bases can be divided into two groups; the pyrimidines and the purines. The pyrimidines are six-membered rings and the purines are six-membered rings joined to a five-membered ring. Adenine and guanine are purines, and the pyrimidines are cytosine and thymine. The structures of the four nitrogenous bases are shown in Figure 1.2.

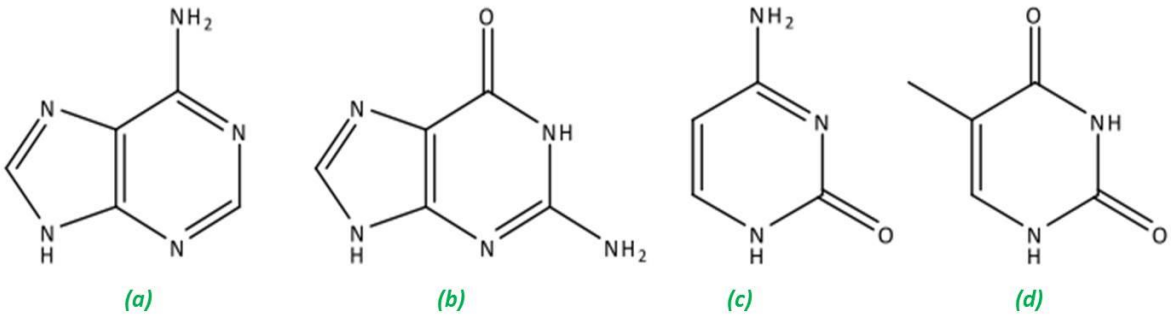

Figure 1.2 The structures of the four nitrogenous bases that form a strand of DNA; (a) adenine, (b) guanine, (c) thymine and (d) cytosine.

In a strand of DNA, the nitrogenous bases are bound together through phosphodiester linkages formed between the 3' hydroxyl group of one nucleotide and the 5' phosphate group of the adjacent nucleotide.[3, 4] The phosphate group on each nucleotide possesses a

negative charge, resulting in the phosphate backbone of DNA being negatively charged at physiological pH (Figure 1.3).

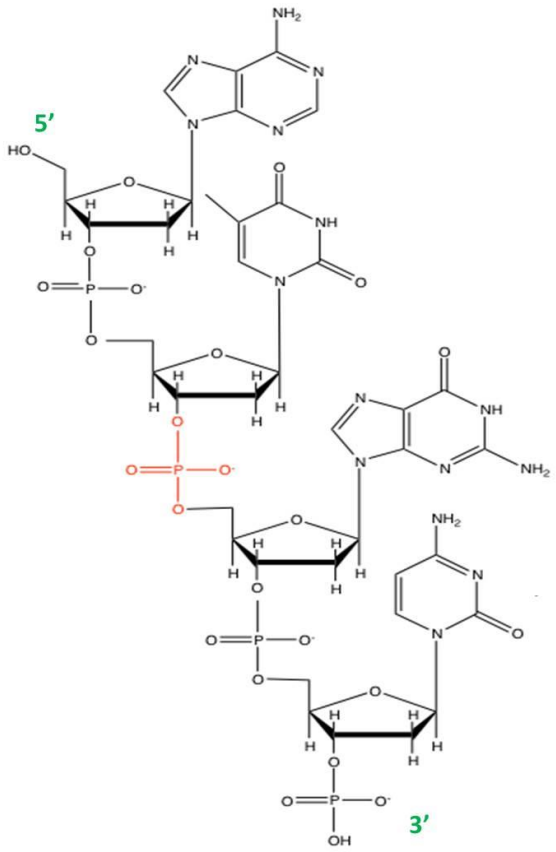

Figure 1.3 Four nucleotide units, each with one of the four nitrogenous bases attached to the deoxyribose sugar, joined together via phosphodiester links (red) between the 3' hydroxyl group of one nucleotide and 5' position of the other.

The order in which the nitrogenous bases appear in a strand of DNA is unique to a particular gene and consequently codes for a specific amino acid sequence, which are the building blocks of proteins.

1.1.2 Secondary Structure

There was a lot of research in the 1930's and 1940's that centred on hereditary characteristics and arising from this there were many proposals on the unit of inheritance.[7] Proteins were originally thought to be the hereditary material, [8] however in 1944 Avery *et al.* proposed that DNA was the fundamental hereditary unit involved in the transformation

of specific strains of bacteria and they concluded that this could also be applied to genes. Consequently, their theory was widely accepted in the scientific community.[6]

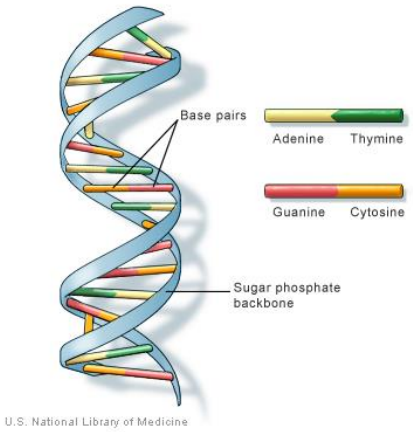

Figure 1.4 A schematic of the structure of the double helix, showing the base pairs formed between the purines and pyrimidines, and the sugar phosphate backbone.[9]

The structure of DNA, however, was not confirmed until 1953 when Watson and Crick first proposed the DNA double helix.[3] This publication came shortly after Pauling suggested that the structure of DNA consisted of three intertwining strands,[10] which was later shown to be incorrect. Watson and Crick discussed the stereochemical issues associated with Pauling's proposed structure and suggested a possible alternative. They suggested a double helical structure that coiled around a central axis with the sugar-phosphate backbone facing outwards and the nitrogenous bases facing inwards (Figure 1.4). The structure was confirmed by X-ray diffraction studies performed by Rosalind Franklin[11, 12] and data interpretation by Maurice Wilkins.[13, 14] Further discussions by Watson and Crick revealed the features of the double helix in more detail and suggested a possible mechanism for replication.[4] The double helix was found to be held together through hydrogen bonds between the nitrogenous bases in the two nucleotide chains. Due to steric considerations derived from X-ray diffraction studies, one of the bases must be a purine and the other a pyrimidine. Specifically, adenine binds to thymine and guanine binds to cytosine (Figure 1.5). The proposed double helix structure was in good agreement with previous work performed by Chargaff *et al.* in 1952 that reported that, in all samples of DNA analysed, the ratios of adenine to thymine and guanine to cytosine were close to unity.[15]

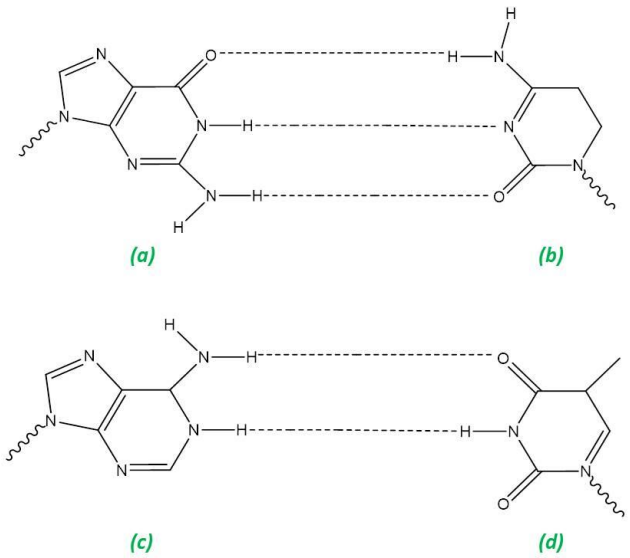

Figure 1.5 Base pairing between (a) guanine and (b) cytosine and between (c) adenine and (d) thymine. The dashed lines represent the hydrogen bonds formed between the bases.

As a result of the specific base pairing elucidated by Watson and Crick, if the sequence of bases on one DNA strand are known, then the sequence of bases on the complementary sequence can be predicted.

1.1.3 The Role of DNA in Molecular Biology

The method of DNA replication proposed by Watson and Crick was experimentally tested in 1958 by Meselson and Stahl who concluded that DNA replication occurred in a semiconservative manner.[16] Each DNA strand in the double helix is referred to as parent molecules since, during replication, each strand acts as a template that will determine the sequence of nucleotides joined together by the sugar phosphate backbone in the new complementary strand. After each replication cycle, two new daughter molecules are produced consisting of one strand from the parent molecule and one newly synthesised strand.

Following the outcomes of the DNA replication studies, Francis Crick proposed the "Central Dogma" of Molecular Biology in 1970.[17] Crick discussed the relationship between DNA, RNA

and proteins, concluding that genetic information comes from DNA and is transferred to RNA and then to proteins. The exact sequence of events is extremely important when genetic information is transferred from DNA resulting in protein synthesis. This is because proteins are synthesised in the cell cytoplasm, however DNA is contained in the nucleus of eukaryotic cells. For genetic information from the DNA to initiate protein synthesis, DNA must first be transcribed into messenger RNA (mRNA), in a process similar to DNA replication. The genetic information is then transferred to the cell cytoplasm by the mRNA, where it is then translated into a sequence of amino acids by the base pairing of mRNA to transfer RNA (tRNA). A schematic of this process is shown in Figure 1.6. The sequence of the amino acids dictates the protein structure and ultimately its functionality.[18]

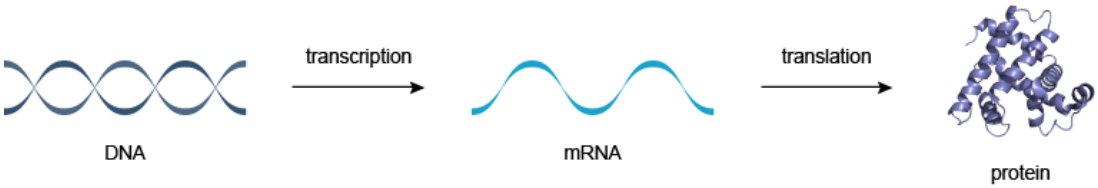

Figure 1.6 A schematic representation of the "Central Dogma" of Molecular Biology showing the movement of genetic information from DNA to RNA to protein.[19]

1.1.4 Alternative DNA Structures

DNA can exist in well-known primary and secondary structures; however there are alternative DNA structures. These include guanine rich DNA sequences known as G-quadruplexes. Interestingly, G-quadruplexes were discovered before the double helix,[20] however it was not until 1962 that the structure was deduced by means of X-ray diffraction studies.[21] The structure was found to consist of four guanine bases forming the core, known as a G-tetrad (Figure 1.7).

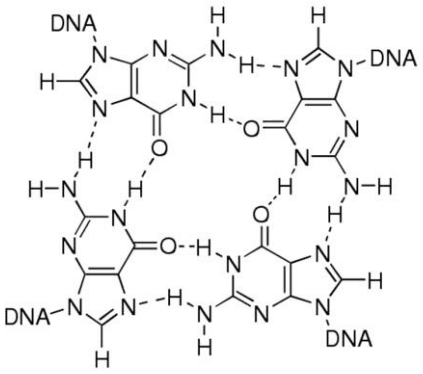

Figure 1.7 The structure of a G-tetrad.[22]

The guanines are held together in a square planar formation by Hoogsteen hydrogen bonding[23] due to the presence of π-π stacking interactions between the G-tetrads sitting on top of each other forming a G-quadruplex structure.[24, 25] The structure of a G-quadruplex is dependent upon the DNA sequence and orientation of the guanine bases. One, two or four separate DNA strands can form the G-quadruplex resulting in unimolecular, bimolecular or tetramolecular structures, respectively (Figure 1.8).[26] The orientation of the G-quadruplex can be further subdivided into parallel (strands proceed in the same 5' to 3' direction) or antiparallel configurations (strands proceed in opposite directions). The stabilisation of G-quadruplexes can occur through the presence of monovalent cations such as Na^+ or K^+,[24, 27] or by small organic molecules such as quinolones[28] or the natural product telomestatin.[29]

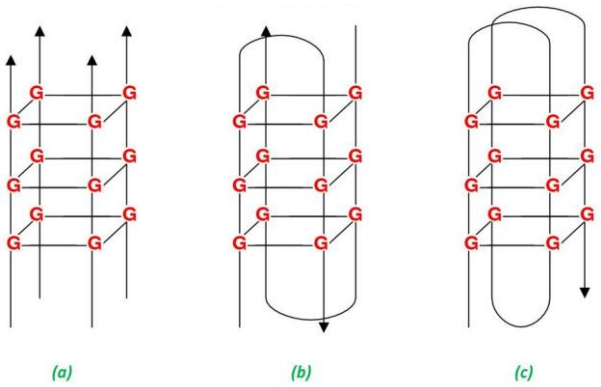

Figure 1.8 Three structural forms of G-quadruplexes. (a) A tetramolecular G-quadruplex consisting of four parallel DNA strands, (b) a bimolecular G-quadruplex where two guanine rich DNA sequences dimerise and (c) a unimolecular G-quadruplex with an antiparallel orientation.[22]

G-quadruplexes can be found in human telomeric DNA and promoter genes.[30-33] Telomeres are nucleoprotein complexes that contain repetitive guanine rich DNA sequences and their main function is to protect the ends of eukaryotic chromosomes from cell degradation and ultimately cell death as they prevent the chromosomes shortening in length during replication. The enzyme telomerase maintains telomere length, however is notably absent in somatic cells. Telomere length is maintained in ~85% of cancers due to telomerase activity; however G-quadruplexes have the ability to inhibit the activity of telomerase by transforming the single stranded DNA into a quadruplex structure. This promotes cell degradation, which is highly advantageous in cancer therapeutics,[29, 34] and this will be discussed further in chapter 3.

1.2 DNA Detection using Fluorescence Spectroscopy

In recent years fluorescence spectroscopy has been the predominant method used for the detection of DNA. This has resulted in the development of synthetic sequences of DNA that possess fluorescent modifications. In particular, research has focussed on the development of assays for the detection of DNA that combine methods of target amplification and fluorescently labelled oligonucleotides.

1.2.1 Introduction to Fluorescence

Fluorescence has been extensively used for DNA detection since changes in the physical properties of DNA when it undergoes a biological event, such as hybridisation or digestion, are difficult to measure and characterise directly. Fluorescent probes are widely used to aid in the analysis of physical changes in the structure of DNA. Fluorescence is defined as the emission of light from a substance that arises from a change in the electronic state of a molecule (Figure 1.9).

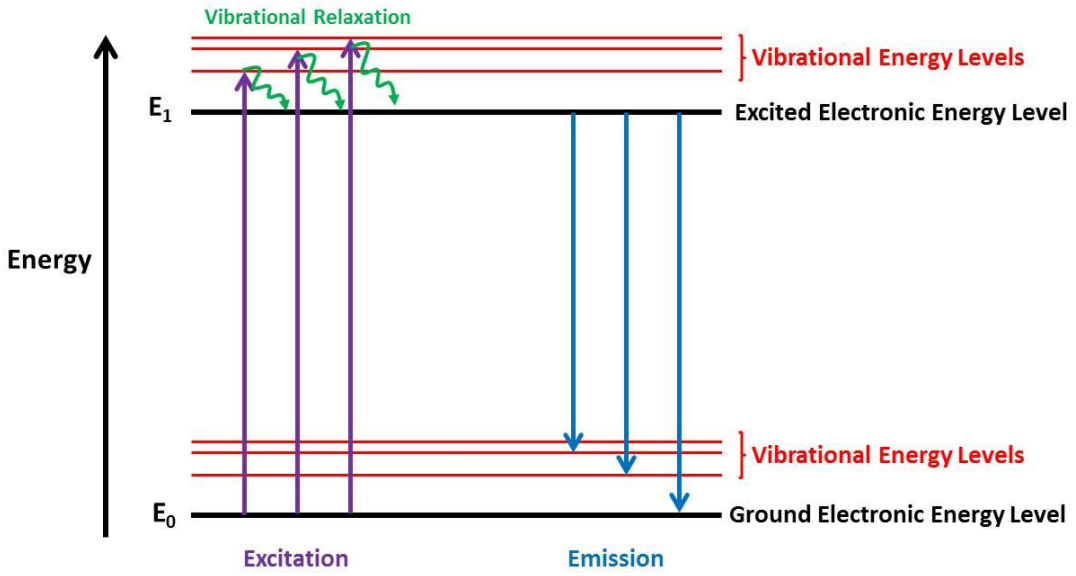

Figure 1.9 A Jablonski diagram showing the process of excitation and emission.

When a species absorbs a photon it is promoted from the ground electronic state (E_0) to a higher vibrational state within the excited electronic energy level (E_1). Vibrational relaxation then occurs, where the excited species relaxes from a higher vibrational energy level to the ground vibrational state of the excited electronic energy level. Relaxation to the ground electronic state then takes place accompanied by the emission of a photon, and this is known as *fluorescence*.

Generally, fluorescence intensity is directly proportional to the concentration of fluorophore present; therefore, the emission spectrum can be used for quantitative analysis as long as the emission wavelength of the molecule under analysis is known. However, there are problems associated with the application of fluorescence as a method of detection. The emission spectrum produced is not specific to the molecule under analysis and therefore no structural information can be deduced from the spectrum. Furthermore, the broad emission peaks observed makes analysis of multiple fluorescent species within the same sample difficult due to a large amount of spectral overlap. Despite these associated problems, fluorescence spectroscopy is extremely sensitive and has proven to be extremely useful for the detection of DNA. Fluorescent labels can be chemically attached or

intercalated into a DNA sequence allowing for detection of a specific target sequence.[35] A common method of DNA detection involving fluorescence is the process called FRET.

1.2.2 Förster Resonance Energy Transfer

Förster resonance energy transfer (FRET) is a chemical phenomenon that involves two molecules.[36] The excitation energy is transferred from a donor fluorophore to an acceptor, which can be either another fluorophore or quencher molecule, via dipole-dipole interactions; however there is no emission of a photon at this point, the fluorescence of the donor molecule is quenched and the acceptor molecule becomes excited followed the emission of light at the wavelength of the acceptor molecule (fluorophore) or the energy is dissipated as heat (quencher) (Figure 1.10). FRET was first discovered by Theodor Förster in 1948.[37]

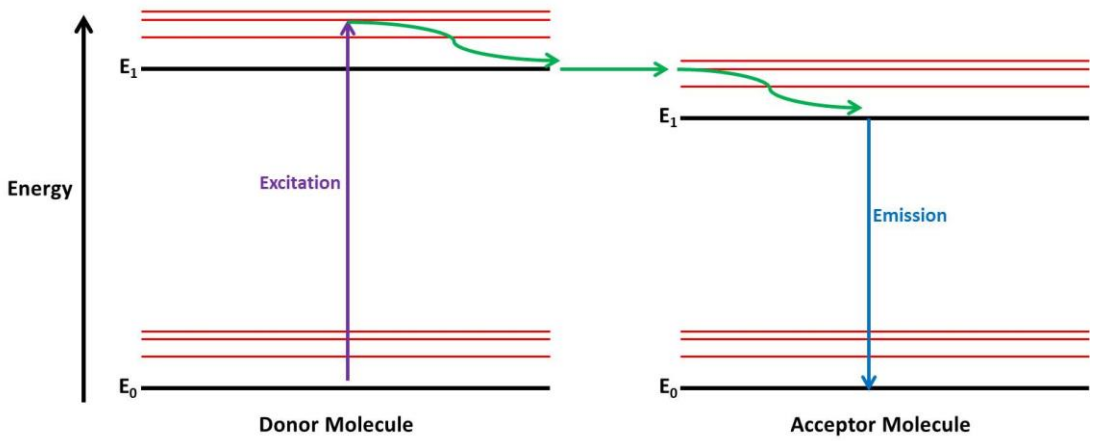

Figure 1.10 A Jablonski diagram showing the process of FRET.

FRET is a non-radiative process where energy is transferred between a donor and acceptor pair of fluorophores. There are two requirements that need to be met when using FRET, firstly the emission spectrum of the donor fluorophore must overlap with the absorption spectrum of the acceptor fluorophore and the distance between the two molecules must be within 1-10 nm.[36]

If a probe sequence of DNA and a target sequence are labelled with a donor and acceptor molecule respectively, the fluorescence of the acceptor molecule can be readily measured if they are within 1-10 nm of each other, for example when the two sequences are hybridised. When they are outwith the required FRET distance, i.e. unhybridised, the acceptor molecule will not be excited and will therefore no longer emit fluorescence. Another possible FRET pair can involve a fluorophore and a quencher molecule, where the quencher accepts the energy from the donor fluorophore molecule but dissipates it as heat rather than light. Therefore, when the FRET pair is within 1-10 nm no fluorescence will be detected; it is only when outwith this distance that fluorescence can be detected. For example, Kawamura *et al.* applied FRET to the detection of telomeric tandem repeat DNA and telomerase activity by using a fluorescein (FAM) labelled probe and the intercalator ethidium bromide.[38] When telomeric DNA was present, it hybridised to the complementary FAM labelled probe producing duplex DNA. Ethidium bromide was then added, which intercalated between the base pairs of the duplex. This resulted in the fluorescence emitted from FAM being quenched by the ethidium bromide. Therefore, when no fluorescence was observed it could be concluded that telomeric DNA was present using the FRET pairing between FAM and ethidium bromide. The amount of quenching was proportional to the concentration of telomeric DNA, as the amount of DNA increased, the level of intercalated ethidium bromide also increased, which resulted in a decrease in fluorescence; therefore the assay developed was quantitative.[38] Based on the theory of FRET and its applicability in DNA detection specific DNA detection strategies have been developed, in particular molecular beacon probes.

1.2.3 Molecular Beacons

The FRET concept was not used for DNA detection until 1996 when Tyagi *et al.* published the design of molecular beacons and their applicability in DNA detection.[39] The concept of molecular beacons is shown in Figure 1.11.

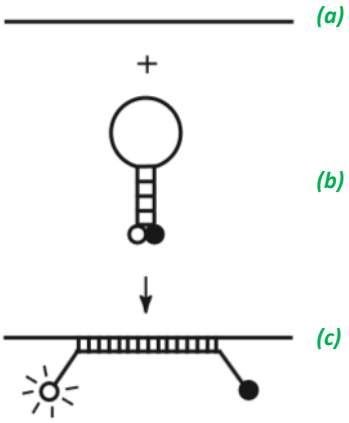

Figure 1.11 The molecular beacon design. When molecular beacons are on their own (b) they are non-fluorescent because the fluorophore and quencher moieties present on the stem sequences are in close proximity (1–10 nm) resulting in fluorescence quenching, however when the probe sequence in the loop hybridises to a target sequence (a), a new duplex is formed (c), which separates the fluorophore and quencher molecules resulting in fluorescence emission.[39]

Molecular beacons are single stranded DNA sequences that contain a stem and loop component. The loop sequence is complementary to a specific target and the stem component is composed of two self-complementary sequences that are non-complementary to the target sequence. A fluorophore molecule is attached to one end of the stem sequence and a quencher molecule is attached to the other. When the molecular beacon is closed, no fluorescence is observed due to the FRET pair being in close proximity (1-10 nm). However, upon addition of the target sequence, hybridisation with the loop sequence will occur, opening the molecular beacon, as the formation of the duplex is more energetically favourable. The molecular beacon goes through a conformational change resulting in the separation of the fluorophore and quencher molecules giving rise to fluorescence emission.[39] Molecular beacons have been widely used in DNA genotyping assays,[40] however clinical samples contain very low concentrations of target DNA, therefore DNA amplification is essential to facilitate fluorescence detection. This is achieved by carrying out the polymerase chain reaction (PCR) prior to the addition of molecular beacons to ensure that there is a sufficient quantity of DNA present to allow for fluorescence detection.

1.2.4 The Polymerase Chain Reaction

Kary Mullis won the Nobel Prize in Chemistry in 1993 for the development of a method of DNA amplification known at the Polymerase Chain Reaction (PCR).[41] The method involves small amounts of DNA being amplified by approximately 2^n, where n is the number of amplification cycles in the reaction.[42, 43] PCR has now been applied to a multitude of applications for example in the fields of forensic science, genetics and molecular diagnostics where small quantities of DNA are required to be amplified prior to analysis.[44] As well as the desired sequence of DNA that is to be amplified, several other components are required to perform PCR: short primer sequences that are complementary to the flanking regions of the target sequence, deoxyribonucleoside triphosphates (dNTPs) and a DNA polymerase, which is an enzyme that can create a new strand of DNA from the dNTPs. The steps required in PCR are shown in Figure 1.12.

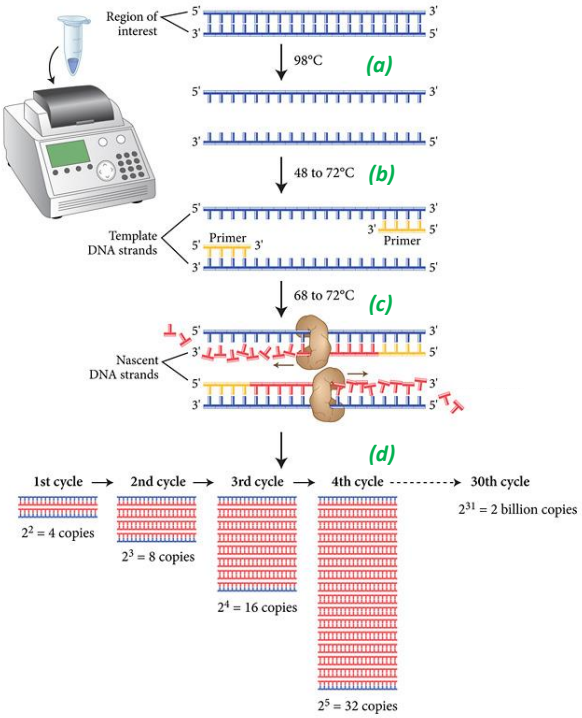

Figure 1.12 The mechanism of the Polymerase Chain Reaction. The first step (a) is denaturation where the temperature is increased to separate the two DNA strands. The second step (b) is the annealing stage where the temperature is lowered to allow the primers to hybridise to the complementary DNA template. Polymerase is then added for primer extension to occur (c) resulting in two new DNA strands. Finally, the process is repeated (d) for a number of cycles and the region of interest is amplified exponentially.[45]

A typical PCR cycle consists of three steps. The reaction starts with a strand separation (denaturation) step where the solution is heated to 95 °C for a short period of time. The reaction is then cooled to 50-65 °C so that the primers can anneal to the separated DNA strands in the flanking areas of the target region. The next step is the extension of the primer sequences using the dNTPs and DNA polymerase, synthesising a new DNA strand in the 3' to 5' direction. Originally *E. coli* DNA polymerase was used; however it could not function at high temperatures so after the denaturation step more enzyme would need to be added.[42] Therefore, the DNA polymerase most commonly used is *Thermus aquaticus* (*Taq)*, which is thermostable at high temperatures, simplifying the method and allowing for automation.[43, 46] The PCR cycle is repeated a number of times resulting in an exponential increase in the amount of amplified target DNA. PCR has been used to successfully detect various disease targets in diagnostic applications, for example the detection of cystic fibrosis amplicons,[47] the human herpes virus 6 (HHV-6)[48] and single nucleotide polymorphisms.[49]

1.2.5 Quantitative PCR

Further developments in PCR led to the process known as *Quantitative* or *Real-Time PCR* (qPCR or RT-PCR), which was designed to amplify and quantify target DNA simultaneously in a closed tube format and would not require any post-PCR quantification methods.[47, 50] Examples of post-PCR quantification involved gel electrophoresis using either agarose or polyacrylamide gels stained with ethidium bromide.[51] This method was time consuming and sometimes provided inaccurate results.

Alternative quantification methods were therefore developed using fluorescently labelled DNA that could be measured during the PCR process.[46, 52, 53] These methods exploited the 5' nuclease activity of *Taq* polymerase and utilised DNA probes labelled with fluorophore and quencher molecules. TaqMan probes, as they are commonly known, result in an increase in fluorescence, which corresponds to an increase in the amount of amplified DNA present. TaqMan probes have a 5' fluorescent modification and at the 3' terminus they possess a quencher molecule and are complementary to the target sequence. When the quencher and fluorophore are in close contact, there is little fluorescence observed; however, when

the *Taq* polymerase synthesises the new DNA strand using dNTPs, due to the 5' nuclease activity of the enzyme the TaqMan probe is digested. This results in the fluorophore and quencher molecules no longer being in close proximity to each other, which increases the fluorescent signal observed (Figure 1.13). The fluorescence intensity is proportional to the amount of DNA amplified, allowing for target DNA quantification during PCR.

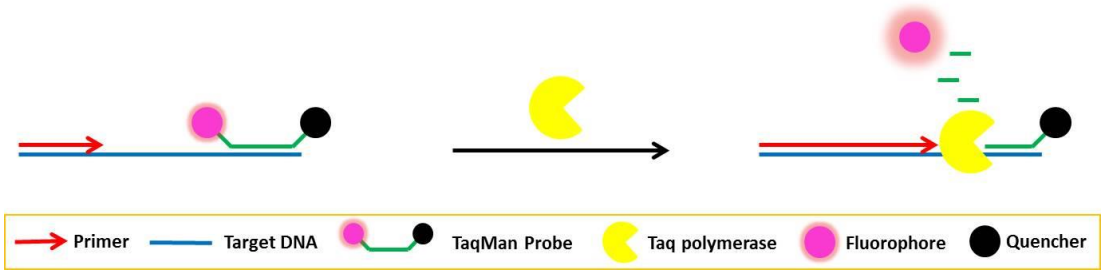

Figure 1.13 A schematic of the TaqMan assay. Taq polymerase digest the TaqMan probes resulting in an increase in fluorescence signal observed when target DNA is present.

TaqMan probes are based on FRET theory, therefore molecular beacon probes could also potentially be used to quantify PCR product. The most common examples of this are known as *Scorpion probes*, which are held in a hairpin configuration with a stem sequence modified with a fluorophore and quencher FRET pair.[49] *Scorpion probes* are attached to the 5' end of the primer used during PCR amplification, with a PCR blocker group (hexaethylene glycol (HEG)) that prohibits the *Taq* polymerase adding dNTPs and the subsequent replication of the *Scorpion probe* sequence (Figure 1.14).[54] The hairpin probe sequence binds to the complementary target sequence as the primer sequence is elongated by the *Taq* polymerase. After amplification the *Scorpion probe* is opened, increasing the distance between the fluorophore and quencher allowing for a fluorescent signal to be observed. Due to the presence of the PCR blocker (HEG), the *Scorpion probe* will not open and the primer will not be elongated if the specific target strand is not present, making this method highly specific.

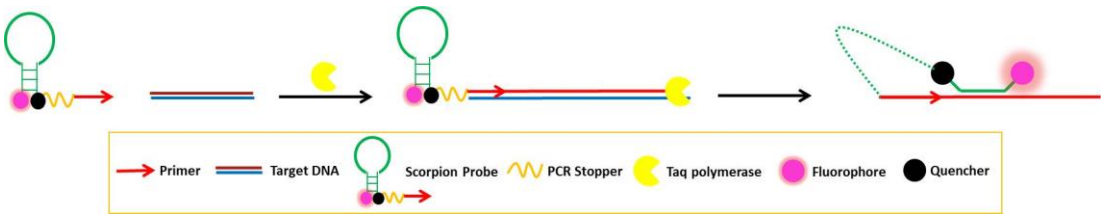

Figure 1.14 Schematic of a *Scorpion probe* assay. Target DNA is detected by selective hybridisation of the unimolecular probe due to the opening of the hairpin configuration resulting in an increase in fluorescence.

Compared to molecular beacons, *Scorpion probes* are considered to be unimolecular, since in a molecular beacon the probe sequence is flanked by two stem sequences. The entire *Scorpion probe* is integrated into the PCR product as it is attached to a primer. As a result of this, hybridisation is faster and more thermodynamically favourable using *Scorpion probes* compared to the beacon configuration.[36]

Fluorescent based methods such as PCR do have disadvantages. For example, PCR is prone to contamination and the non-specific hybridisation of residual DNA, which will make the process more time consuming and decrease the levels of sensitivity and background fluorescent signals from inefficient quenching. With the need for faster and more sensitive methods of detection, research is focussing on the development of novel strategies for disease detection. Major developments have been made in the design of detection assays involving metallic nanoparticles and spectroscopic techniques such as Raman and surface enhanced Raman scattering (SERS).

1.3 Nanoparticles

Nanotechnology is the term used when for technology which uses materials with nanoscale dimensions. The basic concept of nanotechnology was instigated by a lecture delivered by Richard P. Feynman in 1959 with the title “There is plenty of room at the bottom”.[55] He proposed the “bottom up” approach to solving key biological problems on the atomic scale by improving the electron microscope to allow for manipulation of nanoscale materials. Feynman’s proposal is clearly visible through current research in nanotechnology and emerging disciplines such as bionanotechnology.

1.3.1 An Introduction to Nanoparticles

Nanoparticles are defined as particles with one or more dimensions less than 100 nm in size. They can be synthesised from various metals such as gold,[56] silver,[57] copper[58] and platinum.[59] Historically, nanoparticles were used to colour glass and ceramics, the most famous example being the Lycurgus cup, which due to the presence of gold nanoparticles appeared green in reflected light but red in transmitted light.[60] As well as decorative purposes, gold nanoparticles have also been used for medicinal purposes.[56] The first scientific report on the synthesis of gold nanoparticles was by Michael Faraday in 1857.[61] He outlined the formation of colloidal gold from the reduction of aqueous choloroaurate ($AuCl_4^-$). The observation was made that the properties of colloidal solutions differ from the bulk material. It was this discovery that formed the basis of metallic nanoparticle research.

Gold and silver nanoparticles are the most popular form of nanomaterial used for optical applications, with silver nanoparticles being predominantly used in the work discussed in this thesis. Silver nanoparticles are commonly synthesised by the reduction of silver nitrate ($AgNO_3$). The chemical synthesis of silver nanoparticles was first reported by Lee and Meisel in 1982 using citrate to reduce $AgNO_3$.[62] This method is simple to implement and therefore is still widely used today as a method of synthesising silver nanoparticles. A solution of sodium citrate is added to a solution of silver nitrate. The citrate acts as a reducing agent and a stabilising agent for the silver nanoparticles, as it leaves a negative surface layer that repels the nanoparticles from each other making the solution monodispersed.[63] It has been found that citrate is not always the optimal stabilising agent to use depending on the analyte as it can be easily displaced from the nanoparticle surface; therefore, alternative synthesis methods have been developed. Such methods include borohydride reduction of $AgCl_4$,[64] ethelynediaminetetraacetic acid (EDTA) reduction of $AgNO_3$[65] and the hydroxylamine reduction of $AgNO_3$.[66]

Nanoparticles are favoured substrates for diagnostic applications due to their unique optical properties and the ability to control their size and shape. The most commonly used

property of metallic nanoparticles is their localised surface plasmons that are affected when the nanoparticles interact with light of a specific wavelength.

1.3.2 Surface Plasmon Resonance (SPR)

When light interacts with nanoparticles, an oscillating cloud of electrons is induced on the surface of the nanoparticle known as the surface plasmon resonance (SPR). The SPR phenomenon is a result of the collective oscillation of conduction band electrons at the nanoparticle surface induced by interaction with the incoming electromagnetic field (Figure 1.15). When the SPR is associated with nanoparticles, such as gold or silver, the plasmon is referred to as the localised surface plasmon resonance (LSPR).

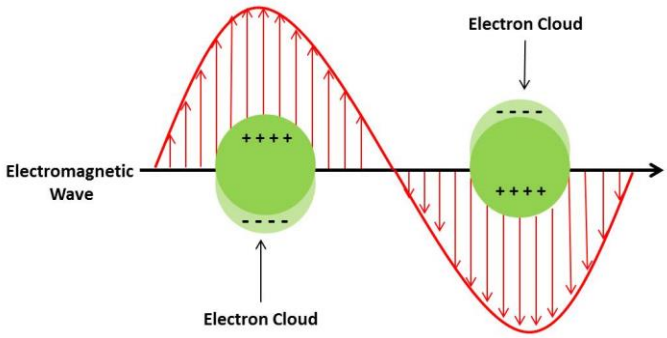

Figure 1.15 A schematic of the surface plasmon resonance induced by an electromagnetic field in a spherical nanoparticle. The interaction with the electromagnetic field causes a net displacement of the negative charge at the positive metal core resulting in a charge difference across the metal sphere.

Gustav Mie first described the SPR phenomenon in 1908, where he applied Maxwell's equation to spherical nanoparticles.[67] He concluded that the plasmon band was due to dipole oscillations of the free electrons in the conduction band occupying the energy states directly above the Fermi energy level.[68] The surface plasmon band for 15 nm gold nanoparticles is 520 nm and for 35 nm silver nanoparticles the surface plasmon band is 400 nm. The surface plasmon band will shift depending on nanoparticle size, shape, the inter-particle distance and changes in the local environment for example the refractive index or the surrounding medium.[69]

The most useful feature of metallic nanoparticles that makes them ideal for bio-sensing applications is the distance dependant nature of the surface plasmon band. When two or more nanoparticles are in close proximity, coupling of the surface plasmons occur, resulting in a red shift of the nanoparticle extinction to longer wavelengths.[70] The red shift is dependent upon the inter-particle distance; the shorter the distance, the larger the red shift.[71] Surface plasmon coupling can also be monitored through a colour change, for example gold nanoparticles change from red to purple when the inter-particle distance decreases.

1.3.3 Nanoparticles used for DNA Detection

Nanoparticles are now widely used in diagnostics, for example in the detection of target DNA. DNA hybridisation is a strong biorecognition event and combining this with metallic nanoparticles has led to the development of successful colorimetric methods of detection. In 1996, two groups, Mirkin *et al.* and Alivisatos *et al.*, both simultaneously reported methods,[72, 73] which instigated a significant amount of research into the conjugation of biomolecules to nanoparticles.[74, 75]

Alivisatos *et al.* developed a method of arranging nanocrystals by exploiting specific DNA hybridisation events.[76] Single stranded DNA sequences were conjugated to individual nanoparticles and upon hybridisation dimers and trimers were created. The method was then further developed using both gold and silver nanoparticles to create a molecular ruler capable of measuring the distance between two nanoparticles. At the same time, Mirkin *et al.* proposed their method for nanoparticle assembly using two different thiolated DNA sequences conjugated to two different batches of 13 nm gold nanoparticles.[72] The two different sequences attached to the nanoparticles were complementary to a region of the same target sequence, therefore upon hybridisation the nanoparticles self assemble into aggregates, reducing their inter-particle distance and causing changes in their surface plasmon resonance, which can be monitored by extinction spectroscopy.

Mirkin and co-workers have developed numerous assays using gold nanoparticles for DNA detection (Figure 1.16).[77-79] His group developed a method for the detection of single base pair mismatches by monitoring the change in melting temperatures of the hybridisation mixtures and then using the "Northwestern Blot" method to visually detect the target DNA with femtomolar detection limits.[80, 81] Additionally, DNA-nanoparticle conjugates in a scannometric DNA array platform were used to detect target DNA in a method which rivals the sensitivity of PCR.[82, 83] More recently, Mirkin *et al.* have reported the design of spherical nucleic acids (SNAs),[75] which are DNA-nanoparticle conjugates that have been widely used in molecular diagnostics, for example they have been used for the detection of mRNA in living cells.[84]

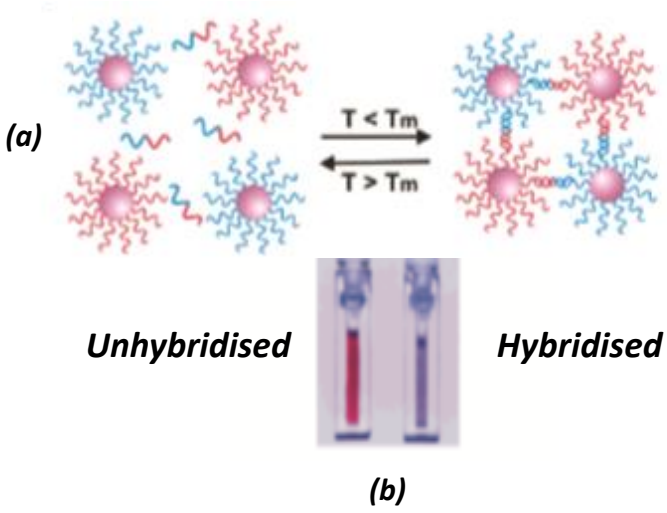

Figure 1.16 (a) A schematic representation of nanoparticle aggregation caused by DNA hybridisation. (b) Aggregation can also be monitored by the change in colour of the gold nanoparticles (red to purple).[77]

Silver nanoparticles, compared to their gold counterparts, are not as widely used in diagnostic research as their synthesis is harder to control. Nevertheless, oligonucleotide-silver nanoparticles (OSN) conjugates have been used; the first report of their use was by Thompson *et al.* in 2008.[85, 86] Similar to the nanoparticle conjugates designed by Mirkin *et al.*,[72] single base pair mismatches were successfully detected using the melting profiles of the DNA sequences. OSN conjugates have not been widely used in diagnostic assays; however; silver nanoparticles possess a high molar extinction coefficient that would increase sensitivity levels when using extinction spectroscopy (Figure 1.17). Also, due to

their optical brightness, silver nanoparticles, and in particular OSN conjugates, can be successfully used in assays involving surface enhanced resonance Raman scattering.[87]

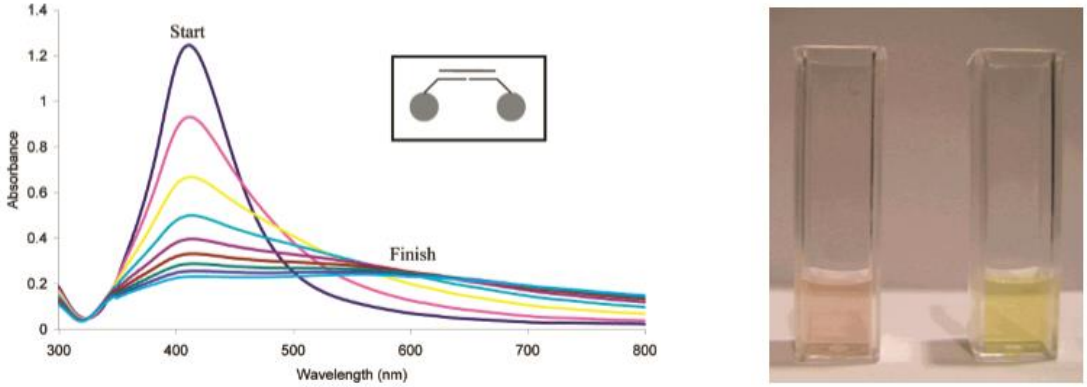

(a) *(b)*

Figure 1.17 (a) Extinction spectra of OSN conjugates in the present of complementary target sequence recorded over a period of time. There is a shift in the surface plasmon band and a change in absorbance due to the aggregation of the silver nanoparticles. (b) Image of the OSN conjugates in the presence of complementary target (left) and non-complementary target (right). With silver nanoparticles, the colour change from yellow to pink indicates nanoparticle aggregation.[85]

1.4 Surface Enhanced Resonance Raman Scattering

Fluorescence based methods such as quantitative PCR are currently the most widely used detection methods in molecular diagnostics.[88] This is due to the ability to fluorescently label DNA, for example, during PCR, fluorescent dye labelled primers are used to monitor DNA amplification, and the wide range of fluorescent labels available for DNA labelling allows for the detection of multiple analytes. However, there are major disadvantages in using fluorescence for the detection of multiple fluorescently labelled analytes such as the broad, overlapping emission spectra that are produced, combined with the possibility of photo-bleaching of the fluorescent dyes and the need for multiple excitation wavelengths. This has led to the investigation into alternative methods for multiplexed analysis and a technique that has proven to be a promising alternative is surface enhanced resonance Raman scattering (SERRS).[89]

1.4.1 Raman Scattering

When a photon of light interacts with a molecule, the photon can either be absorbed, scattered, or it can pass through the molecule with no interaction. Initial studies on the scattering of light involved elastic scattering, where the scattered photons have the same energy as the incident light, in a process known as Rayleigh scattering.[90] The theory of inelastic scattering was first postulated by Smekal in 1923 and was experimentally confirmed in 1928 by Krishnan and Raman.[91, 92] The experiment involved focussing sunlight onto a sample and collecting the scattered light using a second lens. Through the use of optical filters, it was shown that the scattered radiation was different in frequency to the incident light.

When light interacts with a molecule, polarisation of the electron cloud occurs that results in a short lived excited virtual state. Rayleigh scattering involves the distortion of the electron cloud with the nucleus remaining unaffected resulting in small changes in the frequency. The light is therefore scattered at the same frequency as the incident light. Raman scattering involves nuclear motion, a result of the transfer of energy from the incident photon to the molecule (Stokes scattering) or the transfer of energy from the molecule to the scattered photon (anti-Stokes scattering), the processes are shown in the form of a Jablonski diagram in Figure 1.18.[93]

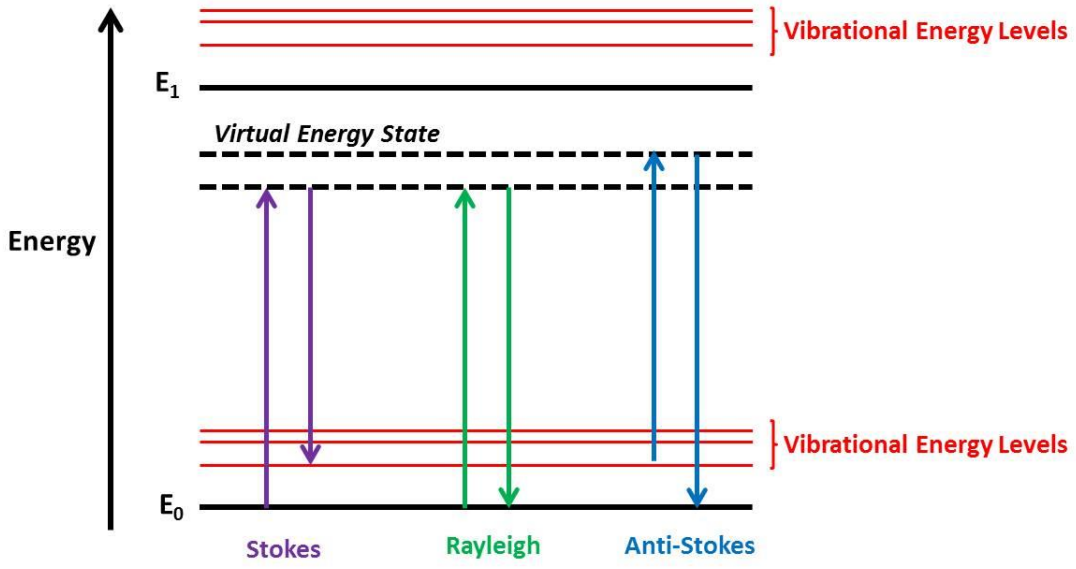

Figure 1.18 A Jablonski diagram illustrating the processes of Rayleigh and Raman scattering.

Stokes scattering occurs when the photons are scattered with less energy than the incident photons, as the molecules are promoted to an excited vibrational state that is higher in energy than the original ground state. At higher temperatures, some molecules will be present in the excited vibrational state and when these molecules lose energy to the scattered photons and return to the ground state, anti-Stokes scattering occurs. At room temperature, the majority of molecules will be present in the ground vibrational state, therefore the intensity of Stokes scattering is likely to be greater than that of anti-Stokes scattering.[93] The population of the energy levels and the ratio of intensities of Stokes and anti-Stokes scattering can be predicted using the Boltzmann equation (Equation 1.1) where N_n is the number of molecules in the excited vibrational energy level, N_m is the number of molecules in the ground vibrational energy level, g is the degeneracy of the energy levels, E_n-E_m is the difference in energy between the vibrational energy levels E_n and E_m, k is the Boltzmann constant (1.3807 x 10^{-23} JK^{-1}) and T is the temperature (K).

$$\frac{N_n}{N_m} = \frac{g_n}{g_m} \exp\left[\frac{-(E_n - E_m)}{kT}\right]$$

Equation 1.1 Boltzmann Equation

The shift in energy between the exciting laser beam and the scattered energy is known as the Raman shift. It corresponds to molecular vibrations, which depends on the number of atoms in the molecule. The frequency of the vibrations is related to the mass of the atoms and bond strength. As a result, Raman spectra provide structural information regarding the molecule under analysis. However, only one in every 10^6-10^8 scattered photons are Raman scattered, meaning that Raman scattering is a relatively weak process.[93] This has led to the development of resonance Raman and surface enhanced Raman scattering as methods of improving the signal obtained from Raman scattering.[93]

1.4.2 Resonance Raman Scattering (RRS)

When using a laser beam with a frequency that is coincident with the frequency of an electronic transition in a molecule, the Raman scattering intensity increases in a process known as resonance Raman scattering (RRS). The signal enhancement from RRS has been reported to be 10^6;[94] however it is typically in the region of 10^3-10^4.[93] The main difference between Raman scattering and RRS is that when using RRS the absorption of a photon results in the excitation of a molecule to an excited state within the first excited electronic state, whereas in Raman scattering the excited molecule reaches a virtual energy state (Figure 1.19). As a result, when RRS is used, more intense spectra are observed as vibrations associated with electronic transitions in a molecule are greatly enhanced, allowing this technique to be used in the identification of molecules in complex biological samples. RRS does have disadvantages, primarily competing fluorescence processes that can result in a high, unwanted fluorescence background.[93]

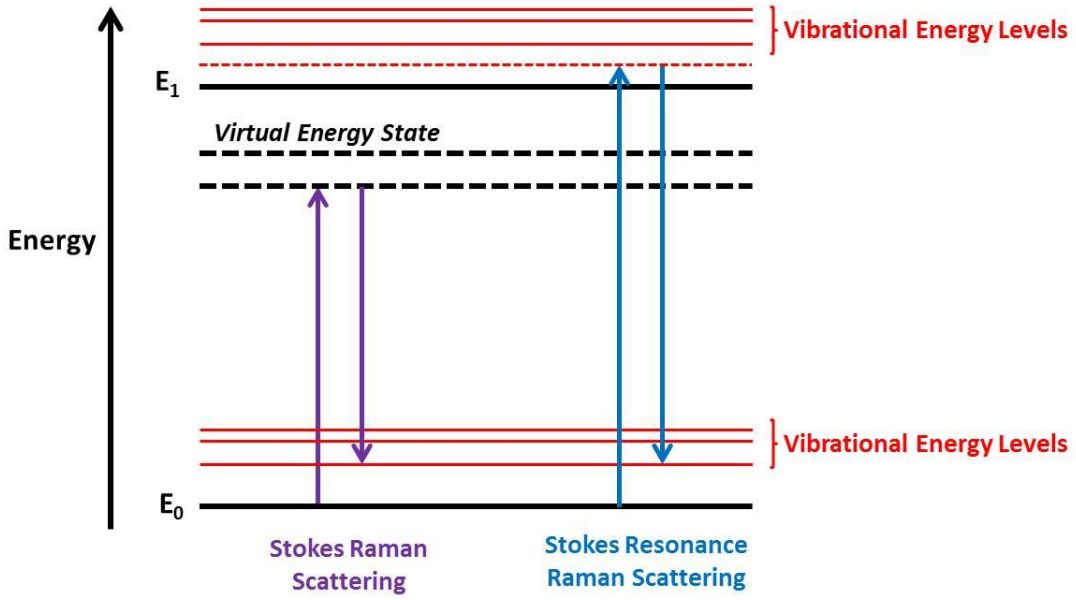

Figure 1.19 A Jablonski diagram illustrating the processes of Raman and resonance Raman scattering.

1.4.3 Surface Enhanced Raman Scattering (SERS)

To overcome the limitations of RRS, surface enhanced Raman scattering (SERS) can be used. SERS was first observed by Fleischman *et al.* in 1974 when they observed an intense Raman signal from pyridine on a roughened silver electrode.[95] The signal was enhanced compared

to that observed when using a smooth silver electrode. The enhancement was initially considered to be a result of the increase in surface area meaning that more pyridine could be adsorbed onto the surface. This was soon disputed by Jeanmarie and Van Duyne and by Albrecht and Creighton.[96, 97] They both concluded that the enhancement observed was not only the result of an increase in surface area. Jeanmarie and Van Duyne proposed that the enhancement was an electromagnetic effect,[96] whereas Albrecht and Creighton suggested that the enhancement was due to a charge transfer effect.[97]

The general opinion is that SERS is a combination of both the electromagnetic effect and the charge transfer effect. The electromagnetic effect is deemed to be the dominant process, which describes the interaction between the surface plasmon and the analyte. When the incident light interacts with the nanoparticle surface it causes the localised surface plasmon to oscillate, which will increase the local field that is experiences by the analyte adsorbed onto the surface causing greater polarisation around the molecule.[98, 99] When the plasmon frequency is in resonance with the laser excitation radiation and the plasmon oscillates perpendicular to the surface, greater enhancement is observed. The plasmon on an individual particle is only in resonance over a small range of wavelengths, so in regions where individual particles or clusters of particles are touching, the electrons can couple with adjacent particles which will result in a resonance being possible over a larger range of wavelengths. These regions are known as “hot spots” and allow the formation of greater electromagnetic fields between the nanoparticles, which will increase signal enhancement.[98] The charge transfer effect is believed to be a smaller contribution to the enhancement factor. It is a result of the formation of a bond between the analyte and the surface. The attachment induces a charge transfer creating a new state that is in resonance with the laser excitation wavelength. The polarisability of the molecule is increased and subsequently increases the scattering effect.[93, 100]

Various metals can be used as the substrate for SERS, such as silver, gold, copper and aluminium. The most common forms are electrodes, thin films and colloidal suspensions of metallic nanoparticles.[101] Silver and gold are the most commonly used for Raman scattering as their surface plasmons have a resonance frequency in the visible region.[93] The greatest

signal enhancement is observed when using silver, due to the greater polarisability of silver giving rise to large surface plasmons.[102]

1.4.4 Surface Enhanced Resonance Raman Scattering (SERRS)

Surface enhanced resonance Raman scattering (SERRS) is a combination of RRS and SERS, which incorporates both surface enhancement and chromophores that are in resonance with the laser excitation to produce enhancements of up to 10^{14}.[93] The first report of SERRS was by Stacy and Van Duyne in 1983.[103] SERRS involves the adsorption of a chromophore onto a roughened metal surface and the laser excitation frequency chosen is close to the absorption maximum of the chromophore. As a result, only vibrations associated to the chromophore are enhanced, allowing for an increase in sensitivity and selectivity.[104]

SERRS overcomes the limitations associated with Raman scattering, as it offers improved sensitivity meaning the laser power can be decreased and will reduce the possibility of sample degradation. Any fluorescence emission will be quenched by the metal surface, meaning Raman peaks will dominate and reduce the fluorescence background in the Raman spectra.[93] Also, the increase in the availability of dye labels that possess different resonant frequencies allows for the detection of multiple analytes by choosing dyes that are in resonance with the available laser excitation wavelength. It is these multiplexing capabilities and increased sensitivity that make SERRS a rival detection method compared to current fluorescence-based methods.[93, 105, 106]

1.4.5 SE(R)RS Detection of DNA

SE(R)RS offers many advantages as a detection method, mainly due to the multiplexing capabilities and the detection of low quantities of DNA.[105] As a result, intensive research has been carried out on the development of SERS-based methods for the qualitative and quantitative detection of DNA.

1.4.5.1 Label Free DNA Detection

SERS has proved to be a highly sensitive method for DNA detection, particularly in the area of label free detection. The four nucleobases give rise to unique SERS spectra due to their differing structures.[107-109] Papadopoulou *et al.* were able to detect single base mismatches with an oligonucleotide sequence using SERS. The oligonucleotides were adsorbed non-specifically onto the nanoparticle surface, the sequences was allowed to adopt a flat conformation onto the surface, which insured that all the bases interacted with the surface resulting in readily observed Raman signals. The single base mismatches were then identified by subtracting the spectra of the target sequence from the mutated sequence.[110] However, analysis of the results using the above approach can be time consuming; therefore detection assays have been developed that exploit specific hybridisation events and changes in the orientation of the structure with respect to the nanoparticle surface.[111] Thiolated poly-adenine DNA sequences were conjugated to gold nanoparticles and signal enhancement of the adenine was observed depending on DNA orientation. When the sequences lie perpendicular to the nanoparticle surface, greater intensity of the adenine peak was observed compared to the DNA lying flat on the surface (Figure 1.20).[111]

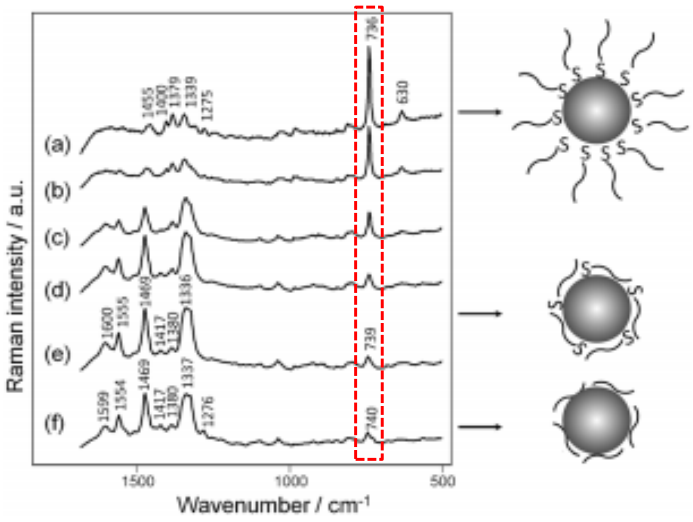

Figure 1.20 The SERS spectra observed with thiolated poly A sequences (a) to (e) with decreasing concentrations. The spectrum shown in (f) is that of unthiolated DNA. Also, the schematic representations of gold nanoparticles with different DNA orientations. The adenine peak used for analysis is highlighted in red.[111]

A molecular beacon assay was also developed to detect the presence of target DNA using this methodology. A molecular beacon in its closed form was attached to a gold nanoparticle through a thiol linker (Figure 1.21). In its closed form, weak adenine peaks were observed; however in the presence of target DNA the beacon opened allowing the adenine peak to be enhanced.[111]

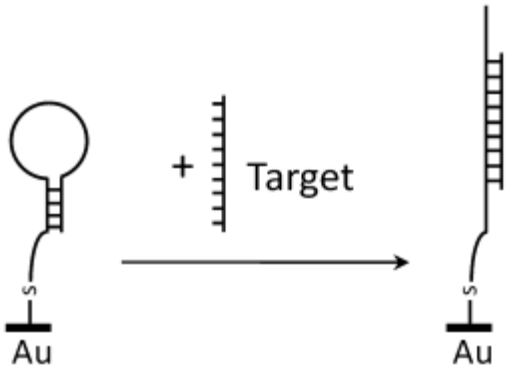

Figure 1.21 A schematic representation of the molecular beacon detection assay. When the target DNA sequences hybridises to the loop sequence of the beacon, a change in conformation occurs resulting in changes in the SERS spectrum.[111]

SERS has proven to be successful for the label free detection of DNA and the four DNA bases, however this does not allow for sequence specific detection as the order of the bases is not obtained, just simply the presence of the bases. To overcome this, dye labelled DNA has been used for the sequence specific detection of target DNA as the spectra generated by the dye is indicative of the presence of a specific target DNA sequence.

1.4.5.2 Fluorescent Dye Labelled DNA Detection

Fluorescent dyes can be covalently attached to DNA sequences and fluorescent labelling of DNA is widely used in fluorescence-based detection methods and has also been used in SERRS.[112] SERRS has been used to detect multiple fluorescent dyes with different absorption maxima and using three different excitation wavelengths, demonstrating that by using the correct choice of fluorescent dye and wavelength, SERRS can be used to quantitatively detect dye labelled DNA.[102] Figure 1.22 illustrates two of the most commonly used fluorescent dye labels; FAM and TAMRA.[113] Both dyes generate unique SERRS spectra

indicative of their structures and have been used throughout this thesis and further discussed in chapters 2, 3 and 4.

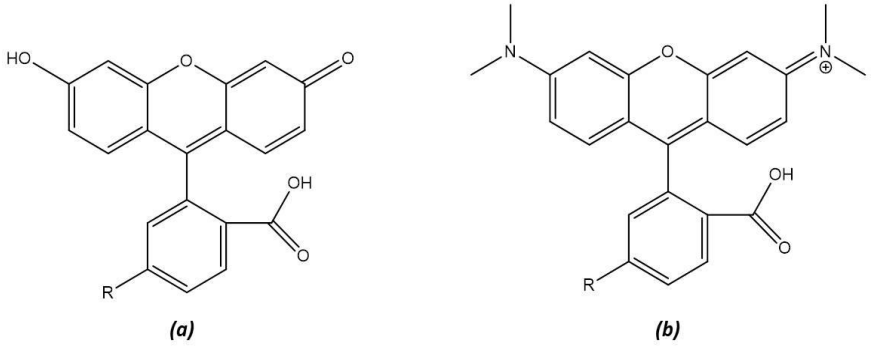

Figure 1.22 The structures of two commonly used dye in fluorescent labelling. (a) FAM (5-(and 6-)-carboxyfluorecein) and (b) TAMRA ((5-(and 6-)-carboxytetramethylrhodamine).

In order to observe the maximum signal intensity using SERRS, the fluorescent dye labelled DNA must either be in close proximity or adsorbed onto the metal surface. Silver nanoparticles possess a citrate layer, which is negatively charged that would repel the negatively charged phosphate backbone of the DNA. Therefore, an aggregating agent is added to facilitate adsorption of the DNA onto the metal surface by reducing the negative charge on the DNA and thereby reducing the level of repulsion. Spermine was found to be the optimal aggregating agent when using SERS for DNA detection.[114] Spermine is a polyamine which acts as a bridge between the two negatively charged species (the silver nanoparticle and the DNA), by interacting with the DNA reducing the negative charge and encouraging the adsorption of the DNA onto the metal surface (Figure 1.23).[105]

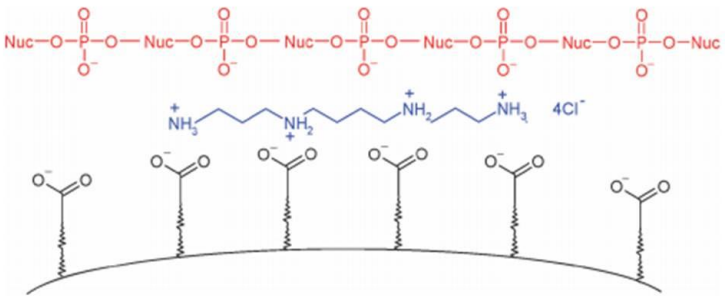

Figure 1.23 A schematic of spermine being used to facilitate the adsorption of DNA onto a nanoparticle surface.[115]

Commercially available dyes like FAM and TAMRA can produce high intensity SERRS signals, however as they are fluorescent dyes, high background signals could also be generated simultaneously with the SERS signals. Metallic nanoparticles are able to reduce the background signals as they can quench the fluorescence emitted from the dyes.[105, 114] However, an alternative approach has been used in DNA labelling involving non-fluorescent dyes in order to eliminate the unwanted fluorescence background.

1.4.5.3 Non-Fluorescent Dye Labelled DNA Detection

SERRS active dyes have been synthesised that produce string SERRS responses with no fluorescent background. These dyes have been designed so that they complex with the nanoparticle surface directly through the formation of bond between the dye and the metal nanoparticle, as opposed to the alternative approach involving electrostatic interactions.[116] The design of these dyes involve benzotriazole moieties that have shown to effectively complex onto silver nanoparticles by displacing the citrate layer and producing a well-defined SERRS spectrum due to the azo group.[106, 117] Benzotriazole forms a stable complex with the nanoparticle surface with fixed orientation that increases the reproducibility of SERRS.[118] Quantitative nanoparticle studies of benzotriazole derivatives have shown that there is concentration dependence in the SERRS intensities observed,[116, 119] however more recently the synthesis of benzotriazole dye has incorporated reactive functional groups to allow the use of SERS to monitor biological reactions.[106, 117, 120] In 2001 Graham *et al.* reported for the first time the use of benzotriazole dyes for the detection of DNA and peptide nucleic acid (PNA).[121] The dye was non-fluorescent and demonstrated the additional labelling chemistry that is possible for SERRS analysis. They noted that further advantages were that due to the strong covalent bonds formed between the metal surface and the benzotriazole dye led to highly reproducible SERS detection.

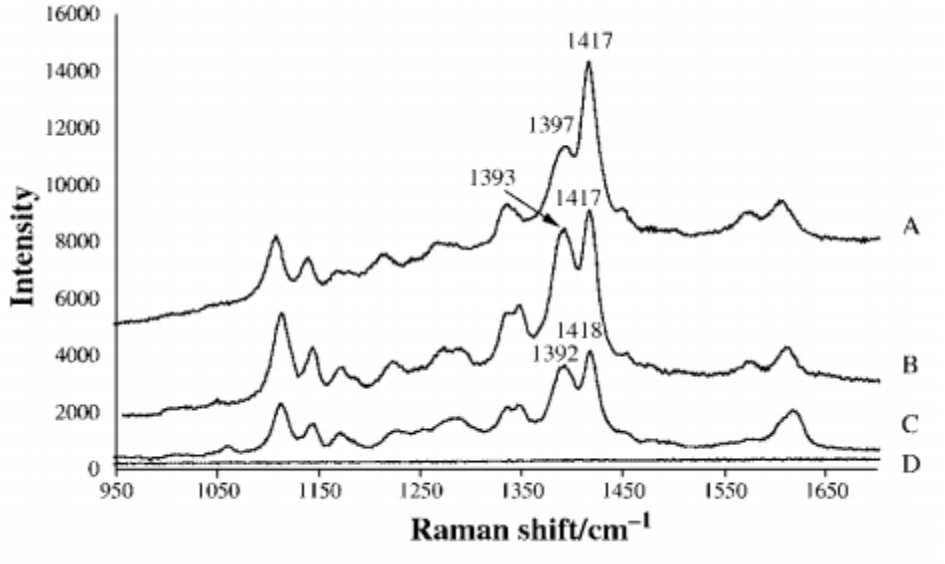

Figure 1.24 The SERS spectra obtained for the free dye (A), dye labelled DNA (B), dye labelled PNA (C) and bare nanoparticles (D). Highlighted peaks at 1393 cm^{-1} and 1417 cm^{-1} are indicative of an azo tautomer.[121]

The use of fluorescent and non-fluorescent dyes attached to DNA sequences can increase the sensitivity of detection of the biomolecules as well as allowing for sequence specific detection. This has led to further studies involving the detection of labelled DNA using SERRS.[122, 102]

1.4.5.4 Quantitative Labelled DNA Detection

Fluorescence emission spectroscopy has been the chosen method of detection for DNA. The method has been proven to produce low limits of detection[123] and furthermore, single molecule detection has been achieved.[124, 125] However, SERRS has now becoming an alternative technique to fluorescence spectroscopy for the detection of DNA. The main advantage that SERRS has is the increased sensitivity in detection by three orders of magnitude[126] and has the potential to detect multiple analytes within the one sample.

The multiplexing capability, i.e. the ability to detect multiple analytes simultaneously, of SERRS is a result of the molecularly specific fingerprint spectra that are obtained. Faulds *et al.* demonstrated the simultaneous detection of five fluorescently labelled DNA

sequences.[105] Five dye labelled DNA sequences were present in the one sample mixture, and by using two different excitation wavelengths all five were quantitatively detected with no need for further chemometric analysis. Two dyes, FAM and R6G were in resonance at 514.5 nm and the other three dyes, BODIPY-TRX, ROX and Cy5.5 were detected using a laser excitation of 633 nm (Figure 1.25). Even though the five fluorescent dyes were in a mixture, there was no decrease in sensitivity compared to when they were analysed individually.

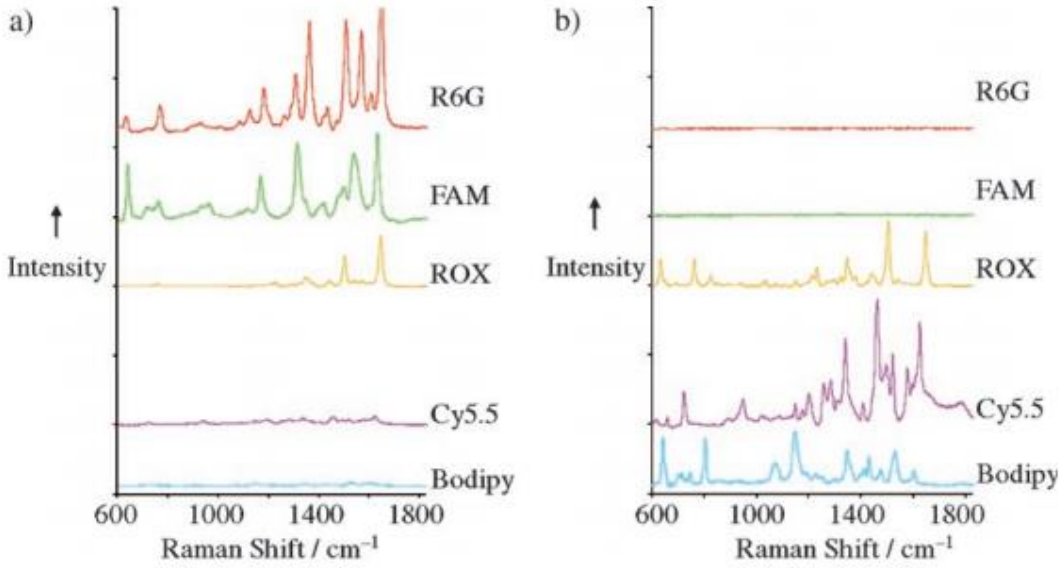

Figure 1.25 The individual SERRS spectra of each dye-labelled oligonucleotide at a) 514.5 nm and b) 632.8 nm.[105]

The multiplex was then further developed for the detection of six dye labelled DNA sequences, however only one excitation wavelength was used combined with multivariate analysis.[113] By using the entire multiplex SERS spectrum and the method of partial least squared analysis involving every combination of the six labelled sequences, each dye labelled sequence was detected and quantified successfully with high levels of sensitivity and selectivity. Based on the advances of SERRS as an analytical technique, Zhong *et al.* used Bayesian methods, on the same data set used by Faulds *et al.*, to detect the specific sequences of disease DNA in multiplex SERRS spectra.[127] The robust method that was developed demonstrated how valuable SERRS has become as an analytical detection method for diagnostic applications.

1.4.5.3 SERS DNA Detection Assays

SERS has been shown to be an appealing alternative to the conventional fluorescence-based methods for the detection of specific DNA sequences. SERS has been applied to the discrimination between base mismatches. The denaturation of double stranded DNA attached to a gold surface was monitored for the detection of wild type, single point mutation (1653C/T) and the triple deletion (Delta F 508) in the CTFR gene, with low limits of detection in the attomolar range.[128] Label free SERS detection of sequence mutations by monitoring the denaturation of DNA was also achieved using the CFTR gene, eliminating the need for labelling DNA sequences prior to analysis.[129] This concept was also applied to the detection of short tandem repeats (STRs) that is required for genetic profiling in forensic applications. SERS, combined with DNA melting, was used to discriminate between different polymorphic repeat sequences of the STR locus D16S539 in PCR products of varying length (121-137 bp).[130] SERS-based DNA detection assays are discussed further in Chapter 2, section 2.1.3.

1.5 Introductory Conclusions

There is a growing need for alternative detection methods that are highly specific and sensitive in molecular diagnostics to enable faster diagnosis and more effective courses of treatment. By using metallic nanoparticles and surface enhanced Raman scattering (SERS), new detection methods have been developed for the simultaneous detection of DNA sequences coding for particular diseases, reducing the time taken for positive diagnosis.

1.6 Project Aims

The overall aim of this research was to develop alternative methods for DNA detection using SERS, to be used in molecular diagnostics. There is a significant need for a fast and reliable detection method for bacterial meningitis due to its rapid onset and high mortality rates. Chapter 2 discusses the development of a SERS-based assay for the detection of three pathogens simultaneously. The presence and the quantity of each pathogen impacts the course of treatment advised for the patient. Using this technique, multiplexed analysis was achieved and it was possible to quantify each pathogen in the multiplex mixture using SERS for the first time. This will prove extremely useful in clinical diagnostics where pathogen quantification is highly desirable.

Recently, there has been an increase in the development of multiplex assays for the simultaneous detection of multiple analytes using fluorescently labelled DNA sequences for SERS detection, however, there are major design considerations needed when employing such assays. When designing SERS multiplex assays, it is essential to determine that all sequences and labels interact with the metal surface and each other in the same way to produce a consistent SERS response. In order to further understand the interactions between fluorescent dyes, DNA and spermine, fluorescence and SERS studies were used to further investigate these interactions. Chapters 3 and 4 discuss the investigative studies performed to gain a better insight into all possible interactions that can occur in a SERS multiplex mixture, allowing for more informed development of multiplex SERS assays.

G-quadruplex DNA has been reported to be an ideal target for cancer therapeutics and therefore detecting the formation of these structures would be extremely useful. Chapter 5 involves the use of SERS to analyse these structures formed after interactions with three specific G-quadruplex stabilising ligands. The aim of this project was to design and develop a method that would readily detect these structures in a selective manner without using any additional labelling agents.

1.7 Introduction References

1. E. S. Lander *et al*, *Nature*, 2001, **409**, 860-921.
2. B. W. S. Robinson, D. J. Erle, D. A. Jones, S. Shapiro, W. J. Metzger, S. M. Albelda, W. C. Parks and A. Boylan, *Thorax*, 2000, **55**, 329-339.
3. J. D. Watson and F. H. C. Crick, *Nature*, 1953, **171**, 737-738.
4. J. D. Watson and F. H. C. Crick, *Nature*, 1953, **171**, 964-967.
5. R. Dahm, *Human Genetics*, 2008, **122**, 565-581.
6. O. T. Avery, C. M. MacLeod and M. McCarty, *Journal of Experimental Medicine*, 1944, **79**, 137-158.
7. M. H. Dawson and R. H. P. Sia, *The Journal of Experimental Medicine*, 1931, **54**, 681-699.
8. R. H. P. Sia and M. H. Dawson, *The Journal of Experimental Medicine*, 1931, **54**, 701-710.
9. Double Helix Structure, http://ghr.nlm.nih.gov/handbook/basics/dna, **2014**.
10. L. Pauling and R. B. Corey, *Proceedings of the National Academy of Sciences of the United States of America*, 1953, **39**, 84-97.
11. R. E. Franklin and R. G. Gosling, *Nature*, 1953, **172**, 156-157.
12. R. E. Franklin and R. G. Gosling, *Nature*, 1953, **171**, 740-741.
13. M. H. F. Wilkins, W. E. Seeds, A. R. Stokes and H. R. Wilson, *Nature*, 1953, **172**, 759-762.
14. M. H. F. Wilkins, A. R. Stokes and H. R. Wilson, *Nature*, 1953, **171**, 738-740.
15. S. Zamenhof, G. Brawerman and E. Chargaff, *Biochimica et Biophysica Acta*, 1952, **9**, 402-405.
16. M. Meselson and F. W. Stahl, *Proceedings of the National Academy of Sciences of the United States of America*, 1958, **44**, 671-682.
17. F. Crick, *Nature*, 1970, **227**, 561-563.
18. Y. Singh, P. Murat and E. Defrancq, *Chemical Society Reviews*, 2010, **39**, 2054-2070.
19. Central Dogma of Molecular Biology, http://www.atdbio.com/content/14/Transcription-Translation-and-Replication#DNA-RNA-and-protein-synthesis, **2014**.
20. I. Bang, *Biochemische Zeitschrift*, 1910, **26**, 293-311.
21. M. Gellert, M. N. Lipsett and D. R. Davies, *Proceedings of the National Academy of Sciences of the United States of America*, 1962, **48**, 2013-&.
22. S. Nelson, L. Ferguson and W. Denny, *Cell & Chromosome*, 2004, **3**, 2.
23. J. L. Huppert, *Chemical Society Reviews*, 2008, **37**, 1375-1384.
24. S. Burge, G. N. Parkinson, P. Hazel, A. K. Todd and S. Neidle, *Nucleic Acids Research*, 2006, **34**, 5402-5415.
25. N. Smargiasso, F. Rosu, W. Hsia, P. Colson, E. S. Baker, M. T. Bowers, E. De Pauw and V. Gabelica, *Journal of the American Chemical Society*, 2008, **130**, 10208-10216.
26. L. Petraccone, E. Erra, V. Esposito, A. Randazzo, L. Mayol, L. Nasti, G. Barone and C. Giancola, *Biochemistry*, 2004, **43**, 4877-4884.
27. N. V. Hud, F. W. Smith, F. A. L. Anet and J. Feigon, *Biochemistry*, 1996, **35**, 15383-15390.
28. R. J. Harrison, S. M. Gowan, L. R. Kelland and S. Neidle, *Bioorganic & Medicinal Chemistry Letters*, 1999, **9**, 2463-2468.
29. M. Y. Kim, H. Vankayalapati, S. Kazuo, K. Wierzba and L. H. Hurley, *Journal of the American Chemical Society*, 2002, **124**, 2098-2099.
30. V. Viglasky, L. Bauer and K. Tluckova, *Biochemistry*, 2010, **49**, 2110-2120.

31. I. A. Pedroso, L. F. Duarte, G. Yanez, K. Burkewitz and T. M. Fletcher, *Biopolymers*, 2007, **87**, 74-84.
32. H.-Q. Yu, D. Miyoshi and N. Sugimoto, *Journal of the American Chemical Society*, 2006, **128**, 15461-15468.
33. G. N. Parkinson, M. P. H. Lee and S. Neidle, *Nature*, 2002, **417**, 876-880.
34. M. Y. Kim, M. Gleason-Guzman, E. Izbicka, D. Nishioka and L. H. Hurley, *Cancer Research*, 2003, **63**, 3247-3256.
35. X. Fei and Y. Gu, *Progress in Natural Science*, 2009, **19**, 1-7.
36. V. V. Didenko, *Biotechniques*, 2001, **31**, 1106-+.
37. T. Forster, *Annalen Der Physik*, 1948, **2**, 55-75.
38. K. Kawamura, H. Yaku, D. Miyoshi and T. Murashima, *Organic & Biomolecular Chemistry*, 2014, **12**, 936-941.
39. S. Tyagi and F. R. Kramer, *Nature Biotechnology*, 1996, **14**, 303-308.
40. L. G. Kostrikis, S. Tyagi, M. M. Mhlanga, D. D. Ho and F. R. Kramer, *Science*, 1998, **279**, 1228-1229.
41. Kary Mullis, Nobel Prize in Chemistry, http://www.nobelprize.org/nobel_prizes/chemistry/laureates/1993/mullis-lecture.html, **2014**.
42. R. K. Saiki, S. Scharf, F. Faloona, K. B. Mullis, G. T. Horn, H. A. Erlich and N. Arnheim, *Science*, 1985, **230**, 1350-1354.
43. R. K. Saiki, D. H. Gelfand, S. Stoffel, S. J. Scharf, R. Higuchi, G. T. Horn, K. B. Mullis and H. A. Erlich, *Science*, 1988, **239**, 487-491.
44. J. A. Lenstra, *Cellular & Moecular Biology*, 1995, **41**, 603-614.
45. Polymerase Chain Reaction, https://www.neb.com/applications/dna-amplification-and-pcr, **2014**.
46. P. M. Holland, R. D. Abramson, R. Watson and D. H. Gelfand, *Proceedings of the National Academy of Sciences of the United States of America*, 1991, **88**, 7276-7280.
47. U. E. M. Gibson, C. A. Heid and P. M. Williams, *Genome Research*, 1996, **6**, 995-1001.
48. F. Fernandez, J. Gutierrez, A. Sorlozano, J. M. Romero, M. J. Soto and F. Ruiz-Cabello, *Microbiological Research*, 2006, **161**, 158-163.
49. N. Thelwell, S. Millington, A. Solinas, J. Booth and T. Brown, *Nucleic Acids Research*, 2000, **28**, 3752-3761.
50. C. A. Heid, J. Stevens, K. J. Livak and P. M. Williams, *Genome Research*, 1996, **6**, 986-994.
51. L. G. Lee, C. R. Connell and W. Bloch, *Nucleic Acids Research*, 1993, **21**, 3761-3766.
52. R. Lang, K. Pfeffer, H. Wagner and K. Heeg, *Journal of Immunological Methods*, 1997, **203**, 181-192.
53. S. A. Bustin, V. Benes, T. Nolan and M. W. Pfaffl, *Journal of Molecular Endocrinology*, 2005, **34**, 597-601.
54. D. Whitcombe, J. Theaker, S. P. Guy, T. Brown and S. Little, *Nature Biotechnology*, 1999, **17**, 804-807.
55. R. P. Feynman, *Caltech Engineering and Science*, 1960, **23**, 22.36.
56. M. C. Daniel and D. Astruc, *Chemical Reviews*, 2004, **104**, 293-346.
57. M. Rycenga, C. M. Cobley, J. Zeng, W. Li, C. H. Moran, Q. Zhang, D. Qin and Y. Xia, *Chemical Reviews*, 2011, **111**, 3669-3712.
58. N. A. Dhas, C. P. Raj and A. Gedanken, *Chemistry of Materials*, 1998, **10**, 1446-1452.
59. Z. Peng and H. Yang, *Nano Today*, 2009, **4**, 143-164.
60. U. Leonhardt, *Nature Photonics*, 2007, **1**, 207-208.

61. M. Faraday, *Philosophical Transactions of the Royal Society of London*, 1857, **147**, 145-181.
62. P. C. Lee and D. Meisel, *Journal of Physical Chemistry*, 1982, **86**, 3391-3395.
63. A. Henglein and M. Giersig, *Journal of Physical Chemistry B*, 1999, **103**, 9533-9539.
64. D. L. Van Hyning and C. F. Zukoski, *Langmuir*, 1998, **14**, 7034-7046.
65. S. M. Heard, F. Grieser, C. G. Barraclough and J. V. Sanders, *Journal of Colloid and Interface Science*, 1983, **93**, 545-555.
66. N. Leopold and B. Lendl, *Journal of Physical Chemistry B*, 2003, **107**, 5723-5727.
67. G. Mie, *Annalen Der Physik*, 1908, **25**, 377-445.
68. M. M. Alvarez, J. T. Khoury, T. G. Schaaff, M. N. Shafigullin, I. Vezmar and R. L. Whetten, *Journal of Physical Chemistry B*, 1997, **101**, 3706-3712.
69. S. K. Ghosh and T. Pal, *Chemical Reviews*, 2007, **107**, 4797-4862.
70. P. K. Jain, X. Huang, I. H. El-Sayed and M. A. El-Sayad, *Plasmonics*, 2007, **2**, 107-118.
71. W. Rechberger, A. Hohenau, A. Leitner, J. R. Krenn, B. Lamprecht and F. R. Aussenegg, *Optics Communications*, 2003, **220**, 137-141.
72. C. A. Mirkin, R. L. Letsinger, R. C. Mucic and J. J. Storhoff, *Nature*, 1996, **382**, 607-609.
73. A. P. Alivisatos, K. P. Johnsson, X. G. Peng, T. E. Wilson, C. J. Loweth, M. P. Bruchez and P. G. Schultz, *Nature*, 1996, **382**, 609-611.
74. C. M. Niemeyer, *Angewandte Chemie-International Edition*, 2001, **40**, 4128-4158.
75. J. I. Cutler, E. Auyeung and C. A. Mirkin, *Journal of the American Chemical Society*, 2012, **134**, 1376-1391.
76. C. Sonnichsen, B. M. Reinhard, J. Liphardt and A. P. Alivisatos, *Nature Biotechnology*, 2005, **23**, 741-745.
77. N. L. Rosi and C. A. Mirkin, *Chemical Reviews*, 2005, **105**, 1547-1562.
78. D. A. Giljohann, D. S. Seferos, W. L. Daniel, M. D. Massich, P. C. Patel and C. A. Mirkin, *Angewandte Chemie-International Edition*, 2010, **49**, 3280-3294.
79. R. L. Letsinger, R. Elghanian, G. Viswanadham and C. A. Mirkin, *Bioconjugate Chemistry*, 2000, **11**, 289-291.
80. J. J. Storhoff, R. Elghanian, R. C. Mucic, C. A. Mirkin and R. L. Letsinger, *Journal of the American Chemical Society*, 1998, **120**, 1959-1964.
81. R. Elghanian, J. J. Storhoff, R. C. Mucic, R. L. Letsinger and C. A. Mirkin, *Science*, 1997, **277**, 1078-1081.
82. T. A. Taton, C. A. Mirkin and R. L. Letsinger, *Science*, 2000, **289**, 1757-1760.
83. J. M. Nam, S. I. Stoeva and C. A. Mirkin, *Journal of the American Chemical Society*, 2004, **126**, 5932-5933.
84. A. E. Prigodich, P. S. Randeria, W. E. Briley, N. J. Kim, W. L. Daniel, D. A. Giljohann and C. A. Mirkin, *Analytical Chemistry*, 2012, **84**, 2062-2066.
85. D. G. Thompson, A. Enright, K. Faulds, W. E. Smith and D. Graham, *Analytical Chemistry*, 2008, **80**, 2805-2810.
86. D. Graham, D. G. Thompson, W. E. Smith and K. Faulds, *Nature Nanotechnology*, 2008, **3**, 548-551.
87. D. Graham, R. Stevenson, D. G. Thompson, L. Barrett, C. Dalton and K. Faulds, *Faraday Discussions*, 2011, **149**, 291-299.
88. J. R. Epstein, I. Biran and D. R. Walt, *Analytica Chimica Acta*, 2002, **469**, 3-36.
89. J. A. Dougan and K. Faulds, *Analyst*, 2012, **137**, 545-554.
90. J. W. Strutt, *Philosophical Magazine Series 4*, 1871, **41**, 107-120.
91. A. Smekal, *Naturwissenschaften*, 1923, **11**, 873-875.
92. C. V. Raman and K. S. Krishnan, *Nature*, 1928, **121**, 501-502.

93. E. Smith and G. Dent, *Modern Raman Spectroscopy: A Practical Approach*, Wiley, 2005.
94. L. Jensen, L. L. Zhao, J. Autschbach and G. C. Schatz, *Journal of Chemical Physics*, 2005, **123**.
95. M. Fleischmann, P. J. Hendra and McQuilla.Aj, *Chemical Physics Letters*, 1974, **26**, 163-166.
96. D. L. Jeanmaire and R. P. Van Duyne, *Journal of Electroanalytical Chemistry and Interfacial Electrochemistry*, 1977, **84**, 1-20.
97. M. G. Albrecht and J. A. Creighton, *Journal of the American Chemical Society*, 1977, **99**, 5215-5217.
98. M. Moskovits, *Reviews of Modern Physics*, 1985, **57**, 783-826.
99. D. Cunningham, R. E. Littleford, W. E. Smith, P. J. Lundahl, I. Khan, D. W. McComb, D. Graham and N. Laforest, *Faraday Discussions*, 2006, **132**, 135-145.
100. A. Otto, *Journal of Raman Spectroscopy*, 1991, **22**, 743-752.
101. W. E. Smith, *Chemical Society Reviews*, 2008, **37**, 955-964.
102. R. J. Stokes, A. Macaskill, P. J. Lundahl, W. E. Smith, K. Faulds and D. Graham, *Small*, 2007, **3**, 1593-1601.
103. A. M. Stacy and R. P. Vanduyne, *Chemical Physics Letters*, 1983, **102**, 365-370.
104. D. Graham, W. E. Smith, A. M. T. Linacre, C. H. Munro, N. D. Watson and P. C. White, *Analytical Chemistry*, 1997, **69**, 4703-4707.
105. K. Faulds, F. McKenzie, W. E. Smith and D. Graham, *Angewandte Chemie-International Edition*, 2007, **46**, 1829-1831.
106. C. J. McHugh, F. T. Docherty, D. Graham and W. E. Smith, *Analyst*, 2004, **129**, 69-72.
107. E. Papadopoulou and S. E. J. Bell, *Journal of Physical Chemistry C*, 2010, **114**, 22644-22651.
108. E. Papadopoulou and S. E. J. Bell, *Journal of Physical Chemistry C*, 2011, **115**, 14228-14235.
109. S. E. J. Bell and N. M. S. Sirimuthu, *Journal of the American Chemical Society*, 2006, **128**, 15580-15581.
110. E. Papadopoulou and S. E. J. Bell, *Angewandte Chemie-International Edition*, 2011, **50**, 9058-9061.
111. E. Papadopoulou and S. E. J. Bell, *Chemical Communications*, 2011, **47**, 10966-10968.
112. K. Faulds, W. E. Smith and D. Graham, *Analytical Chemistry*, 2004, **76**, 412-417.
113. K. Faulds, R. Jarvis, W. E. Smith, D. Graham and R. Goodacre, *Analyst*, 2008, **133**, 1505-1512.
114. K. Faulds, F. McKenzie and D. Graham, *Analyst*, 2007, **132**, 1100-1102.
115. D. Graham and K. Faulds, *Chemical Society Reviews*, 2008, **37**, 1042-1051.
116. G. McAnally, C. McLaughlin, R. Brown, D. C. Robson, K. Faulds, D. R. Tackley, W. E. Smith and D. Graham, *Analyst*, 2002, **127**, 838-841.
117. A. Enright, L. Fruk, A. Grondin, C. J. McHugh, W. E. Smith and D. Graham, *Analyst*, 2004, **129**, 975-978.
118. D. Graham, C. McLaughlin, G. McAnally, J. C. Jones, P. C. White and W. E. Smith, *Chemical Communications*, 1998, 1187-1188.
119. J. C. Jones, C. McLaughlin, D. Littlejohn, D. A. Sadler, D. Graham and W. E. Smith, *Analytical Chemistry*, 1999, **71**, 596-601.
120. A. Grondin, D. C. Robson, W. E. Smith and D. Graham, *Journal of the Chemical Society-Perkin Transactions 2*, 2001, 2136-2141.
121. D. Graham, R. Brown and W. E. Smith, *Chemical Communications*, 2001, 1002-1003.
122. K. Faulds, L. Stewart, W. E. Smith and D. Graham, *Talanta*, 2005, **67**, 667-671.

123. M. J. Espy, J. R. Uhl, L. M. Sloan, S. P. Buckwalter, M. F. Jones, E. A. Vetter, J. D. C. Yao, N. L. Wengenack, J. E. Rosenblatt, F. R. Cockerill and T. F. Smith, *Clinical Microbiology Reviews*, 2006, **19**, 165-256.
124. S. M. Nie, D. T. Chiu and R. N. Zare, *Analytical Chemistry*, 1995, **67**, 2849-2857.
125. H. T. Li, L. M. Ying, J. J. Green, S. Balasubramanian and D. Klenerman, *Analytical Chemistry*, 2003, **75**, 1664-1670.
126. K. Faulds, R. P. Barbagallo, J. T. Keer, W. E. Smith and D. Graham, *Analyst*, 2004, **129**, 567-568.
127. M. J. Zhong, M. Girolami, K. Faulds and D. Graham, *Journal of the Royal Statistical Scoiety: Series C (Applied Statistics),* 2011, **60**, 187-206.
128. S. Mahajan, J. Richardson, T. Brown and P. N. Bartlett, *Journal of the American Chemical Society*, 2008, **130**, 15589-15601.
129. R. P. Johnson, J. A. Richardson, T. Brown and P. N. Bartlett, *Journal of the American Chemical Society*, 2012, **134**, 14099-14107.
130. D. K. Corrigan, N. Gale, T. Brown and P. N. Bartlett, *Angewandte Chemie-International Edition*, 2010, **49**, 5917-5920.

2. Simultaneous Detection and Quantification of Three Bacterial Meningitis Pathogens by SERS

2.1 Introduction

Bacterial meningitis is well known for its rapid onset and high mortality rates, therefore there is a significant need for fast and reliable methods of detection and identification of the specific bacteria present to ensure the most effective method of treatment is administered.[1, 2] A new SERS-based assay for the simultaneous detection and quantification of three bacterial meningitis pathogens was developed. This involved a combination of the enzyme lambda exonuclease (λ-exonuclease), surface enhanced Raman scattering (SERS) and chemometric analysis.[3] The three pathogens that were successfully detected simultaneously and quantitatively were, *Neisseria meningitidis*, *Streptococcus pneumoniae* and *Haemophilus influenzae*.[4]

2.1.1 Bacterial Meningitis

Meningitis is an inflammation of the lining around the brain and spinal cord. Most cases of meningitis are caused by viruses such as herpes, mumps or measles.[1, 5, 6] Unfortunately there are no effective therapies for most viruses that cause meningitis; therefore treatment is aimed at limiting the effects of the symptoms. Meningitis and septicaemia caused by bacteria are usually more serious compared to viral meningitis and require urgent medical attention with appropriate antibiotic therapy. Meningococcal bacteria (*Neisseria meningitidis*) causes meningitis and septicaemia and affects around 3,400 people each year in the UK and Ireland according to an investigation by the Meningitis Research Foundation.[2] Hib meningitis is caused by the bacterium *Haemophilus influenzae* type b. Vaccinations that are administered to infants at the age of two, four and six months have now become available to prevent this form of bacterial meningitis, however prior to this it was the main cause of meningitis in children under the age of 4 in the UK.[7] However, a lot of cases of

bacterial meningitis are in infants that are too young to receive the vaccination.[2] Pneumococcal bacteria (*Streptococcus pneumoniae*) are the second biggest cause of bacterial meningitis in the UK and Ireland. It is caused when these bacteria enter the bloodstream and move into the cerebral spinal fluid (CSF). The bacteria multiply in the CSF and releases toxins which result in inflammation of the brain. If the inflammation of the brain cannot successfully be stopped either by using antibiotics or other treatments, the infection can be fatal. Unfortunately, it can be difficult to diagnose pneumococcal meningitis at the early stages as there are no obvious symptoms. Therefore, upon patient arrival, antibiotics are administered immediately then CSF samples are taken. Results obtained from the culture of the bacteria in the CSF samples can be obscured by the presence of these antibiotics. Diagnosis of the cause of the meningitis is imperative for determining the most effective course of treatment. The assay developed here demonstrated high specificity for the pathogens present, significantly reduced analysis time and the results would not be affected by the presence of antibiotics.

2.1.2 Lambda Exonuclease

Lambda exonuclease (λ-exonuclease) is a highly processive enzyme that digests one strand of double stranded DNA in the 5' to 3' direction.[8-11] The enzyme originates from the bacteriophage lambda and is used in genetic recombination, where the single stranded DNA produced from digestion acts as a substrate during the process of enzyme pairing which then facilitates DNA recombination.[12] For λ-exonuclease to initiate digestion of double stranded DNA, a 5' phosphate group, the enzyme recognition group, is required on the DNA strand which will be the strand the enzyme digests. Studies have shown that the absence of a 5' phosphate significantly reduced the activity of the enzyme.[8]

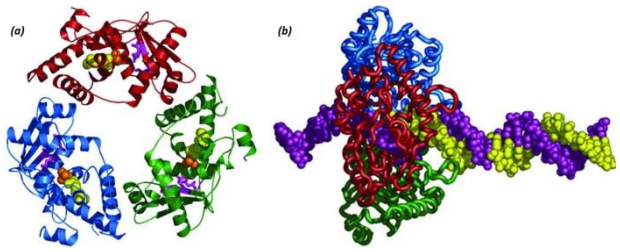

Figure 2.1 (a) Toroidal structure of λ-exonuclease showing the three protein subunits and the central channel. (b) Theoretical model of λ-exonuclease complexed with double stranded DNA, where the substrate has been partially digested.[8]

λ-Exonuclease has a toroidal structure consisting of three protein subunits.[13] A channel passes through the enzyme that decreases in size from 30 Å to 15 Å, allowing double stranded DNA to enter the wider end of the channel, and the digestion products (5' mononucleotides and single stranded DNA) to exit the smaller end of the channel (Figure 2.1).[13] Zhang *et al* further investigated the structure and processive activity of the enzyme.[14] They proposed an *electrostatic ratchet mechanism* where the double stranded DNA substrate is captured in the central channel but not bound to the active site (Figure 2.2). The 5' phosphate is then attracted to a positively charged pocket (Mg^{2+}) where the DNA becomes wedged and the two strands start to unwind. Once the DNA is aligned correctly in the channel/wedge and the Mg^{2+} ions are attached to the duplex, the phosphodiester bond is cleaved yielding 5' mononucleotides and releasing the Mg^{2+} ions that leave through the narrow end of the channel. This then leaves the active site vacant and a newly formed 5' phosphate on the DNA strand, therefore allowing the process to continue until all the phosphodiester bonds are cleaved in the DNA strand. Theoretically, the DNA strand could move backwards, however due to the strong attraction between the 5' phosphate and the positively charged pocket in the active site the DNA is restricted from moving backwards.[14] The favoured substrate for λ-exonuclease activity has been shown to be double stranded DNA.[11]

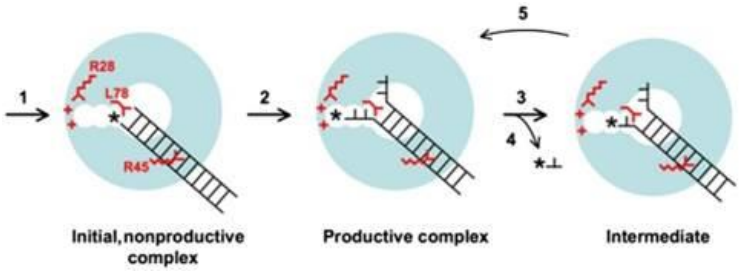

Figure 2.2 Schematic illustrating the mechanism of λ-exonuclease. Step 1, DNA substrate captured in the central channel of the enzyme, where the 5' phosphate is attracted to the positively charged pocket that contains Mg^{2+} ions. DNA substrate now becomes wedged into the positively charged pocket where the two strands unwind, step 2, then the phosphodiester bond is cleaved, step 3. The 5' mononucleotides are expelled from the channel, step 4, leaving the active site vacant for successive cycles of DNA unwinding and bond breaking, step 5.[14]

2.1.3 SERS-Based Assays for DNA Detection

In recent years, there has been a heavy focus on the development of assays using surface enhanced Raman scattering (SERS) for the detection of specific DNA sequences. SERS of the nucleobases has been reported by Bell *et al*,[15] however this does not give any information on the sequence present that is required for disease DNA detection. Therefore, oligonucleotides were designed to incorporate fluorophores that would generate a unique SERS response. In diagnostics, it is not the target disease sequence that is modified with the fluorophore; it is the complementary probe sequence that will possess the fluorophore. Detection of the fluorophore attached to the complementary probe sequence is indicative of the presence of the target sequence through the Watson-Crick base pairing between the two sequences.

SERS was used for the detection of duplex DNA using HEX and R6G to discriminate between the two oligonucleotides based on the SERS signals from the two fluorophores present.[16] Graham *et al* first reported SERS multiplexing for DNA genotyping using a combination of amplification refractory mutation system (ARMS) and SERS for the detection of the three different formats of the cystic fibrosis transmembrane conductance regulator (CFTCR) gene.[17] The multiplexing capability of SERS was used to detect DNA sequences coding for MRSA in a homogeneous assay format.[18] The assay was based on the different affinity that double and single stranded DNA has for the metal surface. When single stranded fluorophore labelled DNA was used, strong SERS intensity was observed, however when double stranded fluorophore labelled DNA was used, low SERS intensity was observed, i.e. the presence of target DNA resulted in a reduction of SERS intensity. This assay was used to the multiplex detection of three genes associated with MRSA using three fluorophores; FAM, HEX and TAMRA. This proved successful using both synthetic DNA and PCR product.[18] Vo-Dinh *et al* developed a "molecular sentinel" approach to the multiplexed detection of DNA using SERS.[19] The molecular sentinel contained a loop DNA sequences with a complementary region to a specific target sequence and the self-complementary stem sequences that hold the sentinel closed in a hairpin loop formation. One of the stem sequences was modified with a thiol group to allow for attachment to the metal surface and the other stem sequence possessed a fluorophore. When the sentinel was closed, the fluorophore was close to the nanoparticle surface therefore intense SERS signals were

observed, however in the presence of target DNA the sentinel opens, the fluorophore then become further away from the nanoparticle surface resulting in a reduction in the SERS signals.[19] The molecular sentinels were used for the multiplex detection of two genes that were biomarkers for breast cancer. Two sentinels were used, one modified with TAMRA, the other with Cy3 and SERS peaks for both fluorophores were used to detect the two breast cancer biomarkers.[19]

Due to the successful application of SERS for the multiplex detection of DNA, it was the chosen technique for the simultaneous detection of the three bacterial meningitis pathogens as other fluorescent based technique do not offer the same extent of multiplexing capabilities.[20, 21] The aim of this work is to simultaneously detect three bacterial meningitis pathogens faster than culture and fluorescence based methods, therefore SERS was used.

2.2 Aims

Due to the significant need for reliable detection methods for bacterial meningitis in a much shorter time frame to improve the chances of patient survival, a SERS-based assay has been developed to fulfil this requirement. This was used to simultaneously detect three bacterial meningitis pathogens, *Neisseria meningitidis*, *Streptococcus pneumoniae* and *Haemophilus influenzae*. Most importantly, by using chemometric analysis, each pathogen within the multiplex mixture was able to be quantified for the first time, which has previously not been done using SERS and is also difficult to achieve in a biological sample mixture.

2.2.1 Exo-SERS Detection Assay

The assay developed for the detection of the bacterial meningitis pathogens was previously optimised for the detection of *Chlamydia trachomatis* and consisted of several steps.[22] First, the synthetic pathogen sequence underwent a sandwich hybridisation event with two complementary sequences, one modified with biotin (*capture probe*) and the other possessed a 5' phosphate to initiate λ-exonuclease digestion and a fluorescent label to aide SERS detection (*reporter probe*), Figure 2.3(i). Streptavidin coated magnetic beads were

then added which retained the newly formed duplex and allowed subsequent wash steps, increasing the specificity of the assay by removing any unbound/excess DNA (Figure 2.3ii and iii). λ-Exonuclease was added and digestion of the 5' phosphate and fluorescent label modified *reporter probe* took place (Figure 2.3iv). This liberated the dye from the duplex that was previously attached to the streptavidin coated magnetic bead. The products of digestion were then added to a mixture of citrate reduced silver nanoparticles and spermine hydrochloride; this was then followed by SERS analysis which generated the SERS spectra of the fluorescent label present on the *reporter probe* (Figure 2.3v and vi). Citrate reduced silver nanoparticles possess a negative surface, therefore spermine hydrochloride was added to reduce this negative charge to enable the negative phosphate backbone of the DNA to come into close proximity of the nanoparticle surface allowing SERS enhancement to occur.

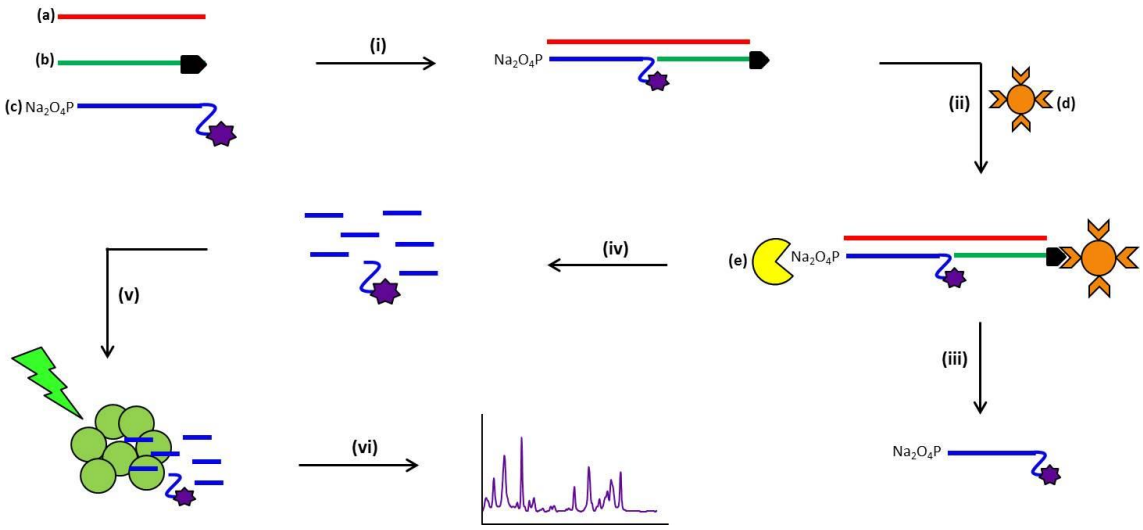

Figure 2.3 Schematic of the SERS detection assay illustrating each step involved. Two chemically modified DNA sequences (b and c) hybridise to a single target DNA sequence (a) in a process known as sandwich hybridisation (i), using 0.3 M PBS at 90 °C for 10 min then 10 °C for 10 min. Streptavidin coated magnetic beads (d) are then added to the reaction mixture (ii) and the newly formed duplex is retained on the beads due to the biotin modification. Subsequent washing steps (iii) take place to remove any excess/unhybridised DNA from the reaction mixture and the beads are resuspended in 30 µL of Exonuclease Buffer (New England Biolabs, Herts, UK). λ-Exonuclease (e) is then added to the reaction mixture for double stranded digestion to occur (iv) for 90 min at 37 °C. The digestion products are then added to a solution containing silver nanoparticles (150 µL) and spermine hydrochloride (20 µL, 0.3 M) (v) and SERS analysis is carried out (vi) using a Raman excitation wavelength of 532 nm and a diode laser.

2.2.2 Selected Fluorescent Dyes

Three fluorescent dyes were required, one for each of the three *reporter probes* corresponding the bacterial meningitis pathogens under analysis. The three dyes chosen were FAM, TAMRA and Cy3, which each produce unique SERS spectra. Figure 2.4 shows the spectra and structures of the three dyes used to label the reporter probes. Table 2.1 lists the Raman peak assignments for each dye.

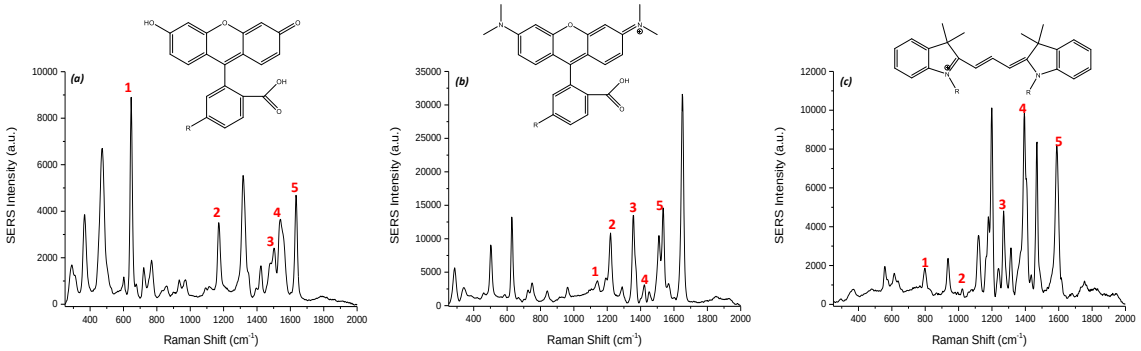

Figure 2.4 SERS spectra and structures of the three fluorescent dyes used; (a) FAM, (b) TAMRA and (c) Cy3.

Table 2.1 Raman peak assignments for the three fluorescent dyes. Red numbering corresponds to the highlighted peaks shown in the spectra in Figure 2.4.

Fluorescent Dye	Raman Shift (cm^{-1})	Assignment
FAM	**(1)** 646	Carboxylic acid, in plane vibration
	(2) 1172	C-O-C symmetrical stretch
	(3) 1503	Central ring breathing
	(4) 1547	-C=C- stretch
	(5) 1635	C=O/C=C symmetrical stretch
TAMRA	**(1)** 1140	C-O-C symmetric stretch
	(2) 1220	=C-H in plane vibration
	(3) 1357	=C-N amine stretch
	(4) 1422-1452	CH3 asymmetric vibration
	(5) 1509-1570	-C=C- aromatic vibrations
Cy3	**(1)** 799	C-C aliphatic chains
	(2) 1022	-C=C- stretch
	(3) 1271, 1394	-C-N- stretch
	(4) 1469	Indole ring vibrations
	(5) 1590	-C=N- stretch

2.3 Experimental

2.3.1 Colloid Synthesis

Silver nanoparticles were synthesised using a modified Lee and Meisel method.[23] Silver nitrate (90 mg) was dissolved in 500 mL distilled water. The solution was heated rapidly to boiling with continuous stirring. Once boiling, an aqueous solution of sodium citrate (1 %, 10 mL) was added quickly. The heat was reduced and the solution was left to boil gently for 90 min with stirring. The colloid was then analysed by UV-vis spectroscopy and the λ_{max} was found to be 411 nm with the full width half-height (FWHH) measured to be 103 nm. The concentration of the colloid was calculated to be 0.3 nM. To minimise issues that arise from batch to batch variation, experiments were performed using the same batch of colloid.

2.3.2 Oligonucleotides

The three target pathogen sequences were those used by Guiver *et al.* for their simultaneous detection using real-time PCR.[4] Biotinylated DNA and unmodified target DNA sequences were purchased on a 0.01 µM scale with HPLC purification from Eurofins MWG (Ebersberg, Germany). 5' phosphate/Dye modified DNA sequences were ordered on a 0.1 µM scale with HPLC purification from Integrated DNA Technologies (Leuven, Belgium).

Table 2.2 Oligonucleotide sequences and modifications used in the SERS detection assay

Name	Sequence (5'-3')	5' Modifications	3' Modifications
Streptococcus pneumoniae	TTCGAGTGTTGCTTATGGGCGCCA	-	-
Streptococcus pneumoniae **"Capture Probe"**	GCAACACTCGAA	-	Biotin
Streptococcus pneumoniae **"Reporter Probe"**	TGGCGCCCATAA	Phosphate	Spacer18-10A-TAMRA
Haemophilus influenzae	CCACGCTCATTCGTTTGATGAGTGGTG	-	-
Haemophilus influenzae **"Capture Probe"**	AACGAATGAGCGTGG	-	Biotin
Haemophilus influenzae **"Reporter Probe"**	CACCACTCATCA	Phosphate	Spacer18-10A-Cy3
Neisseria meningitidis	ATGTGCAGCTGACACGTGGCAATG	-	-
Neisseria meningitidis **"Capture Probe"**	TCAGCTGCACAT	-	Biotin
Neisseria meningitidis **"Reporter Probe"**	CATTGCCACGTG	Phosphate	Spacer18-10A-FAM

2.3.3 Buffer

Exonuclease buffer was supplied by New England Biolabs (Cambridge, UK) consisting of; 67 mM glycine-KOH, 2.5 mM $MgCl_2$ and 50 µg/mL bovine serum albumin (BSA). The pH of the buffer was 9.4. Exonuclease buffer was supplied at 10x concentration and was diluted to 1x concentration when used in the assay.

2.3.4 PCR

PCR was carried out using a Stratagene MX3005P fluorimeter and the commercially available Qiagen PCR reagents. Each reaction had a total volume of 25 µL; 2.5 µL of Qiagen reaction buffer (10x), 1 µL of $MgCl_2$ solution (25 mM), 0.4 µL of deoxynucleoside triphosphates (10 mM), 1 µL of forward primer (10 µM), 1 µL of reverse primer (10 µM), 0.5 µL of Taq Polymerase (5 U), 1 µL of template DNA (approx. $5x10^6$ copies/µL) and made up to the total volume (25 µL) with DEPC treated water. PCR was then carried out using the following thermal profile: 10 min at 95 °C, followed by 45 cycles of 95 °C for 30 s, 58 °C for 1 min then 72 °C for 1 min and a final extension for 1 min at 72 °C.

2.3.5 Gel Electrophoresis

PCR products of each of the three pathogens were run on a 3.5 % w/v agarose gel (3.5 g of agarose in 100 mL TBE Buffer) that was stained with ethidium bromide (2 µL, 10 mM). The gel was poured into a mould and allowed to set. Once the gel was hardened, it was placed within an insulated chamber and filled with 1 x TBE Buffer until the gel was covered. To each well, 15 µL of PCR product premixed with blue loading buffer (5 µL, Bioline). The gel was run for 90 minutes at 160 V.

2.3.6 Detection Assay

A biotinylated modified sequence and a 5' phosphate/fluorophore modified sequence underwent a sandwich hybridisation event with one complementary (target) sequence using a Minicycler PTC-150 system. An aliquot of each DNA sequence (10 µL, 1 µM) was added to a PCR tube containing phosphate buffered solution (70 µL, 0.3 M). The temperature was held at 90 °C for 10 min, and then was lowered to 10 °C for 10 min. For

the *no target* control, the target DNA sequence was omitted and replaced with distilled water, and the *non-complementary* control used a sequence that was not complementary to either of the modified probes in place of the target sequence. Once the sequences were hybridised, 15 µL of Streptavidin coated magnetic beads were added to the PCR tubes and left at room temperature for 30 min. Three washing steps were carried out using phosphate buffered solution (70 µL, 0.3 M). The beads were then resuspended in exonuclease buffer (30 µL, 1x) and lambda exonuclease was added (2 µL, 1 U) for digestion to occur for 90 min at 37 °C. SERS analysis was performed post-digestion.

2.3.7 SERS Analysis

For the limit of detection studies and multiplex assay experiments, SERS was carried out using an Avalon Instrument Ramanstation R3 (Belfast, UK), with an excitation wavelength of 532 nm from a diode laser. Disposable 1.5 mL PMMA semi-micro cuvettes were used. To the cuvette, 30 µL of λ-exonuclease digestion products was added to spermine hydrochloride (20 µL, 0.1 M), distilled water (250 µL) and silver citrate colloid (150 µL). The sample was then mixed thoroughly and immediately analysed by SERS. The spectra were baseline corrected using Grams software. When carrying out limit of detection studies, 5 scans of 5 replicate samples at each concentration were analysed. The equation of the line obtained from the dilution studies was used to calculate the limits of detection. The limit of detection was calculated to be 3 times the standard deviation of the blank, divided by the gradient of the straight line. For the chemometric studies, SERS analysis was performed using an Avalon Plate Reader, with an excitation wavelength of 532 nm. A 96 well plate was placed onto a stage and the instrument's software was used to automatically move the stage so that spectra can be recorded from each well. The accumulation time was 0.01 s and each well was scanned 5 times. A single well can hold 300 µL. Each well contained 30 µL of dye mixture (or post-assay mixture when testing the model), spermine tetrahydrochloride (0.1 M, 20 µL), distilled water (100 µL) and silver citrate colloid (150 µL). To train the PLS prediction model a suitable and reduced number of base line experiments (66 in total) were designed to be performed in the lab. The design of such experiments was based on the theory of Design of Experiments as previously described by Mabbott *et al*.[24] Five scans of five replicates of each of the 66 different dye ratios were analysed and the spectra were averaged prior to model construction. Following this additional samples were

generated to test the model and included: (i) additional dye combinations and (ii) samples after having gone through the complete SERS assay; the latter were included as these are the closest to the clinical scenario.

2.3.8 Chemometrics

Chemometric analysis was performed by Dr. Elon Correa and Prof. Roy Goodacre at the University of Manchester. Data were baseline corrected using the asymmetrical least squared smoothing method.[25] Principal component analysis (PCA) was performed to assess the reproducibility of the data set using Matlab software version R2012a (The MathWorks, Natick, MA, USA). PCA reduces the dimensionality of the SERS data, making it easier to identify any variations in the spectra.[26, 27] PCA was carried out on four different data sets, three consisting of spectra obtained from single pathogen detection experiments and one data set obtained for the multiplex detection of the three pathogens. For quantification of the three pathogens in tertiary mixtures the supervised learning method of partial least squares (PLS) regression was employed. PLS is a multivariate calibration method that relates a set of independent variables *X* (Raman intensities) to a set of dependent variables *Y* (dye-labelled oligonucleotide concentrations). PLS projects the *X* and *Y* variables into sets of orthogonal latent variables, scores of *X* and scores of *Y*, so that the covariance between these two sets of latent variables is maximised.[28] The purpose of PLS is to build a linear model $Y = XB + E$, where B is a matrix of regression coefficients and E represents the difference (error) between observed and predicted Y values.[29] After calibration of the PLS models, validation data (new Raman spectra) not used in model building were used to challenge PLS. These included additional dye-labelled oligonucleotide combinations as well as samples that had gone through the whole SERS assay. If these predictions were correct then this would show that our approach could successfully and simultaneously quantify the three pathogens of bacterial meningitis. The PLS algorithm was run in Matlab version R2012a.

2.4 Results and Discussion

The three bacterial meningitis pathogens, *Neisseria meningitidis*, *Streptococcus pneumoniae* and *Haemophilus influenzae* are the most common causes of acute bacterial meningitis, which is very serious and often fatal infection of the central nervous system.[30, 31] Current methods used for the detection of bacterial meningitis include the culture of the bacteria present in the CSF sample. This method can take up to 36 hours to provide a confirmative results and it has also been reported that the administration of antibiotics prior to sample collection hampers the ability of making a positive identification of the bacteria present.[32, 33] More importantly, there has been an increase in discrepancies between the number of suspected and confirmed cases of bacterial meningitis when using culture based methods.[34, 35] A solution to this problem was to use non-culture based methods such as PCR, and this is now being used extensively for the detection of bacterial meningitis pathogens. PCR involves the amplification of pathogen DNA sequences and provides a universal detection technique for bacteria.[36] However, the disadvantage to using this method is the risk of obtaining false positive results due to the presence of residual bacterial DNA during amplification. The most effective course of treatment for a patient is determined by the positive identification of the bacteria present, therefore a detection method must be developed that can produce reliable confirmative results for bacteria identification to ensure that the best treatment plan had been used for the patient.

As mentioned in section 2.2.1, the assay used for the detection of the three bacterial meningitis pathogens involved several steps. Although PCR product was used in the assay as a way of showing the assay would work using complex samples, by using the enzyme λ-exonuclease the assay would then utilise signal amplification generated by enzyme activity rather than the conventional DNA amplification methods. Firstly, sandwich hybridisation between the target pathogen sequence and the *capture* and *reporter probes* takes place followed by the addition of streptavidin coated magnetic beads and subsequent wash steps to remove any unhybridised/excess DNA. λ-exonuclease is added to allow for the digestion of the *reporter probe* so that the fluorescent label is released from the bead and can be added to a solution of citrate reduced silver nanoparticles and spermine for SERS analysis. The assay demonstrates a high degree of specificity due to the amount of specific events that occur only if the target pathogen is present, i.e. sandwich hybridisation and enzyme

digestion. Whereas, compared to PCR-based methods, these are prone to contamination and non-specific amplification due to the presence of residual DNA. This assay had been optimised for the detection of *Chlamydia trachomatis*, however, the aim of this work was to use this assay to simultaneously detect multiple pathogens which had not been done previously. Furthermore, quantification of each pathogen was to be performed using chemometric analysis.

2.4.1 Oligonucleotide Design

To detect each pathogen individually using this assay, three different DNA sequences were required (Table 2.2). For initial studies, synthetic DNA sequences coding for each pathogen were used as the *target* sequences. Each synthetic pathogen sequence had two complementary synthetic probe sequences, each complementary of half of the *target* sequence (Table 2.2). One probe sequence was modified at the 3' end with a biotin and was referred to as the *capture probe*. The other sequence, referred to as the *reporter probe* was complementary to the other half of the *target* and was modified with a 5' phosphate to enable λ-exonuclease digestion. At the 3' end there was a spacer-18 group which was an 18-atom hexa-ethylene glycol spacer that was used to stop digestion resulting in a sequence of 10 adenine bases and the fluorescent dye on the 3' end being released that would then be free for SERS detection. The 10 adenine bases remained attached to the fluorescent dye post-digestion and previous studies have shown that this adenine "tail" enhances the SERS signal compared to free dye that does not possess a DNA "tail". [22, 37] Figure 2.5a shows the low peak intensities in the SERS spectra that would be obtained if there was only the free dye, i.e. no 10 adenine base "tail". However, when the dye is attached to the DNA "tail", greater SERS intensity is obtained of the dye peaks, in this case the dye was TAMRA (Figure 2.5b). For each of the three pathogens a different fluorescent dye was used to label each target specific *reporter probes*: when detecting *Streptococcus pneumoniae* the fluorescent dye TAMRA was present on the *reporter probe*, for the detection of *Neisseria meningitidis* FAM was the fluorescent dye monitored and finally for the detection of *Haemophilus influenzae* Cy3 was the chosen dye.

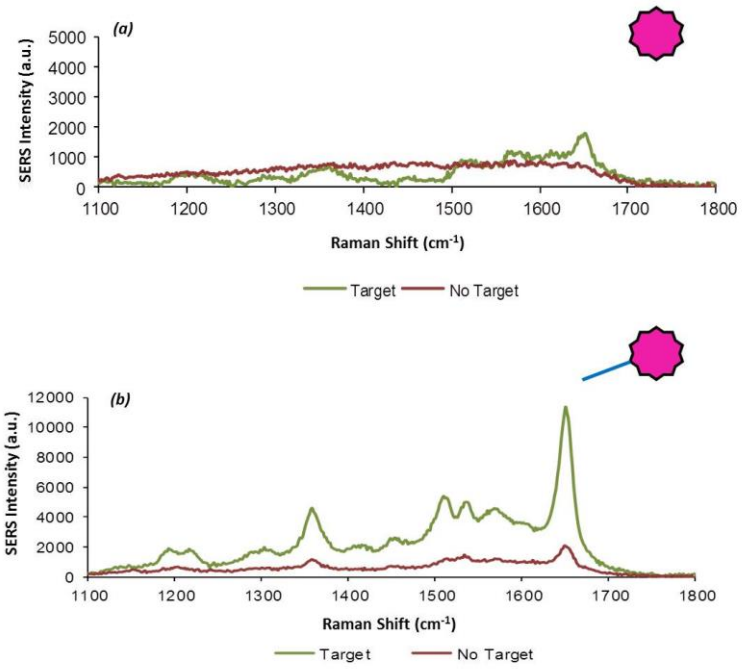

Figure 2.5 (a) SERS spectra obtained after performing the assay when it is only TAMRA dye released post-digestion. (b) SERS spectra obtained when spacer-18 is present in the *reporter probe* sequence so that post-digestion a 10 adenine bases "tail" remains attached to the fluorescent label, TAMRA, meaning when it is added to the nanoparticle-spermine mixture greater SERS enhancement is observed.

2.4.2 Single Pathogen Detection

Single pathogen detection was performed using synthetic target sequences (Table 2.2) then using PCR product. In the first set of experiments, the synthetic target pathogen was added to a solution containing both the *capture* and *reporter* complementary probes. Hybridisation of the complementary probes and target pathogen then took place, followed by the addition of streptavidin coated magnetic beads and subsequent wash steps. The fluorescent dye was then released from the duplex by λ-exonuclease digestion and was added to a mixture of silver citrate nanoparticles and spermine. SERS analysis was then performed and the unique spectrum of the particular dye present was obtained. Along with the detection of the *target* sequence, two control experiments were undertaken each time the assay was performed, *no target* and *non-complementary*. The *non-complementary* control was different for each pathogen detection assay. When detecting *Streptococcus pneumoniae* pathogen, the synthetic sequence for *Neisseria meningitidis* was present and used as the *non-complementary* control. The *Haemophilus influenzae* sequence was the

control when detecting *Neisseria meningitidis* and for the detection of *Haemophilus influenzae*, the synthetic sequence coding for *Streptococcus pneumoniae* was the *non-complementary* control. No SERS peaks from the fluorescent dye labels should have been observed in either control as the synthetic *target* pathogen sequence is not present in the assay and therefore the *reporter probe* will be removed during the wash steps that were performed prior to λ-exonuclease digestion.

The synthetic sequence coding for *Streptococcus pneumoniae* was successfully detected using the Exo-SERS assay. This was carried out by monitoring the characteristic TAMRA peaks in the SERS spectrum (Figure 2.6a), as this was the dye modification on the *reporter probe* complementary to the *Streptococcus pneumoniae* sequence. A prominent peak was observed at around 1650 cm^{-1} that was present due to the C=C bonds in the dye structure and the peaks observed around 1500-1560 cm^{-1} represented the aromatic ring vibrations.[38] All peaks observed in the spectrum were attributed to the structure of TAMRA. As predicted, the *no target* and *non-complementary* controls showed no SERS signal since the *target* pathogen sequence had been omitted from the assay, therefore a fully formed duplex was not obtained, i.e. the *reporter probe* was not present to facilitate SERS detection (Figure 2.6b). *Neisseria meningitidis* was detected successfully, using the respective synthetic *target* DNA sequence, by monitoring the characteristic FAM peaks in the SERS spectrum as this was the dye present on the *reporter probe* complementary to *Neisseria meningitidis* (Figure 2.6c). The peak at 1625 cm^{-1} was a result of the C=C vibrations, and similar to the SERS spectrum of TAMRA, peaks within the range 1400-1500 cm^{-1} represented CH_2 and CH_3 vibrations.[38] Peaks between 1500 and 1600 cm^{-1} were from the aromatic rings in the FAM structure. Again the *no target* and *non-complementary* controls did not produce any SERS peaks as expected since the pathogen sequence was not present in the assay and further analysis at 648 cm^{-1} demonstrated that both controls showed no SERS intensity at this specific characteristic FAM peak (Figure 2.6d). Finally, the synthetic *target* sequence of *Haemophilus influenzae* was also detected successfully using the novel SERS assay by monitoring the characteristic SERS peaks of the dye Cy3, which was chemically attached to the *reporter probe* (Figure 2.6e). Aromatic vibrations were observed between 1500 and 1600 cm^{-1}. The intense peak observed at 1200 cm^{-1} was due to the aliphatic chain in the dye structure.[38] The *non-complementary* control gave no SERS peaks

as expected as the synthetic *target* pathogen sequence was excluded from the assay. This was reaffirmed upon further analysis of the peak at 1586 cm^{-1}. However, upon analysis for the *no target* control, there was a small amount of SERS intensity observed. This can be attributed by the presence of a larger background in the SERS spectrum for this control compared to the *non-complimentary* control and as it was the absolute intensity values used to calculate the peak intensities, negligible SERS intensity could be observed (Figure 2.6f).

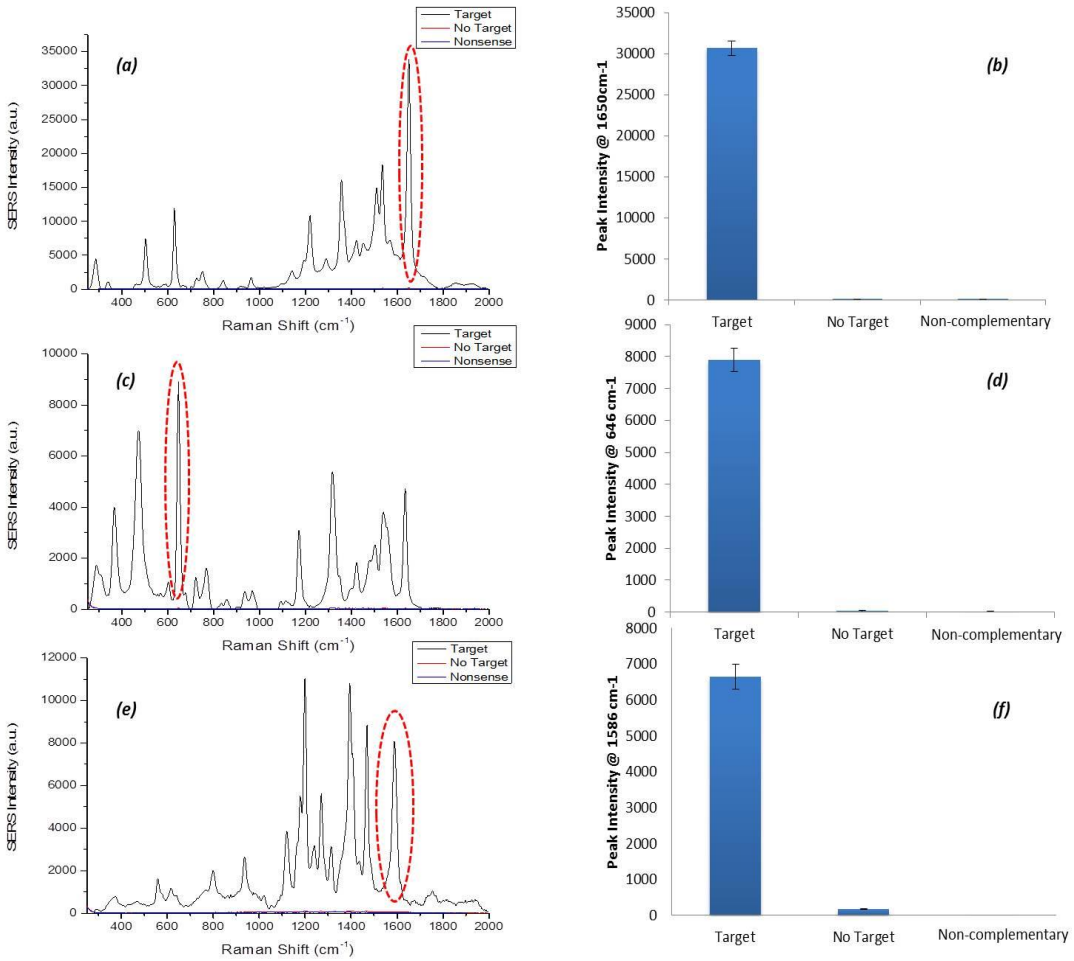

Figure 2.6 SERS spectra obtained from single pathogen detection using the SERS assay: (a) SERS spectra of TAMRA observed when detecting *S. pneumoniae*; (b) SERS peak intensities at 1650 cm^{-1} for assay and both controls when detecting *S. pneumoniae*; (c) SERS spectra of FAM observed when detecting *N. meningitidis*; (d) SERS peak intensities at 646 cm^{-1} for assay and both controls when detecting *N. meningitidis*; (e) SERS spectra of Cy3 observed when detecting *H. influenzae*; (f) SERS peak intensities at 1586 cm^{-1} for assay and both controls when detecting *H. influenza*. SERS spectra were recorded using an excitation wavelength of 532 nm. Peak intensities were obtained by scanning 5 replicate samples 3 times with an accumulation time of 1 s. Averages are shown and error bars are ± one standard deviation.

In summary, when synthetic *target* pathogen DNA was omitted from the assay or a *non-complementary* sequence was present, no SERS signals were obtained, therefore demonstrating the excellent robustness and specificity of this assay for diagnostic purposes.

2.4.3 Determining Target Limits of Detection

With the knowledge that each pathogen could be successfully detected due to the significant SERS enhancement observed when *target* pathogen DNA was present in the assay, a dilution series was carried out to determine the lowest concentration of synthetic *target* pathogen DNA that could be detected using the assay. An initial concentration range of $6x10^{-8}$ M to $1x10^{-9}$ M of synthetic *target* pathogen DNA was added to 1 µM *capture* and *reporter* probes and each step of the SERS assay was performed. The limits of detection were calculated using the equation of the line obtained from the dilution studies and calculating the limit of detection to be 3 times the standard deviation of the blank, divided by the gradient of the straight line (Figure 2.7). The data was normalised using the intensity of the cyclohexane standard measured on the day of analysis. When this SERS assay was previously applied to the detection of *Chlamydia trachomatis* the lowest amount of target DNA was determined to be 77 pM.[22] The calculated limits of detection when using the assay to detect the three pathogens *Neisseria meningitidis*, *Streptococcus pneumoniae* and *Haemophilus influenzae* were 45.3 pM, 99.5 pM and 21.7 pM, respectively.[3] Each limit of detection study of the three pathogens produced linear calibration plots. This is a great result considering the number of steps that need to be carried out (hybridisation, washings, digestion) before the SERS spectra are recorded, emphasising how each event within the assay is highly efficient. The limits of detection obtained for the detection of the three bacterial meningitis pathogens were in the same range to that obtained from the previous study, which indicates the high level of robustness this assay possesses as it can be applied to various different classes of diseases and still have the same levels of sensitivity. More importantly, detection limits in the pico-molar range are highly desirable in clinical diagnostics where the concentrations of disease DNA under analysis are very low and currently very difficult to detect using fluorescence, as it has been previously reported that the limits of detection obtained using SERS are significantly lower to that obtained when using fluorescence.[39]

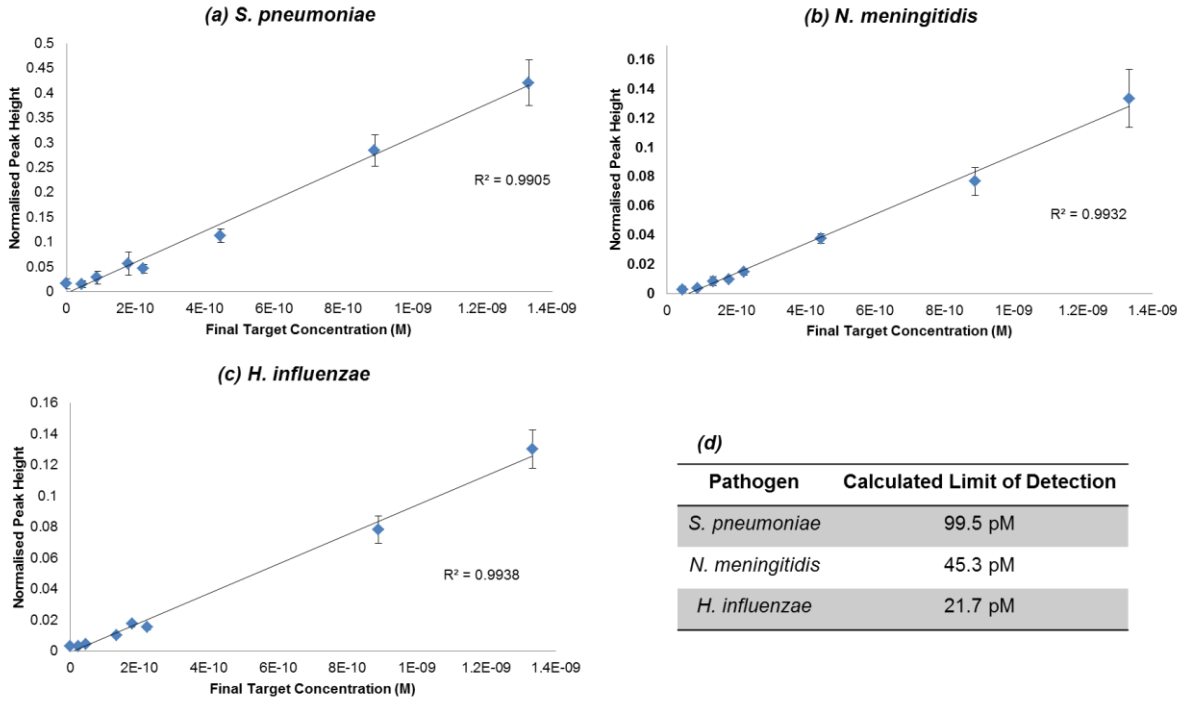

(d)

Pathogen	Calculated Limit of Detection
S. pneumoniae	99.5 pM
N. meningitidis	45.3 pM
H. influenzae	21.7 pM

Figure 2.7 The assay was performed for each pathogen using the specified concentration range. The calibration curves of normalised SERS peak heights for each pathogen are shown: (a) 1650 cm^{-1} peak height used to calculate the limit of detection for *S. pneumoniae*; (b) 646 cm^{-1} peak height used to calculate the limit of detection for *N. meningitidis*; (c) 1586 cm^{-1} peak height used to calculate the limit of detection for *H. influenzae*. Table (d) summarises calculated limits of detection. SERS spectra were recorded using an Avalon Instrument Ramanstation R3, with an excitation wavelength of 532 nm and a diode laser power of 100 mW. Each point represents the average of 5 replicates of each concentration. Error bars are ± one standard deviation.

2.4.4 Pathogen DNA Amplification

The successful results obtained so far used short synthetic exact complement DNA sequences that code for each of the three pathogens. However, this assay has been developed to be used in clinical diagnostics when the pathogen DNA under analysis has been extracted from the bacteria DNA present in the CSF sample extracted from the patient. To ensure that the assay would also produce successful results with clinical samples, pathogen DNA was amplified from plasmid DNA using the polymerase chain reaction (PCR) in order to obtain DNA samples that would be more representative of extracted bacteria DNA from CSF samples as clinical samples were not available. Commercial Qiagen PCR reagents were used to amplify the plasmid DNA of each of the three pathogens. Primers were designed so that they hybridised to the specific region of

interest in the plasmid DNA sequence. The first step of the PCR cycle involved the denaturation of the double stranded plasmid DNA to produce two single strands of DNA using the enzyme activity of Taq polymerase, dNTPs were added in the correct sequence order to produce two newly formed duplex DNA sequences of the bacterial meningitis pathogen under analysis. Successive cycles (40-55) of these steps resulted in a significant increase in the amount of DNA, noted by the increase in the fluorescence emitted from Sybr Green in the amplification plot (Figure 2.8a-c).

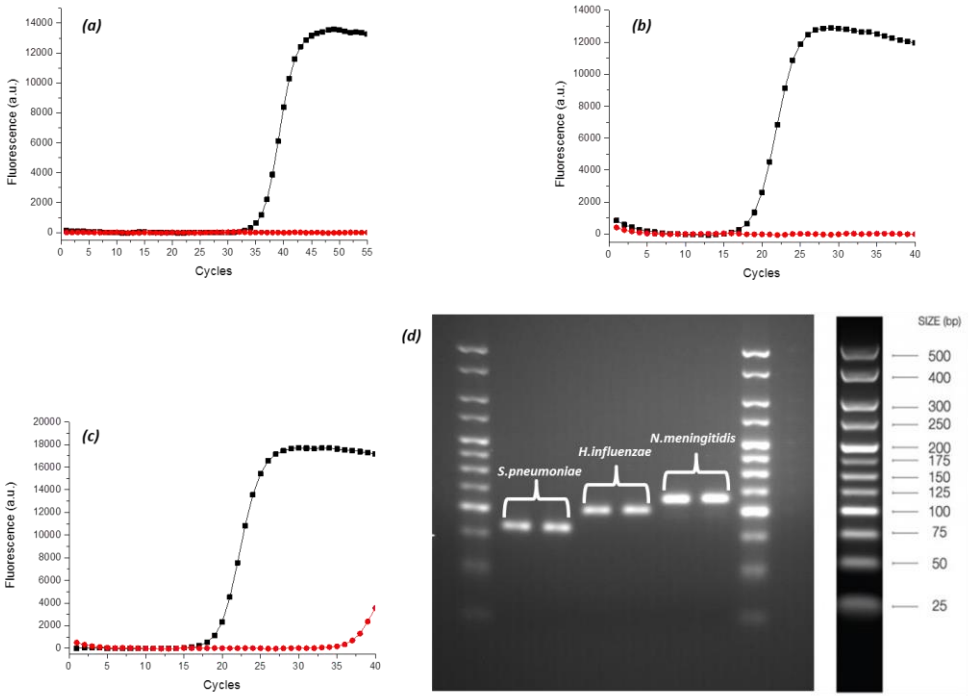

Figure 2.8 Results obtained from PCR performed to obtain amplified DNA product for each pathogen. (a) Amplification plot of the PCR reaction using *Neisseria meningitidis* plasmid DNA (black) and using a control where the plasmid DNA was omitted from the PCR (red). (b) Amplification plot of the PCR reaction using *Streptococcus pneumoniae* plasmid DNA (black) and using a control where the plasmid DNA was omitted from the PCR (red). (c) Amplification plot of the PCR reaction using *Haemophilus influenzae* plasmid DNA (black) and using a control where the plasmid DNA was omitted from the PCR (red). (d) Gel electrophoresis used to size the PCR product obtained from each of the three amplifications. Ethidium bromide stained gel is used to aid the visualisation of the DNA bands and compare them to the ladder standard to determine the size of the PCR product. PCR was carried out using a Stratagene MX3005P with fluorescence detection and commercially available Qiagen PCR reagents. Plasmid DNA was provided by Renishaw Diagnostics Limited.

To ensure the correct size of PCR product was generated using the specific primers and the optimal reagent concentrations, gel electrophoresis was performed (Figure 2.8d). A 3.5 % agarose gel was used that was stained with ethidium bromide (EtBr) to enable the fluorescent identification of the DNA bands. Also used was the Bioline Hyper Ladder V that sized PCR product ranging from 25 to 500 base pairs in length. Loading buffer was premixed with the PCR product before it was added to the wells to facilitate monitoring of the DNA bands while the gel was running. Once the bands were fully separated (90 minutes) the gel was then placed in a BioDoc-It^{TM} Imaging System fitted with a 2UV Transilluminator set at 365 nm. The DNA bands were successfully visualised on the agarose gel and product sizes were estimated to be 80, 100 and 110 base pairs in length for *Streptococcus pneumoniae*, *Haemophilus influenzae* and *Neisseria meningitidis* respectively. These were in good agreement with the predicted product size using the specific primers. Once PCR product for each of the three pathogens was obtained, it was used to investigate if the assay would successfully detect the three pathogens simultaneously using clinically relevant samples.

2.4.5 PCR Product Used in Assay

The assay has previously been performed using short synthetic DNA sequences, the target pathogen sequences were 24 base pairs long and the complementary probes were 12 base pairs in length. PCR product is much longer than synthetic target sequences, the length of PCR product of the three pathogens are stated in the above section (2.4.4). It was vital to demonstrate that the assay would work using the same complementary probes but longer target sequences, i.e. PCR product. The longer pathogen DNA will over hang the probe sequences that in theory would raise issues for the assay to perform efficiently, in terms of the sandwich hybridisation and enzyme digestion. The assay steps were carried as before; however instead of adding synthetic pathogen DNA, pathogen PCR product was added to a solution of the complementary *capture* and *reporter* probes. The hybridisation conditions remained the same, as did the bead addition, washings and enzyme digestion.

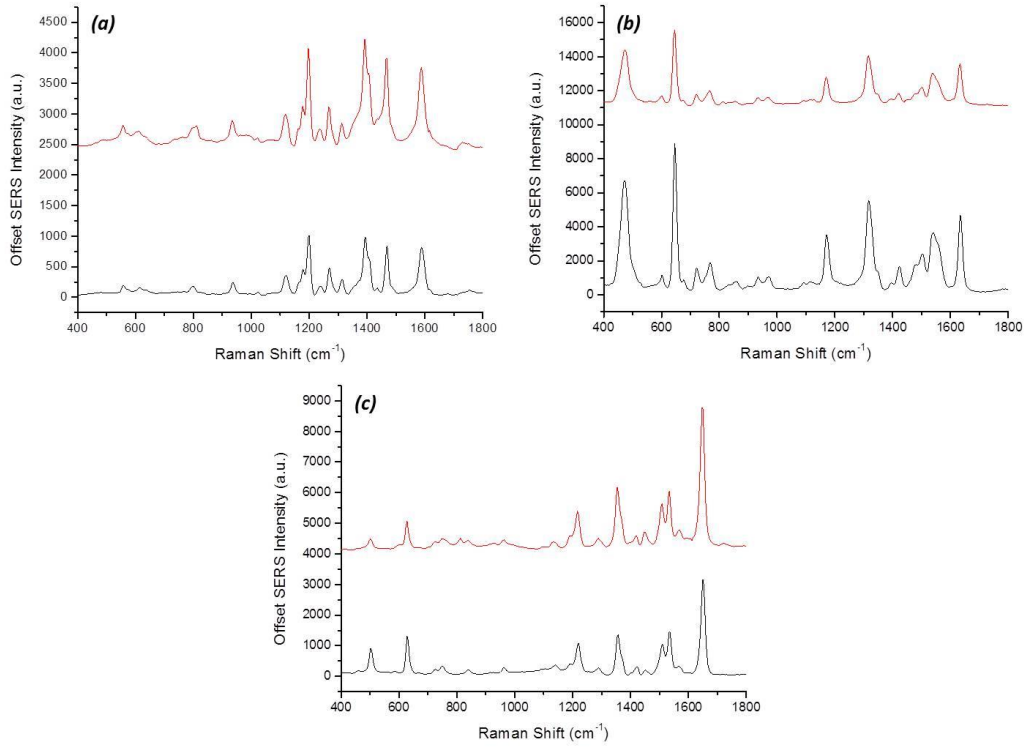

Figure 2.9 Stacked SERS spectra showing the spectra obtained when using PCR product of each pathogen in the assay (red) and the spectra of each dye (black) for comparison. (a) Spectra of *Haemophilus influenzae* PCR product present in the assay (red) and the spectrum of Cy 3 (black). (b) Spectra of *Neisseria meningitidis* PCR product present in the assay (red) and the spectrum of FAM (black). (c) Spectra of *Streptococcus pneumoniae* PCR product present in the assay (red) and the spectrum of TAMRA (black). SERS spectra were recorded using an excitation wavelength of 532 nm with a 10 s (PCR product) or 1 s (dye) accumulation time.

Figure 2.9 shows the spectra obtained when using pathogen PCR product in the assay in place of synthetic pathogen target DNA. For comparison, the individual dye spectra are also shown. As can be seen, the spectra obtained from using PCR product in the assay is that of the dye present on the *reporter* probe. This is a strong indication that the assay does work efficiently when using PCR product, overcoming the issues of hybridisation and enzyme digestion when using longer DNA target sequences. With the knowledge that the assay successfully detects pathogen DNA in both synthetic and PCR product forms, it was now important to determine if the assay could be used for multiplex detection.

2.4.6 Multiplex Pathogen Detection

One of the main aims of this study was to develop a SERS-based assay for the simultaneous detection of three bacterial meningitis pathogens. SERS has been applied to the detection of multiple analytes successfully due to the molecular specific fingerprint spectra that are produced. The three dyes used to detect the pathogens using SERS were FAM (*Neisseria meningitidis*), TAMRA (*Streptococcus pneumoniae*) and Cy3 (*Haemophilus influenzae*). The SERS spectra of FAM and TAMRA are similar which is due to the similarities in their chemical structures (Figure 2.4). By contrast, Cy3 has a markedly different SERS spectrum due to the difference in chemical structure compared to the other two dyes. FAM and TAMRA are xanthene based dyes compared to Cy3, which is an indole based cyanine. Despite the similarity in the SERS spectra of FAM and TAMRA, they can be used successfully in a multiplex system along with Cy3. Multiplex studies were carried out using both synthetic *target* pathogen DNA and with PCR product of each pathogen.

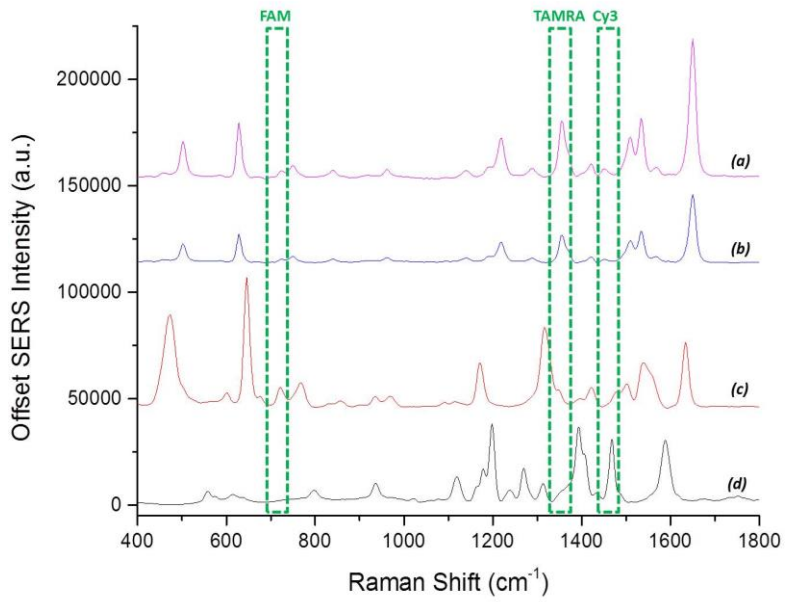

Figure 2.10 Stacked spectra obtained from the simultaneous detection of all three bacterial meningitis pathogens using synthetic target DNA. (a) Multiplex spectra, (b) SERS spectrum obtained when detecting *Streptococcus pneumoniae*, (c) SERS spectrum obtained when detecting *Neisseria meningitidis* and (d) SERS spectrum obtained when detecting *Haemophilus influenzae*. All synthetic target concentrations were 1 µM. SERS spectra were recorded using an excitation wavelength of 532 nm with a 1 s accumulation time. The green boxes show peaks that are unique to each SERS spectrum and hence each pathogen.

Synthetic *target* DNA was used to prove the concept that the three dyes could be used to differentiate between the three pathogens and that they could be detected simultaneously, results are shown in Figure 2.10. Following this, PCR product was then used to establish that the multiplexed assay could be used to analyse clinically relevant CSF samples. For this assay to be considered clinically relevant, it must perform well and produce successful results using pathogen PCR product. As before, with single pathogen detection, all the steps of the assay were performed however in a multiplex scenario, where all three pathogen PCR products and both the complementary probes for each pathogen were present in the one reaction mixture, i.e. nine DNA sequences in total.

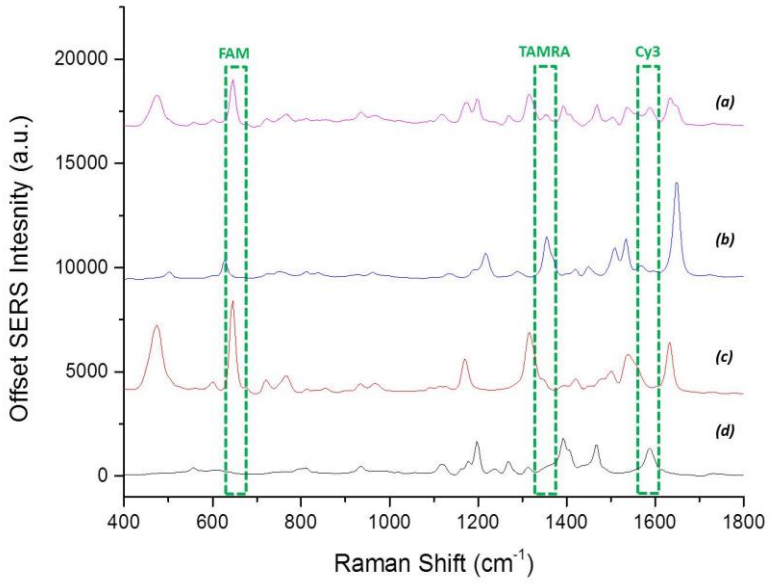

Figure 2.11 Stacked spectra obtained from the simultaneous detection of all three bacterial meningitis pathogens using PCR product. (a) Multiplex spectra, (b) SERS spectrum obtained when detecting *Streptococcus pneumoniae* using PCR product concentration of $2.4x10^4$ copies/µL, (c) SERS spectrum obtained when detecting *Neisseria meningitidis* using PCR product concentration of $1.13x10^5$ copies/µL and (d) SERS spectrum obtained when detecting *Haemophilus influenzae* using PCR product concentration of $7.24x10^5$ copies/µL. SERS spectra were recorded using an excitation wavelength of 532 nm with a 10 s accumulation time. The green boxes show peaks that are unique to each SERS spectrum and hence each pathogen.

Figure 2.11a shows the SERS obtained when detecting all three pathogens simultaneously in the multiplex scenario of the assay. At least one identifiable peak of each dye (Figure 2.11c-d) can be readily observed in the multiplex spectra, indicating that all three targets

have been successfully detected simultaneously using the assay and their presence or absence could be detected using these unique identifying peaks.

2.4.7 Specificity of the Multiplex Detection

When the assay is applied to the detection of one or more of the pathogens, all three *reporter probes* and three *capture probes* will be present, regardless if the target pathogen is present or absent. Therefore, it must be determined that the SERS spectra of the three dyes will only be observed when the associated pathogen is present. The assay was carried out to detect one or more of the pathogens in the presence of all complementary probes by analysis of the SERS spectrum. This was done to ensure that no background signal was obtained from non-complementary probes and that they were all removed through the washing steps in the assay.

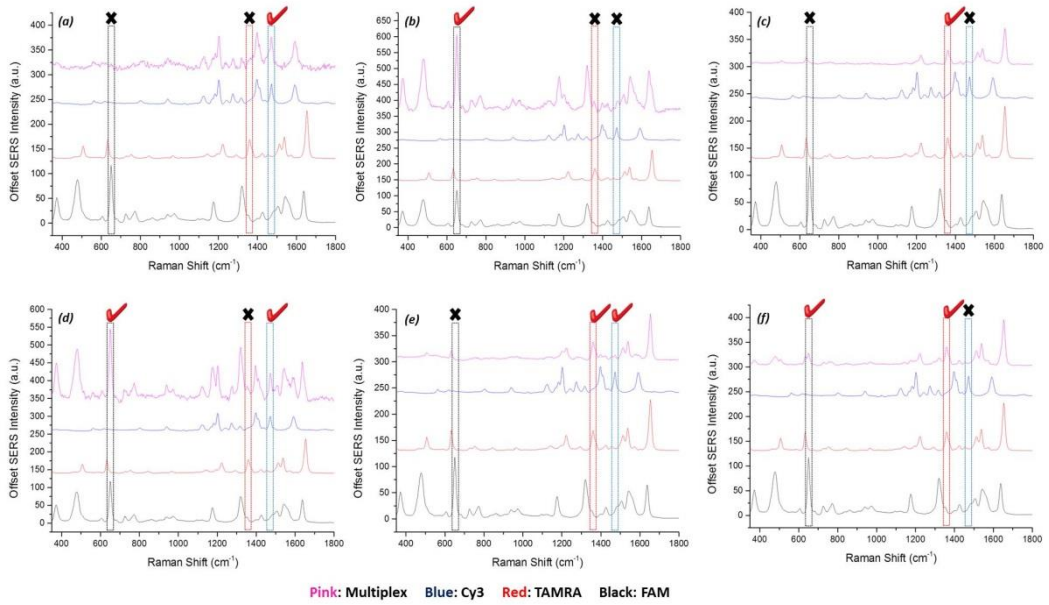

Figure 2.12 Stacked SERS spectra of the different combinations of pathogens and their associated dyes. Each set of spectra have the three dye spectra as references, the blue spectra is Cy3 (*Haemophilus influenzae*), TAMRA (*Streptococcus* pneumoniae) is the red spectra and the black spectra is FAM (*Neisseria meningitidis*). The pink spectra is the SERS spectra after carrying out each step of the assay which should only contain peaks from the pathogen present. Single pathogens in the presence of all complementary probes were detected (a) *Haemophilus influenzae*, (b) *Neisseria meningitidis* and (c) *Streptococcus pneumoniae*. Spectra were taken when detecting two out of the three pathogens with all complementary probes present, (d) *Haemophilus influenzae* and *Neisseria meningitidis*, (e) *Haemophilus influenzae* and *Streptococcus pneumoniae* and finally (f) *Neisseria meningitidis* and *Streptococcus pneumoniae*.

The assay was performed to detect only one of the three pathogens but in the presence of all three *reporter probes* and all three *capture probes*. The SERS spectra of the dye associated with the pathogen present should be the only spectrum observed after the assay is performed due to the multiple washing steps performed that remove any excess or uncomplimentary DNA, regardless of the presence of the other two dyes which should not be seen as the respective target sequence is not present. Figure 2.12a-c are the results obtained when detecting each pathogen individually in such a manner. When detecting *Haemophilus influenzae* and *Streptococcus pneumoniae* individually, it is only the Cy3 or the TAMRA SERS spectra that are observed even when all three dyes are present, showing that the sequences used are highly specific towards the *target* pathogen and in clinical diagnostics this is highly desirable as it would greatly reduce the risk of incorrect pathogen identification. However, when detecting *Neisseria meningitidis* only (Figure 2.12b), peaks from TAMRA and Cy3 were observed arguably at a much lower intensity than that of FAM. To overcome this, the number of wash steps performed after bead addition in the assay could be increased to ensure all non-complementary *reporter probes* are removed prior to enzyme digestions. The results obtained when two target pathogens out of the three were present are shown in Figure 2.12d-f. In each scenario, the unique indicative dye peaks unique to the specific pathogen observed in the spectra are those of the two *reporter probes* that are complementary to the two pathogens present, regardless of the third *reporter probe* being present in the initial assay mixture.

2.4.7 Pathogen Quantification using Chemometrics

The multiplex spectra obtained are multivariate in nature therefore it is difficult to analyse the spectra by eye alone, as can be seen in some of the results obtained in the previous section, where identifiable dye peaks can overlap, for example, the TAMRA and FAM peaks at 1635 cm^{-1} and 1650 cm^{-1}. Furthermore, Cy3 peaks tend to be dominated by TAMRA and FAM spectra therefore, to overcome this, multivariate analysis in the form of principal component analysis and partial least squared regression was performed to generate models to analyse the nature of the multiplex and to quantify the amount of each pathogen present. This was done in collaboration with Prof. Roy Goodacre and Dr. Elon Correa at the University of Manchester.

2.4.7.1 Principle Component Analysis (PCA)

Principal component analysis (PCA) was performed on the multiplex spectra generated from replicate SERS measurements containing equimolar concentrations of each dye labelled oligonucleotide (1 µM), as well as the three separate dye-labelled oligonucleotides (*reporter probes*) associated with each pathogen. The assay was performed to collect the spectra required for each data set. PCA is an excellent approach to reduce the dimensionality of the SERS data.[26]

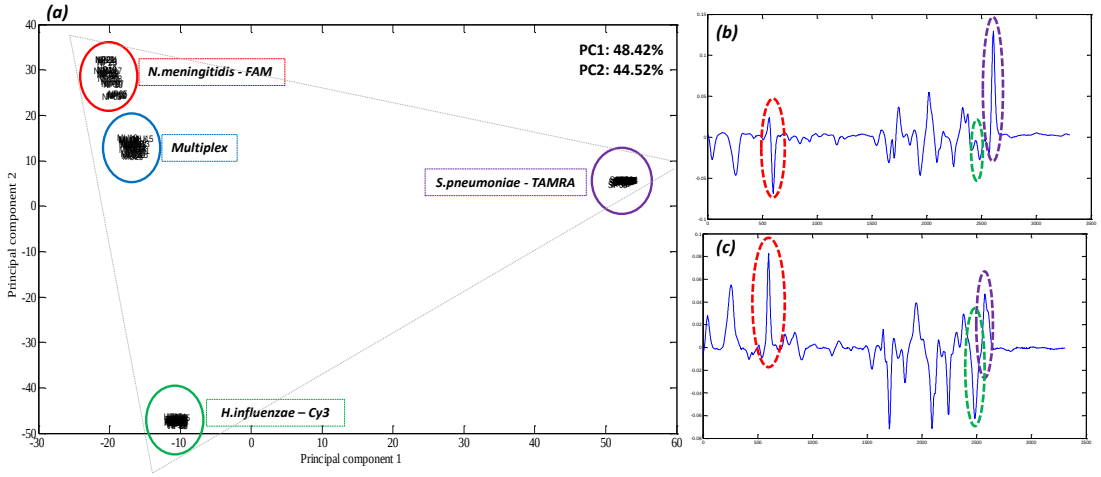

Figure 2.13 (a) PCA scores plot showing the relationship between the multiplex spectra and each of the three single pathogen spectra. 5 scans of each of the 5 replicates were recorded using an excitation wavelength of 532 nm. The loading plots of Principal Component 1 (b) and Principle Component 2 (c) are shown, with FAM, Cy3 and TAMRA peaks highlighted in red, green and purple respectively.

The resulting principal component (PC) scores plot can be seen in Figure 2.13a. The strong relationship the multiplex spectra (blue) has with each of the three pathogen spectra can clearly be seen. The dye-labelled oligonucleotides SERS spectra form the corners of a triangle with the multiplex spectra in between the three dye data sets, indicating the multiplex has some characteristics of each pathogen. Five scans of five replicate samples were collected for each of the four data sets (multiplex, FAM, TAMRA and Cy3) are shown in the PCA plot. Each data set is tightly clustered which strongly indicates that this SERS assay exhibits excellent reproducibility. The PC loading plots for both components are shown in Figure 2.13 b and c. The loadings plot for the first principal component (Figure

2.13b) represents the x-axis of the PCA score plot, with the peaks corresponding to FAM and Cy3 being in the negative region and the TAMRA peak in the positive. The second loadings plot (Figure 2.13c) represents the y-axis of the PCA scores plot that shows the peaks of all three dyes are in the positive region, which is in good agreement with the scores plot. From this PCA analysis, using the two principal components, 92.94 % of the variance within the multiplex data can be explained.

It is noteworthy that the multiplex cluster contains a 1:1:1 mixture of all three *reporter probes* and is positioned closest to the *Neisseria meningitidis* cluster (red), which suggests the multiplex exhibits a stronger FAM signal compared to the other two dye-labelled oligonucleotides due to the FAM spectra perhaps dominating over the other two dye as it may have a greater surface affinity for the nanoparticle. Dye interactions on and off the nanoparticle surface have been investigated in chapters 4 and 5. This means that a more powerful supervised learning method will be needed to accurately quantify the three pathogens in tertiary mixtures.

2.4.7.2 Further Chemometric Analysis for Quantification

Fluorophores are covalently attached to oligonucleotides to aid the detection of DNA sequences. The simultaneous detection of multiple dye labelled oligonucleotides has been successfully achieved using SERS, where 5 labelled oligonucleotides within the one sample were all identified without the need for chemometric analysis.[40] The multiplex was then increased to detect six dye labelled oligonucleotides with the aid of multivariate analysis.[41] Previous chemometric analysis involved the detection of dye labelled oligonucleotides in a premixed solution; the aim of this study was to use chemometric analysis to quantify pathogens in a multiplex mixture after the SERS-based assay had been performed. Initially, mixtures of dye-labelled probes that had not been through the assay were used to generate the models used for predicting the quantities of each pathogen. Following this, the models were tested using dye-labelled oligonucleotides that had been through the SERS-based assay, i.e. post-assay samples. In order to quantify the dye-labelled oligonucleotides in the multiplex, fractional factorial design was used to determine the lowest number of experiments required that would test an equal combination of low, median and high levels

of all three factors (dye-labelled oligonucleotides). Each combination had a final volume of 30 µL and each dye labelled oligonucleotide varied in concentration. This was calculated to be 66 different dye-labelled oligonucleotide ratios, which were analysed by SERS. For ease of visualisation, each set of replicates were averaged to generate 66 SERS spectra prior to PCA. This resulted in the generation of a single PCA scores plot for each dye that shows the quantitative relationship of each of the dye-labelled oligonucleotides within the 66 multiplex SERS mixtures.

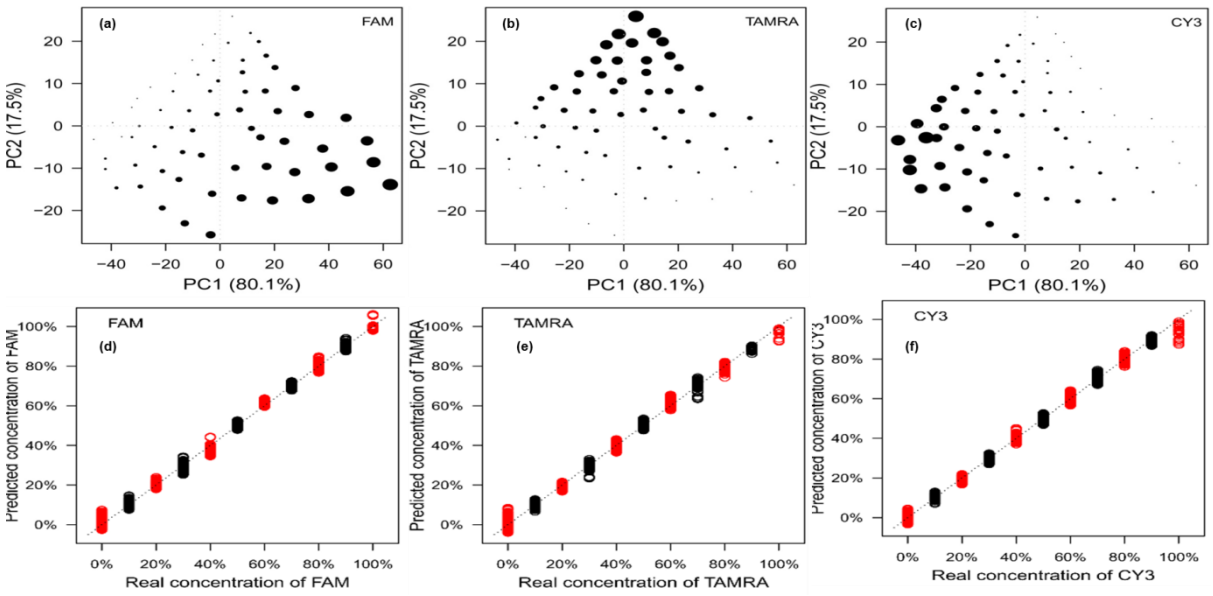

Figure 2.14 (a-c) PCA score plots for each dye-labelled oligonucleotide using averaged replicates of the 66 data points. (d-f) PLS regression models for each dye-labelled oligonucleotide generated using the same 66 average data points. The black spot were used to build the model and the red dots were used to test the linearity of the model. Results show that quantification of each dye is clearly possible.

In Figure 2.14a-c, three PCA plots were produced which have identical PC score locations. The size of the dot is proportional to the concentration of dye-labelled oligonucleotide present in the mixture. The triangular shapes of the score plots are a very good indication that each dye-labelled oligonucleotide present can be quantified. Using the 66 data points generated from the PCA plots, partial least squared (PLS) regression models were constructed (Figure 2.14d-f). The data points were split into two groups, one used to build the PLS model (black) and one used to test the model (red). The three PLS models all show

an expected linear relationship, i.e. they fall on the expected *y=x* line, which further indicates excellent reproducibility and more importantly the dyes can be quantified in a multiplex.

2.4.7.3 Generating and Testing the Chemometric Model

The PCA score plots and PLS regression models were generated using only dye-labelled oligonucleotide mixtures, that is to say that the SERS assay was not performed in full. A second model was then generated that was scaled to a range that would be able to quantify the amount of pathogen present in a post-assay sample. Similar PCA and PLS plots were obtained using the reduced concentrations of the three dye-labelled oligonucleotides and it was now important to test the model. The re-scaled model was tested using "blind" samples, where the actual dye-labelled oligonucleotide concentrations were unknown to the analyst. The results generated by the model (predicted values) were compared to the actual values. Table 2.3 summarises the results obtained from the "blind" test. Some of the best outcomes were the combinations 4, 7 and 10, where there was excellent agreement between the predicted and actual percentages dye-labelled oligonucleotide. However, some of the predicted values were not in good agreement with the actual values, for example, combinations 6, 8 and 12, where the predicted values were much less than the actual values. In particular, in combination 8 the model predicted values for Cy3 and TAMRA where there should not be any dye present, although notably they were very low. With the predictions generated, there is a margin of error and all the results predicted were within these margins (Figure 2.15). Overall, the predicted values are in very good agreement with the actual dye-labelled concentrations used in the assay.

Table 2.3 Comparison of the results obtained from the predictions using the model and the actual dye-labelled oligonucleotide concentrations present.

	Actual Dye-Labelled Oligonucleotide %			Predicted Dye-Labelled Oligonucleotide %		
	FAM	**TAMRA**	**CY3**	**FAM**	**TAMRA**	**CY3**
1	0	0	6.67	0	0	5.53
2	0	0	33.3	0	0	24.7
3	0	6.67	0	0	8.13	0
4	0	6.67	33.3	0	6.27	31.1
5	0	20	20	0	20	17.5
6	0	33.3	6.67	0	25.2	5.73
7	0	33.3	33. 3	0	32	30.2
8	6.67	0	0	5.33	0.2	0.07
9	6.67	0	33. 3	5.8	0	31.1
10	6.67	6.67	6.67	6.2	7.07	6.27
11	6.67	6.67	33.3	6.27	5.8	29.7
12	6.67	20	20	4.07	14.9	16.4
13	6.67	33. 3	0	6.27	25.4	0
14	6.67	33.3	20	4.93	28	18.8
15	6.67	33.3	33.3	6.13	29.9	26.7

The most important testing stage was using samples that had been generated from the detection assay, i.e. post-assay sample testing. This testing was so important as this would mimic the samples that would be used in a clinical environment. The values for pathogen concentration predicted by the model for the post-assay samples were in excellent agreement with the actual concentration values, a very exciting and important result as quantification of pathogen DNA in a clinically relevant sample was successful, regardless of which different pathogens were present. Table 2.4 highlights the results obtained. Combinations 1 and 5 show great agreement between the predicted and actual percentages of the dye-labelled oligonucleotides, however some predictions were not particularly accurate, specifically combinations 6 and 7. The problem here was the model predicted values greater than there should be present. As this testing involved post-assay samples, there is a greater change of incorrect predictions and the greater the values that are predicted could be a results of insufficient wash steps that are needed to remove excess and non-complementary DNA. Nonetheless, the model can be used to successfully predict the amount of each pathogen present in a post-assay multiplex sample.

Table 2.4 Predicted dye-labelled oligonucleotide percentages using post assay samples used to further test the model.

	REAL DYE %			PREDICTED DYE %		
	FAM	**TAMRA**	**CY3**	**FAM**	**TAMRA**	**CY3**
1	6.67	6.67	6.67	7.67	7	6.2
2	6.67	6.67	0	6.4	6.87	0.07
3	6.67	0	6.67	5.87	0	5.93
4	0	6.67	6.67	0	7.27	6.4
5	6.67	0	0	6.47	0	0
6	0	6.67	0	0.8	7.53	2.07
7	0	0	6.67	3.27	0	8.07
8	0	0	0	0.07	0.07	0

Error values were estimated for each dye-labelled oligonucleotide. Normalised root-mean-square error (NRMSE) plots were generated that indicated the error between the actual and predicted concentration values (Figure 2.15). The overlap between the actual concentration values (green) and the predicted concentration values (red) is excellent and indicated that there is a small error associated with the predictions obtained from the PLS model. This emphasises the accuracy and reliability of the chemometric model in predicting the concentration of pathogen present in a multiplex sample. Not only can this detection assay be used to simultaneously detect three bacterial meningitis pathogens, but each pathogen can successfully be quantified in the multiplex using chemometrics.

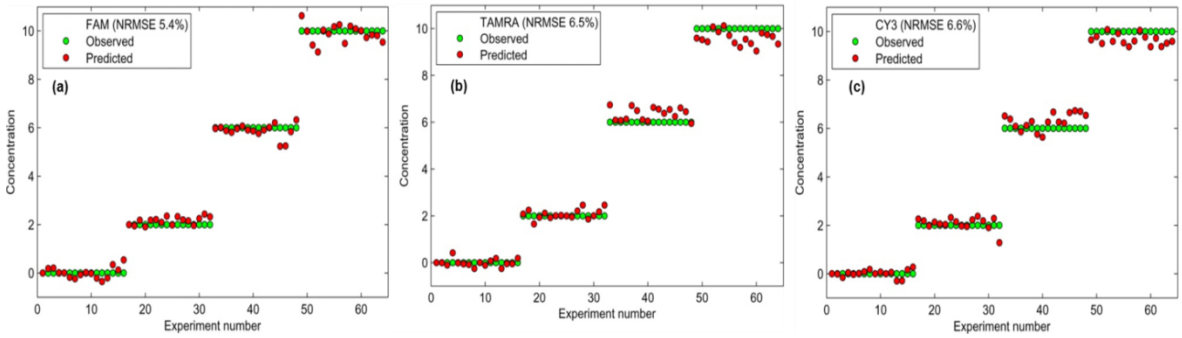

Figure 2.15 Error estimation plots for each dye-labelled oligonucleotide. Overlap between actual values (green) and predicted values (red) shows the closeness of the two values and therefore the normalised root-mean-square error (NRMSE) associated with the predictions.

2.5 Chapter Conclusions

A SERS-based assay was developed for the multiplex detection of three bacterial meningitis pathogens, *Neisseria meningitidis*, *Streptococcus pneumoniae* and *Haemophilus influenzae*. Consideration was taken when designing the dye-labelled oligonucleotide (*reporter*) probe that was used to aid the detection of each pathogen. It was found that instead of having the free dye after enzyme digestion, a spacer molecule that halts enzyme digestion was used in the sequences that left 10 adenine bases attached to the dye that enhanced the SERS peaks unique to that dye. Once the design of the *reporter* probe was finalised, the assay was used to detect each pathogen individually. Successful results were obtained showing the assay to have strong specificity by using two controls, no target and non-complementary where the pathogen sequence was omitted from the assay. Limits of detection studies were performed showing that each pathogen could be detected down to the pico-molar range, advantageous for clinical assays. To determine if this assay developed was suitable for clinical use, PCR product of each pathogen was generated and used in the assay producing equally successive results when using synthetic pathogen DNA. Multiplex studies were then performed using both synthetic DNA and PCR product. The multiplex format of the assay proved to be successful using both forms of the pathogen DNA, which proved that the SERS-based assay can be used for the simultaneous detection of the three bacterial meningitis pathogens. This work was the first report of using chemometric analysis to quantify pathogen DNA is a multiplex post-assay mixture. By using principal component analysis (PCA), generating PLS regression models and multiple testing stages of the models, quantification of each pathogen was successful.

This method of bacterial meningitis detection produces consistent results faster than conventional methods and through the development of the multiplex assay and the use of chemometrics for quantification, this detection method is a promising alternative to current PCR methods of detection and could potentially be applied to a variety of bacterial, fungal and viral diseases.

2.6 Chapter References

1. R. K. Gupta, J. Best and E. MacMahon, *British Medical Journal*, 2005, **330**, 1132-1135.
2. Meningitis Research Foundation, http://www.meningitis.org/, **2014**.
3. K. Gracie, E. Correa, S. Mabbott, J. A. Dougan, D. Graham, R. Goodacre and K. Faulds, *Chemical Science*, 2014, **5**, 1030-1040.
4. C. E. Corless, M. Guiver, R. Borrow, V. Edward-Jones, A. J. Fox and E. B. Kaczmarski, *Journal of Clinical Microbiology* 2001, **39**, 1553-1558.
5. L. Kupila, T. Vuorinen, R. Vainionpaa, V. Hukkanen, R. J. Marttila and P. Kotilainen, *Neurology*, 2006, **66**, 75-80.
6. S. A. E. Logan and E. MacMahon, *British Medical Journal*, 2008, **336**, 36-40.
7. J. McVernon, C. L. Trotter, M. P. E. Slack and M. E. Ramsay, *British Medical Journal*, 2004, **329**, 655-658.
8. K. Subramanian, W. Rutvisuttinunt, W. Scott and R. S. Myers, *Nucleic Acids Research*, 2003, **31**, 1585-1596.
9. K. R. Thomas and B. M. Olivera, *Journal of Biological Chemistry*, 1978, **253**, 424-429.
10. N. G. Nossal and M. F. Singer, *Journal of Biological Chemistry*, 1968, **243**, 913-&.
11. K. S. Sriprakash, N. Lundh, M. Mooonhuh and C. M. Radding, *Journal of Biological Chemistry*, 1975, **250**, 5438-5445.
12. J. W. Little, *Journal of Biological Chemistry*, 1967, **242**, 679-686.
13. R. Kovall and B. W. Matthews, *Science*, 1997, **277**, 1824-1827.
14. J. Zhang, K. A. McCabe and C. E. Bell, *Proceedings of the National Academy of Sciences*, 2011, **108**, 11872-11877.
15. S. E. J. Bell and N. M. S. Sirimuthu, *Journal of the American Chemical Society*, 2006, **128**, 15580-15581.
16. D. Graham, B. J. Mallinder and W. E. Smith, *Angewandte Chemie-International Edition*, 2000, **39**, 1061-+.
17. D. Graham, B. J. Mallinder, D. Whitcombe, N. D. Watson and W. E. Smith, *Analytical Chemistry*, 2002, **74**, 1069-1074.
18. A. MacAskill, D. Crawford, D. Graham and K. Faulds, *Analytical Chemistry*, 2009, **81**, 8134-8140.
19. H. N. Wang and T. Vo-Dinh, *Nanotechnology*, 2009, **20**.
20. M. J. Espy, J. R. Uhl, L. M. Sloan, S. P. Buckwalter, M. F. Jones, E. A. Vetter, J. D. C. Yao, N. L. Wengenack, J. E. Rosenblatt, F. R. Cockerill III and T. F. Smith, *Clinical Microbiology Reviews*, 2006, **19**, 165-256.
21. R. T. Ranasinghe and T. Brown, *Chemical Communications*, 2005, 5487-5502.
22. J. A. Dougan, D. MacRae, D. Graham and K. Faulds, *Chemical Communications*, 2011, **47**, 4649-4651.
23. P. C. Lee and D. Meisel, *Journal of Physical Chemistry*, 1982, **86**, 3391-3395.
24. S. Mabbott, E. Correa, D. P. Cowcher, J. W. Allwood and R. Goodacre, *Analytical Chemistry*, 2012, **85**, 923-931.
25. H. F. M. Boelens, P. H. C. Eilers and T. Hankemeier, *Analytical Chemistry*, 2005, **77**, 7998-8007.
26. D.-H. Kim, R. M. Jarvis, Y. Xu, A. W. Oliver, J. W. Allwood, L. Hampson, I. N. Hampson and R. Goodacre, *Analyst*, 2010, **135**, 1235-1244.

27. S. Mabbott, A. Eckmann, C. Casiraghi and R. Goodacre, *Analyst*, 2013, **138**, 118-122.
28. H. Martens and T. Naes, *Multivariate Calibration*, Wiley, 1991.
29. V. Esposito Vinzi, W. W. Chin, J. Henseler and H. E. Wang, *Handbook of Partial Least Squares*, Springer, 2010.
30. P. B. McIntyre, K. L. O'Brien, B. Greenwood and D. van de Beek, *Lancet*, 2012, **380**, 1703-1711.
31. G. Tzanakaki, M. Tsopanomichalou, K. Kesanopoulos, R. Matzourani, M. Sioumala, A. Tabaki and J. Kremastinou, *Clinical Microbiology and Infection*, 2005, **11**, 386-390.
32. X. Wang, M. J. Theodore, R. Mair, E. Trujillo-Lopez, M. du Plessis, N. Wolter, A. L. Baughman, C. Hatcher, J. Vuong, L. Lott, A. von Gottberg, C. Sacchi, J. M. McDonald, N. E. Messonnier and L. W. Mayer, *Journal of Clinical Microbiology*, 2012, **50**, 702-708.
33. H. Sadighian and M. R. Pourmand, *Iranian Journal of Public Health*, 2009, **38**, 60-68.
34. P. Radstrom, A. Backman, N. Qian, P. Kragsbjerg and C. Pahlson, *Journal of Clinical Microbiology*, 1994, **32**, 2738-2744.
35. G. M. K. Abdeldaim, K. Stralin, J. Korsgaard, J. Blomberg, C. Welinder-Olsson and B. Herrmann, *Bmc Microbiology*, 2010, **10**.
36. R. Ghotaslou, S. Farajnia, F. Yeganeh, S. Abdoli-Oskouei, M. Ahangarzadeh Rezaee and M. Barzegar, *Acta medica Iranica*, 2012, **50**, 192-196.
37. M. M. Harper, J. A. Dougan, N. C. Shand, D. Graham and K. Faulds, *Analyst*, 2012, **137**, 2063-2068.
38. E. Smith and G. Dent, *Modern Raman Spectroscopy: A Practical Approach*, Wiley, 2005.
39. K. Faulds, R. P. Barbagallo, J. T. Keer, W. E. Smith and D. Graham, *Analyst*, 2004, **129**, 567-568.
40. K. Faulds, F. McKenzie, W. E. Smith and D. Graham, *Angewandte Chemie International Edition*, 2007, **46**, 1829-1831.
41. K. Faulds, R. Jarvis, W. E. Smith, D. Graham and R. Goodacre, *Analyst*, 2008, **133**, 1505-1512.

3. Interaction of Fluorescent Dyes with DNA and Spermine using Fluorescence Spectroscopy

3.1 Introduction

Oligonucleotides labelled with fluorescent dyes are widely used as probes for the identification of DNA sequences using detection methods involving optical spectroscopies such as fluorescence and surface enhanced Raman scattering (SERS).[1, 2] Spermine is widely used in SERS and surface enhanced fluorescence (SEF) assays[3] as a charge-reduction aggregating agent as it interacts strongly with the phosphate backbone of the oligonucleotide and is shown to enhance the signal of labelled oligonucleotides. It is important to understand the interactions involving the fluorescent dyes as certain interactions could potentially effect the fluorescence emission observed. Possible interactions include; dye-DNA interactions and dye-spermine interactions. This is also important for SERS based assays as these dye interactions could also affect the SERS intensity observed. By using fluorescence spectroscopy, an understanding into the dye interactions away from the nanoparticle surface could be gained.[4]

3.1.1 Applications of Fluorescent Dyes

Fluorescent dyes are widely used in biological applications, for example in cell imaging,[5] monitoring protein interactions[6] and nucleic acid detection.[7, 8] Nucleic acids are essential in living organisms as they are responsible for storing and transmitting genetic information. Oligonucleotide probes are single stranded nucleic acids that are designed to have high specificity and selectivity towards particular targets such as nucleic acids, proteins and small molecules.[9] Fluorescent labels, such as carboxyfluorecein (FAM) and carboxytetramethylrhodamine (TAMRA) enable highly selective and sensitive detection of biological targets and have become widely used in research and numerous applications

such as the visualisation of DNA amplification in the polymerase chain reaction (PCR).[10, 11] Oligonucleotide-based fluorescent probes consist of a specific DNA sequence covalently attached to a fluorescent dye, Figure 3.1 is a schematic of a oligonucleotide fluorescent probe.[9] Different fluorescent dyes have been used to generate oligonucleotide probes such as TAMRA, fluorescein, HEX and rhodamine-6 green.[12, 13] In fluorescence quenching applications, quencher molecules such as black hole quenchers (BHQ) can also be attached to the oligonucleotide.[14] Fluorescent dyes and quenchers are selected based upon the desired application and considerations such as pH dependence and fluorescent dye position on the DNA sequence must be taken into account.[15-17]

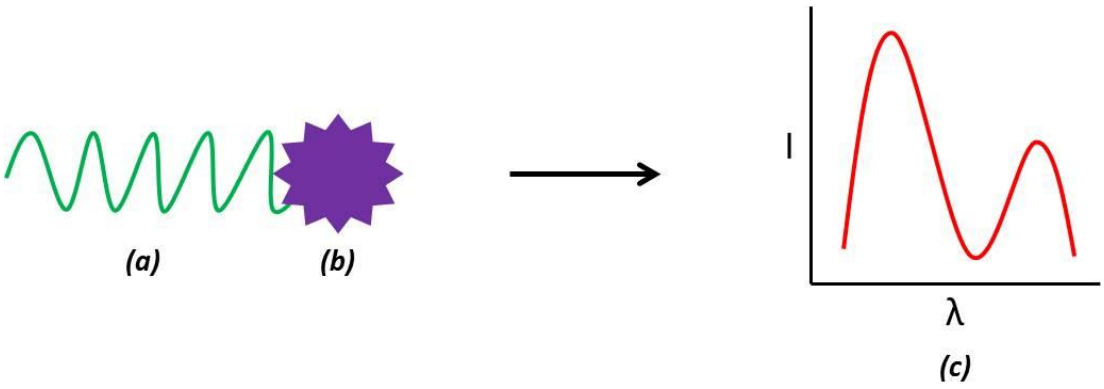

Figure 3.1 Schematic of an oligonucleotide probe. A DNA sequence (a) is covalently attached to a fluorescent dye (b). The fluorophore transforms biorecognition events (e.g. hybridisation) into a fluorescent signal (c).

DNA hybridisation is a recognition event and can be monitored using oligonucleotide probes. These probes are called hybridisation probes and are used in many applications involving the detection of nucleic acids. Applications of hybridisation probes include DNA microarray chips,[18] monitoring intracellular mRNA[19, 20] and monitoring the amplification progress in real time PCR.[21, 22] Hybridisation probes are widely used in molecular biology and molecular diagnostics for the detection of DNA hybridisation using methods such as PCR and fluorescence in-situ hybridisation (FISH).[23] There are two forms of hybridisation probes; binary probes and molecular beacons. Binary probes are mainly used in fluorescence resonance energy transfer (FRET) systems (Figure 3.2a).[10, 20, 24] They are half-complementary probes, one is labelled with a fluorescent dye and the other can be labelled with another fluorescent dye or a quencher molecule. Molecular beacons are the most common form of hybridisation probes and were first reported by Tyagi *et al* in 1996.[19] They

are based on fluorescence quenching and complementary base pairing (Figure 3.2b). Binary probes are advantageous as they do not produce and false positives or non-specific signals; however the kinetics of hybridisation favour molecular beacons, as binary probe hybridisation relies on two events.

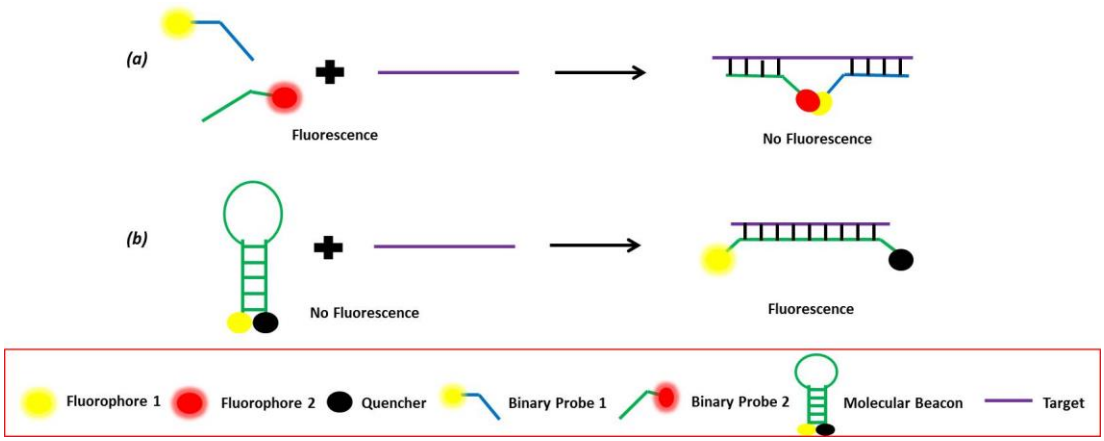

Figure 3.2 A schematic of the two forms of hybridisation probes. (a) Binary probes where before hybridisation there is large fluorescence intensity, then upon hybridisation and due to a FRET mechanism there is a significant reduction in fluorescence intensity. (b) Molecular beacons, the arm sequences are self-complementary, therefore in the absence of target the loop remains closed and fluorescence in quenched due to the proximity of the quencher molecule to the fluorophore. Then upon hybridisation to complementary target sequence, the fluorophore and quencher are separated and fluorescence intensity is significantly increased.

In the field of molecular diagnostics, there is a push for more information rich assays that produce results in a short time frame. This can involve *in situ* detection in a complex matrix such as cell lysate, extracted DNA or PCR product. It is a fair assumption to make that there will be a high chance of the fluorophores interacting with the specific matrix, which can then alter the intensity of the fluorescent dye emission. This is a major consideration when multiple targets/fluorescent dyes are to be detected in the one sample where the interactions that take place will be dye specific.

3.1.2 Base Quenching

Fluorescence emission can be quenched in various ways, for example by using two fluorophores as a FRET pair where one accepts the fluorescence of another thereby quenching the fluorescence (FRET)[25] or using quencher molecules where the energy can be transferred and emitted as heat instead of light. This is what occurs in molecular beacons, fluorescence emitted from a fluorophore will be quenched by a quencher molecule when they are in close proximity, i.e. when the beacon is closed.[19] However, the fluorescence emitted by a fluorophore can also be quenched by a nucleobase, in particular guanine.[26-28] Guanine acts as a fluorescence energy acceptor through a photoinduced electron transfer mechanism.[27, 29] This phenomenon has been used to quantitatively detect specific DNA sequences,[30] protein mutations,[28] and single base alterations.[31] Guanine quenching has also facilitated numerous studies focussing on the hybridisation of complementary oligonucleotides.[28] Nazarenko *et al*. reported that upon hybridisation of complementary DNA sequences, there was only a decrease in the fluorescence intensity emitted by fluorescein when either d(CC) or d(GG) bases and the fluorescent dye were both present at the 5' terminus of the sequence.[17] Therefore, the design of oligonucleotide sequences is important when using fluorescence detection in hybridisation assays for the detection of specific DNA sequences.[32] Although the quenching effect of guanine can be used for the detection of DNA and other biomolecules, it can be considered a major drawback when carrying out fluorescence measurements where quenching of the fluorescence emitted by the fluorophore is undesirable.

3.1.3 Spermine

Polyamines, such as spermine, belong to a large group of biogenic amines that are involved in many physiological functions such as cell growth and proliferation and they are also involved in the synthesis of DNA and RNA.[33] Generally, polyamines are low molecular weight aliphatic amines that are water soluble and have a pK_a of around 10. They are protonated at physiological pH meaning they are polycations, which explains why they have such strong interactions with polyanionic macromolecules such as DNA.[34, 35] Spermine is reported to have a strong interaction with DNA. Basu *et al*. studied the effect of spermine on the aggregation and melting temperatures of calf-thymus DNA. Results showed that

spermine encourages DNA aggregation and can cause the melting temperatures of the DNA to increase as the spermine concentration is increased.[36]

Many molecular studies have been performed to determine the effects of polyamines on double stranded DNA. Models were proposed that showed an interaction between the protonated polyamine group and the negatively charged double stranded DNA focussing on the electrostatic interactions, however direct interactions between the two were discarded.[37, 38] Further studies on polyamine analogues showed that in addition to electrostatic effects between the polyamine and double stranded DNA, structural specificities were also a major component between the interaction of spermine and double stranded DNA.[39] X-Ray diffraction studies of spermine-DNA crystals showed that the spermine was positioned across the major groove of double stranded DNA meaning that the spermine did come into contact with the bases.[40, 41] However, it was still unclear whether these specific binding sites existed in solution samples of spermine-DNA complexes. NMR studies on DNA solutions were carried out which indicated that the spermine-DNA interactions were highly localised therefore, it is not purely a result of electrostatic interactions.[42, 43] It was also believed that the NMR model alone cannot fully explain the spermine-DNA interactions as it was still believed that structural specificities would play a major role.[44] Ruiz-Chica *et al*. studied the interaction between double stranded DNA and spermine by FT-Raman spectroscopy to achieve a deeper understanding of the spermine-DNA interaction in solution.[45] They concluded that there were specific binding sites, between the spermine NH_3^+ groups and either the purine-N7 or thymine-O4 atoms, and this was in addition to the electrostatic effects previously reported.

3.1.3.1 Application of Spermine in SERS

Aggregating agents are essential when using SERS as a method of analysis. For enhancement to occur, the nanoparticles need to aggregate to produce hotspots that generate the enhanced signals.[46-48] The polyamine spermine is an example of an aggregating agent used in SERS analysis, particularly for the detection of DNA. Spermine interacts with DNA, reducing the negative charge of the phosphate backbone allowing the DNA to come into close proximity to the nanoparticle surface and causing an enhancement

in the signal generated.[36] Spermine has also shown to attach onto the nanoparticle surface, changing the overall surface charge to positive that will also encourage aggregation of the nanoparticles.[49] Figure 3.3 is a schematic outlining the action of spermine as an aggregating agent and how this compares to nanoparticle aggregation caused by the addition of a salt.

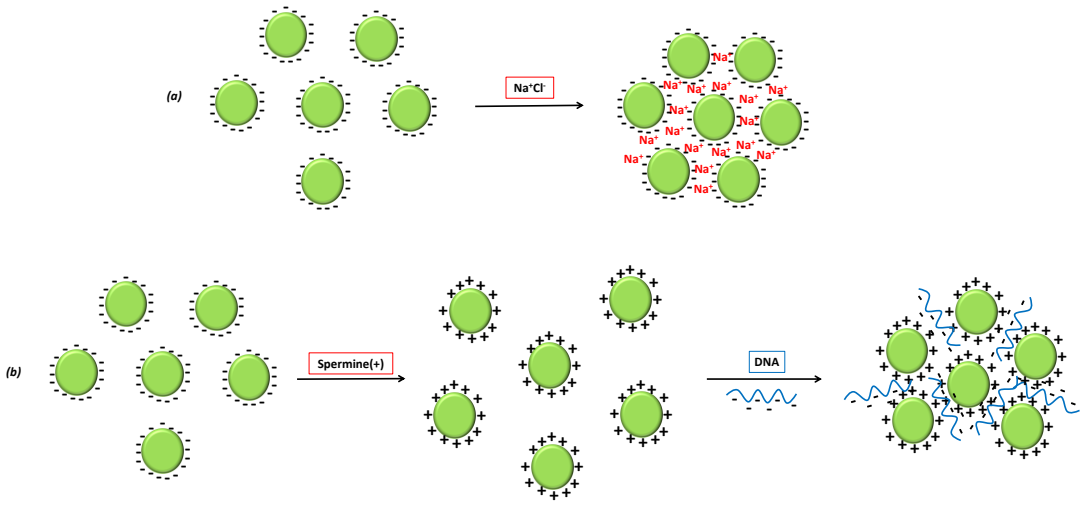

Figure 3.3 A schematic representation of nanoparticle aggregation caused by (a) salt, NaCl and (b) spermine. Aggregation caused by the addition of a salt is due to the charge screening effect that allows the nanoparticles to come closer to one another, whereas nanoparticle aggregation caused by the addition of spermine is a result on the surface charge on the nanoparticle changing from negative to positive, therefore in the presence of negatively charged DNA, the nanoparticles can form aggregates (drawings not to scale).

Spermine is widely used in surface enhanced detection methods such as surface enhanced fluorescence (SEF)[3] and SERS,[2] especially for the detection of DNA. Enhanced fluorescence was obtained from dye labelled DNA using spermine and aggregated silver nanoparticles.[3, 50] SERS detection of unlabelled DNA has also been obtained without the use of fluorescent dyes through the presence of spermine acting as an aggregating and charge reducing agent.[1]

3.2 Aims

Due to the wide application of fluorophores in biological detection assays that use optical techniques such as fluorescence or surface enhanced Raman scattering (SERS), it is

important to gain an insight into the possible interactions that can occur between the different molecules involved and the effect these have on the spectroscopic response. This study used fluorescence spectroscopy to investigate the interactions between two commonly used fluorophores, FAM and TAMRA, with DNA and more importantly the interaction of the two fluorophores with spermine, which is used extensively in metal surface enhanced assays such as SEF and SERS. The effects of spermine addition on the fluorescence intensity of the two fluorophores were compared and different experimental conditions were used, for example changing the pH and reagent concentration. The overall outcome of this study has a significant impact on the choice of fluorophores and experimental conditions when developing a biological detection assay.

3.3 Experimental

3.3.1 Oligonucleotides

All sequences were purchased on a 0.2 µM scale with HPLC purification from Eurofins MWG (Ebersberg, Germany), shown in Table 3.1.

Table 3.1 Modified oligonucleotides and complementary oligonucleotide sequence used in this investigation

Name	Sequence (5'-3')	Modifications
TAMRA labelled oligonucleotide	GGTTCATATAGTTATAATAA	5' TAMRA
FAM labelled oligonucleotide	GGTTCATATAGTTATAATAA	5' FAM
Complementary Sequence	TTATTATAACTATATGAACC	-
FAM Sequence 2	CATTGCCACGTG-Spacer18-10A	3' FAM
Complementary FAM Sequence 2	ATGTGCAGCTGACACGTGGCAATG	-
TAMRA Sequence 2	TGGCGCCCATAA-Spacer18-10A	3' TAMRA
Complementary TAMRA Sequence 2	TTCGAGTGTTGCTTATGGGCGCCA	-

3.3.2 Reagents and Buffers

Spermine hydrochloride and triethylamine (TEA) were purchased from Sigma Aldrich (Dorset, UK) and a stock solution of 0.1 M was prepared and diluted when required.

3.3.3 Fluorescent Instrumentation

Fluorescent measurements were recorded using a Horiba Scientific Fluorolog 3-22, which comprised of an Ushio UXL 450S-O 450 W Xenon short arc lamp as an excitation source, a 200-900 nm double grating excitation and emission monochromators and a R928 Hamamatsu photomultiplier tube. When measuring the FAM fluorescence emission the excitation wavelength was set to 494 nm with a scanning range 500-560 nm and when measuring TAMRA emission the excitation wavelength was set to 560 nm and the scanning range was 570-630 nm. The integration time was set to 0.1 sec and the slits widths were 5 nm for both excitation and emission. For each experiment, three replicate samples were prepared and each replicate was measured five times.

3.3.4 Effects of DNA Attachment on Fluorescence Emission

The fluorescence emission was recorded of the free dyes, F-ITC and TR-ITC, and dye labelled single stranded DNA sequences (FAM and TAMRA) was carried out by adding a solution of the free dye or dye labelled single stranded DNA (100 µL, 1 µM) to a 1.5 mL disposable PMMA microcuvette, containing distilled water (300 µL). Three replicates of each sample were analysed 5 times using the instrumental settings described in section 3.3.3.

3.3.5 Effects of Spermine Addition on Fluorescence Emission

To determine the effect spermine had on the fluorescence emission of the two dyes, free dye or dye labelled single stranded DNA (100 µL, 1 µM) was added to a 1.5 mL disposable PMMA microcuvette containing distilled water (300 µL). Fluorescence measurements were recorded (section 3.3.3) before and after the addition of spermine (50 µL, 0.1 M). Three replicates of each sample were analysed 5 times.

3.3.6 Concentration Studies

Concentration studies were carried out to determine if the effects observed by DNA attachment and spermine addition were concentration dependent.

3.3.6.1 Fluorescent Dye Labelled DNA Concentration Study

An initial concentration of 1 nM to 1 μM of dye labelled single stranded DNA was used to observe the effects of spermine addition at different concentration levels. This was performed by adding FAM or TAMRA labelled single stranded DNA with varying concentrations (100 μL) to a 1.5 mL disposable PMMA microcuvette containing distilled water (300 μL). Fluorescence measurements were recorded before and after the addition of spermine (50 μL, 0.1 M) at each dye labelled single stranded DNA concentration. The instrument settings were those outlined in section 3.3.3. Three replicates of each sample were analysed 5 times.

3.3.6.2 Spermine Concentration Study

The dye labelled single stranded DNA concentration remained constant (1 μL), however the concentration of the spermine added varied from 100 μM to 500 mM. Both FAM and TAMRA labelled single stranded DNA were used. To 1.5 mL disposable PMMA microcuvette containing distilled water (300 μL), dye labelled single stranded DNA (100 μL, 1 μM) and spermine with varying concentration (50 μL) was added. Fluorescence measurements were recorded as described in section 3.3.3. Three replicates of each sample were analysed 5 times.

3.3.7 pH Studies

The fluorescence emission of FAM and TAMRA labelled single stranded DNA sequences was measures before and after spermine addition over a pH range. Three different solutions were used for the pH studies. 250 mM trisodium citrate was prepared and pH was adjusted to 2.9 using HCl. 10 mM phosphate buffered saline, pH 6.9, was prepared by dissolving one tablet (Sigma Aldrich) in 200 mL distilled water. Finally, 1 M NaOH was prepared and pH was measured to be 13.2. The dye labelled single stranded DNA sequence (100 μL, 1 μM) was added to a 1.5 mL disposable PMMA microcuvette that contained one of the four solutions with varying pH (300 μL). Fluorescence measurements were recorded before and after spermine addition (50 μL, 0.1 M) using the instrument settings described in section 3.3.3. Three replicates of each sample were analysed 5 times.

3.3.8 Double Stranded DNA Studies

Fluorescent measurements were recorded under different experimental conditions using FAM or TAMRA labelled double stranded DNA.

3.3.8.1 DNA Hybridisation

To a 1.5 mL eppendorf, both the dye labelled single stranded DNA sequence (100 µL, 1 µM) and the complementary sequence (100 µL, 1 µM) was added to phosphate buffered saline, PBS (200 µL, 0.3 M). DNA hybridisation was carried out using an MJ Research Minicylcer™. The temperature was increased to 90 °C for 10 minutes then decreased to 10 °C for another 10 minutes.

3.3.8.2 Effects of Spermine Addition on Fluorescence Emission

Analysis of the effects of spermine addition on the fluorescence emission of FAM and TAMRA when they were covalently attached to double stranded DNA was carried out by adding a solution of dye labelled double stranded DNA (200 µL, 1 µM) to a 1.5 mL disposable PMMA microcuvette containing distilled water (200 µL). Fluorescence measurements were recorded before and after spermine addition (50 µL, 0.1 M) using the settings outlines in section 3.3.3. Three replicates of each sample were analysed 5 times.

3.3.8.3 Spermine Concentration Study

The same spermine concentration range used in section 3.3.6.2 (100 µM to 500 mM) was applied to the analysis of dye labelled double stranded DNA. Dye labelled double stranded DNA (200 µL, 1 µM) was added to a 1.5 mL disposable PMMA microcuvette containing distilled water (200 µL) followed by a solution of spermine with varying concentration (50 µL). Fluorescence measurements were recorded using the settings described in section 3.3.3. Three replicates of each sample were analysed 5 times.

3.3.8.4 pH Study

The fluorescence emission of FAM and TAMRA labelled double stranded DNA was measured over a pH range. The four solutions used in section 3.3.7; citrate acid (pH 2.9),

distilled water (pH 5.2), PBS (pH 6.9) and NaOH (pH 13.2) were also used in these experiments. Dye labelled double stranded DNA (200 µL, 1 µM) was added to a 1.5 mL disposable PMMA microcuvette containing on of the four solutions with varying pH (200 µL). Fluorescence measurements were recorded before and after the addition of spermine (50 µL, 0.1 M) using the setting described in section 3.3.3. Three replicates of each sample were analysed 5 times.

3.3.9 Triethylamine (TEA) Comparison Studies

For comparison studies, triethylamine (TEA) was added to the sample mixture in place of spermine. Dye labelled single and double stranded DNA was used. For dye labelled single stranded DNA experiments, to a 1.5 mL disposable PMMA microcuvette that contained distilled water (300 µL) dye labelled single stranded DNA (100 µL, 1 µM) was added. For dye labelled double stranded DNA experiments, to a 1.5 mL disposable PMMA microcuvette, distilled water (200 µL) was added followed by dye labelled double stranded DNA (200 µL, 1 µM). Fluorescence measurements were recorded before and after the addition of TEA (50 µL, 0.1 M) using the instrumental settings outlined in section 3.3.3. Three replicates of each sample were analysed 5 times.

3.3.10 Sequence Specification Studies

To determine the effect the particular DNA sequence had on the fluorescence emission of FAM and TAMRA, fluorescence measurements were recorded when FAM and TAMRA were attached to different sequences that were previously used (FAM/TAMRA sequence 2, Table 3.1). Analysis was carried out using dye labelled single and double stranded DNA. For dye labelled single stranded DNA experiments, to a 1.5 mL disposable PMMA microcuvette that contained distilled water (300 µL) dye labelled single stranded DNA (100 µL, 1 µM) was added. For dye labelled double stranded DNA experiments, to a 1.5 mL disposable PMMA microcuvette, distilled water (200 µL) was added followed by dye labelled double stranded DNA (200 µL, 1 µM). Fluorescence measurements were recorded before and after the addition of spermine (50 µL, 0.1 M) using the instrument settings described in section 3.3.3. Three replicates of each sample were analysed 5 times.

3.4 Results and Discussion

Fluorescent labelling is widely used in molecular diagnostics to facilitate the detection of DNA sequences coding for particular diseases. Specific DNA sequences are modified with a fluorescent dye and the response of the fluorophore measured using either fluorescence[51] or surface enhanced Raman scattering (SERS).[52] The development of assays for the detection of multiple targets is of increasing importance as more informative assays are sought and in some formats this involves the comparison of emission or scattering from more than one fluorophore. However, fluorescent dyes are susceptible to interactions with the nucleobases in a DNA sequence[53] and to conditions such as pH and concentration. In addition, spermine has been used extensively in studies involving surface enhanced fluorescence (SEF)[3, 50] and SERS.[1, 2] Spermine, shown in Figure 3.4c, is used to reduce the negative charge on the surface of a nanoparticle and on the DNA allowing the DNA sequence to come into close proximity to the nanoparticle and, if required, to aid nanoparticle aggregation. To characterise the effect of changing conditions and of adding spermine, fluorescence from two commonly used dyes were compared at different pHs and concentrations in the presence and absence of the bases spermine and triethylamine. The two fluorophores used were FAM and TAMRA (Figure 3.4a-b) and for the majority of the experiments the dyes were attached to the same DNA sequence to eliminate the issue of sequence specific affects; however, to determine if the sequence did have an effect on the fluorescence, different sequences attached to FAM and TAMRA were analysed.

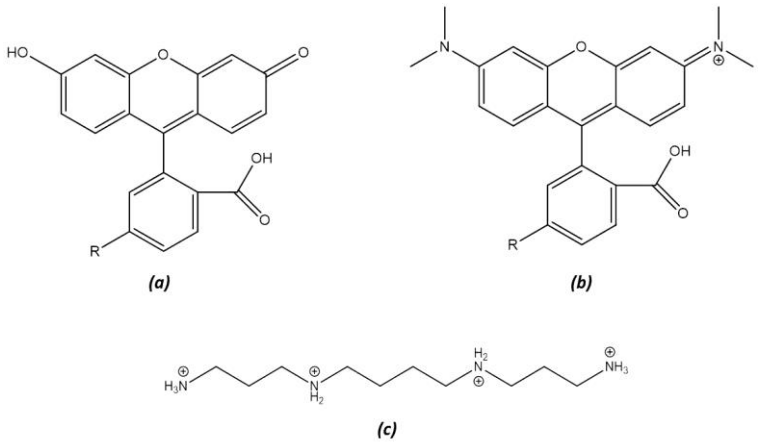

Figure 3.4 The structures of the two fluorophores used in this study and spermine. (a) Structure of FAM, (b) Structure of TAMRA. In both cases R = NHS ester when the fluorophore is attached to an oligonucleotide and R = isothiocyanate when measurements were performed on the *free* dye. (c) Structure of spermine. The structures shown are those present at physiological pH.

3.4.1 Effects of DNA Attachment and Spermine Addition on Fluorescence Emission

Initially the effect on the fluorescence of attachment of the dye to an oligonucleotide sequence and the effect of adding spermine to the dye labelled oligonucleotide on the fluorescence emission were investigated. The fluorescence from 22 nM solutions of the free dyes FAM isothiocyanate (F-ITC) and TAMRA isothiocyanate (TR-ITC) along with FAM labelled oligonucleotide and TAMRA labelled oligonucleotide was measured before and after spermine (50 µL, 0.1 M) addition (Figure 3.5). It should be noted that no change in pH was observed following the addition of spermine, the pH remained at 5.2 throughout the experiments.

Fluorescence spectra were recorded of the free dyes and the dye labelled DNA sequences. The fluorescence emission of FAM decreases when the dye is covalently attached to a DNA sequence (Figure 3.5a) and further comparison of the peak intensity at 518 nm shows the decreases in fluorescence emission in the presence of DNA (Figure 3.5b). The reason for this decrease in the fluorescence is due to the quenching effect of the DNA bases, in particular when guanine is positioned next to the fluorophore, significant quenching occurs. When fluorescence spectra were recorded for TR-ITC and TAMRA labelled DNA, the opposite effects are observed (Figure 3.5c). TAMRA is known to be less susceptible to fluorescence quenching;[27, 29] however in the data presented here, there is a significant increase in fluorescence emission (Figure 3.5d). This could be a result of sequence effects or the presence of DNA that could change the dipole across the molecule that may increase the fluorescence emission.

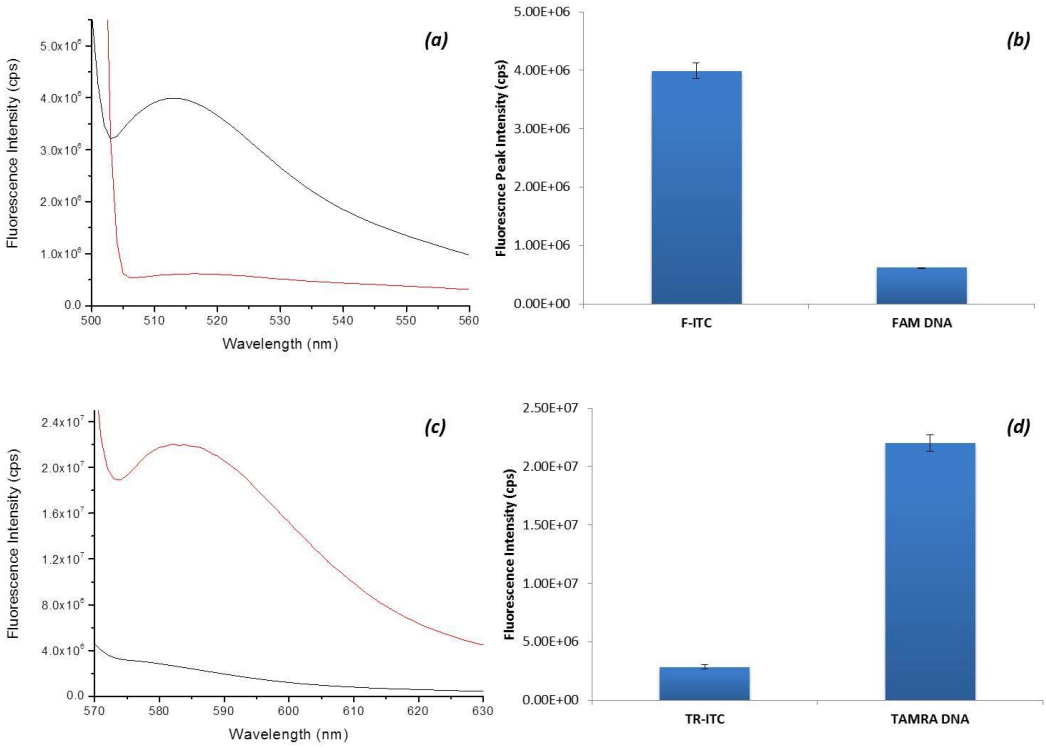

Figure 3.5 Fluorescence spectra observed when analysing the free dyes, F-ITC and TR-ITC, and when the fluorescent dyes are attached to an oligonucleotide sequence (all concentrations are 22 nM). (a) Fluorescence spectra of F-ITC (black) and FAM labelled DNA (red), (b) Fluorescence intensity comparison at 518 nm, (c) Fluorescence spectra of TR-ITC (black) and TAMRA labelled DNA (red) and (d) Fluorescence intensity comparison at 580 nm. For each analysis, 3 replicate samples were analysed 5 times, average spectra are shown. All error bars represent ± one standard deviation.

Fluorescence spectra were then recorded in the absence and presence of spermine. With the exception of TAMRA labelled DNA (Figure 3.6f), the addition of spermine enhances the fluorescence emission of the dye (Figure 3.6a, c, e). The enhancement observed when spermine is added to a solution of FAM labelled DNA and F-ITC; the spermine may be intercalating between the FAM and DNA molecules, reducing the base quenching effect. Spermine added to a solution of TR-ITC does not induce the same level of enhancement compared to that of F-ITC and FAM labelled DNA. The measurements were recorded at pH 5.2, and with the pK_a of spermine being 10.5 and the pK_a of the carboxylic acid in the TAMRA structure is around 3, both the dye and spermine will be positively charged resulting in little interaction between the two molecules; therefore the lower impact on the fluorescence emission.

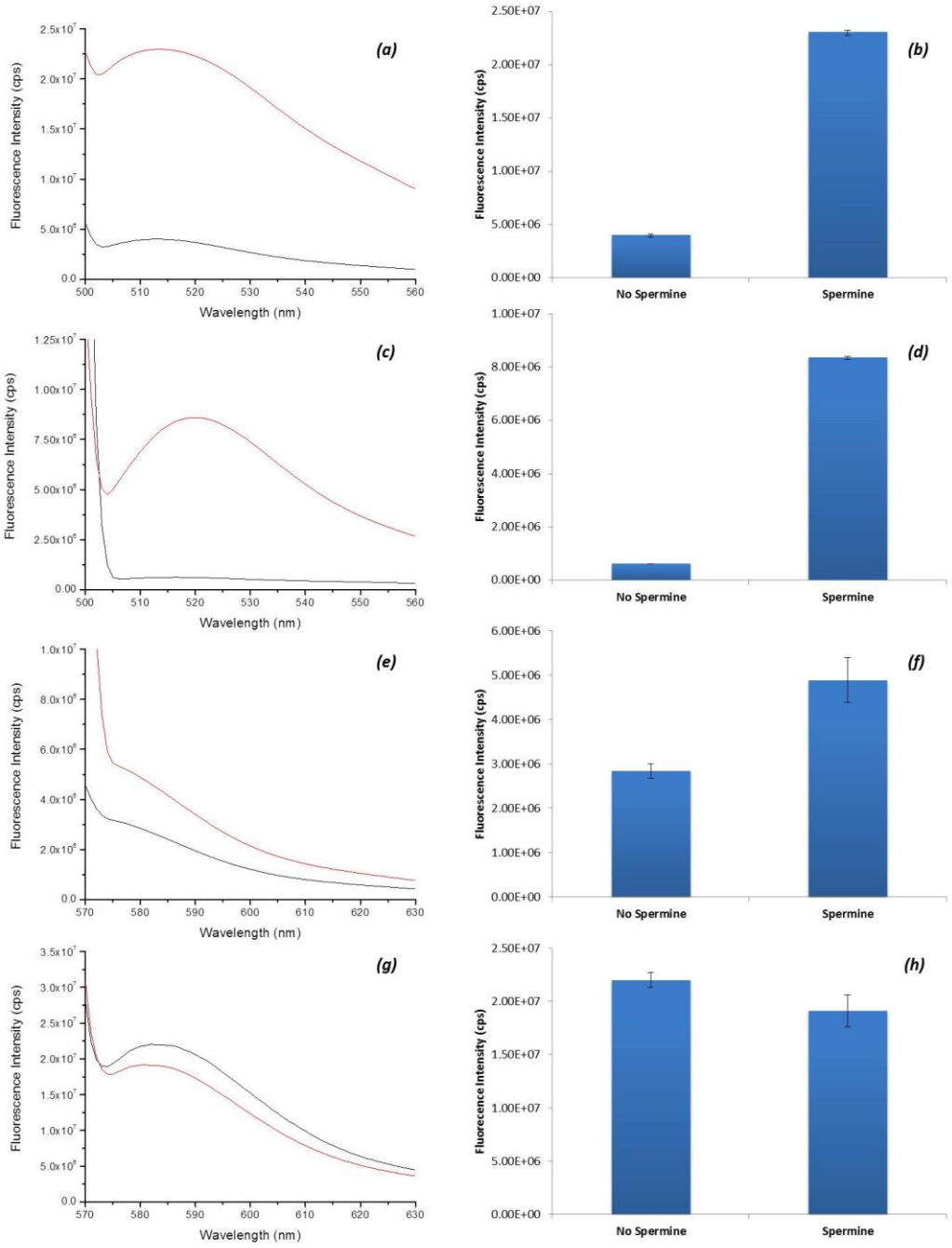

Figure 3.6 The fluorescence spectra observed in the absence (black) and presence (red) of spermine and comparisons of fluorescence intensity at λ_{em}. (a) Fluorescence spectra of F-ITC (22 nM) and (b) fluorescence intensity at 518 nm, (c) fluorescence spectra of FAM labelled DNA (22 nM) and (d) fluorescence intensity at 518 nm. (e) Fluorescence spectra of TR-ITC (22 nM) and (f) fluorescence intensity at 580 nm, (g) fluorescence spectra of TAMRA labelled DNA (22 nM) and (h) fluorescence intensity at 580 nm. For each analysis, 3 replicate samples were analysed 5 times, average spectra are shown. All error bars represent ± one standard deviation.

The presence of spermine has now been shown to have an effect on the fluorescence emission of the fluorescent dyes FAM and TAMRA. The experimental conditions remained constant for the above measurements; however it was unknown what the effect of changing the concentration of dye/DNA, the pH and the attached DNA sequence would have on the fluorescence observed before and after spermine addition.

3.4.2 Concentration Studies

It was important to determine if the spermine-induced enhancement observed with the fluorescent dye FAM was dependent on the concentration of FAM-labelled oligonucleotide present. It was also necessary to ascertain if changing the concentration of TAMRA labelled DNA, would affect whether spermine either enhanced or decreases the fluorescence intensity.

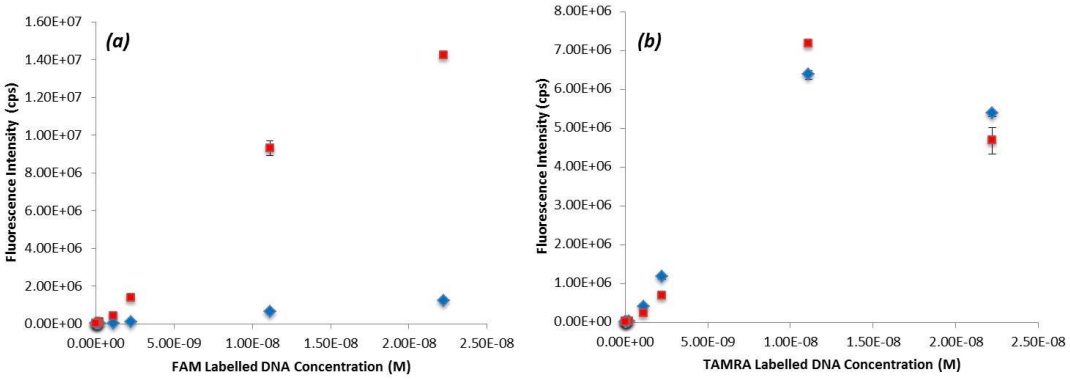

Figure 3.7 Fluorescence intensity at varying fluorescent dye labelled DNA concentrations. (a) Fluorescence intensity at 518 nm for varying the concentration of FAM-labelled oligonucleotide, in the presence (red) and absence (blue) of spermine, 3 replicate samples were analysed 5 times each, error bars represent ± 1 standard deviation. (b) Fluorescence intensity at 580 nm for varying the concentration of TAMRA-labelled oligonucleotide, in the presence (red) and absence (blue) of spermine, 3 replicate samples were analysed 5 times each, error bars represent ± 1 standard deviation.

Figure 3.7a shows that the relationship between fluorescence intensity and FAM labelled oligonucleotide concentration over the range 22 pM to 22 nM is approximately linear except at the highest concentration. It can also be observed that the enhancement

attributed to the addition of spermine is greater at higher concentrations of FAM labelled oligonucleotide. However, the concentration dependence of the fluorescence emission for TAMRA oligonucleotide shows a decrease in intensity at the highest concentration (Figure 3.7b). It can also be noted that TAMRA does not experience any significant fluorescence enhancement in the presence of spermine compared to FAM. The sudden decrease in TAMRA intensity at the highest concentration (22 nM) is a result of TAMRA having self-quenching properties that can occur at these concentrations. This effect is also observed for other rhodamine derivatives.[54]

Concentration studies were also performed whereby the fluorescent dye labelled DNA concentration was kept constant (22 nM) and the spermine solution concentration was decreased from 50 mM to 11 μM.

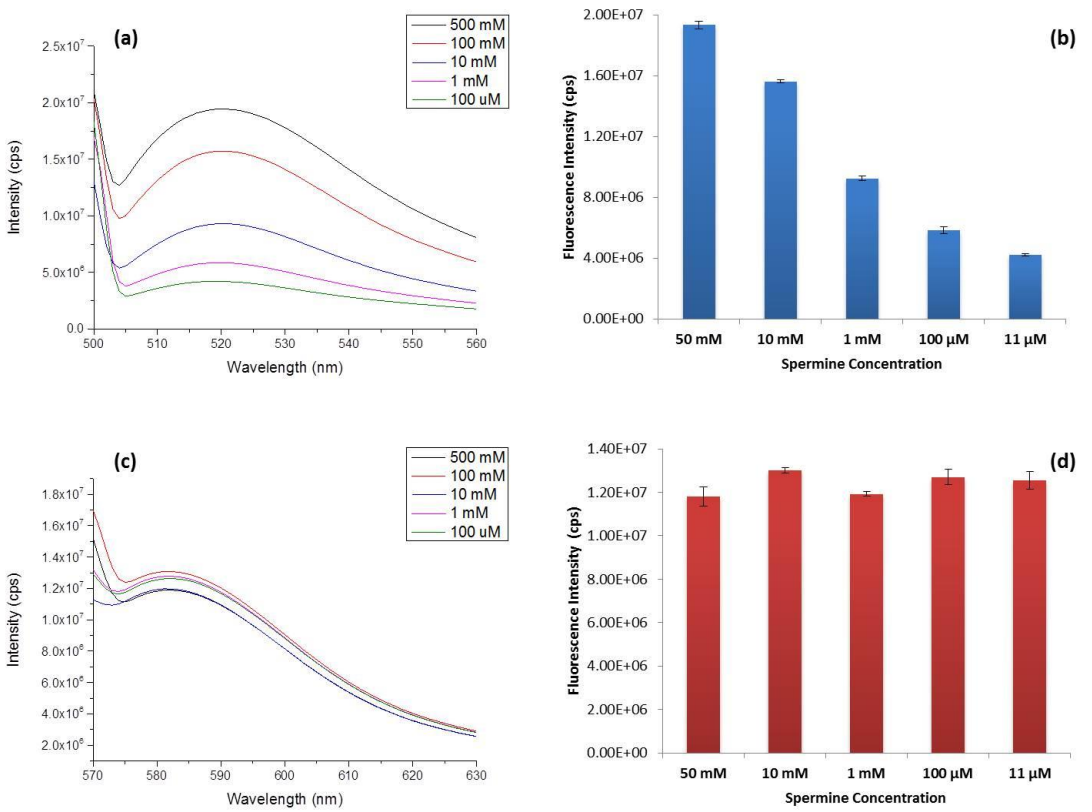

Figure 3.8 Results obtained when varying concentrations of spermine (50 mM to 11 µM) were added to the solution of fluorescent dye labelled oligonucleotides. (a) Fluorescence spectra obtained when decreasing concentrations of spermine were added to a 22 nM solution of FAM-labelled oligonucleotide. (b) Comparison of fluorescence intensities at 518 nm over the concentration range of spermine added. (c) Fluorescence spectra obtained when decreasing concentrations of spermine were added to a 22 nM solution of TAMRA-labelled oligonucleotide. (d) Comparison of fluorescence intensities at 580 nm over the concentration range of spermine added. 3 replicate samples were analysed 5 time and the error bars represent ± 1 standard deviation.

The effect of spermine on the FAM labelled oligonucleotide can be seen in Figure 3.8a-b. The FAM fluorescence intensity decreased with decreasing spermine concentration, emphasising the strong interaction there is between spermine and FAM. Therefore; the addition of spermine does significantly enhance the fluorescence intensity of FAM and this effect is concentration dependent. However, when the spermine concentration is decreased in the presence of TAMRA labelled oligonucleotide, there is very little change in fluorescence intensity, indicating that there is very little dependence between the spermine concentration and TAMRA intensity (Figure 3.8c-d). Regardless of the spermine

concentration being decreased, there was always an excess of spermine molecules compared to dye labelled DNA molecules.

3.4.3 pH Studies

All previous experiments were carried out at a pH of 5.2; therefore it was imperative to investigate the intensity dependence and also the spermine enhancement affect at different pHs. Fluorescence measurements of FAM and TAMRA labelled oligonucleotides were recorded at pH 2.9, 5.2, 6.9 and 13.2, and there was no change in pH when spermine was added. When the pH increased, the fluorescence intensity of FAM increased as did the spermine attributed enhancement at all pHs, however the effect was much greater at pH 5.2 (Figure 3.9a-b). In contrast, the fluorescence intensity of the TAMRA oligonucleotide varied less with pH as previously reported but there is a significant increase at pH 5.2 (Figure 3.9c-d).[55, 56] There is a small enhancement due to the addition of spermine at pH 6.9 but at the other pHs there is a small decrease.

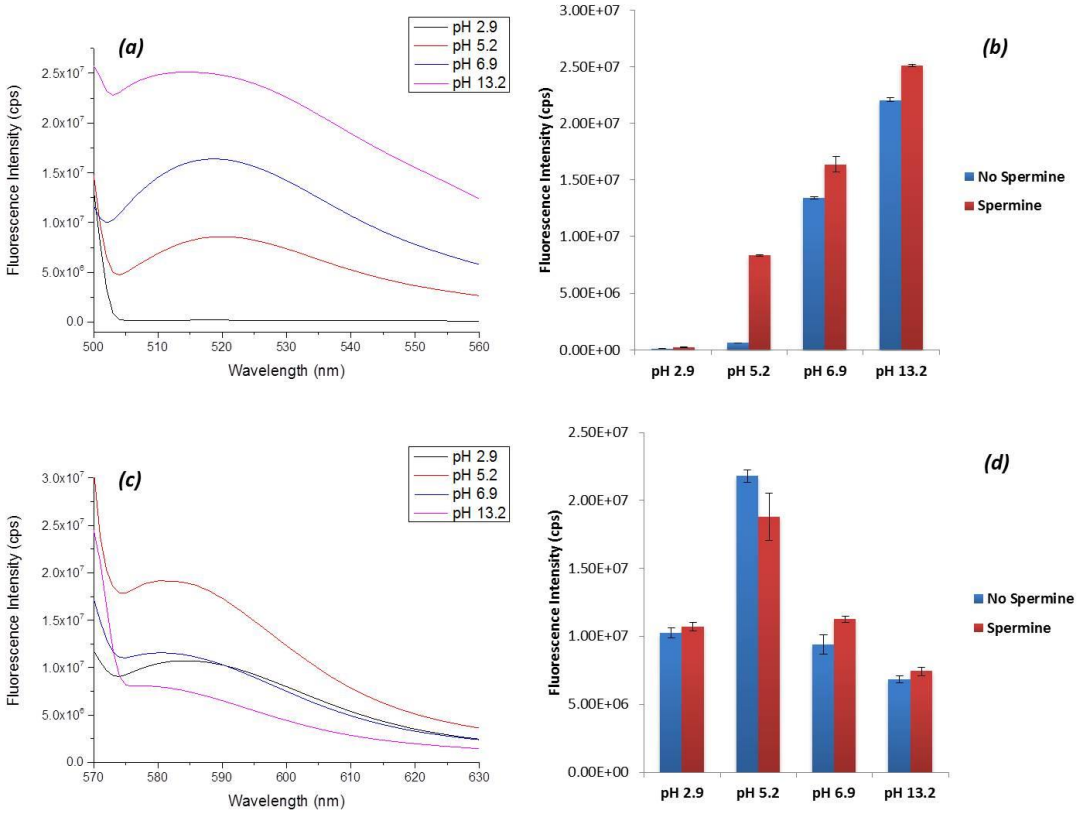

Figure 3.9 Fluorescence measurements obtained after varying the pH of the solution. (a) Fluorescence spectra of FAM-labelled oligonucleotides (22 nM) when the pH was altered. (b) Fluorescence intensity analysis at 518 nm. (c) Fluorescence spectra of TAMRA-labelled oligonucleotides (22 nM) when the pH was altered. (d) Fluorescence intensity at 580 nm, 3 replicate samples were analysed 5 times and the error bars represent ± 1 standard deviation.

The efficiency of the emission of FAM and TAMRA is dependent upon the dipole across the molecule and this is affected by changes in substitution pattern around the ring. This can clearly be seen in the results shown in Figure 3.5, where the covalent attachment of the dye to an oligonucleotide sequence increases the FAM efficiency and decreased TAMRA efficiency. The carboxylic acid group of FAM has a pK_a of 3.9 (Figure 3.4) and the phenolic group a pK_a of 9.5, therefore at pH 5.2 FAM will exist in solution in equilibrium between the lactone and ionic forms (Figure 3.10 b).[57, 58] The lactone form only gives very weak fluorescence. Therefore; the positively charged spermine would be expected to bind across the molecule forming an acid base complex, thus altering the equilibrium in favour of the ionic form.

With the exception of strongly acidic conditions, TAMRA exists in equilibrium between its protonated and zwitterionic forms and its non-fluorescent lactone form (Figure 3.10 b). The pKa of the carboxylic acid is very low (pKa~3), therefore across the pH range used, TAMRA will be present mainly in the zwitterionic form with some of the protonated form at the lowest pH.[59] The spectra show changes in the emission wavelength and intensity as the equilibrium changes, maximum emission occurs at pH 6.9, where the zwitterion form should predominate. Covalent attachment to an oligonucleotide causes a notable increase in intensity (Figure 3.5), presumably by stabilising the zwitterionic form and increasing the dipole. An acid base pair will form with the spermine but the effect on the dipole will be more limited and more complex due to the positive charge on the TAMRA.

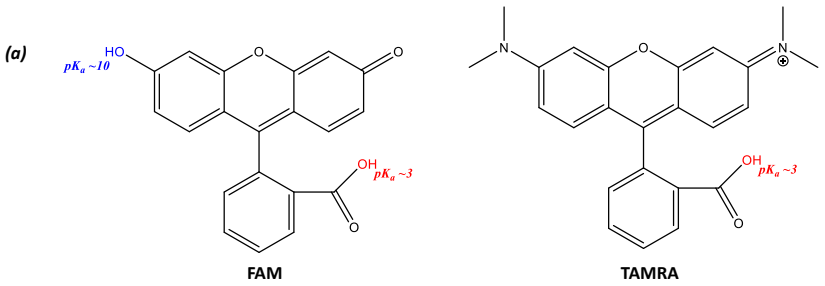

Figure 3.10 The structures of the chromophores at varying pH. (a) The structures of FAM and TAMRA labelled with the pK_a's of the carboxylic acid and phenol groups. (b) The varying structures of both FAM and TAMRA with changing pH. The ring-open form of FAM is fluorescent and increases in fluorescence emission with increasing pH. At higher pH the phenolic OH will also ionise. Ring-closed lactone form of FAM present at acidic pH which is non-fluorescent. The protonated form of TAMRA and zwitterion, both present at neutral and alkaline pH and fluorescent. The lactone form of TAMRA is non-fluorescent and exists at extremely acidic pH.

Therefore, attaching DNA to fluorescent dyes, changing the spermine concentration or the pH of the buffer solutions will all have an effect on the fluorescence emission of FAM and TAMRA. All previous results were obtained using dye labelled single stranded DNA, the next part of this study was to determine what effect changing the experimental conditions would have on the fluorescence emission of the dyes when they were attached to double stranded DNA.

3.4.4 Double Stranded DNA Studies

It was imperative to know what the affect the presence of spermine would have on the fluorescence intensity if it was double stranded DNA instead of single stranded. As before, the spermine concentration was decreased from 50 mM to 11 µM and added to a solution of double stranded DNA (22 nM). When spermine was added to a solution of FAM labelled double stranded DNA there was a slight decrease in fluorescence emission, as was the case when spermine was added to TAMRA labelled double stranded DNA (Figure 3.11a). When spermine concentration studies were performed using FAM and TAMRA labelled double stranded DNA, the fluorescence intensity of both fluorescent dyes did not vary greatly (Figure 3.11b). This suggests that when either fluorophore is attached to double stranded DNA, due to the already reported strong interaction with spermine and double stranded DNA,[45] it is this interaction that dominates. The spermine has little or no interaction with FAM or TAMRA resulting in little change in intensity, regardless of spermine concentration.

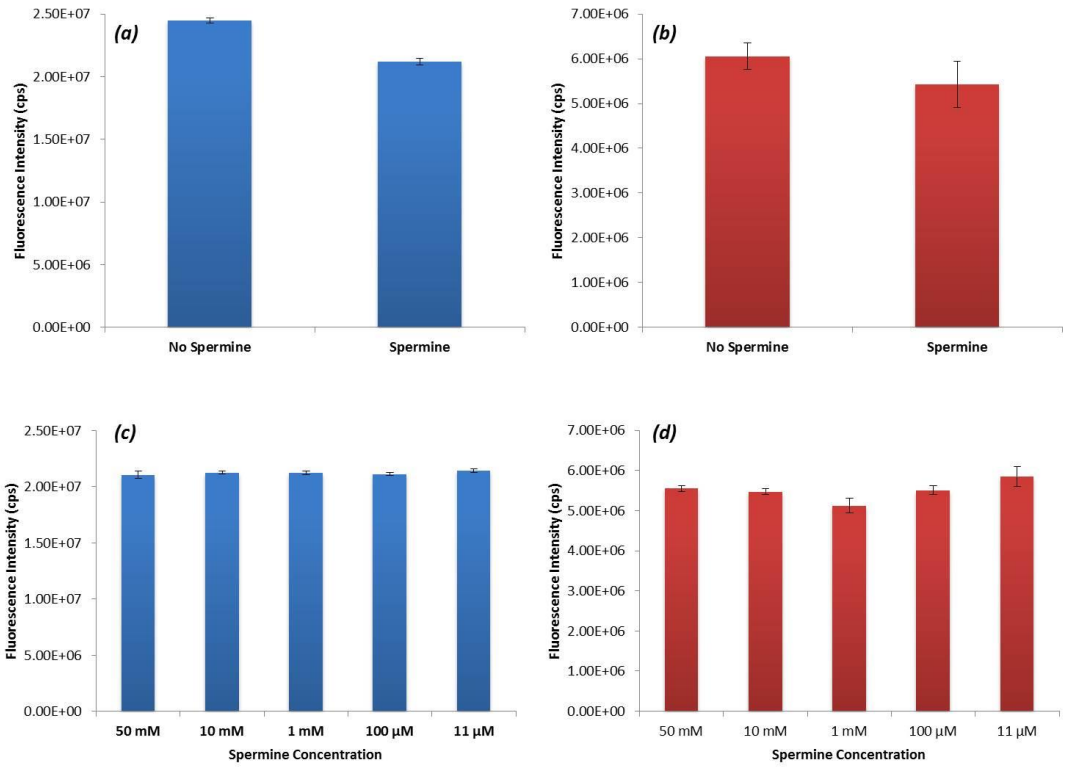

Figure 3.11 Fluorescence intensity comparisons obtained when fluorescent dyes were attached to double stranded DNA (22 nM). (a) Fluorescence intensity measured at 518 nm of FAM labelled double stranded DNA in the absence and presence of spermine (b) Fluorescence intensity measured at 580 nm of TAMRA labelled double stranded DNA in the absence and presence of spermine. (c) Fluorescence intensity at 518 nm of FAM labelled double stranded DNA with decreasing spermine concentration from 50 mM to 11 µM. (d) Fluorescence intensity at 580 nm of TAMRA labelled double stranded DNA with decreasing spermine concentration from 50 mM to 11 µM. For each experiment, 3 replicate samples were analysed 5 times and the error bars represent ± 1 standard deviation.

The pH dependence of the fluorescence of both fluorescent dyes in the double stranded DNA form is markedly different compared to that observed when they were attached to single stranded DNA. The FAM intensity at pH 2.9 was again low but at pH 5.2 and above it was nearly constant and greater than in the single stranded form (Figure 3.12a) even in the presence of spermine, it most likely that the ionic form of the dye is favoured due to steric hindrance. In contrast, the fluorescence intensity of TAMRA was lower than that observed in the single stranded form and surprisingly decreased significantly with increasing pH with no sharp increase in intensity at pH 6.9 (Figure 3.12b). In strongly alkaline conditions, the hydrogen bonds between the base pairs will break resulting in two single DNA strands.[60] Therefore at pH 13.2 the DNA attached to the fluorophore may no longer be in duplex form

so theoretically the fluorescence intensity observed should be similar to that of single stranded DNA at pH 13.2. However at all pHs the fluorescence is lower than at the equivalent pH for the single stranded form, suggesting that the covalent attachment causes a change in dipole which reduced the emission efficiency. The lack of a sharp increase in intensity at pHs where the zwitterion would be expected to form suggests that the covalently bound fluorescent dye is attached to the DNA in a way which prevents the true zwitterion formation.

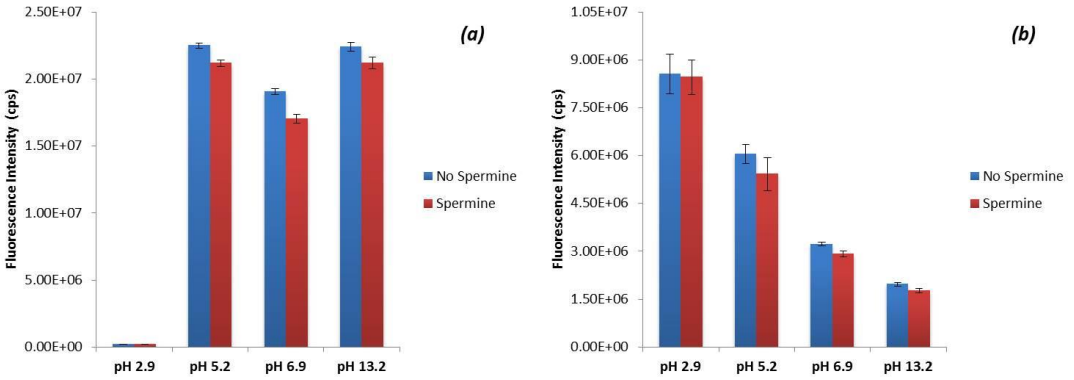

Figure 3.12 Fluorescence intensity comparisons obtained when fluorophores were attached to double stranded DNA. (a) Fluorescence peak intensities at 518 nm comparing the change in FAM fluorescence with changing pH. (b) Fluorescence peak intensities at 580 nm comparing the change in TAMRA fluorescence with changing pH. For each experiment, 3 replicate samples were analysed 5 times and the error bars represent ± 1 standard deviation.

3.4.5 Triethylamine (TEA) Comparison Studies

The presence of spermine does affect the emission of the fluorescent dyes. To understand the interaction between spermine and the two fluorescent dyes and if it was related to an acid-base relationship, the pH dependence experiments were repeated using a simple non-nucleophilic base, triethylamine (TEA), and both single and double stranded DNA (Figure 3.13). With the single stranded FAM oligonucleotide, maximum fluorescence was obtained at pH 5.2 and above, a result that was similar to that found for the double stranded product with no spermine and a greater effect than that obtained with spermine (Figure 3.11a). Perhaps not surprisingly for the double stranded FAM oligonucleotide, the spermine had little effect (Figure 3.13c). The TEA is present in excess and may form an acid base pair with both the carboxylic acid and phenolic groups by pH 5.2, whereas spermine is likely to be already bound across the molecule and may not affect the phenolic group.

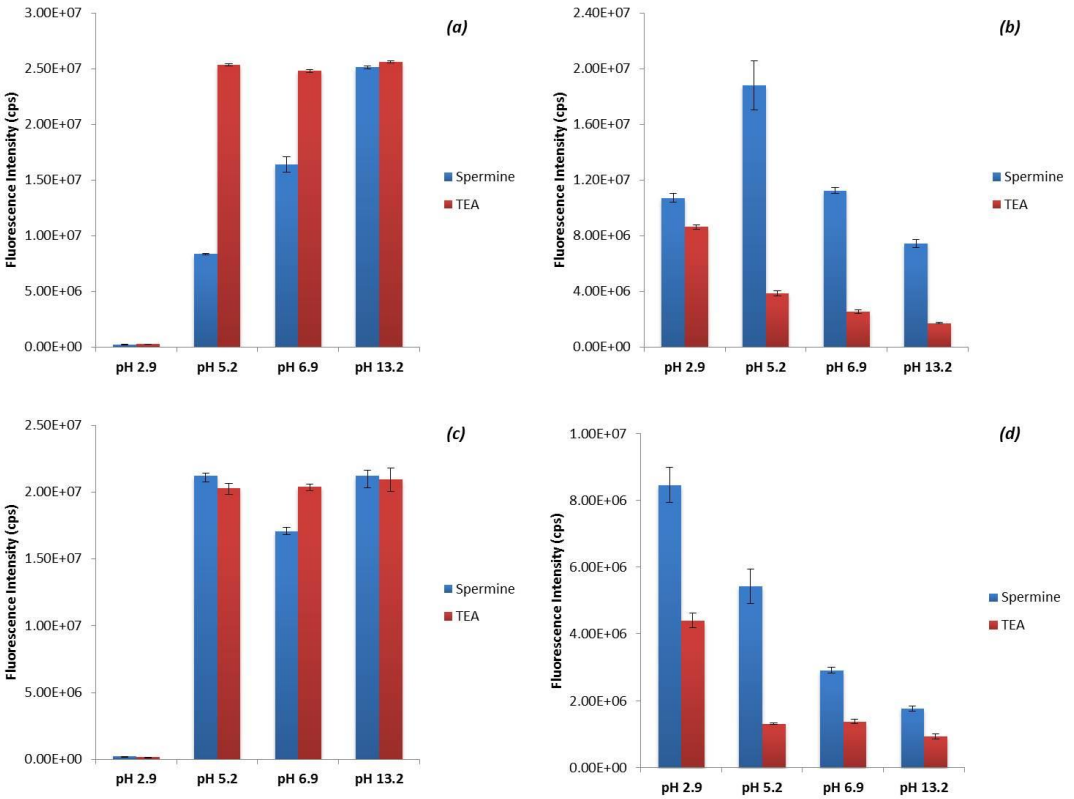

Figure 3.13 (a) Fluorescence intensity comparison obtained when TEA or spermine was added to a solution of FAM labelled single stranded DNA (22 nM). (b) Fluorescence intensity comparison obtained TEA or spermine was added to a solution of TAMRA labelled single stranded DNA (22 nM). (c) Fluorescence intensity comparison obtained TEA or spermine was added to a solution of FAM labelled double stranded DNA (22 nM) (d) Fluorescence intensity comparison obtained TEA or spermine was added to a solution of TAMRA labelled double stranded DNA (22 nM). For each experiment, 3 replicate samples were analysed 5 times and the error bars represent ± 1 standard deviation.

For double stranded TAMRA labelled DNA (Figure 3.13d), the fluorescence emission decreased as the pH increased and there was a much greater reduction in intensity at every pH compared to that observed when spermine was added. This suggested that TEA could be acting as a quencher to TAMRA, which is surprising as this should not be the case. The more likely explanation is that the excess base is interacting with part of the xanthine structure, probably the electron rich oxygen in the bridge, to alter the electronic structure and reduce the dipole. This may also be part of the reason it is so efficient at increasing the fluorescence efficiency of FAM. The fact that one effect is enhancement and the other

reduction of fluorescence is reasonable since the efficiency of emission depends on the dipole and this will be altered differently in FAM and TAMRA, which will ultimately be affected by changing pH as the fluorescent and non-fluorescent forms of the dyes will exist at differing pHs.

3.4.6 Sequence Specificity

The FAM and TAMRA labelled oligonucleotides used so far both had the same DNA sequence attached to the fluorophores, eliminating the issue of sequence specific effects. To investigate whether a change in oligonucleotide sequence would affect the fluorescence intensity observed, fluorescent measurements were recorded when the FAM and TAMRA fluorophores were attached to different oligonucleotide sequences. Table 3.1 in the experimental section lists the sequences used for these experiments, sequence 1 FAM/TAMRA are those used in previous experiments and sequence 2 FAM/TAMRA were used for comparison to determine if there was any sequence related influences on the effects observed.

Fluorescent measurements were recorded on the different sequences of single and double stranded labelled oligonucleotides. When single stranded labelled oligonucleotides were analysed, for both FAM and TAMRA, the fluorescence intensity observed when the fluorophores were attached to sequence 2, was always greater than that observed when using sequence 1 (Figure 3.14a,c). This can be explained by the base quenching that FAM and TAMRA experienced due to the dGG present at the 5' terminus next to the fluorescent dye of sequence 1. It has previously been reported that the guanine base is the more efficient quencher of all the nucleobases, especially when they are positioned adjacent to the fluorescent dye, which is the case for sequence 1.[17] For double stranded oligonucleotide experiments, varied results are obtained (Figure 3.14b,d). When FAM was attached to the duplex sequences, sequence 1 generated the higher fluorescence intensity compared to sequence 2. This could be a result of the complementary strands now causing more base quenching than the single stranded counterparts when FAM is attached to the oligonucleotide. When TAMRA is attached to the double stranded oligonucleotides, there

were no significant changes in fluorescence intensity when the sequences attached were different, which was due to TAMRA being less susceptible to base quenching.

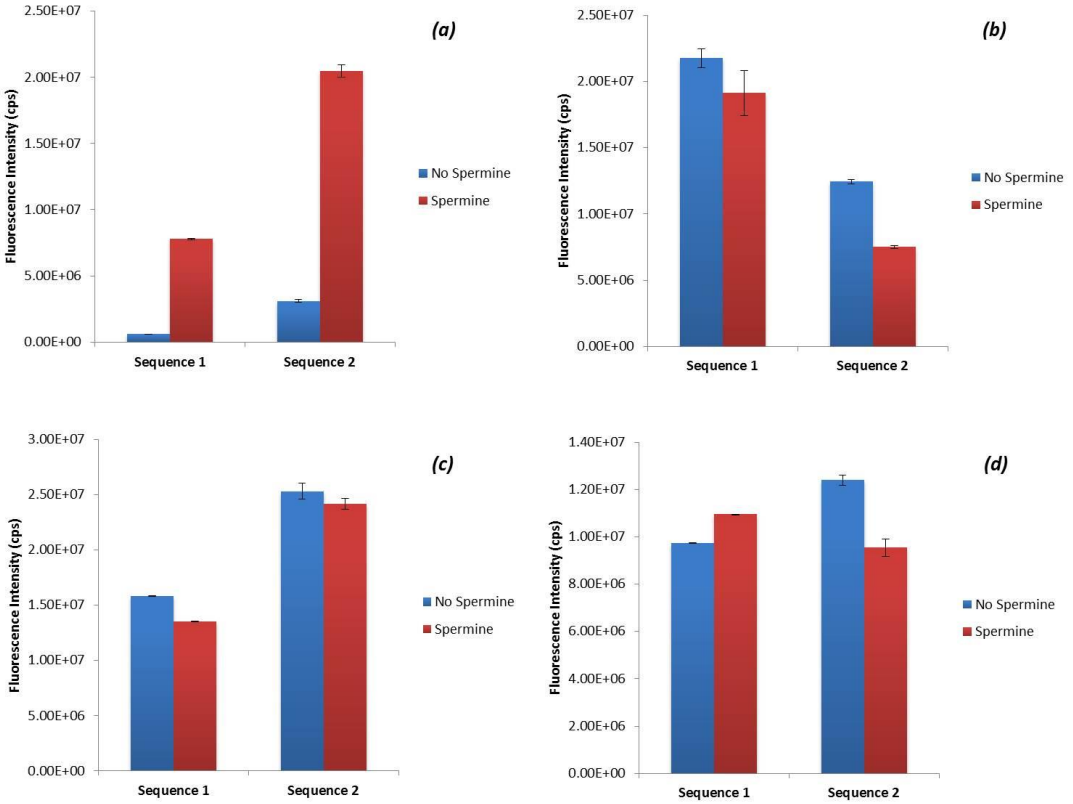

Figure 3.14 Fluorescence intensity comparisons obtained when fluorescent dyes were attached to different oligonucleotide sequences. (a) Fluorescence peak intensities at 518 nm comparing the change in FAM fluorescence when it is attached to two different single stranded oligonucleotides, sequence 1 and 2 (22 nM). (b) Fluorescence peak intensities at 518 nm comparing the change in FAM fluorescence when it is attached to two different double stranded oligonucleotides, sequence 1 and 2 (22 nM). (c) Fluorescence peak intensities at 580 nm comparing the change in TAMRA fluorescence when it is attached to two different single stranded oligonucleotides, sequence 1 and 2 (22 nM). (d) Fluorescence peak intensities at 580 nm comparing the change in TAMRA fluorescence when it is attached to two different double stranded oligonucleotides, sequence 1 and 2 (22 nM). For each experiment, 3 replicate samples were analysed 5 times and the error bars represent ± 1 standard deviation.

The sequence that is covalently attached to the fluorescent dye has shown to have an effect on the emission of the two fluorescent dyes, FAM and TAMRA. The trends reported in previous sections are relevant to only the same sequence that is attached to both FAM and TAMRA (Table 3.1). The main reason sequence specificities arise is due to base

quenching effects. Previous literature has reported that the presence of guanine bases, dGG, on the 5' terminus next to the fluorescent dye results in a significant amount of base quenching as observed in the results for sequence 1 (Figure 3.5).

3.5 Chapter Conclusions

This investigative study has shown that fluorescent dyes that are commonly used in biological detection assays are susceptible to interactions with the oligonucleotide sequence that they are attached to and to the polyamine spermine. Both interactions have a significant effect on absolute fluorescence intensity which can potentially impact the use of these fluorescent dyes in detection assays. The polyamine spermine is widely used in SERS and SEF based detection methods;[1-3, 50] therefore it was of great importance to consider the interaction of spermine with the fluorescent dyes as the overall signal can be affected. Two fluorescent dyes were compared, FAM and TAMRA. When spermine was added to the free dye F-ITC and FAM labelled oligonucleotides, there was a significant fluorescence enhancement. This was a result of the reduction in base quenching experienced by FAM, due to the design of sequence 1 that contains dGG in the 5' terminus next to FAM, as the spermine would intercalate between adjacent oligonucleotide sequences and would reduce the base quenching effect. Conversely, TAMRA did not exhibit the same fluorescence enhancement as observed with FAM. TAMRA is a positively charged fluorescent dye and therefore the polycation spermine would not have a strong interaction with this dye, compared to the negatively charged FAM.

In fluorescence assays, the relative intensities of the fluorescent dyes vary with pH and concentration and evidence of aggregation of DNA causing reduced fluorescence was found. In addition, the formation of a double strand alters the emission efficiency significantly. If spermine is added, or another base such as TEA, large changes in emission efficiency occur that is dependent on the base that is added. The fluorescence emitted from the fluorescent dye and the enhancement achieved by the addition of spermine can be affected by the oligonucleotide sequence attached to the dye, ultimately due to the level of base quenching that occurs. When spermine was added to the FAM labelled

oligonucleotide sequence, the emission is enhanced as the spermine intercalates between the DNA and FAM reducing the base quenching effect. TAMRA labelled DNA does not experience the same enhancement, a consequence of the positive charge present on TAMRA at the pH used for analysis or that TAMRA is less susceptible to base quenching prior to spermine addition.

The major reason for this study was to establish the extent to which the fluorescence will be affected in different conditions thus providing the knowledge to construct assays for the detection of multiple oligonucleotide sequences labelled with different fluorescent dyes. In the experiments discussed in this chapter, the two fluorescent dyes were analysed separately and more complexity is to be expected if they are mixed. However, for a deeper understanding as to why the emission efficiency of different fluorophores changes dependent upon experimental conditions and addition of a base, more experimental and computational analysis will need to be performed. Nevertheless, the results obtained emphasise the great consideration when selecting the conditions, reagents, and oligonucleotide design that is required if fluorescence intensities are to be compared in the development of biological detection assays.

The two fluorescent dyes, FAM and TAMRA are commonly used for the simultaneous detection of multiple targets using SERS, for example they were two of the three dyes used in Chapter 2 in the SERS-based assay for the simultaneous detection of three bacterial meningitis pathogens. This fluorescence study has shown the interactions that can occur between the two dyes and DNA, and how the presence of spermine affects the fluorescence emission. The fluorescence was further affected by changing experimental conditions, such as concentration and pH. It is reasonable to assume that these changing conditions may lead to changes in the SERS spectra obtained, where it is changes in peak positions or relative peak intensities. The following chapter will discuss the affect changing concentration and pH has on the SERS spectra of FAM and TAMRA, with more emphasis on the dye present in a mixture, i.e. a multiplex SERS mixture.

3.6 Chapter References

1. C. Y. Wu, W. Y. Lo, C. R. Chiu and T. S. Yang, *Journal of Raman Spectrosscopy*, 2006, **37**, 799-807.
2. D. van Lierop, Z. Krpetic, L. Guerrini, I. A. Larmour, J. A. Dougan, K. Faulds and D. Graham, *Chemical Communications*, 2012, **48**, 8192-8194.
3. R. Gill and E. C. Le Ru, *Physical Chemistry Chemical Physics*, 2011, **13**, 16366-16372.
4. K. Gracie, W. E. Smith, P. Yip, J. U. Sutter, D. J. S. Birch, D. Graham and K. Faulds, *Analyst*, 2014, **139**, 3735-3743.
5. J. S. Paige, T. Nguyen-Duc, W. Song and S. R. Jaffrey, *Science*, 2012, **335**, 1194-1194.
6. G. MacBeath and S. L. Schreiber, *Science*, 2000, **289**, 1760-1763.
7. A. Castro, F. R. Fairfield and E. B. Shera, *Analytical Chemistry*, 1993, **65**, 849-852.
8. A. Castro and R. T. Okinaka, *Analyst*, 2000, **125**, 9-11.
9. B. Juskowiak, *Analytical and Bioanalytical Chemistry*, 2011, **399**, 3157-3176.
10. A. A. Marti, S. Jockusch, N. Stevens, J. Y. Ju and N. J. Turro, *Accounts of Chemical Research*, 2007, **40**, 402-409.
11. J. W. Liu, Z. H. Cao and Y. Lu, *Chemical Reviews*, 2009, **109**, 1948-1998.
12. M. Hahn, J. Wilhelm and A. Pingoud, *Electrophoresis*, 2001, **22**, 2691-2700.
13. B. G. Moreira, Y. You, M. A. Behlke and R. Owczarzy, *Biochemical and Biophysical Research Communications*, 2005, **327**, 473-484.
14. M. K. Johansson, H. Fidder, D. Dick and R. M. Cook, *Journal of the American Chemical Society*, 2002, **124**, 6950-6956.
15. R. M. Clegg, A. I. H. Murchie, A. Zechel, C. Carlberg, S. Diekmann and D. M. J. Lilley, *Biochemistry*, 1992, **31**, 4846-4856.
16. M. Sauer, K. H. Drexhage, U. Lieberwirth, R. Muller, S. Nord and C. Zander, *Chemical Physics Letters*, 1998, **284**, 153-163.
17. I. Nazarenko, R. Pires, B. Lowe, M. Obaidy and A. Rashtchian, *Nucleic Acids Research*, 2002, **30**, 2089-2095.
18. J. L. Mergny, A. S. Boutorine, T. Garestier, F. Belloc, M. Rougee, N. V. Bulychev, A. A. Koshkin, J. Bourson, A. V. Lebedev, B. Valeur, N. T. Thuong and C. Helene, *Nucleic Acids Research*, 1994, **22**, 920-928.
19. S. Tyagi and F. R. Kramer, *Nature Biotechnology*, 1996, **14**, 303-308.
20. Y. Sei-Iida, H. Koshimoto, S. Kondo and A. Tsuji, *Nucleic Acids Research*, 2000, **28**.
21. X. H. Peng, Z. H. Cao, J. T. Xia, G. W. Carlson, M. M. Lewis, W. C. Wood and L. Yang, *Cancer Research*, 2005, **65**, 1909-1917.
22. S. A. E. Marras, S. Tyagi and F. R. Kramer, *Clinica Chimica Acta*, 2006, **363**, 48-60.
23. T. Ried, A. Baldini, T. C. Rand and D. C. Ward, *Proceedings of the National Academy of Sciences*, 1992, **89**, 1388-1392.
24. R. A. Cardullo, S. Agrawal, C. Flores, P. C. Zamecnik and D. E. Wolf, *Proceedings of the National Academy of Sciences of the United States of America*, 1988, **85**, 8790-8794.
25. V. V. Didenko, *Biotechniques*, 2001, **31**, 1106-+.
26. M. Torimura, S. Kurata, K. Yamada, T. Yokomaku, Y. Kamagata, T. Kanagawa and R. Kurane, *Analytical Sciences*, 2001, **17**, 155-160.
27. D. S. Xiang, K. Zhai and L. Z. Wang, *Analyst*, 2013, **138**, 5318-5324.
28. T. Maruyama, T. Shinohara, H. Ichinose, M. Kitaoka, N. Okamura, N. Kamiya and M. Goto, *Biotechnology Letters*, 2005, **27**, 1349-1354.
29. S. Ranjit and M. Levitus, *Photochemistry and Photobiology*, 2012, **88**, 782-791.
30. S. Kurata, T. Kanagawa, K. Yamada, M. Torimura, T. Yokomaku, Y. Kamagata and R. Kurane, *Nucleic Acids Research*, 2001, **29**, e34.

31. C. Dohno and I. Saito, *Chembiochem*, 2005, **6**, 1075-1081.
32. S. A. E. Marras, F. R. Kramer and S. Tyagi, *Nucleic Acids Research*, 2002, **30**, e122.
33. C. Moinard, L. Cynober and J. P. de Bandt, *Clinical Nutrition*, 2005, **24**, 184-197.
34. E. Agostinelli, M. P. M. Marques, R. Calheiros, F. Gil, G. Tempera, N. Viceconte, V. Battaglia, S. Grancara and A. Toninello, *Amino Acids*, 2010, **38**, 393-403.
35. E. Larque, M. Sabater-Molina and S. Zamora, *Nutrition*, 2007, **23**, 87-95.
36. H. S. Basu and L. J. Laurence, *Journal of Biological Chemistry*, 1987, **244**, 243-246.
37. M. Suwalsky, W. Traub, U. Shmueli and J. A. Subirana, *Journal of Molecular Biology*, 1969, **42**, 363-373.
38. A. M. Liquori, L. Costantino, V. Crescenzi, V. Elia, E. Giglio, R. Puliti, M. De Santis Savino and V. Vitagliano, *Journal of Molecular Biology*, 1967, **24**, 113-122.
39. T. J. Thomas and V. A. Bloomfield, *Biopolymers*, 1984, **23**, 1295-1306.
40. S. Jain, G. Zon and M. Sundaralingam, *Biochemistry*, 1989, **28**, 2360-2364.
41. L. D. Williams, C. A. Frederick, G. Ughetto and A. Rich, *Nucleic Acids Research*, 1990, **18**, 5533-5541.
42. B. Andreasson, L. Nordenskioeld, W. H. Braunlin, J. Schultz and P. Stilbs, *Biochemistry*, 1993, **32**, 961-967.
43. W. H. Braunlin, T. J. Strick and M. T. Record, *Biopolymers*, 1982, **21**, 1301-1314.
44. D. Esposito, P. Del Vecchio and G. Barone, *Journal of the American Chemical Society*, 1997, **119**, 2606-2613.
45. J. Ruiz-Chica, M. A. Medina, F. Sánchez-Jiménez and F. J. Ramírez, *Biophysical Journal*, 2001, **80**, 443-454.
46. R. C. Jin, *Angewandte Chemie-International Edition*, 2010, **49**, 2826-2829.
47. K. Faulds, W. E. Smith and D. Graham, *Analytical Chemistry*, 2004, **76**, 412-417.
48. K. L. Wustholz, A.-I. Henry, J. M. McMahon, R. G. Freeman, N. Valley, M. E. Piotti, M. J. Natan, G. C. Schatz and R. P. Van Duyne, *Journal of the American Chemical Society*, 2010, **132**, 10903-10910.
49. D. Graham, W. E. Smith, A. M. T. Linacre, C. H. Munro, N. D. Watson and P. C. White, *Analytical Chemistry*, 1997, **69**, 4703-4707.
50. R. Gill, L. Tian, W. R. C. Somerville, E. C. Le Ru, H. van Amerongen and V. Subramaniam, *Journal of Physical Chemistry C*, 2012, **116**, 16687-16693.
51. D. S. Xiang, C. L. Zhang, L. Chen, X. H. Ji and Z. K. He, *Analyst*, 2012, **137**, 5898-5905.
52. K. Gracie, E. Correa, S. Mabbott, J. A. Dougan, D. Graham, R. Goodacre and K. Faulds, *Chemical Science*, 2014, **5**, 1030-1040.
53. C. A. M. Seidel, A. Schulz and M. H. M. Sauer, *The Journal of Physical Chemistry*, 1996, **100**, 5541-5553.
54. M. Massey, W. R. Algar and U. J. Krull, *Analytica Chimica Acta*, 2006, **568**, 181-189.
55. A. Aneja, N. Mathur, P. K. Bhatnagar and P. C. Mathur, *Journal of Biological Physics*, 2008, **34**, 487-493.
56. M. R. Longmire, M. Ogawa, Y. Hama, N. Kosaka, C. A. S. Regino, P. L. Choyke and H. Kobayashi, *Bioconjugate Chemistry*, 2008, **19**, 1735-1742.
57. M. Adamczyk and J. Grote, *Bioorganic & Medicinal Chemistry Letters*, 2003, **13**, 2327-2330.
58. R. Sjöback, J. Nygren and M. Kubista, *Spectrochimica Acta Part A: Molecular and Biomolecular Spectroscopy*, 1995, **51**, L7-L21.
59. A. Pedone and V. Barone, *Physical Chemistry Chemical Physics*, 2010, **12**, 2722-2729.
60. M. Ageno, E. Dore and C. Frontali, *Biophysical Journal*, 1969, **9**, 1281-1311.

4. Interaction of Fluorescent Dyes with Spermine and DNA Using Surface Enhanced Raman Spectroscopy (SERS)

4.1 Introduction

SERS offers many advantages as a method for DNA analysis due to the low limits of detection[1, 2] that can be obtained ant the ability to detect multiple analytes in a sample mixture using the molecularly specific fingerprint spectra that are observed and without the need for any separation steps. To obtain the optimal SERS signals for successful DNA detection, a DNA probe sequences has to be designed that contains a surface seeking group for nanoparticle attachment and also a chromophore, which will provide a resonance contribution with the excitation laser wavelength to give a large increase in sensitivity.[3] The chromophore that has to be attached to the DNA sequence can be either a fluorescent label, such as TAMRA or FAM, as the metallic surface is capable of quenching the fluorescence emission[4] or it can be a specifically designed SERS dye (section 1.4.5.3). Through careful design of the SERS probe, sensitive and specific DNA detection can be achieved.

4.1.2 SERS Probes for DNA Detection

SERS probes designed for DNA detection can involve commercially available fluorescent dyes that are covalently attached to the DNA sequence of interest. Fluorescent dyes are commonly used in SERS probes due to the simple chemistry that is involved to attach the dyes to a DNA sequence and because of the quenching ability of the nanoparticle surface. There are numerous examples where commercially available dyes were attached to SERS probes and used for DNA detection.[5-9] Faulds *et al.* labelled DNA sequences with eight commercially available fluorescent dyes and each were shown to be easily detected using SERS.[10] Limits of detections were calculated for each dye, showing that quantitative SERS

analysis at low concentration levels could be readily achieved, something that was not possible using fluorescence based methods. Further to this, Stokes *et al*. analysed 13 DNA sequences that were each labelled with a commercially available fluorophore.[11] This emphasised the power of SERS to be used to successfully quantify DNA sequences that are labelled with fluorescent dyes.

4.1.3 Multiplex Detection of Fluorescent Dye Labelled Probes

Multiplex detection is the ability to detect multiple labels (fluorescent dye labelled DNA sequences) at the same time without using any separation procedures.[12] Multiplex detection can involve a 2-plex, an example being the multiplex analysis of mutations within the cystic fibrosis gene.[7] The specific DNA sequences used in that study were labelled with a rhodamine dye and HEX. A 3-plex system was then developed for the detection of SERS probe sequences that corresponded to particular gene sequences from *E. coli*.[13] Following this, a multiplex system was developed for the detection of 5 dye labelled DNA sequences using two laser excitation frequencies (514.5 and 633 nm).[14] Three of the dyes would give low limits of detection at 514.5 nm excitation and the other two at 633 nm excitation. When all 5 oligonucleotides were mixed together in the one sample, using the 514.5 nm laser excitation signals from three dyes, FAM, R6G and ROX, were easily observed and when using the 633 nm excitation laser the other two dyes, BODIPY and Cy 5.5 could then be identified in the SERS spectrum. The fluorescent dye ROX produced signals at both laser excitations. To increase the SERS multiplex to the detection of 6 or more labelled DNA sequences, chemometric analysis will be required to clearly identify the presence or absence of the fluorescent dye labels in the multiplex mixture.[15]

4.1.4 Interactions within the Multiplex Mixture

Nanoparticles are often used for the detection of DNA sequences using SERS. For example, silver nanoparticles can be prepared with a citrate layer that will possess a net negative charge on the nanoparticle surface.[16] Therefore, to allow the negatively charge phosphate backbone of a DNA sequence to adsorb onto the negatively charges silver nanoparticle surface, a method involving the reduction of these charges is required. One approach involves electrostatic layering using either poly(L-lysine) or spermine.[17] Spermine was found

to facilitate the maximum adsorption of DNA onto the nanoparticle surface. Spermine is discussed in more detail in chapter 3 section 3.1.3. The two fluorescent dyes used within this study are TAMRA and FAM; structures are shown in Figure 3.3. These are charged dyes, with TAMRA being positive and FAM negative. The charge on the dye, or indeed any analyte to be detected, can have a significant effect on the SERS intensity observed. Negatively charged dyes like FAM tend to produce poor SERS intensity due to the repulsion between the dye and the negatively charged nanoparticle surface, whereas positively charged dyes such as TAMRA produce a greater SERS intensity due to the ease of surface adsorption. The use of spermine can overcome these electrostatic repulsions.

With various charged components in a SERS multiplex mixture, it is reasonable to assume numerous interactions can take place. These interactions, such as the ones between dye labelled DNA and spermine, enhance the SERS signal observed. However, there are other interactions that can reduce the SERS intensity and these interactions can also be dye specific. It is important to understand all possible interactions that can occur, especially when using SERS for the simultaneous detection of multiplex analytes as each fluorescent dye present must produce sufficient SERS intensity to be identified and then quantified.

4.2 Aims

Previous work (chapter 3) demonstrated that the presence of spermine can either enhance or reduce the fluorescence emission of two fluorescent dyes, FAM and TAMRA, which may have an effect on the SERS spectra observed for the two dyes. Therefore, studies into the effects of these interactions between the dyes, DNA, spermine and the silver nanoparticle surface under different experimental conditions were undertaken. The effect of changing the experimental conditions the surface adsorption of the analytes (dye or dye labelled DNA) and how it will affect the SERS response was investigated. These studies involved the SERS analysis of free dyes as well as the fluorescent dyes covalently attached to single or double stranded DNA. It is important to understand the possible interactions between these fluorescent labels using SERS as the results will have an impact on the design of multiplex SERS-based detection assays.

4.3 Experimental

4.3.1 Colloid synthesis

Silver nanoparticles were synthesised using a modified Lee and Meisel method.[16] Silver nitrate (90 mg) was dissolved in 500 mL distilled water. The solution was heated rapidly to boiling with continuous stirring. Once boiling, an aqueous solution of sodium citrate (1 %, 10 mL) was added quickly. The heat was reduced and the solution was left to boil gently for 90 min with stirring. The colloid was then analysed by UV-vis spectroscopy and the λ_{max} was found to be 406 nm with the full width half-height (FWHH) measured to be 82 nm. The concentration of the colloid was calculated to be 0.18 nM. To minimise issues that arise from batch to batch variation, experiments were performed using the same batch of colloid.

4.3.2 Oligonucleotides

All sequences were purchased on a 0.2 µM scale with HPLC purification from Eurofins MWG (Ebersberg, Germany), shown in Table 5.1.

Table 4.1 Modified oligonucleotides and complementary oligonucleotide sequence used in this investigation

Name	Sequence (5'-3')	5' Modifications
TAMRA labelled oligonucleotide	GGTTCATATAGTTATAATAA	TAMRA
FAM labelled oligonucleotide	GGTTCATATAGTTATAATAA	FAM
Complementary Sequence	TTATTATAACTATATGAACC	-

4.3.3 SERS Instrumentation

SERS analysis was carried out using an Avalon Instrument Ramanstation R3 (Belfast, UK), with an excitation wavelength of 532 nm from a diode laser. Disposable 1.5 mL PMMA semi-micro cuvettes were used. Instrument settings were 5 x 1 second accumulations with 0.5 cm^{-1} resolution. Data was baseline corrected using Grams software (AI 7.00). In some experiments, the 1 second exposure time had to be reduced due to saturation of the detector. The data was corrected to account for the change in exposure time.

4.3.4 Fluorescent Dye Analysis

Analysis of the free dyes was carried out by preparing TR-ITC and F-ITC 1 μM solution of each dye. To a microcuvette, the free dye (10 μL, 1 μM) was added to a solution of spermine (20 μL, 0.1 M), distilled water (220 μL) and citrate reduced silver nanoparticles (150 μL), in that order. SERS analysis was then performed immediately as described in section 4.3.3. Each sample was prepared in triplicate and an average SERS spectrum was calculated.

4.3.5 Fluorescent Dye Labelled Single Stranded DNA Analysis

Single stranded DNA labelled with either TAMRA or FAM were also analysed using SERS, sequences are shown in Table 4.1. Analysis was carried out by preparing 1 μM solutions of TAMRA and FAM labelled single stranded DNA. The dye labelled DNA (10 μL, 1 μM) was added to a cuvette followed by spermine (20 μL, 0.1 M), distilled water (220 μL) and citrate reduced silver nanoparticles (150 μL), in that order. SERS analysis was then performed immediately as described in section 4.3.3. Each sample was prepared in triplicate and an average SERS spectrum was calculated.

4.3.6 Fluorescent Dye Labelled Double Stranded DNA Analysis

When analysing double stranded labelled DNA, DNA hybridisation had to be performed prior to SERS analysis. To a sample vial, dye labelled DNA (10 μL, 1 μM) and the complementary sequence (10 μL, 1 μM) were added to a solution of phosphate buffered saline, PBS (20 μL, 0.3 M). The sample vial was placed in a heating block at 90 °C for 10 minutes and then cooled to 10 °C for 10 minutes. For SERS analysis, the double stranded labelled DNA (20 μL, 1μM) was added to a solution of spermine (20 μL, 0.1 M), distilled water (210 μL) and citrate reduced silver nanoparticles (150 μL). SERS analysis was then performed immediately as described in section 4.3.3. Each sample was prepared in triplicate and an average SERS spectrum was calculated.

4.3.7 Concentration Studies

For dye concentration studies discussed in sections 4.4.2.1and 4.4.2.2, a final concentration range of 2.2 pM to 22 nM was prepared. The concentration study performed in section 4.2.2.3 involved a range from 0.13 nM to 24.7 nM. The free dyes and dye labelled oligonucleotides were analysed both individually and in a mixture of both. For individual analysis, fluorescent dye, dye labelled single stranded DNA or dye labelled double stranded DNA (10 µL, 10 µL or 20 µL) was added to a solution of spermine (20 µL, 0.1 M), distilled water (220 or 210 µL) and silver citrate reduced nanoparticles (150 µL). SERS analysis was then performed immediately. For mixture analysis, 10 µL of each fluorescent dye or dye labelled DNA was added to a solution of spermine (20 µL, 0.1 M), distilled water (220 µL) and silver citrate reduced nanoparticles (150 µL). The varying concentrations of each fluorescent dye or fluorescent dye labelled DNA were prepared prior to SERS analysis.

4.3.8 Time Studies

Time studies, using TR-ITC/F-ITC and TAMRA/FAM labelled single or double stranded DNA, were performed to determine what affect the order of addition of the analyte had on the SERS intensities observed. The fluorescent dyes were treated as primary or secondary probes based on their order of addition. To a microcuvette, the primary fluorescent dye or dye labelled single stranded DNA (10 µL, 1 µM) was added to a mixture of spermine (20 µL, 0.1 M), distilled water (220 µL) and citrate reduced silver nanoparticles (150 µL). Following this, the secondary fluorescent dye or dye labelled single stranded DNA was added and SERS analysis started immediately. SERS measurements were recorded every 5 minutes for 20 minutes. When time studies were performed using fluorescent dye labelled double stranded DNA, the same order of addition was followed however there were two volume changes, the amount of dye labelled DNA added was increased to 20 µL and the amount of distilled water was reduced to 210 µL.

4.3.9 pH Studies

SERS spectra were recorded using buffers with varying pHs to determine what affect changing the pH had on the SERS intensity of the characteristic peaks of the fluorescent dyes. Table 4.2 lists the four solutions used for the pH studies.

Table 4.2 Solutions of varying pH

pH	Solution
2.9	Citrate/HCl
5.2	Distilled Water
6.9	Phosphate Buffered Saline (PBS)
13.2	NaOH

250 mM trisodium citrate was prepared and pH was adjusted to 2.9 using HCl. 10 mM phosphate buffered saline, pH 6.9, was prepared by dissolving one tablet (Sigma Aldrich) in 200 mL distilled water. Finally, 1 M NaOH was prepared and pH was measured to be 13.2. The distilled water used throughout all of the experiments had a measured pH of 5.2. Samples for analysis were prepared as follows; fluorescent dye or dye labelled single stranded DNA (10 µL, 1 µM) was added to spermine (20 µL, 0.1 M), one of the four solutions listed in Table 5.2 (220 µL) and citrate reduced silver nanoparticles (150 µL). For double stranded DNA studies, 20 µL of dye labelled DNA was added to the cuvette and the amount of solution added was reduced to 210 µL. SERS analysis was carried out immediately. Each sample was prepared in triplicate and an average SERS spectrum was calculated.

4.3.10 Nanoparticle Characterisation

4.3.10.1 Nanosizing

Dynamic light scattering (DLS) measurements were performed to determine the effect of changing the pH of the solution had on the nanoparticles. This was carried out by adding citrate reduced silver nanoparticle (400 µL) and one of the solutions in Table 4.2 (400 µL) to a cuvette and performing the measurement using a Malvern Zetasizer nano ZS system. Measurements of all four solutions were also recorded after the addition of spermine (80 µL, 0.1 M).

5.3.8.2 Zeta Potential

The zeta potential for each of the four solutions used for the nanosizing measurements (section 4.3.10.1) was performed using the same instrument. Samples were prepared in a

similar way, citrate reduced silver nanoparticles (400 µL) were added to one of the four solutions (400 µL). The dip cell was placed into the cuvette and analysis followed.

4.4 Results and Discussion

Detection of nucleic acids, proteins and small molecules has been readily achieved using surface enhanced Raman scattering (SERS), through the ability to label these biomolecules with fluorescent dyes.[18] Due to the multiplexing capabilities of SERS, more than one fluorescently labelled biomolecule can be detected in the same sample mixture.[19] These methods of detection rely on each of the fluorescent dyes present producing equivalent amounts of signal so that each one can be readily detected. Ideally, they will have similar Raman cross sections and affinity for the metal surface, so that one dye does not dominate over the others in the multiplex. However, interactions can occur between the fluorescent dyes on and off the nanoparticle surface that will ultimately affect the overall SERS response that is obtained. These interactions can be due to the presence of other molecules such as aggregating agents like spermine, or can be a result of the electrostatic interactions due to the charge on the fluorescent dyes compared to the nanoparticle. Within the scope of this work, fluorescently labelled DNA will be detected using SERS.

Before any studies were performed, SERS spectra of TAMRA isothiocyanate (TR-ITC), FAM isothiocyanate (F-ITC), TAMRA labelled oligonucleotide and FAM labelled oligonucleotide were recorded to determine if the SERS spectrum changed upon covalent attachment of the fluorescent dye to a DNA sequence (Figure 4.1). To achieve this free dye or dye labelled DNA (10 µL, 1 µM) was premixed with spermine (20 µL, 0.1 M)and then added to silver nanoparticles (150 µL).

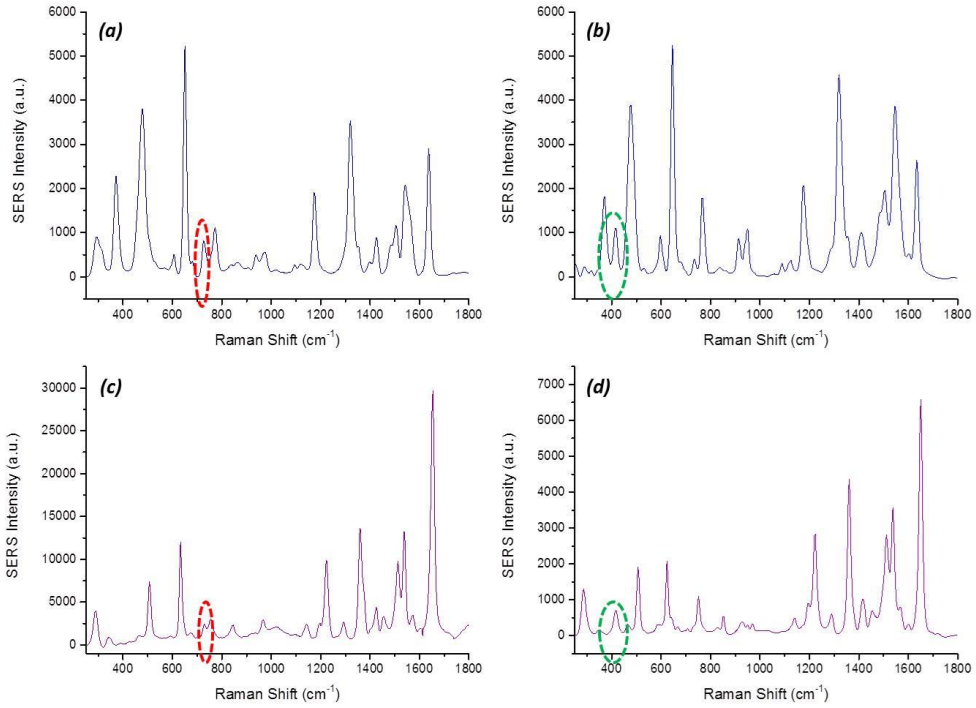

Figure 4.1 SERS spectra of the fluorescent dyes TAMRA and FAM when attached and unattached to an oligonucleotide (22 nM) premixed with spermine (0.1 M) and added to silver nanoparticles. (a) SERS spectrum of FAM labelled oligonucleotide, (b) SERS spectrum of FAM isothiocyanate (F-ITC), (c) SERS spectrum of TAMRA labelled oligonucleotide and (d) SERS spectrum of TAMRA isothiocyanate (TR-ITC). Additional DNA peaks are highlighted in red and isothiocyanate peaks in green. Spectra were recorded using an excitation wavelength of 532 nm with a 1 s accumulation time.

The SERS spectra observed when FAM and TAMRA are attached to an oligonucleotide sequence (Figure 4.1 a, c) contain an additional peak at 730 cm^{-1}, which is attributed to the presence of an oligonucleotide sequence, in particular the adenine base.[20] An additional peak is observed at 417 cm^{-1} in the spectra of the free dyes, F-ITC and TR-ITC, due to the presence of the isothiocyanate group attached to the free dyes (Figure 4.1 b, d). There was a shift in all peak positions of 4 cm^{-1} between the free dye and dye-oligonucleotide forms. The peaks chosen for analysis were 646 cm^{-1} and 650 cm^{-1} for F-ITC and FAM labelled oligonucleotide, and 1650 cm^{-1} and 1654 cm^{-1} for TR-ITC and TAMRA labelled oligonucleotide respectively. Furthermore, there are some changes in relative peak intensities upon attachment of the fluorescent dye to an oligonucleotide sequence, for

example, the 1575 cm^{-1} peak in the F-ITC spectrum compared to that in the FAM labelled oligonucleotide where there is a change in frequency of the ring vibrations due to the attachment of DNA. Changes in relative peak intensities are also a result the change in orientation of the fluorescent dye with respect to the nanoparticle surface when it is attached or unattached to DNA.

4.4.1 Affinity of Fluorescent Dye to the Nanoparticle Surface

Previous studies have shown that different intensities of SERS spectra are observed when the fluorescent dye is attached to single stranded DNA, double stranded DNA or when it is in its free form. In 2009, MacAskill *et al.* used SERRS for the detection of specific DNA sequences based on the different affinity between single and double stranded DNA and the silver nanoparticle surface. Results showed that reduced SERS intensity was observed when double stranded DNA was attached to the fluorescent dye FAM, whereas an increase in SERS intensity was observed when single stranded DNA was attached to FAM.[21] Following this, Harper *et al.* demonstrated the different affinities that TAMRA labelled single and double stranded and the free dye TAMRA has for the silver nanoparticle surface. It was shown that TAMRA labelled single stranded DNA has the highest affinity for the nanoparticle surface producing the most intense SERS spectrum, followed by TAMRA labelled double stranded DNA whereas the free dye TAMRA was shown to have no affinity for the surface resulting in no SERS intensity observed.[22] Both studies used different experimental conditions to those used in this work; EDTA reduced silver nanoparticles compared to citrate reduced silver nanoparticles were used and the pH of the buffer was 7.4, whereas the pH of the SERS solution in this instance was 5.2. These changes in conditions could potentially affect the affinity the fluorescent dyes and dye labelled DNA sequences have for the nanoparticle surface.

The difference in SERS intensity observed when the fluorescent dye is free or attached to single or double stranded DNA is due to the difference in electrostatic attraction between the nucleobases and the nanoparticle. However, the fluorescent dyes themselves are also charged, TAMRA is positive whereas FAM is negative. Free dye or dye labelled DNA was added to a solution of spermine, distilled water and citrate reduced silver nanoparticles.

SERS spectra were recorded for TR-ITC/TAMRA labelled DNA and F-ITC/FAM labelled DNA. The results obtained for TAMRA are given in Figure 4.3.

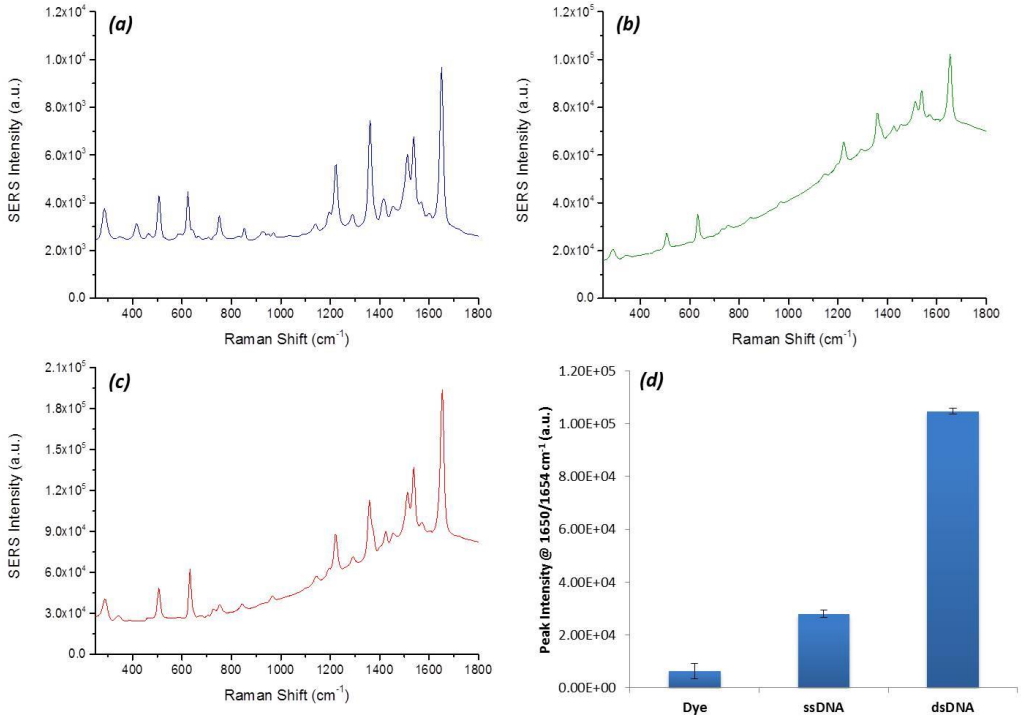

Figure 4.2 SERS analysis of (a) TR-ITC (22 nM) (b) TAMRA labelled single stranded DNA (22 nM) and (c) TAMRA labelled double stranded DNA (22 nM). (d) Further peak analysis at 1650 cm^{-1} for TR-ITC and 1654 cm^{-1} for TAMRA covalently attached to DNA. SERS spectra were recorded using an excitation wavelength of 532 nm. Peak intensities were obtained by scanning 5 replicate samples 3 times with an accumulation time of 1 s. Averages are shown and error bars are ± one standard deviation.

When the SERS spectra were recorded of TR-ITC (Figure 4.2a), TAMRA labelled single stranded DNA (Figure 4.2b) and TAMRA labelled double stranded DNA (Figure 4.2c), varying peak intensities were observed. The strongest SERS intensity was observed when TAMRA was attached to double stranded DNA and the weakest was when the dye was in free form. This is a result of the combined electrostatic attraction between the positively charged TAMRA and the negative nanoparticle surface, and between the negatively charged phosphate backbone of the oligonucleotide and the positively charged spermine. TAMRA labelled single stranded DNA also experiences these electrostatic interactions but not to

the same extent. The free dye has no attraction to the positively charged spermine, only to the negatively charged nanoparticle surface, which does not produce the same SERS intensity as the dye labelled oligonucleotides. The fluorescence background also varies, most notably when TAMRA is covalently attached to single stranded DNA where the largest background signal is observed (Figure 4.2b). This suggests that the TAMRA labelled single stranded DNA is orientated in such a way that the fluorescent dye is positioned away from or unable to come close to the nanoparticle surface, increasing the background fluorescence i.e. decreasing the fluorescence quenching caused by the nanoparticle. The results shown here are different to those obtained by Harper *et al.*[22] In that study, TAMRA labelled single stranded DNA produced the largest SERS intensity with the free dye producing no SERS peaks. The main difference between the two studies is the silver nanoparticles used; Harper *et al*. used EDTA reduced silver nanoparticles whereas in this study citrate reduced silver nanoparticles were used. The surface layer on the nanoparticles will be different, which will ultimately affect the affinity between dye/DNA and the nanoparticle surface. Furthermore, Harper *et al.* found that the pH greatly affected the degree of affinity the DNA had for the nanoparticle surface and found that pH 8.3 gave the greatest discrimination, whereas pH 5.2 was used throughout these experiments.[22, 23]

The results obtained from SERS analysis of F-ITC (Figure 4.3a), FAM labelled single stranded DNA (Figure 4.3b) and FAM labelled double stranded DNA (Figure 4.3c) are different compared to those obtained from the SERS analysis of TR-ITC/TAMRA labelled DNA. The highest SERS intensity was observed when the FAM was free and when it was covalently attached to single stranded DNA as the dye will be closest to the nanoparticle surface. There are two possible reasons why FAM labelled double stranded DNA produced the lowest intensity. Firstly, the strong interaction between spermine and double stranded DNA that could dominate over any interactions between the dye and spermine, resulting in FAM being positioned further away from the nanoparticle surface producing the lowest SERS intensity and highest fluorescent background (Figure 4.3c), or there could be a stronger interaction between the negatively charged phosphate backbone that is exposed in single stranded DNA and the positively charge spermine, resulting in higher SERS intensity observed for FAM labelled single stranded DNA (Figure 4.3b). The results obtained here agree with those shown by MacAskill *et al.* where double stranded DNA attached to FAM

gave lower SERS intensity compared to single stranded DNA attached to FAM, a result due to the electrostatic interaction between the nucleobases, spermine and the nanoparticle surface.[21] MacAskill *et al.* did not analyse FAM as the free dye (F-ITC), therefore there is no previous data on the comparison between F-ITC and FAM labelled single stranded DNA.

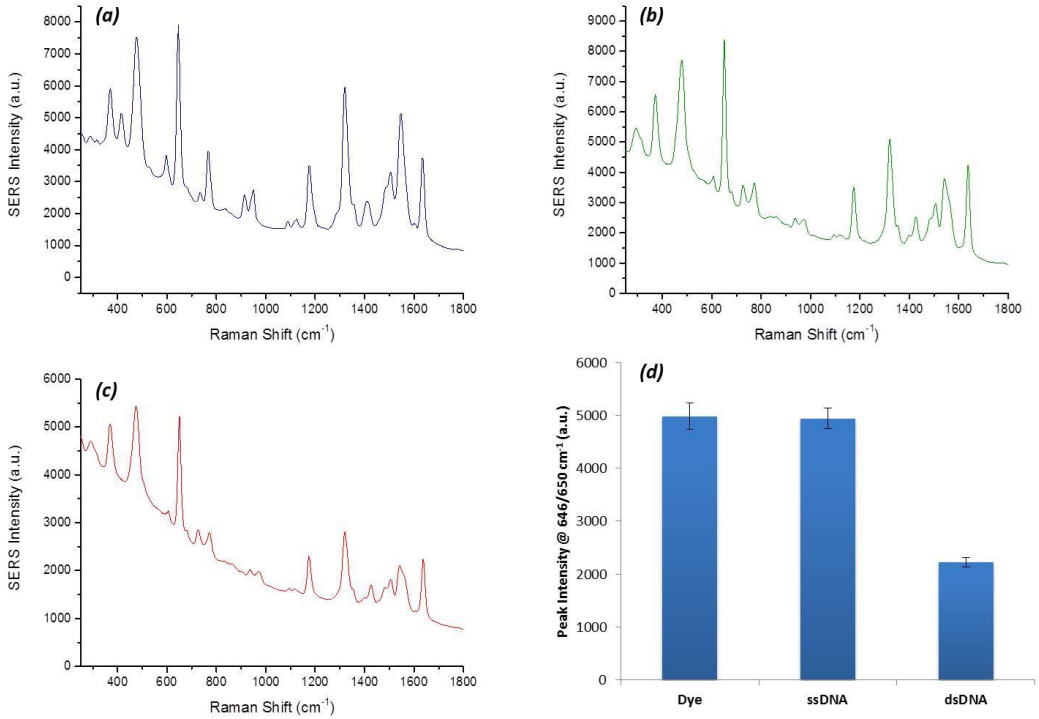

Figure 4.3 SERS analysis of (a) F-ITC (22 nM) (b) FAM labelled single stranded DNA (22 nM) and (c) FAM labelled double stranded DNA (22nM). (d) Further peak analysis at 646 cm^{-1} for F-ITC and 650 cm^{-1} for FAM covalently attached to DNA. SERS spectra were recorded using an excitation wavelength of 532 nm. Peak intensities were obtained by scanning 5 replicate samples 3 times with an accumulation time of 1 s. Averages are shown and error bars are ± one standard deviation.

When analysing the free dyes and dye labelled DNA using fluorescence spectroscopy, the fluorescence intensity changed depending on the DNA attachment to the dye. Fluorescence results for TAMRA demonstrated the maximum intensity was observed when single stranded DNA was attached to TAMRA, with TR-ITC and double stranded TAMRA labelled DNA producing similar fluorescent intensities (Figure 3.5). Comparing this to the SERS spectra shown in Figure 4.2, the change in fluorescence background of the spectra correlates to the fluorescence intensity results, with single stranded DNA showing the

highest fluorescence background (Figure 4.2 b). For FAM fluorescence comparison, the intensity was not greatly affected by DNA attachment, which is reflected in the SERS spectra (Figure 4.3 a-c) where the fluorescence background does not change significantly as it does with TAMRA. Therefore, both the SERS and fluorescence data have shown that attachment of a DNA sequence to a fluorescent dye will affect the fluorescence emission of the dye, which also correlates with the fluorescent background in the SERS spectra. The electrostatic interactions that arise due to the attachment of DNA to the fluorescent dye have shown to have an effect on the fluorescence emission (Figure 3.5), however changes in the SERS spectra of the dyes are also observed such as additional DNA peaks and a shift in all peak positions.

These results were based on separate analysis of the individual fluorescent dyes. As can be seen, each produced different SERS intensities depending on their attachment to oligonucleotides. However, the focus of this study was to determine what the outcome would be when the two fluorescent dyes were both present in mixtures, both in free forms and when they were covalently attached to an oligonucleotide sequence.

4.4.2 Effects of Changing Fluorescent Dye Concentration

The SERS intensity observed of the free dyes and dye labelled DNA sequences has a linear relationship with changing concentration, i.e. as the concentration of the analyte is increased, the SERS intensity also increases.[11, 14] However, it was important to determine what happens to the relative intensities of the two fluorescent dyes then present in a mixture when only the concentration of one fluorescent dye is changed. This is extremely important as it will ultimately affect the ability to quantify each dye present and ensure that one dye does not dominate or displace the other from the nanoparticle surface in the mixture. Four concentration studies were performed, two using the free forms of the fluorescent dyes, TR-ITC and F-ITC, and two using the TAMRA and FAM labelled single stranded DNA. The peaks monitored were the same as those stated previously.

4.4.2.1 Fluorescent Dyes (TR-ITC and F-ITC)

Two different scenarios were investigated, one involved changing the concentration of F-ITC from 2.2 pM to 22 nM while keeping the concentration of TR-ITC constant (22 nM). The other involved changing the concentration of TR-ITC (2.2 pM to 22 nM) while F-ITC concentration remained at 22 nM, at these concentrations the dyes will be above monolayer coverage on the nanoparticle surface. When varying the concentration of TR-ITC that was added to a solution of F-ITC, the FAM and TAMRA peaks at 646 cm^{-1} and 1650 cm^{-1} respectively were monitored. The results are given in Figure 4.4, it can be seen that the FAM peak at 646 cm^{-1} does not increase in intensity as would be expected since the concentration is not increasing. However, as the TR-ITC concentration is increased, the peak intensity of TAMRA also increases and at the highest concentration where the two dyes are in equimolar concentration, TAMRA intensity is higher than that of FAM (Figure 4.4a). This suggests that as TAMRA increases in concentration, it is capable of displacing FAM from the nanoparticle surface, resulting in a higher TAMRA SERS peak intensity, which is in good agreement with Figures 4.2 and 4.3 that show TAMRA producing much higher SERS intensity than FAM. When varying the concentration of F-ITC added to TR-ITC (22 nM), the F-ITC peak intensity does increase with increasing concentration, however not to the same extent with increasing TR-ITC concentration (Figure 4.4 b). At the highest concentration (22 nM), the F-ITC peak intensity at 646 cm^{-1} is not greater than that of TR-ITC at 1650 cm^{-1}, suggesting that when TR-ITC is added first, it is strongly attached to the nanoparticle surface and is not readily displaced by F-ITC.

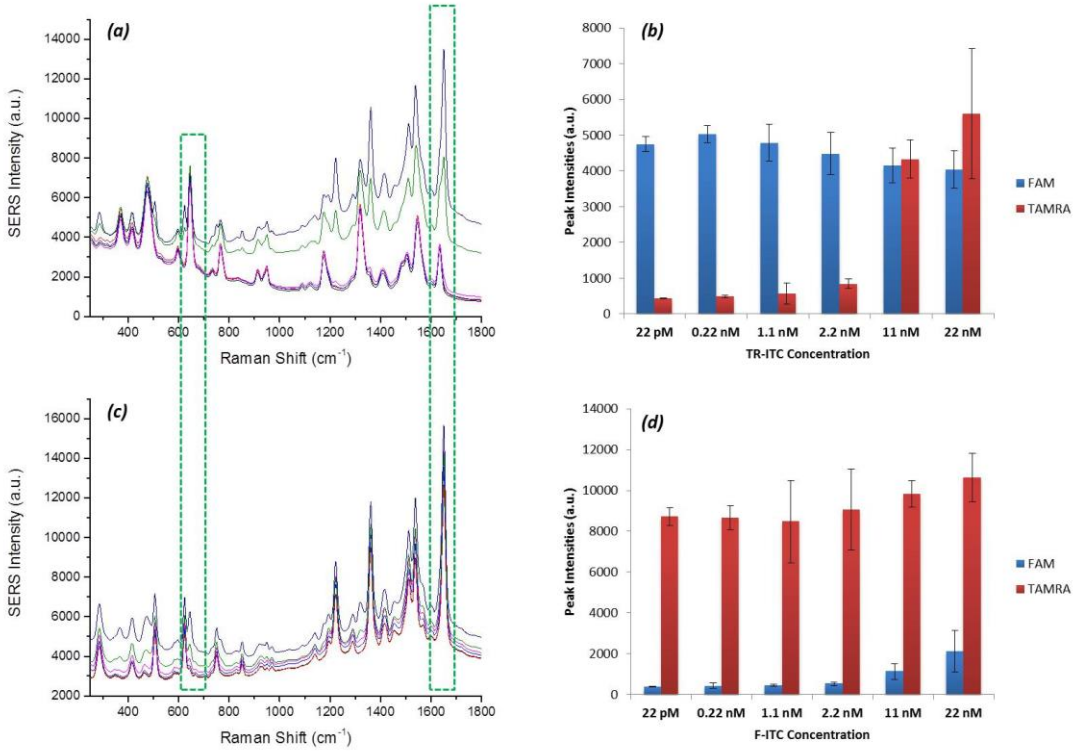

Figure 4.4 Results obtained when analysing the SERS peak intensities of TR-ITC (1650 cm^{-1}) and F-ITC (646 cm^{-1}) when one dye concentration is varied from 2.2 pM to 22 nM. Blue data represents F-ITC peak intensity and red data represents TR-ITC peak intensity. (a) SERS spectra with increasing TR-ITC concentration, (b) Peak intensity comparison when varying concentration of TR-ITC. (c) SERS spectra with increasing F-ITC concentration and (d) Peak intensity comparison when varying concentration of F-ITC. SERS spectra were recorded using an excitation wavelength of 532 nm and a 1 s accumulation time. Peak intensities were obtained by scanning 5 replicate samples 3 times with an accumulation time of 1 s. Averages are shown and error bars are ± one standard deviation.

4.4.2.2 Single Stranded TAMRA and FAM Labelled DNA

The same concentration studies were performed using fluorescent dye labelled single stranded DNA. When varying concentrations of TAMRA labelled DNA (2.2 pM to 22 nM) was added to FAM labelled DNA (22 nM), the TAMRA peak intensity at 1654 cm^{-1} increased as the concentration increased and, similar to that observed in Figure 4.5, there was no increase in the FAM peak intensity at 650 cm^{-1}. The higher concentrations, 0.2 nM to 22 nM, there was a slight decrease in intensity (Figure 4.5 a). Compared to the results obtained when varying the free dye concentration (Figure 4.4 a), at the highest concentration (22 nM), the TAMRA peak intensity is not greater than that of FAM. This suggests that when TAMRA is covalently attached to DNA, it is not able to displace FAM

labelled DNA as readily as the free form dyes due to the presence of the oligonucleotide sequences. At the highest concentration, 22 nM, it is above monolayer coverage. Figure 4.6b shows the results obtained when monitoring peak intensities when varying concentrations of FAM labelled DNA is added to TAMRA labelled DNA (22 nM). When TAMRA is added first, is strongly adheres to the nanoparticle, evidenced by the high peak intensity, similar to that observed when adding TR-ITC first. However, even when the concentration of FAM labelled DNA was increased, there is no increase in peak intensity at 650 cm^{-1}, suggesting that FAM labelled DNA is not able to displace TAMRA labelled DNA from the nanoparticle surface due to the electrostatic interactions between the charged dyes, negative DNA and the negative nanoparticle surface. The interaction between DNA, spermine and the nanoparticle surface is most likely to be the strongest, more so that the electrostatic interactions involving the charged dyes.

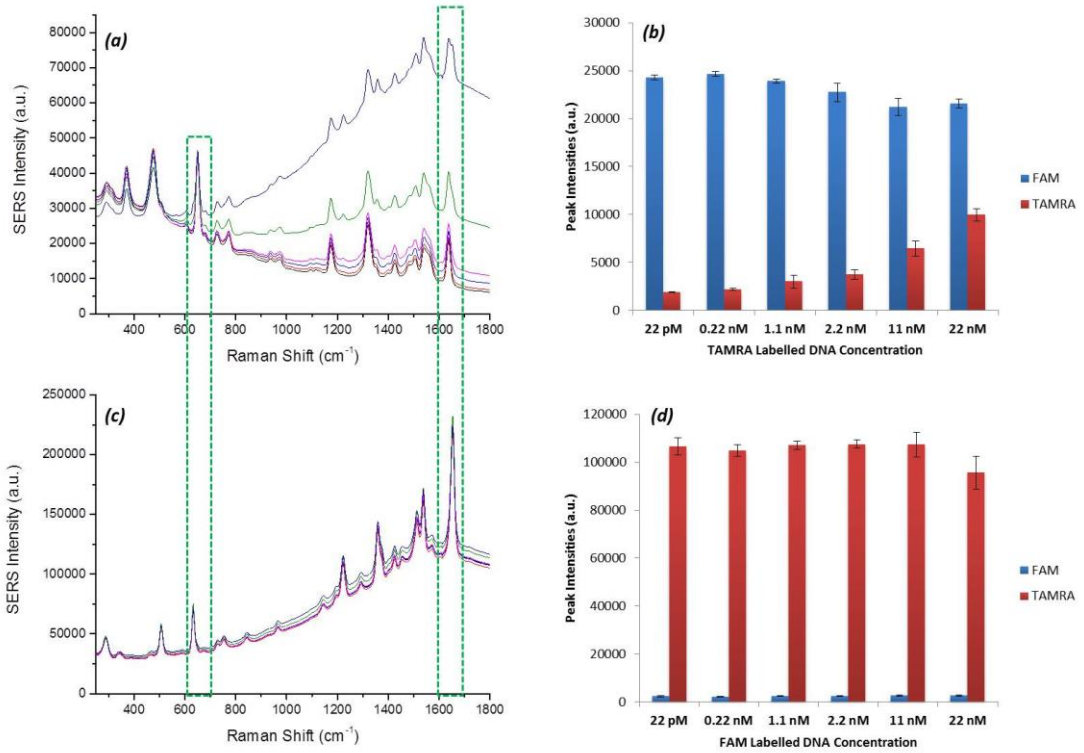

Figure 4.5 Results obtained when analysing the SERS peak intensities of TAMRA labelled DNA, at 1654 cm^{-1} (red) and FAM labelled DNA at 650 cm^{-1} (blue) when one concentration is varied from 2.2 pM to 22 nM (peaks are highlighted in the green boxes). (a) SERS spectra with increasing TAMRA labelled oligonucleotide and (b) peak intensity comparison with varying concentrations of TAMRA labelled DNA. (c) SERS spectra with increasing FAM labelled DNA concentration and (d) peak intensity comparison with varying concentrations of FAM labelled DNA. SERS spectra were recorded using an excitation wavelength of 532 nm and a 1 s accumulation time. Peak intensities were obtained by scanning 5 replicate samples 3 times with an accumulation time of 1 s. Averages are shown and error bars are ± one standard deviation.

4.4.2.3 Increasing Concentration of Both Fluorescent Dyes

Concentration studies were then performed using fluorescent dye labelled single stranded DNA and increasing both dye labelled DNA concentrations from 0.13 nM to 24.7 nM simultaneously. The lower concentrations were used so that the analysis was performed below monolayer coverage. Figure 4.6a shows the SERS spectra obtained when increasing the concentrations of both FAM and TAMRA labelled DNA. By monitoring the TAMRA and FAM peak intensities (1654 cm^{-1} and 650 cm^{-1} respectively), when they are present in the mixture (red data set) and when they are separate (blue data set), a clearer understanding of what happens on the nanoparticle surface with changing concentration can be obtained

(Figure 4.6b, c). Comparing both TAMRA and FAM dye labelled DNA when they are present separately, and in the mixture, the same response to changing concentration is observed for both dyes. At very low concentrations, below monolayer coverage around 0.13 nM to 1.3 nM, the oligonucleotides are likely to lie flat on the nanoparticle surface due to the attractive forces between the spermine and phosphate backbone and that there is space available on the nanoparticle surface (Figure 4.6 d(i)). There is then a plateau region from 2.6 nM to 16.9 nM suggesting that there is no more space on the nanoparticle surface for the dye labelled oligonucleotides to lie flat resulting in the formation of a second layer producing a slight increase in SERS intensity (Figure 4.6d(ii)). At the higher concentrations, 18.2 nM to 24.7 nM, the mixed monolayers on the surface may form into clusters or more layers with complex geometry. These may be head to tail structures with the dyes at the same or opposite ends with one pointing down to the surface and one away from the surface (Figure 4.6d(iii)). Therefore, above monolayer coverage, some dyes will lie off the surface and some are on it in equal measures, linking the SERS response to the increase in fluorescence. The fluorescence is not necessarily enhanced as this would require the correct distance between the fluorescent dye and the nanoparticle; it simply may not be as quenched at higher concentrations.

The blue data sets shown in Figure 4.7 represent the peak intensities observed when the dye labelled DNA sequences are both increased, however they are not present in a mixture. For both FAM and TAMRA labelled DNA, within this concentration range monolayer coverage is not reached as there is no plateau region observed. This is reasonable as monolayer coverage will be attained at lower dye concentrations when they are present in the mixture (red data sets), as there will be more dye labelled oligonucleotides present in that volume. This concentration study highlights why spermine is powerful in SERS as it influences the orientation of the dye labelled oligonucleotide through dye-DNA or DNA-DNA interactions resulting from the presence of spermine. Furthermore, results shown in Chapter 4 demonstrate the presence of spermine also influences the fluorescence emission of FAM and TAMRA; spermine enhances the fluorescence emission of FAM but has a lesser effect on TAMRA.

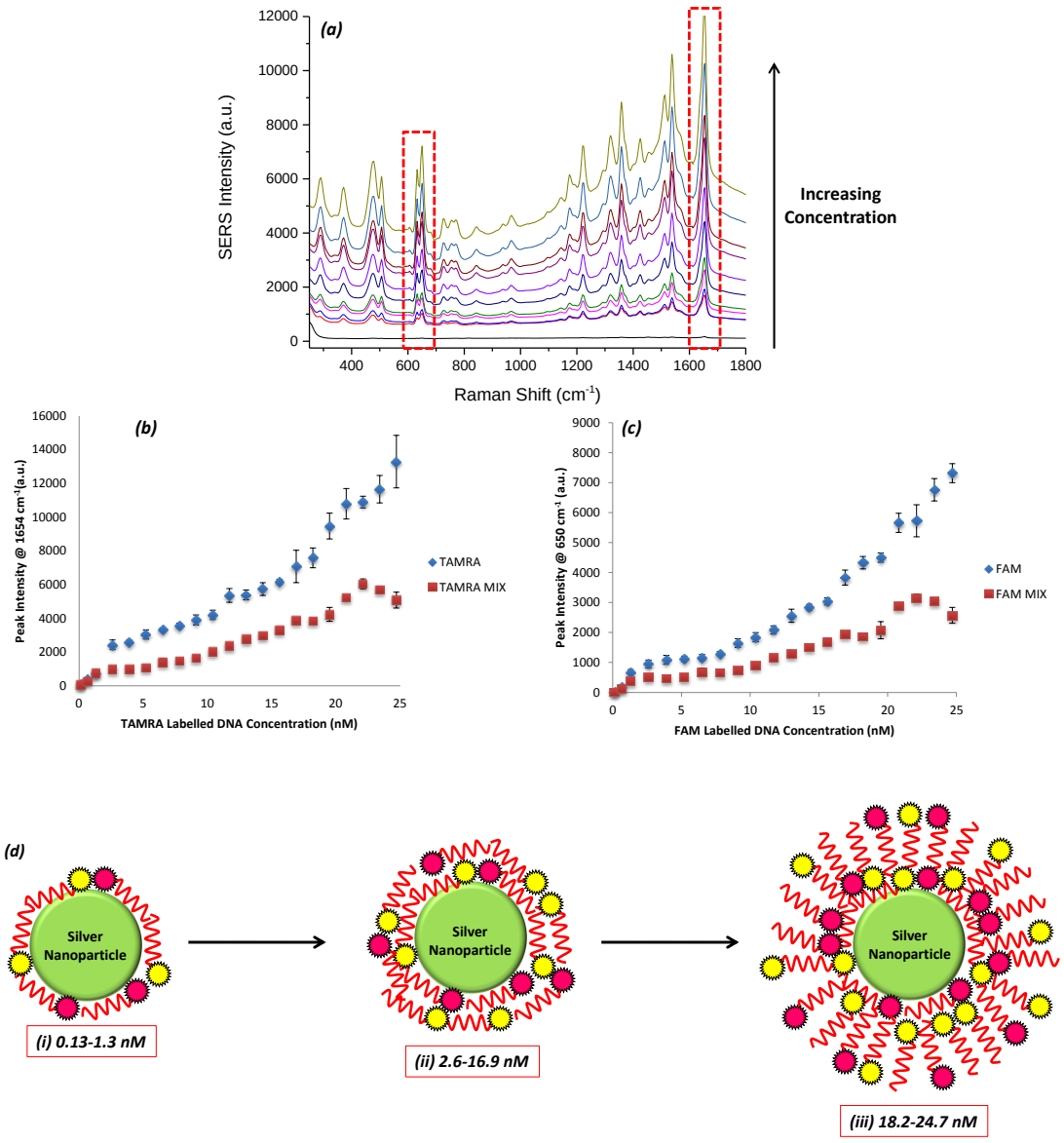

Figure 4.6 SERS spectra and peak intensity comparisons when increasing the concentration of both TAMRA and FAM labelled single stranded DNA simultaneously from 2.2 pM to 22 nM. (a) SERS spectra obtained when increasing the concentration of FAM and TAMRA labelled DNA. The 650 cm^{-1} FAM peak and 1654 cm^{-1} TAMRA peak are highlighted. (b) Peak intensity values at 1654 cm^{-1} comparing TAMRA labelled single stranded DNA when it is in a mixture (red) and when it is increased separately (blue). (c) Peak intensity values at 650 cm^{-1} comparing FAM labelled single stranded DNA when it is in a mixture (red) and when it is increased separately (blue). SERS spectra were recorded using an excitation wavelength of 532 nm and a 1 s accumulation time. Peak intensities were obtained by scanning 5 replicate samples 3 times with an accumulation time of 1 second. Averages are shown and error bars are ± one standard deviation. (d) A schematic representation of the orientation of the dye labelled DNA sequences when the concentration is increased (not to scale).

As demonstrated by the concentration studies performed, there is a marked difference in SERS intensity between TAMRA and FAM, either attached to an oligonucleotide or free, when both are present in a mixture. Order of addition of the dye labelled oligonucleotides plays a major role in the overall intensity observed as does the concentration of the free dye or dye labelled DNA. All concentration studies involved immediate SERS analysis after dye addition, therefore it was important to determine what happened to the SERS intensity of the fluorescent dyes over a time period.

4.4.3 Time Studies

For the two dyes to be used successfully in a SERS multiplex, it is imperative to understand the optimum sample preparation conditions required to enable identification of both dyes in a mixture. Previous experiments involved the two fluorescent dyes being premixed directly before SERS analysis resulting in spectra containing peaks from both dyes (Figure 4.7). The spectrum observed when the two fluorescent dyes are premixed is shown in Figure 4.7a and the individual spectra of TR-ITC and F-ITC are shown in Figure 4.7 b and c respectively. The multiplex spectrum contains peaks from both dyes, highlighted with asterisks.

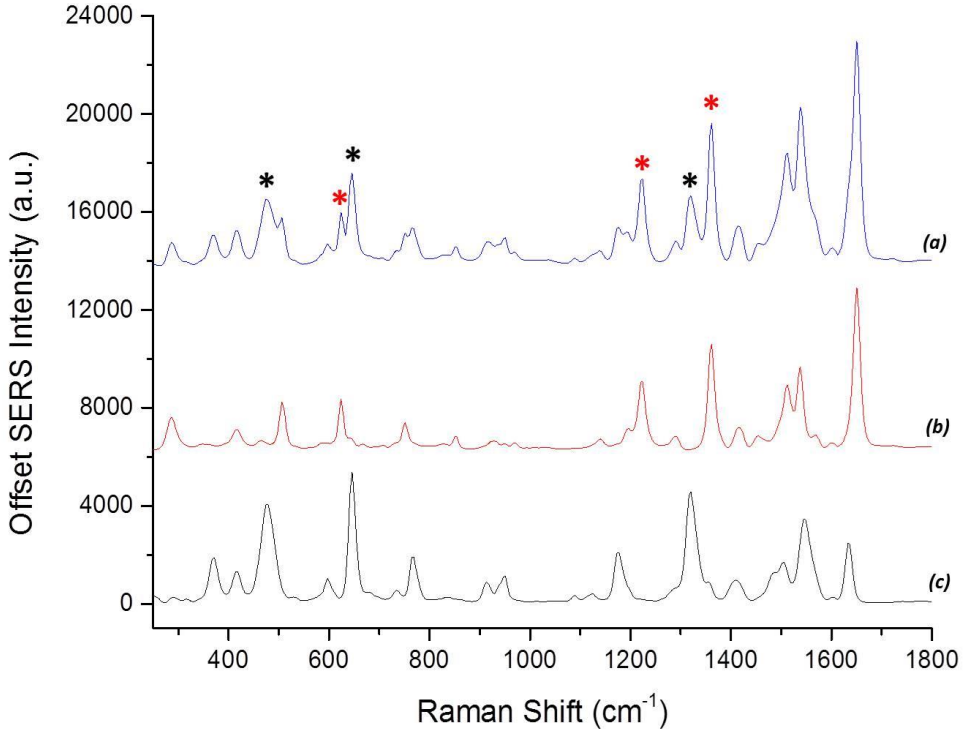

Figure 4.7 The SERS spectra of (a) the two fluorescent dyes, TR-ITC and F-ITC (both 22 nM), premixed directly before SERS analysis, (b) TR-ITC (22 nM) and (c) F-ITC (22 nM). TR-ITC peaks are highlighted with the red asterisk and the F-ITC speaks are highlighted by the black asterisk. SERS spectra were recorded using an excitation wavelength of 532 nm and a 1 second accumulation time.

Concentration studies have shown that the order of addition of fluorescent dye affects the SERS spectra produced (section 4.4.2). Therefore, studies were performed that did not focus on changing the concentration of the free dyes or dye labelled DNA, but what happened to the SERS intensity of the two dyes after initial addition to the mixture over a period of time. The unique peaks for TAMRA and FAM were monitored over a period of 20 minutes, with SERS spectra collected every 5 minutes.

4.4.3.1 Free Dyes Time Study

The SERS spectra of F-ITC and TR-ITC (22 nM) were monitored over a period of time. TR-ITC was added to the solution of spermine and silver nanoparticles followed by F-ITC immediately before SERS analysis. The order of addition of the fluorescent dyes was

reversed for the second time study. TR-ITC was added first to the cuvette containing spermine, distilled water and citrate reduced silver nanoparticles followed by the addition of F-ITC and spectra were recorded every 5 minutes for 20 minutes. The TAMRA peak at 1650 cm^{-1} decreases over time. A peak at 646 cm^{-1} due to F-ITC was observed, showing that F-ITC does interact with the nanoparticle surface; however does not vary much over time. The intensity observed at 1650 cm^{-1} is higher indicating a stronger interaction with the nanoparticle when it comes to TR-ITC (Figure 4.8a-c).

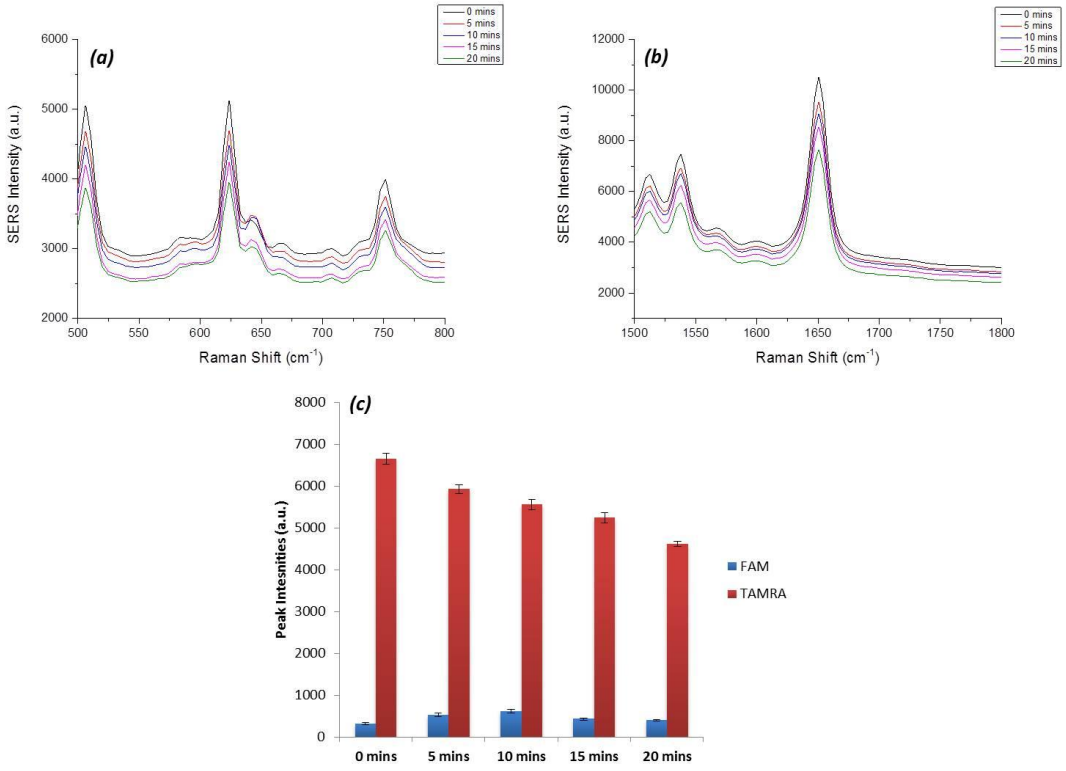

Figure 4.8 Results obtained when monitoring the SERS intensity for 20 minutes. TR-ITC (22 nM) was added first to the sample mixture followed by F-ITC (22 nM). (a) SERS spectra focussing on 646 cm^{-1} peak monitored for F-ITC, (b) SERS spectra focussing on 1650 cm^{-1} peak monitored for TR-ITC. (c) Comparison of the TR-ITC peak (red) and the F-ITC peak (blue). SERS spectra were recorded using an excitation wavelength of 532 nm and a 1 second accumulation time. Peak intensities were obtained by scanning 5 replicate samples 3 times with an accumulation time of 1 s. Averages are shown and error bars are ± one standard deviation.

The second time study involved the addition of F-ITC first, followed by the addition of TR-ITC. The intensity of the 1650 cm^{-1} TAMRA peak does not significantly increase over time; however the intensity of the 646 cm^{-1} F-ITC peak decreased (Figure 4.9a-c). This suggests that TR-ITC is displacing F-ITC from the nanoparticle surface, further indicating the stronger

affinity that TR-ITC has for the nanoparticle surface compared to F-ITC and is in good agreement with initial results shown in Figures 4.2 and 4.3. This is further highlighted when considering the change in background fluorescence, which decreases over time. This could be a result of the dyes coming closer to the nanoparticle surface over time, especially TR-ITC, allowing for the fluorescence to be quenched.

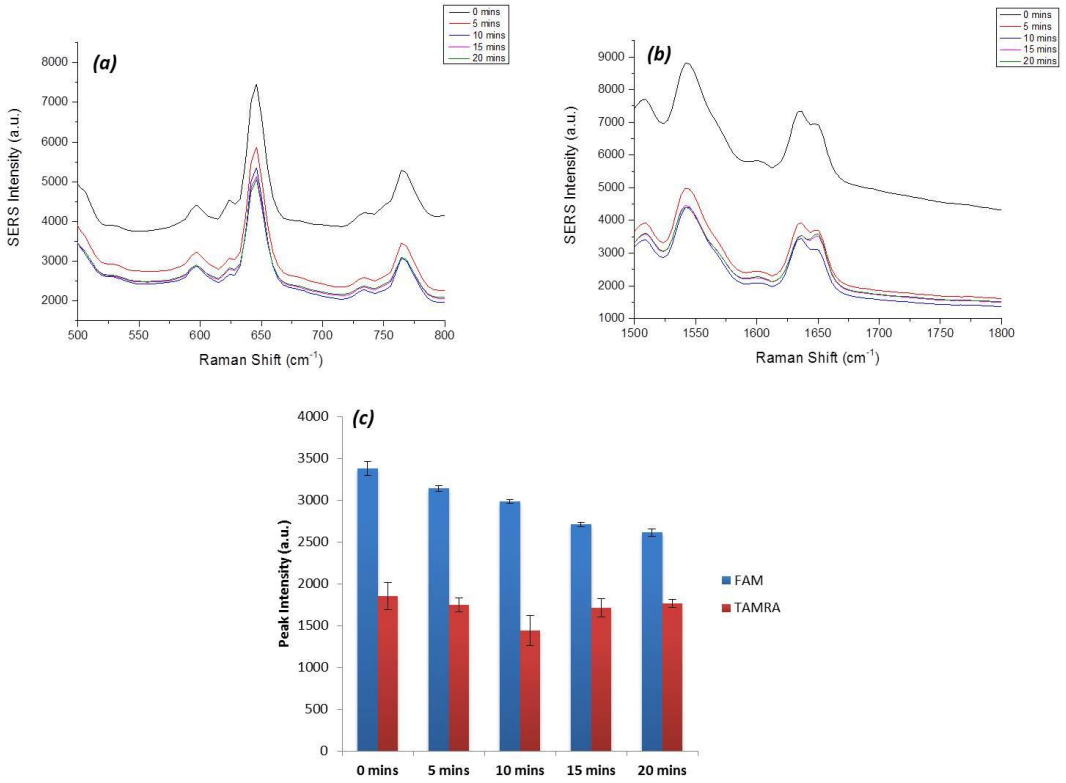

Figure 4.9 Results obtained when monitoring the SERS intensity for 20 minutes. F-ITC (22 nM) was added first to the sample mixture followed by TR-ITC (22 nM). (a) SERS spectra focussing on 646 cm^{-1} peak monitored for F-ITC, (b) SERS spectra focussing on 1650 cm^{-1} peak monitored for TR-ITC. (c) Comparison of the TR-ITC peak (red) and the F-ITC peak (blue). SERS spectra were recorded using an excitation wavelength of 532 nm and a 1 second accumulation time. Peak intensities were obtained by scanning 5 replicate samples 3 times with an accumulation time of 1 second. Averages are shown and error bars are ± one standard deviation.

4.4.3.2 Single Stranded DNA Time Study

Similar time studies were then carried out using single stranded DNA labelled with either FAM or TAMRA. Initially, FAM labelled single stranded DNA was added to a solution containing TAMRA labelled single stranded DNA and SERS spectra were monitored. Then

the converse was carried out, FAM labelled single stranded DNA was added initially followed by TAMRA labelled single stranded DNA. SERS spectra were then recorded at 5 minute intervals for 20 minutes. The TAMRA and FAM peaks that were monitored for intensity comparisons were 1654 cm^{-1} and 650 cm^{-1} respectively.

Figure 4.10a-c shows that when TAMRA labelled single stranded DNA was added initially to the sample mixture followed by FAM labelled single stranded DNA, TAMRA dominated the SERS spectrum. This suggests that there is a very strong interaction between the TAMRA labelled single stranded DNA and the nanoparticle surface. As observed in Figure 4.2, TAMRA labelled single stranded DNA does have a stronger affinity for the nanoparticle surface, especially compared to TR-ITC. Therefore, when FAM labelled single stranded DNA is added last, FAM cannot displace TAMRA labelled DNA and come into close enough contact with the nanoparticle surface for signal enhancement. The stronger attraction that TAMRA has for the nanoparticle surface is likely to be a result of electrostatic attraction between the positive dye and the negative nanoparticle surface. Again, there is a decrease in the background fluorescence over time, most notable at the TAMRA peak at 1654 cm^{-1} (Figure 4.10b), as the fluorescence is being quenched when the dye labelled single stranded DNA sequences is coming closer to the nanoparticle surface. The differences observed between the time studies involving the free dyes and dye labelled single stranded DNA is another effect observed due to the attachment of a DNA sequence, which has been shown to cause changes in the SERS spectra in Figure 4.1.

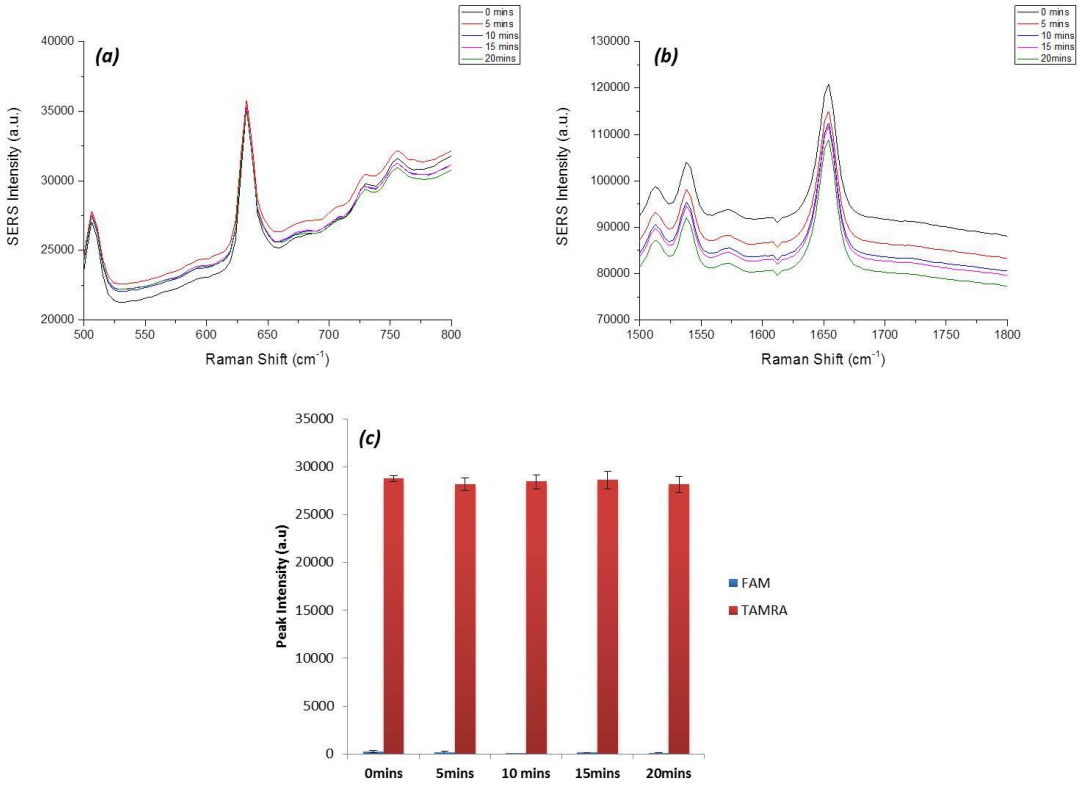

Figure 4.10 Results obtained when monitoring the SERS intensity for 20 minutes. TAMRA labelled single stranded DNA (22 nM) was added first to the sample mixture followed by FAM labelled single stranded DNA (22 nM). (a) SERS spectra focussing on 650 cm^{-1} peak monitored for FAM labelled single stranded DNA, (b) SERS spectra focussing on 1654 cm^{-1} peak monitored for TAMRA labelled single stranded DNA. (c) Comparison of the TAMRA peak (red) and the FAM peak (blue). SERS spectra were recorded using an excitation wavelength of 532 nm and a 1 s accumulation time. Peak intensities were obtained by scanning 5 replicate samples 3 times with an accumulation time of 1 s. Averages are shown and error bars are ± one standard deviation.

When FAM labelled single stranded DNA was added first, FAM peaks are strong in the SERS spectrum (Figure 4.11 a and b). The intensity of the 650 cm^{-1} FAM peak remains constant over the 20 minutes, whereas the intensity of the 1654 cm^{-1} TAMRA peak increases, despite there being no increase in concentration (Figure 4.11c). This suggests that TAMRA is coming closer to the nanoparticle surface over time, and if this continues TAMRA could eventually displace FAM on the surface and dominate the SERS spectrum. This is in agreement with results shown in Figures 4.2 and 4.3, where TAMRA produces the higher SERS intensity compared to FAM regardless of their covalent attachment to DNA. There is also a change in the background signal, however it does not decrease in a similar way as shown in

Figure 4.9. This difference that is observed could be a result of the attachment of the dyes to single stranded DNA sequences that will affect the orientation and therefore the distance between the dye and the nanoparticle surface. There is no clear pattern with the change in background fluorescence of the time period and this could be a result of the formation of mixed layers where the dyes will not be uniformly positioned with respect to the nanoparticle surface.

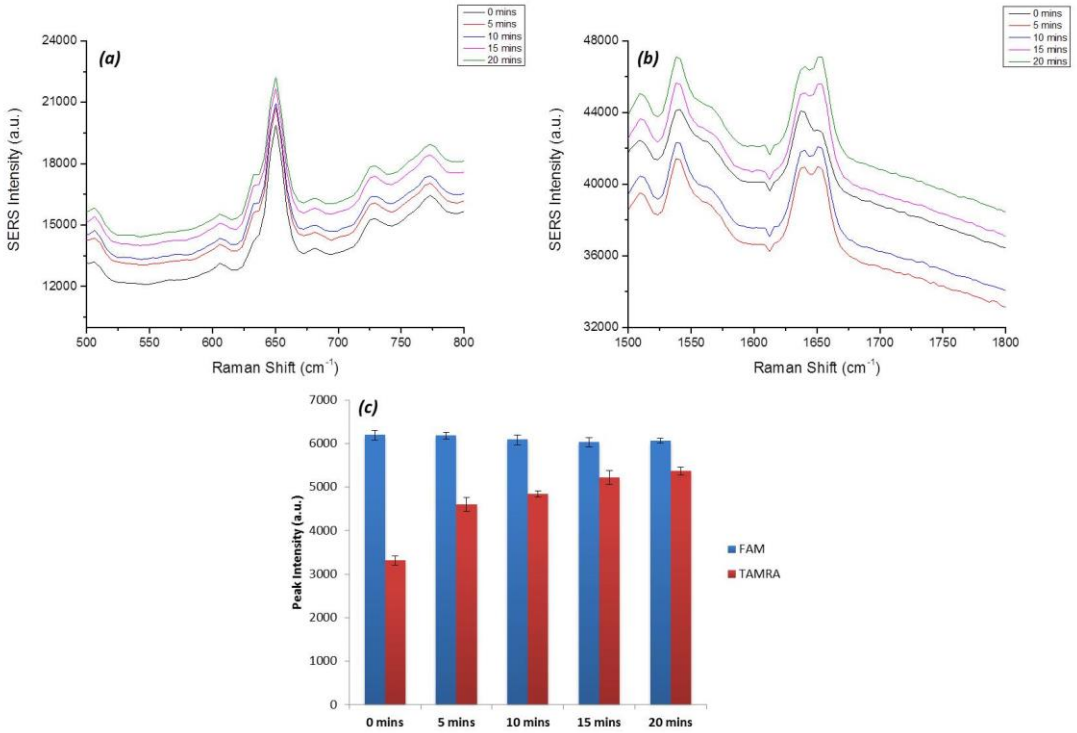

Figure 4.11 Results obtained when monitoring the SERS intensity for 20 minutes. FAM labelled single stranded DNA (22 nM) was added first to the sample mixture followed by TAMRA labelled single stranded DNA (22 nM). (a) SERS spectra focussing on 650 cm^{-1} peak monitored for FAM labelled single stranded DNA, (b) SERS spectra focussing on 1654 cm^{-1} peak monitored for TAMRA labelled single stranded DNA. (c) Comparison of the TAMRA peak (red) and the FAM peak (blue). SERS spectra were recorded using an excitation wavelength of 532 nm and a 1 s accumulation time. Peak intensities were obtained by scanning 5 replicate samples 3 times with an accumulation time of 1 s. Averages are shown and error bars are ± one standard deviation.

4.4.3.3 Double Stranded DNA Time Study

TAMRA and FAM labelled DNA sequences were hybridised to their complementary sequences to determine the effect double stranded labelled DNA would have on the intensity of the SERS spectra over the time period. Two samples were analysed, one where TAMRA labelled double stranded DNA was added first to the sample mixture followed by FAM labelled double stranded DNA, and the reverse of this where FAM labelled double stranded DNA was added first.

When TAMRA labelled double stranded DNA is added first, there was no significant increase in intensity at 650 cm^{-1} indicative of the presence of FAM and as the time study progressed, TAMRA intensity at 1654 cm^{-1} decreased (Figure 4.12). Figure 4.12c suggests that when TAMRA labelled double stranded DNA is added initially, it adsorbs directly onto the surface; however over time a layer of TAMRA double stranded DNA could form around the nanoparticle surface where TAMRA is positioned further away from the surface resulting in a decrease in peak intensity. Regardless, TAMRA is positioned closer to the surface and as a result dominated the SERS spectrum throughout the time study. An observed decrease in the background signal suggests that over the time period TAMRA labelled double stranded is coming in closer proximity to the nanoparticle surface, quenching the fluorescence.

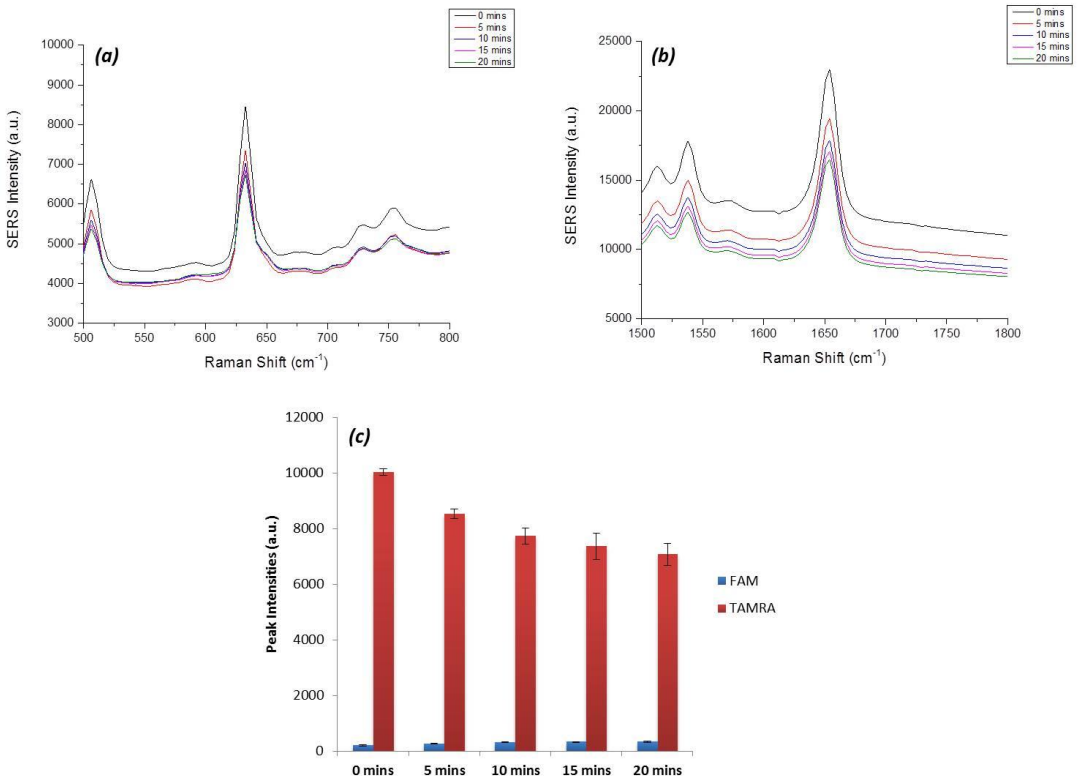

Figure 4.12 Results obtained when monitoring the SERS intensity for 20 minutes. TAMRA labelled double stranded DNA (22 nM) was added first to the sample mixture followed by FAM labelled double stranded DNA (22 nM). (a) SERS spectra focussing on 650 cm^{-1} peak monitored for FAM labelled double stranded DNA, (b) SERS spectra focussing on 1654 cm^{-1} peak monitored for TAMRA labelled double stranded DNA. (c) Comparison of the TAMRA peak (red) and the FAM peak (blue). SERS spectra were recorded using an excitation wavelength of 532 nm and a 1 s accumulation time. Peak intensities were obtained by scanning 5 replicate samples 3 times with an accumulation time of 1 s. Averages are shown and error bars are ± one standard deviation.

Similar to the results obtained from the time studies involving the free dyes (Figure 4.9) and dye labelled single stranded DNA (Figure 4.11), when FAM labelled double stranded DNA is added first followed by TAMRA labelled double stranded DNA, the FAM peak intensity is readily observed at 650 cm^{-1}. The intensity of the peaks are lower than that when TAMRA labelled DNA is added first (2,000 a.u. compared to 10,000 a.u.); however, based on results shown in Figure 4.3 and 4.4 this is to be expected as TAMRA does produce higher SERS peak intensities compared to FAM. The TAMRA peak intensity does increase over time (Figure 4.13c). A potential competing effect to the displacement of FAM by TAMRA is the formation of layers consisting of dye labelled DNA. When TAMRA labelled DNA is added first, a layer could form around the nanoparticle resulting in high TAMRA SERS intensity and upon

addition of FAM labelled DNA, a second layer may form; however this will be further from the nanoparticle surface and therefore FAM SERS intensity is low. Conversely, when FAM labelled DNA was added initially followed by TAMRA labelled DNA, a layer of FAM labelled DNA could form around the nanoparticle and this time in closer proximity resulting in the observable FAM peak intensities. Even when TAMRA labelled DNA is added last, it may still be capable of forming a layer around the FAM labelled DNA over time and as it produces higher SERS intensity separately (Figure 4.2), TAMRA peak intensity will also be readily observed. This layer could be positioned further away from the nanoparticle surface due to the increase in background signal observed.

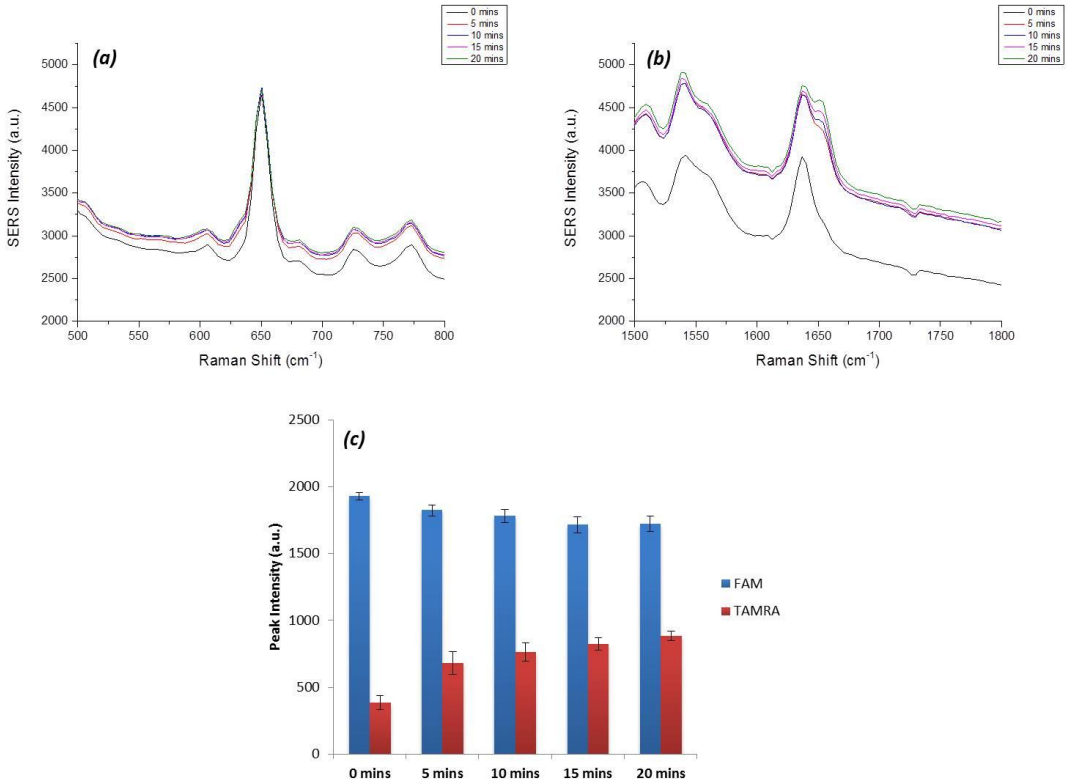

Figure 4.13 Results obtained when monitoring the SERS intensity for 20 minutes. FAM labelled double stranded DNA (22 nM) was added first to the sample mixture followed by TAMRA labelled double stranded DNA (22 nM). (a) SERS spectra focussing on 650 cm^{-1} peak monitored for FAM labelled double stranded DNA, (b) SERS spectra focussing on 1654 cm^{-1} peak monitored for TAMRA labelled double stranded DNA. (c) Comparison of the TAMRA peak (red) and the FAM peak (blue). SERS spectra were recorded using an excitation wavelength of 532 nm and a 1 s accumulation time. Peak intensities were obtained by scanning 5 replicate samples 3 times with an accumulation time of 1 s. Averages are shown and error bars are ± one standard deviation.

The results obtained from these time studies show the major impact that order of addition has on the SERS intensity observed for both fluorescent dyes. Another major consideration is that the order of addition is dependent upon the fluorescent dye being bound or unbound to DNA and whether the DNA is either single or double stranded. These are not the only factors that will affect the design considerations of a SERS based assay. Changing experimental conditions such as pH has been shown in chapter 3 to greatly influence the fluorescence emission of TAMRA and FAM; therefore it is reasonable to assume that varying the pH could potentially affect the SERS spectra of the two dyes.

4.4.4 pH Effects on SERS Intensity

The effect of changing the pH on the SERS intensity of each fluorescent dye solution was investigated. The free fluorescent dyes, fluorescent dye labelled single stranded DNA and fluorescent dye labelled double stranded DNA were analysed under four different pHs. The solutions used were citrate/HCl (pH 2.9), distilled water (pH 5.2), phosphate buffered saline (pH 6.9) and NaOH (pH 13.2), found in Table 4.2.

4.4.4.1 TAMRA

TR-ITC, TAMRA labelled single stranded DNA or TAMRA labelled double stranded DNA were added to a solution of spermine, one of the four varying pH solutions and citrate reduced silver nanoparticles. The SERS spectra obtained and the comparisons of peak intensities can be found in Figure 4.14.

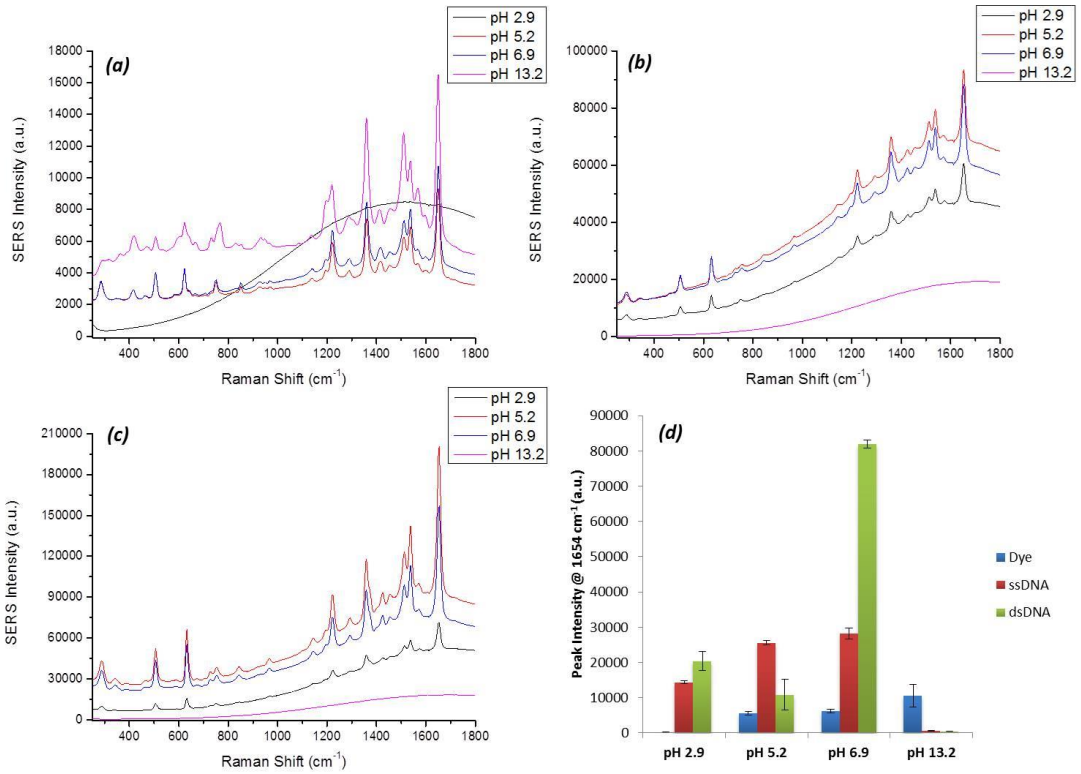

Figure 4.14 Results obtained from varying the pH of the solution of TR-ITC or TAMRA labelled DNA (22 nM). (a) SERS spectra of TR-ITC with changing pH, (b) SERS spectra of TAMRA labelled single stranded DNA with changing pH and (c) SERS spectra of TAMRA labelled double stranded DNA with changing pH. (d) Comparison of the peak intensities at 646/650 cm^{-1} and 1650/1654 cm^{-1} over the pH range for TR-ITC (blue), TAMRA labelled single stranded DNA (red) and TAMRA labelled double stranded DNA (green). SERS spectra were recorded using an excitation wavelength of 532 nm and a 1 s accumulation time. Peak intensities were obtained by scanning 5 replicate samples 3 times with an accumulation time of 1 s. Averages are shown and error bars are ± one standard deviation.

SERS analysis of TR-ITC solutions of varying pH (Figure 4.14a), show that no SERS signal was observed at pH 2.9, and the highest intensity SERS signal was observed at pH 13.2. TR-ITC is a positive dye and therefore has a strong affinity for the negatively charged surface of the nanoparticle, further enhanced at pH 13.2. SERS results obtained when analysing TAMRA labelled single stranded DNA at the varying pH solutions (Figure 4.14b) are different to those obtained for TR-ITC. SERS spectra are observed at acidic and neutral pH, however at pH 13.2 there is a significant reduction in intensity. For TAMRA labelled double stranded DNA, high intensity at 1654 cm^{-1} is observed at pH 6.9 (Figure 4.14c). These results are in good agreement with Figure 4.2, where double stranded TAMRA labelled DNA has a higher

affinity for the nanoparticle surface compared to single stranded DNA. At pH 13.2, TAMRA exists in its protonated form that is fluorescent and DNA becomes denatured which has resulted in no SERS signal observed for either single or double stranded TAMRA labelled DNA. As shown in chapter 3 (Figure 3.8), changing the pH will cause structural changes in the fluorescent dyes. This is evident in Figure 4.14a as there is a change in the relative peak intensities at 1500-1600 cm^{-1} suggesting that TR-ITC has a different structure at pH 13.2 compared to the other pHs, structures are shown in chapter 3 Figure 3.10.

4.4.4.2 FAM

To investigate the effect of pH on the SERS signals from F-ITC, FAM labelled single stranded DNA or FAM labelled double stranded DNA was added to a solution of spermine, one of the four varying pH solutions and citrate reduced silver nanoparticles. The SERS spectra obtained and the peak intensity comparisons can be found in Figure 4.15.

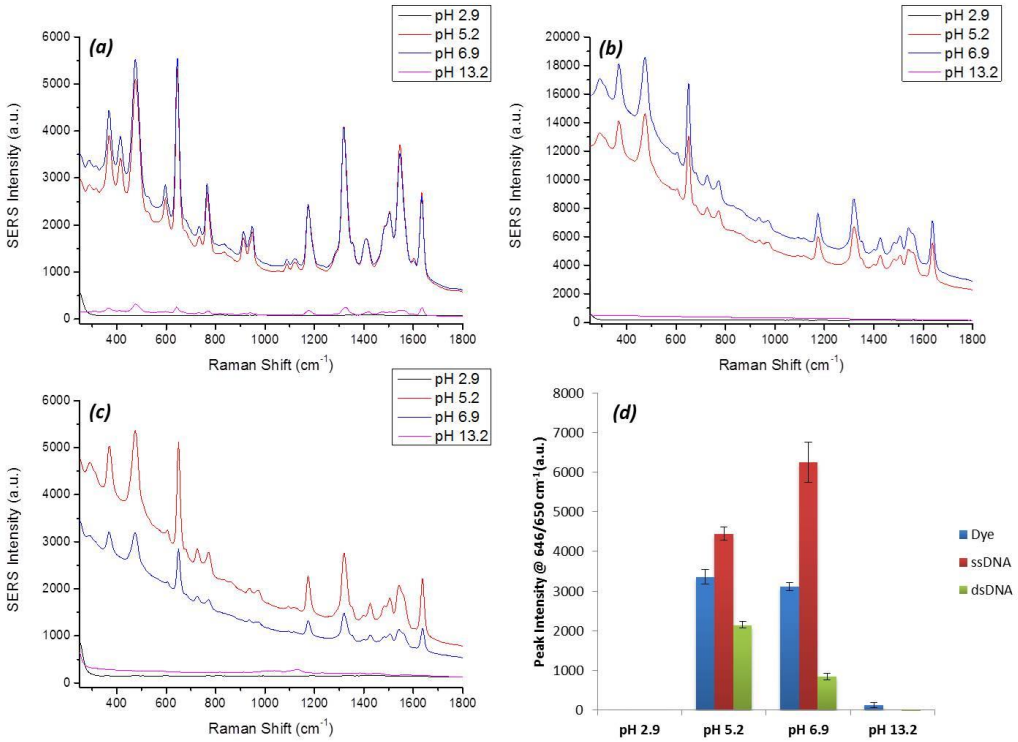

Figure 4.15 SERS obtained from varying the pH of F-ITC or FAM labelled DNA (22.2 nM). (a) SERS spectra of F-ITC with changing pH, (b) SERS spectra of FAM labelled single stranded DNA with changing pH and (c) SERS spectra of FAM labelled double stranded DNA with changing pH. (d) Comparison of the peak intensities at 646/650 cm^{-1} and 1650/1654 cm^{-1} over the pH range for F-ITC (blue), FAM labelled single stranded DNA (red) and FAM labelled double stranded DNA (green). SERS spectra were recorded using an excitation wavelength of 532 nm and a 1 s accumulation time. Peak intensities were obtained by scanning 5 replicate samples 3 times with an accumulation time of 1 s. Averages are shown and error bars are ± one standard deviation.

At pH 5.2 and 6.9, F-ITC gives the optimal SERS intensity (Figure 4.15a); in acidic and alkaline conditions the SERS intensity is greatly reduced. SERS intensity obtained when the pH of FAM labelled single stranded DNA was changed gave similar results to F-ITC (Figure 4.15b). Again with double stranded FAM labelled DNA, no SERS intensity is observed at pH 2.9 or pH 13.2 and the intensity observed at pH 5.2 and 6.9 is lower than that for F-ITC and single stranded DNA (Figure 4.15c).

When changing the pH of the solution, the fluorescence emission and SERS intensities of both TAMRA and FAM are greatly affected. With respect to fluorescence, the structures of

the dyes changed with varying the pH (Figure 3.10). As the pH was increased, FAM changed from its non-fluorescent lactone structure to its ring opened structure that was highly fluorescent, which explained the increase in FAM fluorescence with increase in pH. Analysing the same pH solutions containing F-ITC or FAM labelled DNA, SERS signals were only observed within the pH range 5.2 to 6.9. An increase in SERS intensity was not observed and therefore did not show the same response compared to fluorescence emission. Varying the pH did not affect the fluorescence emission of TAMRA as the dye exists in two forms in the pH range used, either the zwitterion or the protonated form that are both fluorescent (Figure 3.10). The SERS intensity observed of TR-ITC and TAMRA labelled DNA with varying pH showed an increase in SERS intensity for TR-ITC when the pH increased, however at pH 13.2 no SERS signals were observed for TAMRA labelled DNA (Figure 4.14d). There is no direct relationship between fluorescence and SERS when varying the pH, a reason for this may be that in SERS the silver nanoparticles will also be affected by changing pH, which was not an issue when performing fluorescence analysis.

4.4.5 Nanoparticle Characterisation at Different pH

It has already been discussed in chapter 3 section 3.4.3 that changing the pH of a solution will have an effect on the structure of the fluorescent dye; however changing the pH will also have an effect on the nanoparticles. This will ultimately affect the ability of the analyte to interact with the nanoparticle surface and the stability of the nanoparticles. For example, changing the pH could remove/displace the citrate from the surface of the nanoparticle or it could cause uncontrolled aggregation. Both these situations could potentially inhibit the interaction of spermine with the nanoparticle surface could reduce the ability of the dye or dye labelled DNA to adsorb onto the surface of the nanoparticle and affect the reproducibility of the SERS response. The effect of changing the pH on the nanoparticles was investigated by measuring the size and zeta potential of the nanoparticle at different pH in the presence and absence of spermine.

Citrate reduced silver nanoparticles were added to each of the four solutions with varying pH and the particle size was measure before and after spermine addition (Figure 4.16). SERS measurements were previously recorded at a pH of 5.2, and as can be seen in Figure

4.16, varying the pH away from 5.2 causes nanoparticle aggregation that will be uncontrolled, as the particle size in the absence of spermine at pH 5.2 is approximately 60 nm, when the pH is changed this increases significantly to between 600 and 800 nm. The presence of spermine does cause aggregation of the nanoparticles, however this is controlled. At pH 6.9, the aggregation will be caused by the presence of the salt in PBS solution. At extremely acidic and alkaline pH, the surface charge on the nanoparticle will change inducing uncontrolled aggregation.

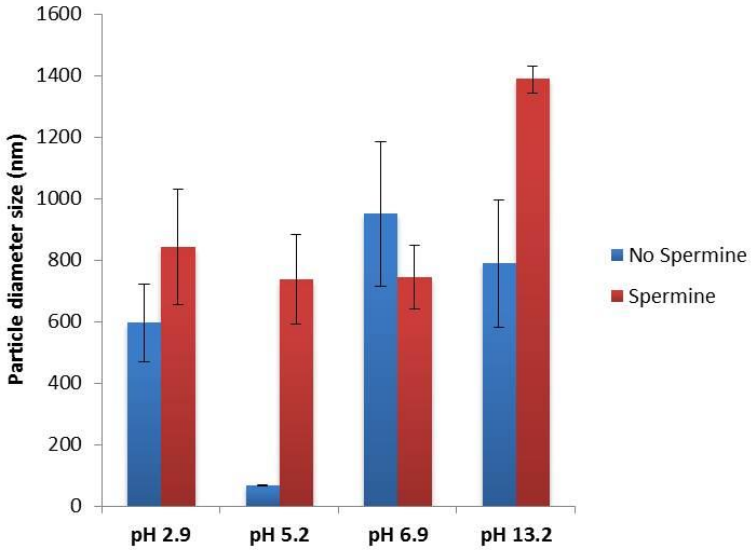

Figure 4.16 Size of the citrate reduced silver nanoparticles when changing the pH. Measurements were taken before (blue) and after (red) spermine addition. Three replicate measurements were taken for each sample. Error bars represent ±1 standard deviation.

The Zeta potential of each of the four different pH solutions containing nanoparticles and spermine was then measured. The Zeta potential provides information regarding the charge on the nanoparticle surface. As the silver nanoparticles possess a negatively charged citrate layer on the surface, the more negative the value the more stable the nanoparticles are in solution. Results are shown in Figure 4.17 and they provide a clearer understanding as to what is happening on the nanoparticle surface at the various pHs.

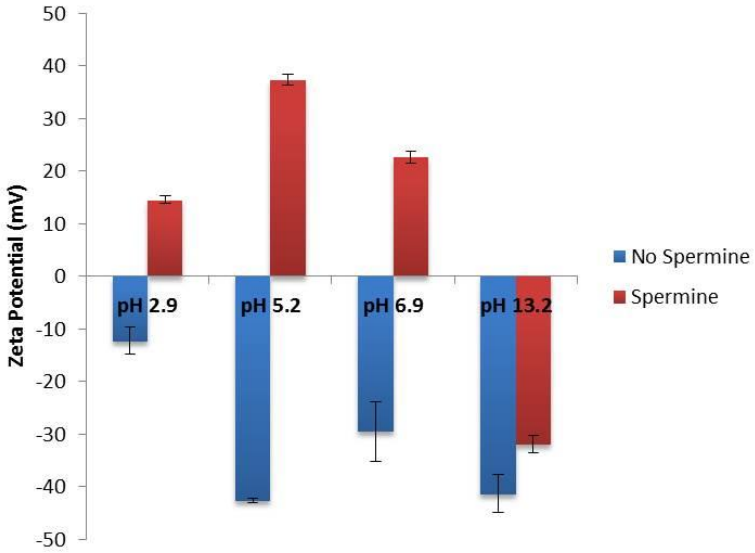

Figure 4.17 Zeta potential of the citrate reduced silver nanoparticles when changing the pH. Measurements were taken before (blue) and after (red) spermine addition. Three replicate measurements were taken for each sample. Error bars represent ±1 standard deviation.

The addition of the polycation spermine changes the surface charge from negative to positive at acidic and neutral pHs. However at pH 13.2, addition of spermine does not change the charge on the surface of the nanoparticle to positive. The pKa of spermine is around 10.5, therefore at pH 13.2 spermine is no longer a polycation and as a result cannot create a positive charge on the surface of the nanoparticle. This explains why there is no SERS observed at pH 13.2 of dye labelled DNA. SERS relies on the interaction of the analyte (fluorescent dye or DNA) with the nanoparticle surface. This can only occur if spermine is present to reduce the negative charge on the nanoparticle surface allowing the negative DNA to come close to the surface. Fluorescence studies demonstrated that at pH 13.2, fluorescence intensity was observed (Figure 3.9), however in these fluorescence measurements there is no dependence on the presence of spermine to observe a signal.

At low pH, the nanoparticle/spermine solution is positive, allowing for optimal nanoparticle-DNA interactions to occur. However at pH 13.2, there is a net negative charge on the nanoparticle surface causing a high degree of repulsion between the DNA and surface, therefore the analyte cannot come close enough to the nanoparticle resulting in poor SERS intensity. At physiological pH, TAMRA will favourably make contact with the

nanoparticle surface, whereas FAM will preferentially interact with the polycation spermine (Figure 4.18). These differences in proximity to the nanoparticle surface explain why TAMRA produces a higher SERS intensity compared to FAM.

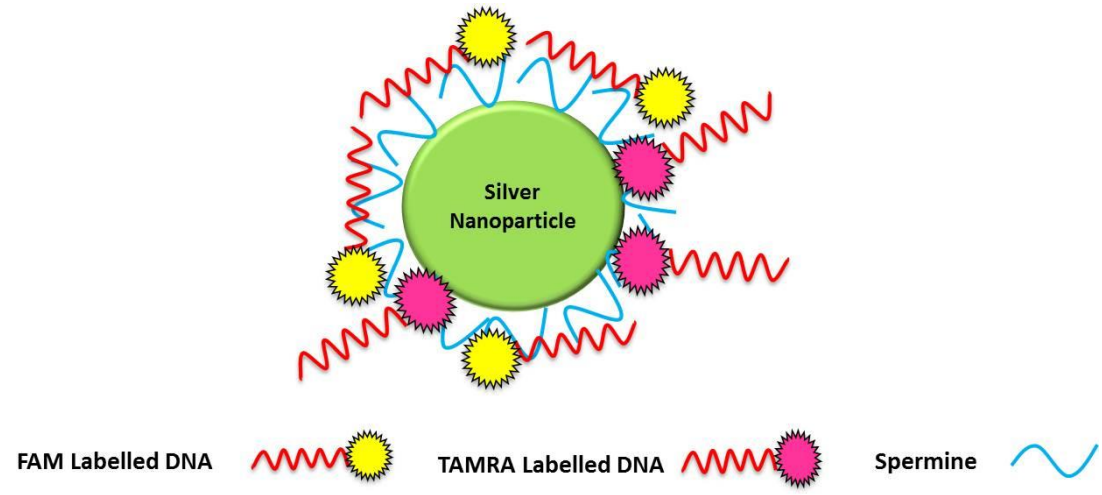

Figure 4.18 Schematic of the interactions between the silver nanoparticles, spermine, FAM labelled DNA and TAMRA labelled DNA in neutral pH conditions.

As discussed in chapter 4, changing pH also affects the structural form of the fluorescent dyes. TAMRA can exist in three forms; protonated, zwitterion and lactone. The lactone form is non-fluorescent and is present in acidic conditions, whereas the fluorescent protonated and zwitterion forms are present at neutral and alkaline pH. FAM exists in equilibrium between the non-fluorescent lactone form and the ring open fluorescent form that exists at higher pH. When putting these interactions in context of SERS, the decrease in fluorescence at low pH would reduce the background in the SERS spectra, giving a better signal-to-noise ratio. However, at low pH there is also a reduced SERS intensity as at pH 2.9, the stability of the nanoparticles are greatly reduced (Figure 4.17), which results in the poor signal enhancement.

To summarise, the SERS intensity and fluorescence emission of FAM and TAMRA are highly dependent on pH. In the limits of the pH range, for dye labelled DNA no SERS signals are observed at acidic and alkaline pH; however FAM fluorescence increases with increasing pH and TAMRA produces fluorescence regardless of the pH. SERS spectra of the dyes are

strongly affected by the stability of the nanoparticles as would be expected. When the pH used was changed away from 5.2, uncontrolled nanoparticle aggregation occurs resulting in the loss of SERS signals. This was a factor that was not of concern in the fluorescence studies. Spermine is required to observe SERS signals of fluorescent dye labelled DNA, however when using alkaline pH the ability of spermine to do this is prevented as it is no longer protonated therefore will not reduce the charge on the nanoparticle surface allowing the negatively charged DNA to come into close proximity for SERS signals to be observed.

4.5 Chapter Conclusions

The SERS intensity of two fluorescent dyes, TAMRA and FAM, were investigated under different experimental conditions. Studies were performed when the dyes were free (TR-ITC and F-ITC) and when they were attached to either single or double stranded DNA. The presence of the DNA sequence had an effect on the SERS spectra obtained due to the interactions involving the DNA sequence and the fact that the proximity of the dye to the nanoparticle surface will be affected. The two fluorescent dyes produce different peak intensities that is affected if they are free or attached to DNA. Also, the charge on the fluorescent dye will have a major effect on the SERS intensity. SERS intensity increases when TAMRA is covalently attached to a DNA sequence, which is a result of an increase in electrostatic attraction between the dye labelled DNA, spermine and the nanoparticle surface. F-ITC and FAM labelled single stranded DNA produced higher SERS intensity compared to FAM labelled double stranded DNA, which is in agreement with previous work by MacAskill *et al*. that showed double stranded DNA had a lower affinity for the nanoparticle surface as the negative nucleobases were not exposed to induce electrostatic interaction with the positive spermine.[21]

The order of addition of the fluorescent dyes was also investigated using time studies. Results concluded that the dye that was added first produced the strongest intensity. TAMRA was found to have a stronger interaction with the nanoparticle surface, demonstrated clearly in the studies involving fluorescent dye labelled single stranded DNA.

When FAM labelled single stranded DNA was added first, FAM SERS intensity was readily obtained, with TAMRA intensity increasing over time. However, when TAMRA labelled single stranded DNA was added first no FAM intensity was observed throughout the time study.

Studies into the effects of varying pH on the SERS intensity were performed. The optimal pH for the greatest SERS intensity was found to be in the region of pH 5.2. At the other pHs, uncontrolled nanoparticle aggregation was observed. Furthermore, at pH 13.2, spermine was not able to reduce the negative charge on the nanoparticle surface as it is no longer a polycation, resulting in repulsion between the negative DNA and negative nanoparticle surface. TR-ITC was an exception to this, which can be explained by the positive charge on the dye that has a strong affinity for the negative nanoparticle surface. Simultaneous analysis of the fluorescent dyes produce lower SERS intensity compared to the individual analysis of the two dyes. This is a result of the competition between the two fluorescent dyes on the nanoparticle surface. This is a strong consideration for multiplexing SERS analysis as there is a decrease in sensitivity.

The combination of the fluorescence and SERS studies has provided a detailed insight into the interactions between spermine and the fluorescent dyes TAMRA and FAM and the effect of changing experimental conditions has on the SERS signals observed for the two dyes. For both fluorescence and SERS, the covalent attachment of TAMRA or FAM to a DNA sequence results in a change in intensity. This is of major significance when using SERS or fluorescence for the detection of dye labelled DNA and, more importantly, when multiplex detection is required as the two dyes are affected differently by DNA attachment. Fluorescence studies of the free dyes and dye labelled oligonucleotides at different pHs demonstrated that different structures of the dyes will be present when the pH is changed. These structural changes affected the fluorescence emission of the dyes. With the information on the structures of the dyes at different pHs, SERS spectra were recorded of the free dyes and dye labelled DNA sequences. At acidic and alkaline pH, no SERS signals of FAM or TAMRA labelled DNA were observed, a result of uncontrolled aggregation of the nanoparticles at these pHs. The resulting SERS spectrum observed for the multiplex

detection of FAM and TAMRA labelled DNA will be strongly affected by the nature of the DNA sequence attached and the experimental conditions used. By undertaking these studies, it has been shown how important experimental set up such as order of addition, pH and the presence of spermine will ultimately determine if the two dyes FAM and TAMRA can be identified and quantified successfully in multiplex detection.

4.6 Chapter References

1. K. Kneipp, H. Kneipp, G. Deinum, I. Itzkan, R. R. Dasari and M. S. Feld, *Applied Spectroscopy*, 1998, **52**, 175-178.
2. S. M. Nie and S. R. Emery, *Science*, 1997, **275**, 1102-1106.
3. D. Cunningham, R. E. Littleford, W. E. Smith, P. J. Lundahl, I. Khan, D. W. McComb, D. Graham and N. Laforest, *Faraday Discussions*, 2006, **132**, 135-145.
4. A. Ruperez, R. Montes and J. J. Laserna, *Vibrational Spectroscopy*, 1991, **2**, 145-154.
5. D. Graham, W. E. Smith, A. M. T. Linacre, C. H. Munro, N. D. Watson and P. C. White, *Analytical Chemistry*, 1997, **69**, 4703-4707.
6. N. R. Isola, D. L. Stokes and T. Vo-Dinh, *Analytical Chemistry*, 1998, **70**, 1352-1356.
7. D. Graham, B. J. Mallinder and W. E. Smith, *Angewandte Chemie-International Edition*, 2000, **39**, 1061-1063.
8. Y. W. C. Cao, R. C. Jin and C. A. Mirkin, *Science*, 2002, **297**, 1536-1540.
9. K. Faulds, L. Stewart, W. E. Smith and D. Graham, *Talanta*, 2005, **67**, 667-671.
10. K. Faulds, W. E. Smith and D. Graham, *Analytical Chemistry*, 2004, **76**, 412-417.
11. R. J. Stokes, A. Macaskill, P. J. Lundahl, W. E. Smith, K. Faulds and D. Graham, *Small*, 2007, **3**, 1593-1601.
12. D. Graham and K. Faulds, *Chemical Society Reviews*, 2008, **37**, 1042-1051.
13. F. T. Docherty, M. Clark, G. McNay, D. Graham and W. E. Smith, *Faraday Discussions*, 2004, **126**, 281-288.
14. K. Faulds, F. McKenzie, W. E. Smith and D. Graham, *Angewandte Chemie International Edition*, 2007, **46**, 1829-1831.
15. K. Faulds, R. Jarvis, W. E. Smith, D. Graham and R. Goodacre, *Analyst*, 2008, **133**, 1505-1512.
16. P. C. Lee and D. Meisel, *Journal of Physical Chemistry*, 1982, **86**, 3391-3395.
17. L. P. Zhou, J. Yang, C. Estavillo, J. D. Stuart, J. B. Schenkman and J. F. Rusling, *Journal of the American Chemical Society*, 2003, **125**, 1431-1436.
18. M. M. Harper, K. S. McKeating and K. Faulds, *Physical Chemistry Chemical Physics*, 2013, **15**, 5312-5328.
19. J. A. Dougan and K. Faulds, *Analyst*, 2012, **137**, 545-554.
20. S. E. J. Bell and N. M. S. Sirimuthu, *Journal of the American Chemical Society*, 2006, **128**, 15580-15581.
21. A. MacAskill, D. Crawford, D. Graham and K. Faulds, *Analytical Chemistry*, 2009, **81**, 8134-8140.
22. M. M. Harper, J. A. Dougan, N. C. Shand, D. Graham and K. Faulds, *Analyst*, 2012, **137**, 2063-2068.
23. M. M. Harper, PhD Thesis, University of Strathclyde, 2013.

5. Qualitative SERS Analysis of G-quadruplex DNAs Using Selective Stabilising Ligands

5.1 Introduction

Nucleic acids are of key biological importance due to their range of functions and ability to form different structures. A key example is G-quadruplexes that are nucleic acid structures formed by guanine rich sequences. G-quadruplexes are found in different regions of the genome such as telomeres and promoter genes. This work involved the design of a method for analysing the formation of G-quadruplexes using surface enhanced Raman spectroscopy (SERS). Three ligands that specifically bind to and stabilise G-quadruplexes were used that each have their own unique SERS response. When the ligands were bound to a G-quadruplex no SERS spectra were observed, however when the ligand was added to a solution of DNA with a different topology such as a duplex structure, the ligands do not bind and remain free in solution to produce SERS spectra. This resulted in an "on to off" method for the detection of G-quadruplex formation using SERS.[1]

5.1.1 G-quadruplex DNA

G-quadruplexes are guanine rich DNA sequences that have the ability to form stable structures under physiological conditions *in vivo*.[2, 3] G-quadruplexes are composed of G-quartets that are a result of Hoogsteen hydrogen-bonding between guanines that stack on top of each other resulting in four-stranded helical structures that are held together by π-π interactions.[4, 5] The structure and stability of G-quadruplexes is known to be dependent on several factors such as the nature of the sequence, flanking nucleotides, loop length, and most importantly the presence of monovalent cations such as K^+ and Na^+.[6-8] The specific cation that is present influences the topology of the G-quadruplex, for example in the presence of Na^+, human telomeric DNA sequence $AG_3(T_2AG_3)_3$ folds into an anti-parallel structure, whereas in the presence of K^+, (T_2AG_3) repeats can fold into at least five distinct

quadruplex structures, the most common being the parallel and anti-parallel configurations (Figure 5.1).[9, 10]

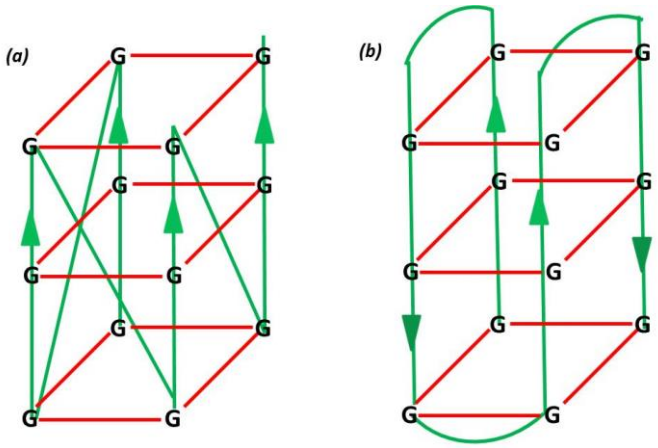

Figure 5.1 Depending on how the individual guanine bases are arranged, quadruplexes can adopt different topologies. (a) When all the strands are in the same 5'-3' direction (green arrows), the quadruplex is termed parallel. (b) If one or more of the strands are in a different 5'-3' direction, the quadruplex has adopted an anti-parallel topology. The red lines represent the G-quartets held together through π-π stacking interactions.

Studies have shown that guanine rich DNA sequences can spontaneously fold into G-quadruplex DNA structures *in vitro* and more recent studies have shown that quadruplexes have certain functions *in vivo*.[3] G-quadruplexes are involved in regulating telomere maintenance, as well as transcription, replication and translation.[4] Telomeres are nucleoprotein complexes and their main function is to protect the ends of eukaryotic chromosomes by containing repetitive guanine-rich DNA.[2] In somatic cells, telomeres are shortened in length by 50-200 bases after each successive cell division cycle due to the inability of DNA polymerase to replicate the telomeric DNA strand as the 3' OH group at the extreme end of the chromosome is unavailable. When telomeres are shortened critically, they reach the hayflick limit and the cells become senescent and induce apoptotic signals resulting in cell death. However, telomere length is maintained in around 85% of cancerous cells due to the enzyme telomerase, which is notably absent in somatic cells. Telomerase is an enzyme that can add TTAGGG repeats to 3' end of DNA strands in telomere regions, which would usually be shortened in the absence of telomerase during successive cycles of cell division.[11] The formation of a G-quadruplex at telomere ends will inhibit the activity of telomerase because it isolates the substrate needed for telomerase activity, the single

stranded DNA.[12] The ability of G-quadruplexes to inhibit telomerase activity makes them ideal targets in cancer therapeutics.

5.1.2 G-quadruplex Stabilising Ligands

There has been extensive research on the development of G-quadruplex ligands, in particular those that target the human telomeric repeat [$d(T_2AG_3)_4$], and in turn would block the action of telomerase.[13-15] G-quadruplexes have a larger π-surface area compared to duplex DNA because of the four coplanar bases compared to only two in duplex DNA. The majority of small molecules that can bind to these structures also have large π-surface areas to maximise the formation of π-π interactions.[16] Small organic molecules can therefore lead to cell death by displacing the protective telomeric components or isolating the substrate (single stranded DNA) needed for telomerase activity.[17, 18] Telomestatin is a natural product that was isolated from the bacterium *Streptomyces anulatus* and has been shown to be a very potent telomerase inhibitor.[19] As mentioned previously, monovalent ions such as Na^+ or K^+ are required for G-quadruplex formation, however telomestatin itself has the capability to convert linear DNA into G-quadruplex structures without the need for these monovalent cations.[12] Kim *et al.* demonstrated the first experimental evidence that telomestatin selectively facilitates the formation or stabilisation of intra-molecular G-quadruplexes, particularly quadruplexes produced from the human telomeric sequence. Their results concluded that telomestatin was the first natural product that could inhibit telomerase activity as it facilitates the formation of stable G-quadruplex structures.[17] There are several other G-quadruplex-interactive compounds such as, anthraquinones,[20, 21] perylenes[22, 23] and quinolones[24] that have all been shown to inhibit telomerase.

G-quadruplexes can be used as potential therapeutic targets for anti-cancer therapy.[25] The ligand 2,6-diamidoanthraquinone was shown to stabilise a G-quadruplex structure and inhibit telomerase activity.[20] Since then, many classes of ligands have been reported as G-quadruplex stabilising agents, however very few of these have shown specificity towards the targeted G-quadruplex structure over other DNA topologies. Some ligands have also been shown to indirectly inhibit telomerase by displacing the telomere binding proteins that then induce a DNA damage response, as opposed to forming a G-quadruplex

structure.[26, 27] Therefore, there has been great interest in developing strong and selective quadruplex binding agents that can detect the formation of G-quadruplex structures *in vivo*.[18]

5.1.3 Current Methods of G-quadruplex Analysis

The structure and stability of G-quadruplexes have been extensively investigated using various methods.[28] Several spectroscopic techniques can be used such as UV molecular absorption,[29] circular dichroism (CD) spectroscopy,[30] fluorescence (FRET)[31] and NMR.[32] UV/CD techniques have the more sensitive instrumental response to the interaction between the G-quadruplex strands. Additionally, CD can be used to determine if the G-quadruplex has a parallel or anti-parallel configuration.[33] However, more detailed molecularly specific information on binding events and analysis of the formation of G-quadruplexes can be obtained using Raman spectroscopy.

5.1.3.1 The use of Raman and SERS for DNA Analysis

Raman spectroscopy is an alternative technique which can be used to analyse the structure of macromolecules such as DNA. It has been successfully applied to the investigation of the phosphodiester backbone conformation and the hydrogen-bonding interactions of G-quadruplexes.[34] Muira *et al.* identified specific Raman markers as indicators of the presence of parallel or anti-parallel G-quadruplexes.[35] Raman spectroscopy is limited by the relatively low cross section of the Raman scattering process compared to other techniques such as fluorescence and absorption spectroscopy. Surface enhanced Raman scattering (SERS) has now become an alternative method as it overcomes the limitations associated with Raman spectroscopy.[36] The high sensitivity achieved when using SERS is due to the enhancement of the Raman cross section when the analyte is in close proximity to a metal surface , for example a silver or gold colloidal suspension. There have been several studies involving the direct detection of DNA bases or sequences using SERS. For example, Kneipp *et al.* used SERS for the detection of adenine bases[37] and Bell *et al.* successfully used SERS for the label free detection of DNA bases,[38-43] emphasising the capability of SERS to be a successful method for direct DNA detection.

The detection of the formation of specific DNA structures has proven to be more difficult using SERS due to the high dependence that the enhancement of Raman scattering has on the orientation of the DNA with respect to the metallic surface. Rusciano *et al.* developed the application of SERS to investigate the stability of G-quadruplexes by using SERS to gain information on the structure of guanine-rich DNA sequences. G-quadruplex structures with different structural features such as the orientation of glycosidic bonds and distortions in the sugar-phosphate backbone were analysed. SERS analysis allowed the stabilities to be compared using fluctuations in the spectra resulting in the discovery of specific Raman markers of G-quadruplex DNA.[44] This demonstrated for the first time that SERS can be an extremely useful technique for the analysis of the stabilities of different G-quadruplex structures.

Breuzard *et al.* demonstrated that is was possible to use SERS to analyse DNA structures and in particular to investigate the stability of G-quadruplexes using derivatives of ethidium bromide.[45] Ethidium bromide has a weak stabilising effect on G-quadruplexes compared to the three ethidium bromide derivatives also used, which had a stronger stabilising effect. When ethidium bromide intercalated with double stranded DNA, SERS signals were completely lost. When ethidium bromide and its derivatives were complexed to a G-quadruplex structure, there was a decrease in ethidium bromide SERS intensity. The methods used by Breuzard *et al.* are similar to what the methods used in this study; however there are some major differences. Ligands that specifically bind to G-quadruplexes and also stabilise their formation were used. These ligands also produced a unique Raman response and had no affinity for duplex DNA.

5.2 Chapter Aims

G-quadruplexes have been shown to be ideal targets for cancer diagnostics. By using SERS to analyse the formation of G-quadruplexes, a new method was to be designed that would be an appealing alternative to the fluorescence-based methods currently available. Three ligands, synthesised by Dhamodharan *et al.,*[46] known to stabilise G-quadruplex structures were used and their ability to act as Raman reporters assessed. Using the combination of

SERS and the three ligands, a highly specific method for the analysis of G-quadruplex formation was developed. By combining the therapeutic stabilising nature of the ligands and their Raman reporter capabilities, it is hoped that this method can be further developed and used as a diagnostic tool for anti-cancer therapies.

5.2.1 G-Quadruplex Stabilising Ligands and their Method of Analysis

This work used SERS for the qualitative detection of the formation of G-quadruplex structures. SERS was used to monitor the formation of G-quadruplexes based on the unique SERS response given by three G-quadruplex stabilising ligands. When each ligand was added to a solution containing G-quadruplex DNA, they bind strongly to this DNA structure and upon addition of silver nanoparticles, no interaction happens between the ligand and nanoparticles therefore no SERS response is obtained (Figure 5.2a). However, when the ligand was added to a solution of duplex DNA, it remains unbound and free in solution. Therefore when silver nanoparticles are added, aggregation occurs due to the interaction of the ligand with the nanoparticles, resulting in the unique SERS spectrum associated with that particular ligand (Figure 5.2b).

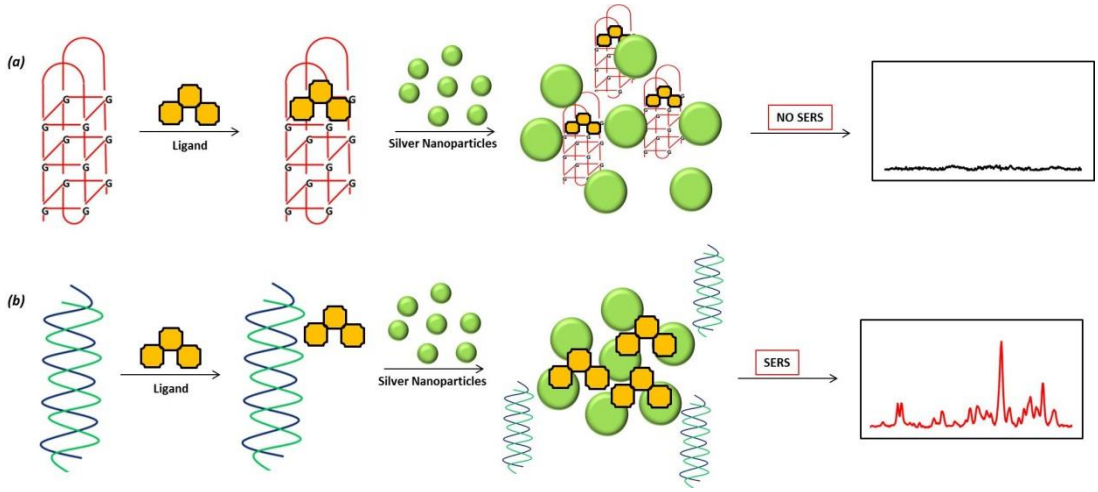

Figure 5.2 A schematic overview of the qualitative detection of G-quadruplex DNA. (a) When the stabilising ligand is added to a solution containing G-quadruplex DNAs, the ligand strongly binds to the G-quadruplex and when silver nanoparticles are added, the ligand is not free to induce aggregation and a unique SERS response is not observed. (b) When the stabilising ligand is added to a solution containing duplex DNAs, the ligand does not bind to this DNA structure, therefore in the presence of silver nanoparticles, aggregation occurs resulting in a SERS response from the ligand.

This work was carried out in collaboration with Prof. Pradeepkumar from IIT Bombay, who synthesised the ligands used in this study. 360A was previously studied by Granotier *et al*,[47] and the other two ligands, 3AQN and 6AQN (Figure 5.3), were previously shown to stabilise various G-quadruplexes (telomeric, *C-KIT1*, *C-KIT2* and *C-MYC*) selectively over duplex DNA.[46] This was the first study that utilised SERS as the method of analysis due to the ability of the three ligands to act as Raman reporters. Several guanine-rich DNA sequences were used including the human telomeric sequence, the sequence from the promoter gene *C-MYC* and the sequence peroxidase deoxyribozyme.

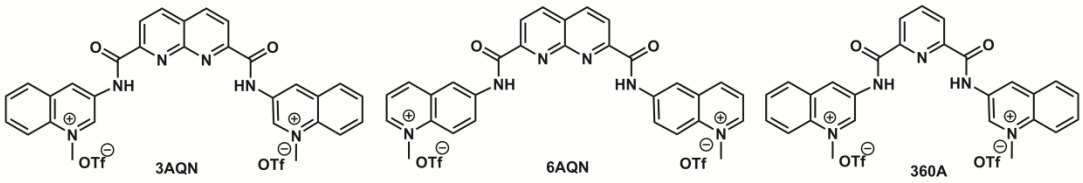

Figure 5.3 The structures of the three selective G-quadruplex binding ligands. From left: 3AQN (3-amino-quinolinium naphthyridine); 6AQN (6-amino-quinolinium naphthyridine) and 360A (3-amino-quinolinium pyridine).

5.3 Experimental

5.3.1 Ligand Synthesis

The three ligands (3AQN, 6AQN and 360A) used in this study were provided and synthesised as reported previously by Dhamodharan *et al*.[46]

5.3.2 Colloid Synthesis

Silver nanoparticles were synthesised using a modified Lee and Meisel method.[48] Silver nitrate (90 mg) was dissolved in distilled water (500 mL). The solution was heated rapidly to boiling with continuous stirring. Once boiling, an aqueous solution of sodium citrate (1 %,

10 mL) was added quickly. The heat was reduced and the solution was left to boil gently for 90 minutes with stirring. The colloid was then analysed by UV-vis spectroscopy and the λ_{max} was 403 nm with the full width half-height (FWHH) measured to be 124 nm. The concentration of the colloid was calculated to be 0.2 nM.

5.3.3 Oligonucleotides

All DNA sequences were purchased on a 0.2 µM synthesis scale with HPLC purification from Eurofins MWG (Ebersberg, Germany).

Table 5.1 The DNA sequences used in this work consisting of three G-quadruplex sequences and a self-complementary duplex sequence used as a control.

Name	Description	Sequence (5' – 3')
Peroxidase Deoxyribozyme	Quadruplex	GTGGGTAGGGCGGGTTGG
Human Telomeric DNA	Quadruplex	AGGGTTAGGGTTAGGGTTAGGG
***C-MYC* Promoter**	Quadruplex	TGAGGGTGGGTAGGGTGGGTAA
Control	Duplex (Self complementary)	CAATCGGATCGAATTCGATCCGATTG
Molecular Beacon	Molecular Beacon	GGGTTAGGGTTTTTTCCTTTGTTTGTTTTTGGGTTAGGG
Loop Complementary Sequence	Single Stranded DNA	AAAAACAAACAAAGGAAAAAA

5.3.4 SERS Analysis of the Stabilising Ligands

To determine if the ligands could act as Raman reporters, analysis was performed using two different types of nanoparticles and two laser excitations. Silica coated gold nanoparticles (420 µL) or citrate reduced silver nanoparticles (420 µL) were added to a disposable PMMA microcuvette containing one of the three ligands (20 µL, 50 µM). SERS analysis was performed using a Renishaw inVia microscope system with a laser excitation of 633 nm. The sample mixture in the PMMA microcuvette was analysed using a 20 x long working distance objective and an accumulation time of 1 second. WiRE 2.0 software (Renishaw PLC) was used to collect the spectra which were then baseline corrected using a multipoint polynomial fit and level and zero mode using Grams software (AI 7.00). When using the second excitation laser, each ligand (20 µL, 50 µM) was added to a well within a 96 well plate containing citrate reduced silver nanoparticles (280 µL). Samples were analysed using

an Avalon Plate Reader (Belfast, UK) with a laser excitation wavelength of 532 nm. The plate was placed onto a stage and the instrument's software was used to automatically move the stage to allow the spectra to be recorded from each well, with an accumulation time of 1 second. Spectra were collected and baseline corrected using Grams software (AI 7.00). All experiments were carried out using 3 replicate samples, where the spectra were averaged.

5.3.5 Determining the Aggregation Abilities of the Ligands

To determine if the ligands induced nanoparticle aggregation, UV-Vis absorption spectra were collected using a Cary 300 Bio UV-vis spectrometer. Samples were analysed in 1 cm quartz cuvettes and scanned from 200 to 800 nm. To the cuvettes, ligand (50 µL, 50 µM), citrate reduced silver nanoparticles (50 µL) and distilled water (350 µL) was added. Size and zeta measurements were carried out using a Malvern Zetasizer Nano Series. To a 2-sided 1 cm plastic cuvette, one of the ligands (100 µL, 50 µM), citrate reduced nanoparticles (300 µL) and distilled water (400 µL) was added. A Malvern dip cell kit was used for zeta measurements. Size measurements were taken every minute for 10 minutes and the process was repeated with 3 replicate samples, with an average value taken.

5.3.6 SERS of Ligands Bound to G-quadruplexes

To determine if the binding of the ligands to G-quadruplexes has any effect on the SERS signals observed, the following SERS experiments were carried out. Prior to SERS analysis, each ligand (20 µL, 50 µM) was incubated with the peroxidase deoxyribozyme quadruplex sequence (20 µL, 50 µM) at room temperature for 30 minutes. The mixture of ligand and quadruplex (40 µL) was added to a well containing citrate reduced silver nanoparticles (260 µL). An Avalon Plate Reader (Belfast, UK) with an excitation laser of 532 nm was used. SERS analysis was performed as described in section 5.3.4.

5.3.7 SERS of Ligands Bound to Duplex DNA

SERS analysis of the ligands in the presence of duplex DNA was also carried out. Self-complementary single stranded DNA was used as the duplex control. DNA hybridisation

was carried out using a heating block where a solution of single stranded DNA (50 µL, 50 µM) was added to phosphate buffered saline solution (50 µL, 0.3 M, pH 6.9) and the temperature was increased to 90 °C for 10 minutes then decreased to 10 °C for 10 minutes. Prior to SERS analysis, each ligand (20 µL, 50 µM) was incubated with the duplex sequence (20 µL, 50 µM) at room temperature for 30 minutes. The mixture of ligand and duplex DNA (40 µL) was added to a well containing citrate reduced silver nanoparticles (260 µL). An Avalon Plate Reader (Belfast, UK) with an excitation laser of 532 nm was used. SERS analysis was performed as described in section 5.3.4.

5.3.8 The use of an Aggregating Agent to Observe SERS of DNA

The SERS spectra observed using the ligands and either G-quadruplex or duplex DNA contained no SERS peaks attributed to the presence of DNA. This was overcome by using an additional aggregation agent such as $MgSO_4$. Experiments were carried out using both duplex and G-quadruplex DNA. Prior to SERS analysis, each ligand (20 µL, 50 µL) was incubated with either duplex or quadruplex DNA (20 µL, 50 µM) at room temperature for 30 minutes. Added to each well was the ligand-DNA mixture (40 µL), the aggregating agent $MgSO_4$ (20 µL, 0.1 M) and citrate reduced silver nanoparticles (240 µL). An Avalon Plate Reader (Belfast, UK) with an excitation laser of 532 nm was used. SERS analysis was performed as described in section 5.3.4.

Samples were also analysed using a Renishaw inVia microscope system with a laser excitation of 785 nm. The sample mixture was added to a microcuvette and analysed using a 20 x long working distance objective and an accumulation time of 10 seconds. WiRE 2.0 software (Renishaw PLC) was used to collect the spectra which were then baseline corrected using a multipoint polynomial fit and level and zero mode using Grams software (AI 7.00).

5.3.9 Concentration Studies

Concentration studies were carried out using each ligand and the peroxidase deoxyribozyme quadruplex sequence. The concentration of the ligands remained at 50 µM

and the G-quadruplex DNA concentration was decreased in increments from 50 μM to 5 nM. Prior to SERS analysis, each ligand (20 μL, 50 μM) was incubated with the peroxidase deoxyribozyme quadruplex sequences (20 μL, *X* M) for 30 minutes at room temperature. An Avalon Plate Reader (Belfast, UK) with an excitation laser of 532 nm was used with a 1 second accumulation time. SERS analysis was performed as described in section 5.3.4. Triplicate samples were analysed and average spectra were taken.

5.3.10 Monovalent Cation Study

The ligands have the ability to induce the formation of G-quadruplexes without the need for monovalent cations. Either a solution of NaCl (20 μL, 100 mM) or KCl (20 μL, 100 mM) was added to the sample mixture. Duplex DNA and quadruplex DNA were both used. The ligand 3AQN (20 μL, 50 μM) was incubated with either duplex or quadruplex DNA (20 μL, 50 μM) for 30 minutes at room temperature. To a well within the 96 well plate, the ligand-DNA mixture (40 μL), either KCl or NaCl (20 μL, 100 mM) were added to citrate reduced silver nanoparticles (240 μL). An Avalon Plate Reader (Belfast, UK) with a laser excitation wavelength of 532 nm was used with an accumulation time of 1 second. SERS analysis was performed as described in section 5.3.4. Triplicate samples were analysed and average spectra were taken.

5.3.11 Varying the G-quadruplex DNA Sequence

Previous experiments were carried out using only one G-quadruplex sequence, the peroxidase deoxyribozyme G-quadruplex sequence. Experiments were performed using different G-quadruplex forming sequences (Table 3.1), the human telomeric sequence and the promoter gene *C-MYC*. One ligand, 3AQN, was used. The ligand 3AQN (20 μL, 50 μM) was incubated with one of the G-quadruplex sequences or the duplex DNA (20 μL, 50 μM) at room temperature for 30 minutes. To a well, the 3AQN-DNA mixture (40 μL) was added to citrate reduced silver nanoparticles (260 μL). An Avalon Plate Reader (Belfast, UK) with a laser excitation wavelength of 532 nm was used with a 1 second accumulation time. SERS analysis was performed as described in section 5.3.4. Triplicate samples were analysed and average spectra were taken.

5.3.12 Development of a Positive Assay using SERS

A new assay was designed using a molecular beacon probe that contained G-quadruplex sequences, which form the stem. The molecular beacon sequence and the sequence complementary to the loop are found in Table 3.1. The molecular beacon sequence (20 µL, 50 µM) was incubated with the ligand 6AQN (20 µL, 50 µM) for 30 minutes at room temperature. DNA hybridisation was carried out using a heating block, where the molecular beacon and 6AQN mixture (40 µL) were added to a sample vial along with the complementary sequence (20 µL, 50 µM) and phosphate buffered saline (60 µL, 0.3 M). The temperature was increased to 90° for 10 minutes then decreased to 10 °C for 10 minutes. This mixture (120 µL) was added to citrate reduced silver nanoparticles (180 µL) into a well in a 96 well plate. An Avalon Plate Reader (Belfast, UK) with a laser excitation wavelength of 532 nm was used with a 10 second accumulation time. SERS analysis was performed as described in section 5.3.4. Triplicate samples were analysed and average spectra were taken.

5.4 Results and Discussion

Bisquinolinium ligands such as 360A are known to selectively bind and stabilise G-quadruplex DNA over duplex DNA.[49-51] Dhamodharan *et al.* reported two new derivatives of bisquinolinium carboxamide, each having 1,8-napthryidine as the central core (Figure 5.3).[46] Biochemical and biophysical studies were used to investigate the interaction between the ligands and different nucleic acids. Circular dichroism (CD) melting assays indicated that the ligands have a greater stabilising effect on G-quadruplex DNA compared to duplex DNA. CD studies were also used to investigate the potential of these ligands to induce G-quadruplex formation. As observed with the natural product isolated from the bacteria *Streptomyces anulatus*, telomestatin, in the absence of monovalent cations the ligands are capable of inducing the formation of a G-quadruplex structure. A Fluorescent Intercalator Displacement (FID) assay demonstrated the ligands (3AQN, 6AQN and 360A) have high binding affinity and selectivity for quadruplex DNA over duplex DNA. In the work reported here, SERS was used for the direct detection of the interaction of these ligands with G-quadruplex DNA and due to the Raman reporter capabilities of the ligands, no additional fluorescent agent was required.

5.4.1 Determinig the Potential of G-Quadruplex Ligands as Raman Reporters

For this novel SERS-based method to be successful, it was important to determine if any of the three ligands could be used as Raman reporters. SERS experiments were performed to determine what metallic nanoparticle would be the optimal SERS substrate and what laser excitation wavelength was best to observe the most intense and clearly defined SERS spectra of each ligand. Silica coated gold nanoparticles and citrate reduced silver nanoparticles were used, along with two laser excitations wavelengths of 532 nm and 633 nm. Results are shown in Figure 5.4, which demonstrate that when silica coated gold nanoparticles were used, the SERS response from the ligands was very poor. However, when using citrate reduced silver nanoparticles, SERS peaks of each ligand were readily observed using both excitation wavelengths, with a 532 nm laser excitation wavelength producing sharper SERS peaks. Therefore, for this study, citrate reduced silver nanoparticles and a laser excitation wavelength of 532 nm was used in the detection of the formation of G-quadruplexes.

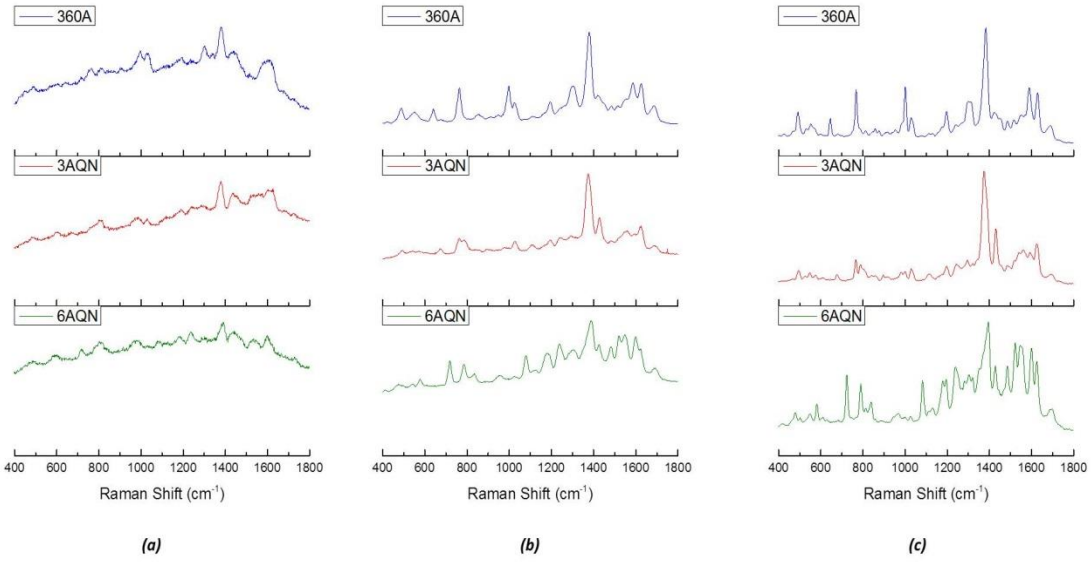

Figure 5.4 SERS spectra obtained for each stabilising ligand using silica coated gold or citrate reduced silver nanoparticles and two different excitation wavelengths. (a) SERS spectra of the three ligands using silica coated nanoparticles and an excitation laser of 633 nm, (b) SERS spectra of the three ligands using citrate reduced silver nanoparticles with 633 nm excitation laser and (c) SERS spectra of the three ligands using citrate reduced silver nanoparticles with 532 nm excitation laser. Spectra were obtained using either a 633 or 532 nm laser excitation and an accumulation time of 1 s.

A SERS response was obtained for each ligand using silver citrate reduced nanoparticles due to the aggregation caused by the ligand. No additional aggregating agent was added to observe the SERS spectra shown in Figure 5.4b-c. When silica coated gold nanoparticles were used, aggregation was inhibited due to the silica coating on the nanoparticle meaning the ligands could not encourage the formation of nanoparticle clusters resulting in low SERS peak intensity (Figure 5.4a). To confirm that the ligands were able to aggregate the nanoparticles, UV-Visible spectroscopy and dynamic light scattering (DLS) measurements were recorded for each of the three ligands mixed with silver citrate nanoparticles (Figure 5.5).

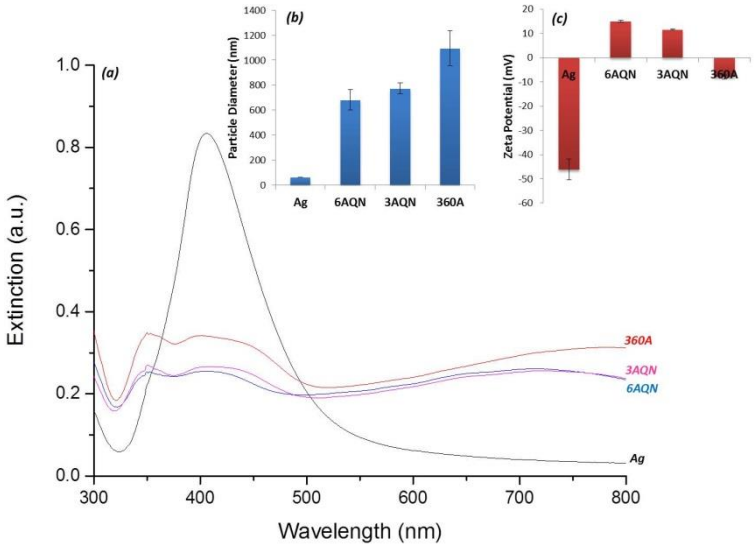

Figure 5.5 UV-Visible and DLS analysis of nanoparticle aggregation caused by each ligand. (a) Extinction spectra of silver nanoparticles (black), and aggregated silver nanoparticles in the presence of 6AQN (blue), 3AQN (pink) or 360A (red). (b) Comparison of particle sizes in free nanoparticles and nanoparticles in the presence of each ligand. (c) Zeta potential measurements of free nanoparticles and the nanoparticles in the presence of each ligand. For sizing and zeta potential analysis, 3 replicate measurements were averaged and error bars represent ±1 standard deviation.

The strong SERS intensity observed when analysing each of the three ligands was assumed to be a result of induced nanoparticle aggregation. It was important to confirm that the reason for the successful SERS analysis was a result of the aggregating ability of the ligands without the addition of an aggregating agent. Therefore, further investigative analysis was

performed to show nanoparticle aggregation caused by the presence of the ligands. Extinction spectra in Figure 5.5a shows that in the presence of each ligand, there is a dampening in the SPR band at 406 nm, broadening of the peak and also the appearance of an additional peak at 750 nm. This indicates that nanoparticle aggregation is occurring resulting in the formation of nanoparticle clusters. This was further confirmed by measuring the size of the nanoparticles, which demonstrates a significant increase when the ligands are present (Figure 5.5b), and zeta potential analysis demonstrating that the surface charge on the nanoparticles is reduced, reducing the repulsion between nanoparticles allowing for aggregates to form in the presence of the ligands (Figure 5.5c). Particle sizing values when the ligands were present were significantly higher compared to nanoparticles present on their own, and the largest increase in size was produced form the ligand 360A. This suggests that when using 360A, the nanoparticles over-aggregate which is in agreement with the zeta potential of -7.2, indicating that the nanoparticles have very little surface repulsion allowing for large aggregates to form. For 3AQN and 6AQN, similar particle size and zeta potential values were obtained, which was expected as they are isomers (Figure 5.3). These results confirmed that the ligands induce nanoparticle aggregation resulting in intense SERS spectra, unique to each ligand.

5.4.2 SERS of Ligands Bound to G-quadruplex DNA

From the previous results, it has been shown that the ligands do give a unique SERS response. The three ligands have shown to selectively bind to and stabilise G-quadruplexes.[46] As demonstrated, when the ligands are free in solution, unique SERS spectra are obtained. However, upon ligand binding to the G-quadruplex, it was unknown what would happen to the SERS intensity of each ligand. There could be several outcomes, for example a change or reduction in SERS signal due to changes in the orientation of the ligands when they are bound to G-quadruplexes. To determine the effect on SERS intensity of the ligands when they were bound to a G-quadruplex sequence, each ligand was incubated for 30 minutes with the peroxidase deoxyribozyme quadruplex sequence (Table 5.1) followed by SERS analysis.

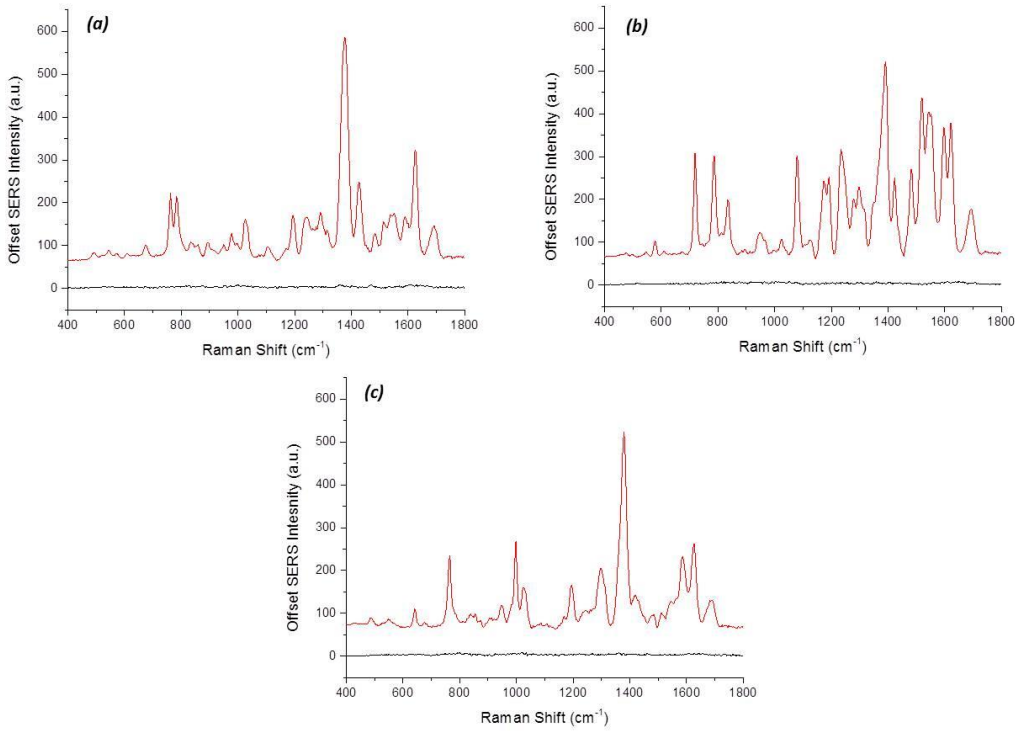

Figure 5.6 SERS spectra of free ligand (red) and peroxidase deoxyribozyme complex (black): (a) spectra of 3AQN free and complexed to G-quadruplex DNA, (b) spectra of 6AQN free and complexed to G-quadruplex sequence and (c) spectra of 360A free and complexed to G-quadruplex sequence. Spectra were obtained using a 532 nm laser excitation wavelength and an accumulation time of 1 s.

Figure 5.6 illustrates that there was a significant reduction in SERS signal when each of the three ligands were bound to the G-quadruplex sequence. Each ligand has bound strongly to the G-quadruplex structure, therefore preventing the ligands from interacting with the nanoparticles resulting in no aggregation and a significant reduction in the SERS intensity for each ligand. However, when the ligands are free in solution in the absence of the G-quadruplex sequence, nanoparticle aggregation occurs and strong SERS signals are observed for each ligand.

5.4.3 Specificity of the G-Quadruplex Stabilising Ligands

To demonstrate the specificity that the three stabilising ligands have towards G-quadruplex sequences, i.e. to ensure that the ligands only bind to G-quadruplex structures and do not have the same affinity for other DNA topologies, SERS analysis of the interaction between

the ligands and duplex DNA compared to G-quadruplex DNA was performed. Each ligand was incubated with either double stranded DNA or the G-quadruplex DNA for 30 minutes prior to SERS analysis. The duplex sequence is designed so that it does not fold into a G-quadruplex sequence, by ensuring guanine rich sequences were not used. The results are shown in Figure 5.6. For each ligand, SERS signals were obtained when the duplex DNA sequence was added in place of a G-quadruplex sequence. This confirms that the ligands specifically bind to G-quadruplex DNA and in the presence of duplex DNA, they remain free in solution to interact with the nanoparticle surface, causing aggregation, and resulting in a significant SERS response (Figure 5.2).

Three individual peaks were chosen for each ligand: 1380 cm^{-1}, 719 cm^{-1} and 1379 cm^{-1} for 3AQN, 6AQN and 360A, respectively. These peaks arise from the presence of aromatic nitrogens present in the structures.[52] Further peak intensity analysis was performed at these peak positions to highlight the high specificity these ligands have for G-quadruplex DNA. In each case, when the ligand is bound to the G-quadruplex sequence there is a significant decrease in the peak intensities compared to the duplex control, summarised in Figure 5.7d. When comparing the absolute peak intensities of the ligands when they are free in solution (Figure 5.6) and when they are in the presence of duplex DNA (Figure 5.7d), there is a slight decrease in intensity when the ligand is mixed with duplex DNA. The ligands are known to preferentially bind to G-quadruplex DNA more strongly compared to duplex DNA. However, the decrease in SERS intensity suggests that some of the ligand molecules are interacting with the duplex DNA, resulting in less nanoparticle-ligand interactions, to such an extent that a decrease is observed. Nevertheless, the discrimination between SERS intensity when the ligands are bound to duplex DNA or G-quadruplex DNA is still significant.

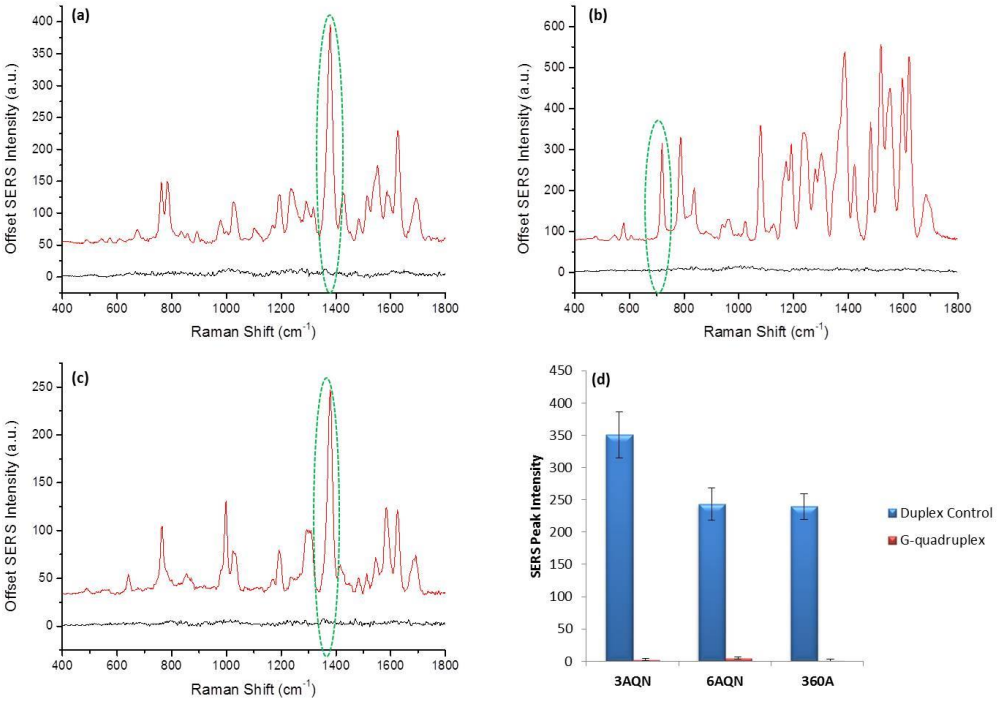

Figure 5.7 SERS spectra of each ligand binding to the peroxidase deoxyribozyme quadruplex (black) and the spectra obtained when the ligand is in the presence of duplex DNA control sequence (red): (a) spectra of 3AQN binding events; (b) spectra of 6AQN binding events and (c) spectra of 360A binding events. All three ligands and G-quadruplex DNA were used at 50 µM.(d), A comparison of the peak intensities of unique peaks of each ligand, highlighted by the green circle. In the spectrum of 3AQN, the peak at 1380 cm^{-1} was used for comparison studies, the peak at 719 cm^{-1} in the 6AQN spectrum was chosen and for 360A peak intensity studies the unique peak at 1379 cm^{-1} was used. Spectra were obtained using a 532 nm laser excitation wavelength and an accumulation time of 1 s. All peak intensities were obtained by scanning 3 replicate samples 5 times with an accumulation time of 1 s. Averages are shown and error bars represent ± one standard deviation.

5.4.4 Addition of an Aggregating Agent

When the ligands are adsorbed directly onto the surface of silver nanoparticles, in the absence of a G-quadruplex sequence, they cause nanoparticle aggregation resulting in the unique SERS spectra of the ligands. However, there was no observation of any peaks for the DNA itself. DNA peaks might be expected to appear from the presence of the G-quadruplex-ligand spectra as all the ligand was sequestered allowing the G-quadruplex to adsorb onto the silver nanoparticle surface to produce intense DNA signals. However, this was not the

case even though SERS analysis of DNA has been widely reported.[53] This is due to the absence of an aggregating agent like spermine or $MgSO_4$ that would reduce the repelling negative charges of the DNA and nanoparticle, facilitating SERS enhancement of the G-quadruplex DNA.

Experiments were undertaken, where the aggregating agent magnesium sulphate ($MgSO_4$), previously used by Bell *et al*,[38] was added to the solution containing the ligand, DNA and nanoparticles. Two laser excitation wavelengths were used, 532 nm which has been used throughout the entire study and also 785 nm as it has been reported the use of $MgSO_4$ and a laser excitation of 785 nm will result in the appearance of DNA peaks in the SERS spectrum.[38]

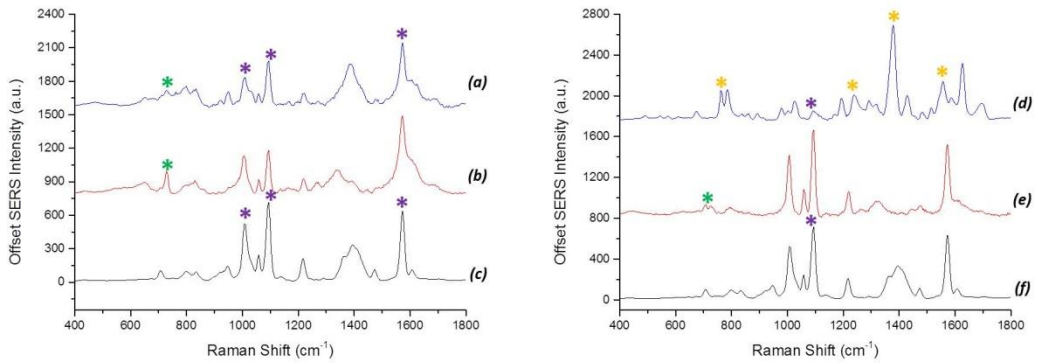

Figure 5.8 SERS spectra obtained when $MgSO_4$ was added to mixture containing duplex or G-quadruplex DNA (50 µM), 3AQN (50 µM) and silver nanoparticles. (a) SERS spectrum of 3AQN bound to peroxidase deoxyribozyme sequence, (b) SERS spectrum of the peroxidase deoxyribozyme sequence only, (c) SERS spectrum of silver nanoparticles and aggregating agent $MgSO_4$. (d) SERS spectrum of 3AQN and duplex DNA, (e) SERS spectrum of duplex DNA and (f) SERS spectrum of silver nanoparticle and $MgSO_4$. Coloured markers are used to assign peaks in the spectra. DNA peaks are marked with *, peaks from $MgSO_4$ aggregated silver nanoparticles marked with * and 3AQN peaks are marked with *. SERS spectra were recorded using a 532 nm laser excitation wavelength with a 4 s accumulation time.

When adding $MgSO_4$ to a solution containing G-quadruplex DNA and silver nanoparticles and using a 532 nm laser excitation, an identifiable DNA peak can be observed at 728 cm^{-1}, noted with * in Figure 5.8b. When the ligand 3AQN is added, DNA peaks are still observed however at a lower intensity, Figure 5.8a.[38] The other more intense peaks observed are due

to the aggregated silver nanoparticles (Figure 5.8c). When the ligand is added to a solution containing duplex DNA and silver nanoparticles, SERS signals from 3AQN are obtained, however no DNA peaks are observed. In Figure 5.8e, when adding $MgSO_4$ to duplex DNA, there is a visible DNA peak at 723 cm^{-1}, however when adding $MgSO_4$ to a solution containing 3AQN and duplex DNA, any observable DNA peaks are masked by the intense ligand SERS peaks (*), which have been further enhanced due to the increase in aggregation caused by $MgSO_4$ where enhanced silver citrate peaks are also observed (*) shown in Figure 5.8d.

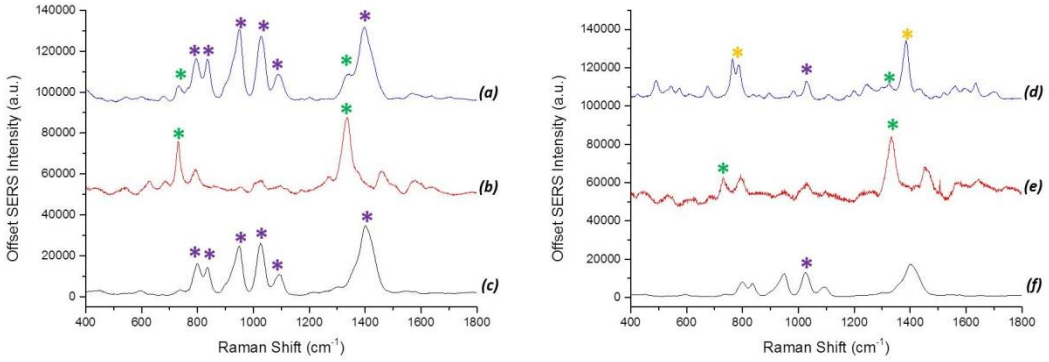

Figure 5.9 SERS spectra obtained when $MgSO_4$ was added to mixture containing duplex and G-quadruplex DNA (50 µM), 3AQN (50 µM) and silver nanoparticles. (a) SERS spectrum of 3AQN bound to peroxidase deoxyribozyme sequence, (b) SERS spectrum of the peroxidase deoxyribozyme sequence only, (c) SERS spectrum of silver nanoparticles and aggregating agent $MgSO_4$. (d) SERS spectrum of 3AQN and duplex DNA, (e) SERS spectrum of duplex DNA and (e) SERS spectrum of silver nanoparticle and $MgSO_4$. Coloured markers are used to assign peaks in the spectra. DNA peaks are marked with *, peaks from $MgSO_4$ aggregated silver nanoparticles marked with * and 3AQN peaks are marked with *. SERS spectra were recorded using a 785 nm laser excitation with a 10 s accumulation time.

Performing the same experiments using a 785 nm laser excitation wavelength produced different results. When using G-quadruplex DNA added to aggregated silver nanoparticles and when it was bound to 3AQN (Figure 5.9a-b), prominent DNA peaks at 730 cm^{-1} and 1334 cm^{-1} can be observed in the absence and presence of 3AQN. This is due to the addition of the aggregating agent $MgSO_4$, which has reduced the negative charge on the phosphate backbone of the DNA allowing it to come into close proximity with the nanoparticle surface producing DNA SERS peaks. When using duplex DNA, again DNA peaks are observed in the absence of the ligand (Figure 5.8e) and when 3AQN is present. Ligand

peaks as well as the DNA peak at 1334 cm^{-1} can be observed (Figure 5.8d). Additional peaks are due to the aggregated silver nanoparticles labelled with "*" and spectra are shown in Figure 5.9c and e. This is different to the spectra obtained using the 532 nm laser excitation wavelength. There are also spectral differences between G-quadruplex DNA and duplex DNA; this could be for two reasons. First the orientation of the DNA in relation to the surface of the nanoparticle strongly affects the SERS spectra observed and secondly, the composition of the DNA sequence, i.e. the amount of each base, will affect the relative intensity of certain peaks.[42, 53]

This result shows that if it was required, using $MgSO_4$ and a 785 nm laser excitation, DNA peaks can be observed as well as ligand peaks. However in this study, the ability of the ligand itself to aggregate the nanoparticles was exploited therefore there was no need for an additional aggregating agent. Also SERS analysis was performed using a 532 nm laser excitation wavelength, which would make observing DNA peaks difficult when the ligand was present, when no additional aggregating agent such as $MgSO_4$ was present to facilitate the adsorption of DNA onto the nanoparticle surface.

5.4.5 Concentration Ratio of Ligand and G-quadruplex DNA

The previous results presented (Figure 5.6) were obtained when the ligands and G-quadruplex DNA were in equimolar concentrations (50 µM). Experiments were carried out to determine how the SERS response would be affected when reducing the concentration of G-quadruplex DNA and keeping the concentration of the ligand constant. As this is a negative SERS method, where signal decreases in the presence of the targeted G-quadruplex sequence, it was essential to determine at what concentration ratio between the G-quadruplex and ligands does this "on to off" method occurs.

Figure 5.10 summarises the results obtained when the concentration of G-quadruplex DNA was reduced in increments from 50 µM to 5 nM. The G-quadruplex DNA at varying concentrations was incubated with each ligand (50 µM) for 30 minutes prior to SERS analysis. It can be seen that when the G-quadruplex concentration is reduced to below

5 µM a SERS response was obtained due to insufficient G-quadruplex DNA available to sequester all of the ligand resulting in a signal being obtained. This demonstrated that, as was expected, the ratio of ligand to G-quadruplex DNA is critical (Table 5.2). As the concentration of the G-quadruplex decreases, the ligand molecules will be in excess. The less G-quadruplex molecules available to sequester the ligand molecules, the more ligand molecules will be available for nanoparticle interaction resulting in SERS signals. When ligand concentration is constant at 50 µM and when the ligand is in 100 times excess than the G-quadruplex DNA, SERS signals are observed.

Table 5.2 Ratio of ligands to G-quadruplex at each concentration used.

Concentration of G-quadruplex DNA (M)	Ligands : G-quadruplex
$5x10^{-5}$	1 : 1
$1x10^{-5}$	1 : 0.2
$5x10^{-6}$	1 : 0.1
$5x10^{-7}$	1 : 0.01
$5x10^{-8}$	1 : 0.001
$5x10^{-9}$	1 : 0.0001
0	1 : 0

For example, if the formation of a G-quadruplex was to be monitored using a particular concentration of DNA then a corresponding ligand concentration should be used. It is likely that if lower concentrations of ligand were used, an aggregating agent would be required as the amount of ligand present would not be enough to induce aggregation of the nanoparticles that was previously obtained. It can be clearly seen in Figure 5.10 that by using the correct ratio of G-quadruplex DNA to ligand results in a clear, sharp “on to off” signal being obtained upon formation of the G-quadruplex structure.

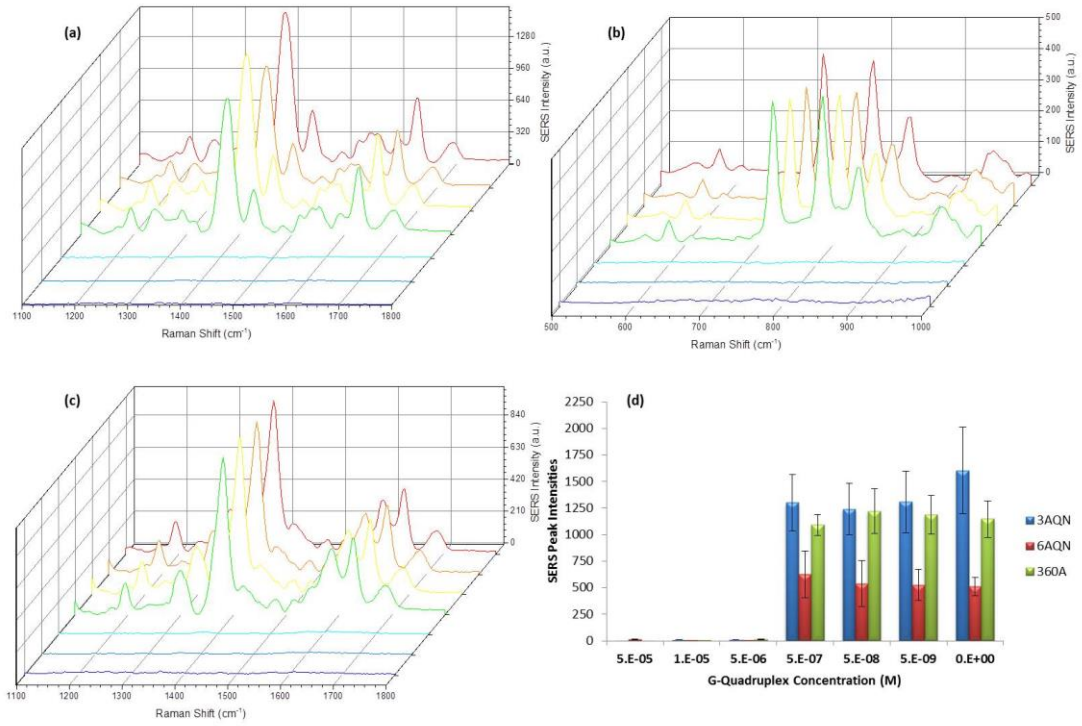

Figure 5.10 SERS spectra obtained from G-quadruplex concentration studies using each of the three ligands. The G-quadruplex concentration was reduced from 50 µM (dark blue) to 10 µM (light blue), 5 µM (turquoise), 0.5 µM (green), 50 nM (yellow), 5 nM (orange) and no G-quadruplex present (red). The concentration of the ligands remained constant at 50 µM. (a) SERS spectra of 3AQN obtained when reducing the G-quadruplex concentration. (b) SERS spectra of 6AQN obtained when decreasing the G-quadruplex concentration. (c) SERS spectra of 360A obtained when decreasing the G-quadruplex concentration. (d) Peak intensity comparisons for each of the three ligands using; 1380 cm^{-1} for 3AQN comparisons, 719 cm^{-1} for 6AQN comparisons and 1379 cm^{-1} peak intensity comparisons. Spectra were obtained using a 532 nm laser excitation wavelength and an accumulation time of 1 s. All peak intensities were obtained by scanning 3 replicate samples 5 times with an accumulation time of 1 s. Averages are shown and error bars represent ± one standard deviation.

5.4.6 Presence and Absence of Monovalent Cations

For further investigation into the effects of changing the experimental conditions, the ligand 3AQN was used. The importance of a monovalent cation such as Na^+ or K^+ has been highlighted as their presence induces the formation of a G-quadruplex structure from the guanine rich single stranded substrate.[4, 28, 54, 55] The ligands used in this study not only stabilise and bind to G-quadruplexes; they also induce the formation of the G-quadruplex structures without the need for monovalent cations,[46] the presence of a cation influences the orientation of the G-quadruplex.[17, 56]

SERS analysis was performed using 3AQN in the presence of duplex and G-quadruplex DNA, and adding either 100 mM NaCl or 100 mM KCl to provide the monovalent cations and investigating the effect this had on the SERS signals observed. Figure 5.11(a-c) shows the SERS spectra obtained when 3AQN is in the presence of duplex DNA and in a solution of NaCl, KCl or water for SERS analysis. Figure 5.11d is the SERS spectra observed when G-quadruplex DNA was present. The intensity of the peak at 1380 cm^{-1} was measured and plotted in Figure 5.11e illustrating that there was a slight decrease in the absolute SERS intensity when the monovalent ions were absent due to the reduced aggregation of the nanoparticles that would have been caused by the salt. However, the discrimination between the duplex DNA and the G-quadruplex DNA was still very significant. SERS signals were only observed when G-quadruplex DNA was absent; no SERS signals were observed when the ligand was bound to a G-quadruplex sequence, regardless of the salt conditions.

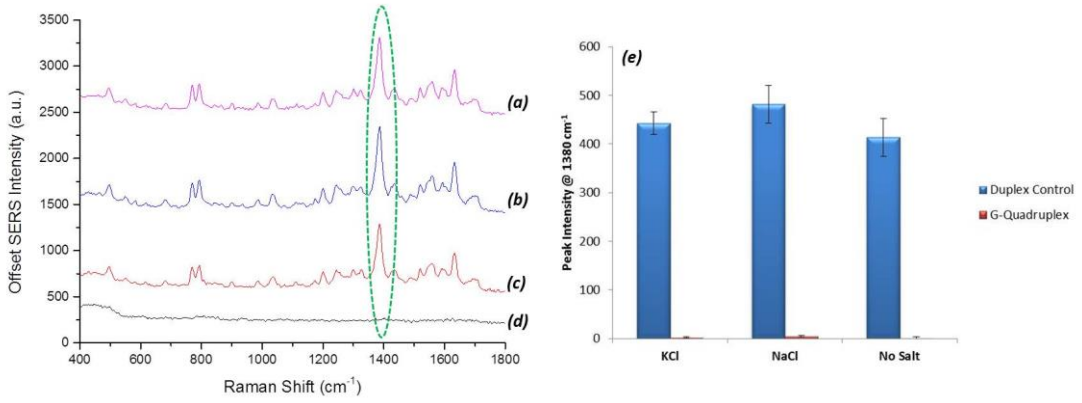

Figure 5.11 SERS spectra of 3AQN complexed to the duplex DNA control sequence in the presence of (a) Na^+ ions, (b) K^+ ions, (c) no monovalent ions and (d) 3AQN bound to G-quadruplex. Spectra were also recorded in the different salt conditions when 3AQN was complexed to the peroxidase deoxyribozyme quadruplex sequence. (e) Comparison of peak intensities using the unique peak at 1380 cm^{-1}. Spectra were obtained using a 532 nm laser excitation wavelength and an accumulation time of 1 s. All peak intensities were obtained by scanning 3 replicate samples 5 times with an accumulation time of 1 s. Averages are shown and error bars represent ± one standard deviation.

This further highlights the potential of using 3AQN as a stabilising agent for the formation of G-quadruplex DNA as SERS has shown it stabilises the G-quadruplex in the absence of monovalent cations.

5.4.7 Applicability of the Ligands for the Analysis of Other G-quadruplex Sequences

The ligands have been shown to selectively bind to G-quadruplex DNA compared to duplex DNA, however this has so far only been demonstrated using one G-quadruplex sequence, peroxidase deoxyribozyme. To show that these ligands can have a wider application for G-quadruplex analysis, two other sequences were used in the investigation. G-quadruplex forming sequences are also found in the promoter regions of oncogenes such as *C-MYC*. The *C-MYC* oncogene is the most common malfunctioning gene in human cancers; therefore it is an appealing target for anti-cancer therapies.[57] The human *C-MYC* gene is highly regulated and any changes in its expression are a crucial point in cancer progression. Detection of these guanine-rich sequences is extremely beneficial to the field of cancer diagnostics. Experiments were performed using the ligand 3AQN and two alternative G-quadruplex sequences, the human telomeric DNA sequence and the proto-oncogene *C-MYC* (Table 5.1).

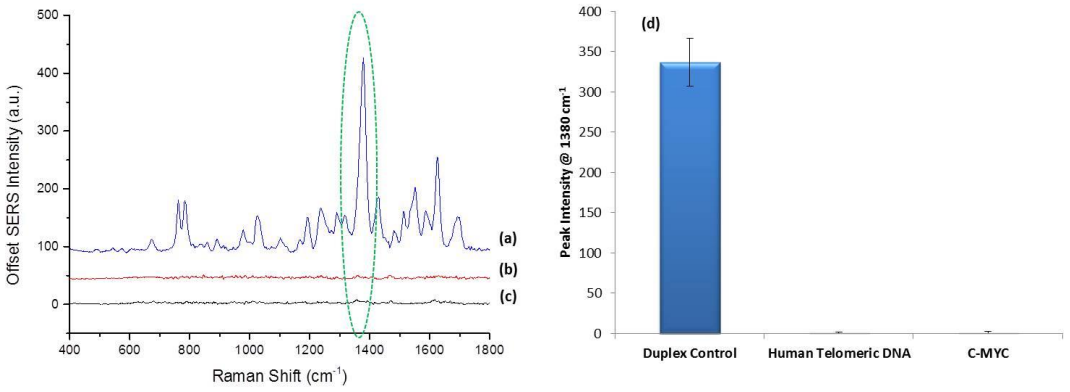

Figure 5.12 SERS spectra of 3AQN (50 µM) in the presence of (a) control duplex DNA (50 µM), (b) human telomeric DNA (50 µM), (c) *C-MYC* DNA (50 µM) and (d) a comparison of peak intensity at 1380 cm^{-1}. Spectra were obtained using a 532 nm laser excitation wavelength and an accumulation time of 1 second. All peak intensities were obtained using the 1380 cm^{-1} peak by scanning 3 replicate samples 5 times with an accumulation time of 1 s. Averages are shown and error bars represent ± one standard deviation.

Figure 5.12(a-c) illustrates that the 3AQN ligand peaks are only observed in the absence of guanine-rich DNA sequences, regardless of the nature of the G-quadruplex sequence whether it be human telomeric DNA or the *C-MYC* sequence. This demonstrates the strong affinity 3AQN has for the topology of a G-quadruplex, regardless of where it is found in the biological system and in the absence of any monovalent cations. Figure 5.12d shows the results from plotting the SERS intensity of 3AQN peak at 1380 cm^{-1}. It can clearly be seen that there is a large discrimination between the ligand in the presence of duplex DNA and when the ligand is bound to a G-quadruplex sequence. These results reaffirm the concept of using SERS and stabilising ligands such as 3AQN as a reliable qualitative method for analysing the formation of G-quadruplexes.

5.4.8 Design of a Molecular Beacon Probe for a G-Quadruplex Detection Assay

The method of analysis of G-quadruplex formation relied upon the loss of SERS signal to confirm the presence of a G-quadruplex sequence. Successful results were obtained when analysing the formation of a G-quadruplex using three ligands that not only specifically bound to G-quadruplexes but also acted as Raman reporters. In an effort to make use of these ligands combined with SERS analysis for a positive SERS detection method, an assay was designed that would only give an increase in SERS signal when the desired target was present (Figure 5.13).

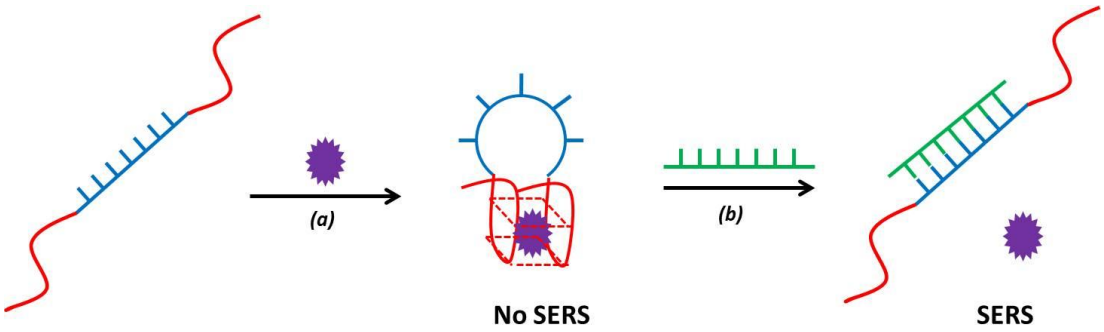

Figure 5.13 A schematic of the positive SERS assay using the ligands and G-quadruplex forming sequences. (a) In the presence of one of the stabilising ligands, the G-quadruplex structure forms resulting in a hairpin formation with the G-quadruplex in the stem region. (b) When a sequence complementary to the loop is present, the G-quadruplex opens releasing the ligand resulting in a SERS signal being observed.

Bourdoncle *et al.* designed a molecular beacon probe using the formation of a G-quadruplex as the stem sequence.[58] The stem sequence of a molecular beacon usually relies on Watson and Crick base pairing; however molecular beacons can now be formed using G-quadruplex structures. Using this design, an assay has been developed where upon the addition of one of the stabilising ligands (3AQN, 6AQN or 360A), the molecular beacon assembles and the stem sequences are in the form of a G-quadruplex, while a loop sequence is also formed. Since the ligand is bound to the G-quadruplex sequence, there will be no SERS signals. However, upon addition of a complementary target sequence that will hybridise to the loop sequence, the G-quadruplex stem will open, releasing the ligands and producing a SERS signal.

Preliminary experiments have been performed using a molecular beacon designed probe where the loop sequence was 39 bases long and the stem sequence was the peroxidase deoxyribozyme quadruplex sequence discussed previously. The ligand chosen for this study was 6AQN.

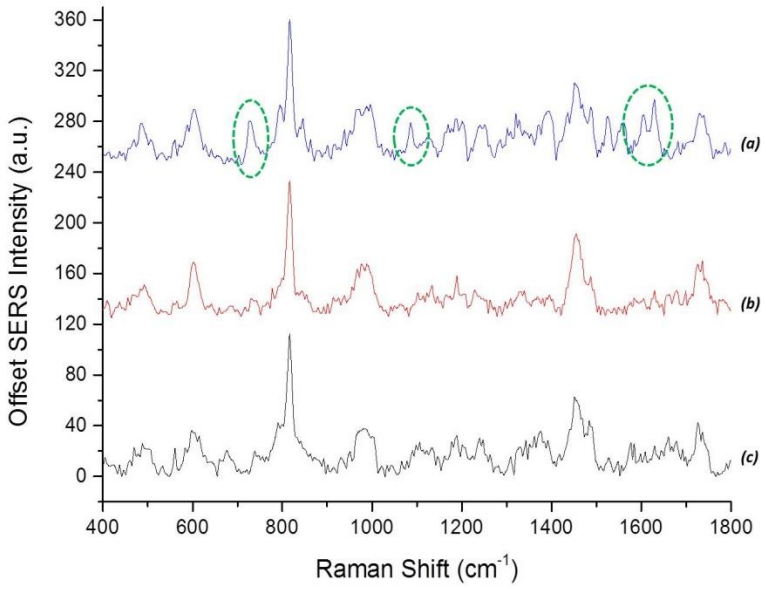

Figure 5.14 SERS spectra obtained when using the molecular beacon formed using G-quadruplex stems. (a) SERS spectra when the complementary sequence was added that opened the molecular beacon releasing the ligand resulting in SERS signal (green circles). Two control spectra were obtained using a non-complementary sequence (b) or no DNA sequences (c). SERS spectra were obtained using a 532 nm laser excitation wavelength and an accumulation time of 1 s.

Using the new assay format, when the complementary sequence was present, hybridisation took place opening the loop and separating the G-quadruplex stems, releasing 6AQN. SERS signals were observed that were attributed to the release of the ligand from the G-quadruplex, highlighted by the green circles in Figure 5.14a. These peaks were not present in the control spectra (Figure 5.14b, c). The intensity of the ligand peaks is low compared to previous ligand studies (section 5.4.2). Optimisation of the assay conditions, specifically the hybridisation between the complementary sequence and the loop sequence will need to be performed to increase the SERS intensity observed. However, preliminary results demonstrate the potential of this new assay, involving G-quadruplexes and stabilising ligands that act as Raman reporters, to be used successfully as a biological detection assay.

5.5 Chapter Conclusions

Analysis of the formation of G-quadruplex DNA sequences found in the peroxidase deoxyribozyme, telomeric region and in the proto-oncogene *C-MYC* has been demonstrated using a SERS-based approach. Studies were performed using three G-quadruplex stabilising ligands; 3AQN, 6AQN and 360A. Each ligand successfully detected the formation of a G-quadruplex sequence with high specificity demonstrated by comparing the interaction of the ligands with duplex DNA. Further studies were performed using 3AQN that demonstrated the added stabilising effect that the ligands possess, due to the fact that monovalent cations, usually required for G-quadruplex formation, are not needed when using these ligands as they can induce the G-quadruplex formation. SERS measurements can be taken without the addition of any fluorescent agents and without the presence of any salt. Since the ligands were known to bind to and stabilise various G-quadruplexes, the SERS-based method was extended to the analysis of any G-quadruplex forming sequences present in a biological system with successful results. The absence of an aggregating agent resulted in the lack of DNA peaks in the SERS spectra; however results show that by changing the experimental conditions, both ligand and DNA peaks could be readily observed. The method developed was novel in nature and provided a new and information rich approach to the analysis of higher order DNA structures and demonstrates the future possibilities of studies involving G-quadruplexes as key biological targets.

Following the success of using these ligands as Raman reporters, a new assay was designed where a molecular beacon probe with a G-quadruplex sequence of DNA as the stem was used. The presence of one of the stabilising ligands allowed the molecular beacon to remain closed, however in the presence of a target sequence of DNA complementary to the loop region of the beacon, the molecular beacon opened and released the ligand resulting in a SERS signal being observed. The results obtained are preliminary; however they do suggest that this assay method will be successful. The optimisation of the experimental conditions forms the basis of future work on this project.

5.6 Chapter References

1. K. Gracie, V. Dhamodharan, P. I. Pradeepkumar, K. Faulds and D. Graham, *Analyst*, 2014, DOI: 10.101039/c4an00551a
2. I. A. Pedroso, L. F. Duarte, G. Yanez, K. Burkewitz and T. M. Fletcher, *Biopolymers*, 2007, **87**, 74-84.
3. E. Y. Lam, D. Beraldi, D. Tannahill and S. Balasubramanian, *Nature Communications*, 2013, **4**, 1796-1796.
4. H. J. Lipps and D. Rhodes, *Trends in cell biology*, 2009, **19**, 414-422.
5. G. N. Parkinson, M. P. H. Lee and S. Neidle, *Nature*, 2002, **417**, 876-880.
6. Y. Chen and D. Yang, in *Current Protocols in Nucleic Acid Chemistry*, John Wiley & Sons, Inc., 2001.
7. S. Burge, G. N. Parkinson, P. Hazel, A. K. Todd and S. Neidle, *Nucleic Acids Research*, 2006, **34**, 5402-5415.
8. N. V. Hud, F. W. Smith, F. A. L. Anet and J. Feigon, *Biochemistry*, 1996, **35**, 15383-15390.
9. B. Heddi and A. T. Phan, *Journal of the American Chemical Society*, 2011, **133**, 9824-9833.
10. A. T. Phan, *FEBS Journal*, 2010, **277**, 1107-1117.
11. D. Hanahan and R. A. Weinberg, *Cell*, 2011, **144**, 646-674.
12. M. Y. Kim, M. Gleason-Guzman, E. Izbicka, D. Nishioka and L. H. Hurley, *Cancer Research*, 2003, **63**, 3247-3256.
13. S. Neidle and G. Parkinson, *Nature Reviews Drug Discovery*, 2002, **1**, 383-393.
14. L. Oganesian and T. M. Bryan, *Bioessays*, 2007, **29**, 155-165.
15. D. J. Patel, A. T. Phan and V. Kuryavyi, *Nucleic Acids Research*, 2007, **35**, 7429-7455.
16. J. L. Huppert, *Chemical Society Reviews*, 2008, **37**, 1375-1384.
17. M. Y. Kim, H. Vankayalapati, S. Kazuo, K. Wierzba and L. H. Hurley, *Journal of the American Chemical Society*, 2002, **124**, 2098-2099.
18. G. Biffi, D. Tannahill, J. McCafferty and S. Balasubramanian, *Nature Chemistry*, 2013, **5**, 182-186.
19. K. Shin-ya, K. Wierzba, K.-i. Matsuo, T. Ohtani, Y. Yamada, K. Furihata, Y. Hayakawa and H. Seto, *Journal of the American Chemical Society*, 2001, **123**, 1262-1263.

20. D. Y. Sun, B. Thompson, B. E. Cathers, M. Salazar, S. M. Kerwin, J. O. Trent, T. C. Jenkins, S. Neidle and L. H. Hurley, *Journal of Medicinal Chemistry*, 1997, **40**, 2113-2116.
21. M. A. Read, A. A. Wood, J. R. Harrison, S. M. Gowan, L. R. Kelland, H. S. Dosanjh and S. Neidle, *Journal of Medicinal Chemistry*, 1999, **42**, 4538-4546.
22. H. Y. Han, C. L. Cliff and L. H. Hurley, *Biochemistry*, 1999, **38**, 6981-6986.
23. A. Rangan, O. Y. Fedoroff and L. H. Hurley, *Journal of Biological Chemistry*, 2001, **276**, 4640-4646.
24. R. J. Harrison, S. M. Gowan, L. R. Kelland and S. Neidle, *Bioorganic & Medicinal Chemistry Letters*, 1999, **9**, 2463-2468.
25. S. Balasubramanian, L. H. Hurley and S. Neidle, *Nature Reviews Drug Discovery*, 2011, **10**, 261-275.
26. S. Neidle, *Febs Journal*, 2010, **277**, 1118-1125.
27. S. Balasubramanian and S. Neidle, *Current Opinion in Chemical Biology*, 2009, **13**, 345-353.
28. H.-Q. Yu, D. Miyoshi and N. Sugimoto, *Journal of the American Chemical Society*, 2006, **128**, 15461-15468.
29. M. Fialova, J. Kypr and M. Vorlickova, *Biochemical and Biophysical Research Communications*, 2006, **344**, 50-54.
30. Y. Xu, Y. Noguchi and H. Sugiyama, *Bioorganic & Medicinal Chemistry*, 2006, **14**, 5584-5591.
31. F. He, Y. Tang, S. Wang, Y. Li and D. Zhu, *Journal of the American Chemical Society*, 2005, **127**, 12343-12346.
32. O. Y. Fedoroff, M. Salazar, H. Han, V. V. Chemeris, S. M. Kerwin and L. H. Hurley, *Biochemistry*, 1998, **37**, 12367-12374.
33. V. Viglasky, L. Bauer and K. Tluckova, *Biochemistry*, 2010, **49**, 2110-2120.
34. C. Wei, G. Jia, J. Yuan, Z. Feng and C. Li, *Biochemistry*, 2006, **45**, 6681-6691.
35. T. Miura and G. J. Thomas, *Biochemistry*, 1994, **33**, 7848-7856.
36. K. Kneipp, H. Kneipp, I. Itzkan, R. R. Dasari and M. S. Feld, *Chemical Reviews*, 1999, **99**, 2957-2975.
37. K. Kneipp, H. Kneipp, V. B. Kartha, R. Manoharan, G. Deinum, I. Itzkan, R. R. Dasari and M. S. Feld, *Physical Review E*, 1998, **57**, R6281-R6284.
38. S. E. J. Bell and N. M. S. Sirimuthu, *Journal of the American Chemical Society*, 2006, **128**, 15580-15581.
39. E. Papadopoulou and S. E. J. Bell, *Journal of Physical Chemistry C*, 2010, **114**, 22644-22651.
40. E. Papadopoulou and S. E. J. Bell, *Analyst*, 2010, **135**, 3034-3037.
41. E. Papadopoulou and S. E. J. Bell, *Journal of Physical Chemistry C*, 2011, **115**, 14228-14235.
42. E. Papadopoulou and S. E. J. Bell, *Chemical Communications*, 2011, **47**, 10966-10968.
43. E. Papadopoulou and S. E. J. Bell, *Chemistry-a European Journal*, 2012, **18**, 5394-5400.
44. G. Rusciano, A. C. De Luca, G. Pesce, A. Sasso, G. Oliviero, J. Amato, N. Borbone, S. D'Errico, V. Piccialli, G. Piccialli and L. Mayol, *Analytical Chemistry*, 2011, **83**, 6849-6855.
45. G. Breuzard, J. M. Millot, J. F. Riou and M. Manfait, *Analytical Chemistry*, 2003, **75**, 4305-4311.
46. V. Dhamodharan, S. Harikrishna, C. Jagadeeswaran, K. Halder and P. I. Pradeepkumar, *Journal of Organic Chemistry*, 2012, **77**, 229-242.

47. C. Granotier, G. Pennarun, L. Riou, F. Hoffschir, L. R. Gauthier, A. De Cian, D. Gomez, E. Mandine, J. F. Riou, J. L. Mergny, P. Mailliet, B. Dutrillaux and F. D. Boussin, *Nucleic Acids Research*, 2005, **33**, 4182-4190.
48. P. C. Lee and D. Meisel, *Journal of Physical Chemistry*, 1982, **86**, 3391-3395.
49. J. F. Riou, L. Guittat, P. Mailliet, A. Laoui, E. Renou, O. Petitgenet, F. Mégnin-Chanet, C. Hélène and J. L. Mergny, *Proceedings of the National Academy of Sciences*, 2002, **99**, 2672-2677.
50. G. Pennarun, C. Granotier, L. R. Gauthier, D. Gomez, F. Hoffschir, E. Mandine, J. F. Riou, J. L. Mergny, P. Mailliet and F. D. Boussin, *Oncogene*, 2005, **24**, 2917-2928.
51. A. De Cian, E. DeLemos, J.-L. Mergny, M.-P. Teulade-Fichou and D. Monchaud, *Journal of the American Chemical Society*, 2007, **129**, 1856-1857.
52. E. Smith and G. Dent, *Modern Raman Spectroscopy: A Practical Approach*, Wiley, 2005.
53. G. Rusciano, A. C. De Luca, G. Pesce, A. Sasso, G. Oliviero, J. Amato, N. Borbone, S. D'Errico, V. Piccialli, G. Piccialli and L. Mayol, *Analytical Chemistry*, 2011, **83**, 6849-6855.
54. K. W. Lim, S. Amrane, S. Bouaziz, W. X. Xu, Y. G. Mu, D. J. Patel, K. N. Luu and A. T. Phan, *Journal of the American Chemical Society*, 2009, **131**, 4301-4309.
55. J. L. Huppert, *FEBS Journal*, 2010, **277**, 3452-3458.
56. E. Izbicka, R. T. Wheelhouse, E. Raymond, K. K. Davidson, R. A. Lawrence, D. Y. Sun, B. E. Windle, L. H. Hurley and D. D. Von Hoff, *Cancer Research*, 1999, **59**, 639-644.
57. A. Siddiqui-Jain, C. L. Grand, D. J. Bearss and L. H. Hurley, *Proceedings of the National Academy of Sciences*, 2002, **99**, 11593-11598.
58. A. Bourdoncle, A. Estévez Torres, C. Gosse, L. Lacroix, P. Vekhoff, T. Le Saux, L. Jullien and J. L. Mergny, *Journal of the American Chemical Society*, 2006, **128**, 11094-11105.

6. Conclusions

There is a growing need for much more informative methods of detection and analysis of biomolecules such as DNA. Surface enhanced Raman scattering (SERS) has been used for the development of a biological detection assay and for the analysis of the formation of specific DNA structures. There is a need for understanding the interactions between biomolecules, fluorescent dyes and the metal surfaces by obtaining information on such interactions, much more informed decisions can be made when designing biological detection assays using SERS.

A SERS-based assay was developed for the multiplex detection of three bacterial meningitis pathogens. Through careful design of the reporter probe, enhanced SERS signals of the fluorescent dye that was complementary to one of the pathogens were observed. The assay involved several steps; sandwich hybridisation, bead washing and enzyme digestion using λ-exonuclease. For the assay to successfully detect the pathogens, each step had to be efficiently carried out. Each pathogen was detected successfully indicating that the assay was working to maximum efficiency. To further confirm this; two control experiments were carried out, one where the target pathogen was omitted from the assay and another where a non-complementary was added in place of the target pathogen. Upon SERS analysis, no signal was observed showing the high specificity of the assay. To demonstrate the sensitivity of the detection method, limits of detection studies were performed using each pathogen, which were all calculated to be in the pico-molar range ideal for detection in clinical samples that would contain low quantities of target pathogen. PCR product of each pathogen was then used to determine if the assay could still be used for the detection of longer DNA sequences that would mimic a clinical environment. SERS signals of the fluorescent dyes associated with each pathogen were readily observed using PCR product. Following these studies, the three pathogens were detected simultaneously using synthetic DNA and PCR product, therefore the SERS-based assay was successfully implemented for the multiplex detection of the three pathogens. Furthermore, for the first time each pathogen was quantified in the post-assay mixture using chemometric methods such as principle component analysis (PCA) and partial least squared regression (PLS).

There is an increase in the development of multiplex assays involving DNA, fluorescent dyes and, when using SERS as the analysis method, spermine. Investigation into the interactions that occur between fluorescent dyes, in particular FAM and TAMRA, DNA and spermine were carried out using fluorescence and SERS. By using fluorescence to investigate these interactions, an understanding of what interactions were happening away from the nanoparticle was obtained. When spermine was added to a solution of F-ITC or FAM labelled DNA, fluorescence enhancement was observed; however, this was not observed using TR-ITC or TAMRA-labelled DNA. It was also noted that when the fluorescent dyes were covalently attached to DNA, the fluorescence decreased through base quenching caused by the DNA. All these competing interactions will ultimately have an effect on their relative intensities in a multiplex detection assay.

SERS studies involving FAM and TAMRA were then performed based on the information generated from the fluorescence studies. As with observed in fluorescence, covalent attachment to a DNA sequence affects the SERS intensity observed of the two fluorescent dyes. Conversely, in the presence of spermine TAMRA produced the more intense SERS signals compared to FAM. This could be a combined effect from the orientation of the dyes with respect to the nanoparticle surface and the charges these dyes possess. Each component under analysis is charged; therefore electrostatic interactions will have a major impact on the SERS intensity observed. Different experimental conditions were also applied to the analysis, demonstrating that careful selection of reagents and conditions needed when designing multiplex assays.

SERS was then applied for the detection of the formation of G-quadruplex DNA. Three quadruplex sequences were analysed; peroxidase deoxyribozyme, human telomeric DNA and the promoter gene *C-MYC*. G-quadruplex DNA structures are ideal target for cancer diagnostics as they sequester the substrate, single stranded DNA, needed for the progression of cancer cells. SERS analysis of DNA and in particular G-quadruplex DNA has been reported previously, however additional labelling or aggregating agents were required. By using three ligands; 360A, 3AQN and 6AQN, SERS analysis of G-quadruplex

formation was successful without the need for fluorescent labelling or nanoparticle aggregation agents such as $MgSO_4$. These ligands selectively bind to and stabilise G-quadruplex DNA, and in addition have the ability to aggregate nanoparticles and can also act as Raman reporters. Therefore, by using these ligands alone, the formation of a G-quadruplex can be detected using SERS based upon the unique SERS spectra of each ligand.

This thesis involved the application of SERS for the multiplex detection of three bacterial meningitis pathogens and for the detection of the formation of G-quadruplex DNA using stabilising ligands. Further to this, investigative studies using fluorescence and SERS analysis demonstrated the consideration needed when designing SERS-based assays involving the detection of fluorescent dye labelled DNA.

7. Further Work

The work presented in this thesis has shown the potential of SERS as an alternative detection method compared to the much used fluorescence-based methods for the detection of DNA.

The SERS-based assay used for the simultaneous detection and quantification of three bacterial meningitis proved successful. However, for this assay to be fully implemented into clinical diagnostics, bacteria extracted from human CSF samples must be used in the assay using the same reporter probes and if SERS signals are observed then the assay can be deemed as a clinical diagnostic assay. Chemometric analysis is a powerful tool and was used to readily quantify pathogens in the assay mixture. Due to the power if this technique, the multiplex can be increased to detect and quantify more than three pathogens.

Fluorescence and SERS studies into the interactions between fluorescent dyes (FAM and TAMRA), DNA and spermine produced results that allowed for a more informed approach to assay design. However, there is potential to increase the scope of these investigations by introducing more fluorescent dyes and by using different DNA sequences to gain a better understanding of the sequence specificity when measuring the fluorescence emission of SERS spectra of fluorescent dyes.

The formation of G-quadruplex DNA was successfully detected using SERS. Our collaborators in IIT Bombay are designing new ligands that will specifically bind to different G-quadruplex structures and using the “on to off” SERS method, these new ligands not only provide information on the presence of the G-quadruplex, but discrimination between different G-quadruplex sequences will also be achieved. Further to this, there is a potential application for these ligands to detect G-quadruplexes *in vivo*.

An assay has been designed using a molecular beacon with G-quadruplex sequences for stem sequences to produce a SERS signal only when target is present, i.e. a positive SERS assay. Proof of concept work has been performed however more focus on the optimisation of experimental conditions is required to improve the SERS signal observed. This would then combine the formation of G-quadruplexes and the Raman reporter ligands to be used in a SERS assay used for the detection of specific target DNA.

Appendix: Publications and Presentations

Publications

1. Simultaneous detection and quantification of three bacterial meningitis pathogens by SERS. **K. Gracie**, E. Correa, S. Mabbott, J. Dougan, D. Graham, R. Goodacre, K. Faulds, *Chemical Science*, 2014, **5**, 1030-1040
2. Qualitative SERS analysis of G-quadruplex DNAs using selective stabilising ligands. **K. Gracie**, V. Dhamodharan, P. I. Predeepkumar, K. Faulds, D. Graham, *Analyst*, 2014, DOI: 10.101039/c4an00551a
3. Interaction of fluorescent dyes with DNA and spermine using fluorescence spectroscopy. **K. Gracie**, W. E. Smith, P. Yip, J. U. Sutter, D. J. S. Birch, D. Graham, K. Faulds, *Analyst*, 2014, **139**, 3735-3743
4. Interactions of FAM and TAMRA labelled DNA in a multiplex SERS system. **K. Gracie**, K. Harding, W. E. Smith, D. Graham, K. Faulds, *in preparation*

Oral Presentations

1. Using Optical Spectroscopies for the Detection and Analysis of Biological Materials, Nanolight, September 2013, University of Strathclyde
2. Simultaneous Detection and Quantification of Bacterial Meningitis using SERS and Lambda Exonuclease, RSC Analytical Research Forum (ARF), July 2013, University of Hertfordshire & GSK
3. Simultaneous Detection of Bacterial Meningitis using SERS and Lambda Exonuclease, Pittcon Conference, March 2013, Philadelphia, USA
4. Multiplex Detection of Periodontal Diseases Using SERS and Lambda Exonuclease, University of Strathclyde Inorganic Section Meeting, June 2012, West Brewery

Poster Presentations

1. Multiplexed SERS detection of Periodontal Diseases, Poster Presentation, RSC Analytical Research Forum (ARF), July 2012, University of Durham **(prize winner)**
2. Using SERS to Simultaneously Detect Periodontal Diseases, Poster Presentation, Nano Meets Spectroscopy (NMS), September 2011, NPL London
3. Enzymatic Detection of Pathogen DNA, Poster Presentation, RSC Analytical Research Forum (ARF), July 2011, University of Manchester **(prize winner)**